IntechOpen

Molecular Docking

Edited by Dimitrios P. Vlachakis

MOLECULAR DOCKING

Edited by **Dimitrios P. Vlachakis**

Molecular Docking
http://dx.doi.org/10.5772/intechopen.69830
Edited by Dimitrios P. Vlachakis

Contributors

Sadia Sultan, Kamran Ashraf, Gurmeet Kaur Surindar Singh, Rafael Trindade Maia, Vinícius Amador, Ravi Varala, Bollikolla Hari Babu, Lucia Pintilie, Amalia Stefaniu, Luis Chacon, Abel Suárez, Carlos Cortés, Mario Valle, Norma Flores-Holguín, Linda-Lucila Landeros-Martinez, Daniel Glossman-Mitnik, Erasmo Orrantia-Borunda, Zhong-Ru Xie, Darby L. Woodling, Marisa A. Stewart, Mark Andrew Phillips, Dimitrios P. Vlachakis

Notice

First published in London, United Kingdom, 2018 by IntechOpen
eBook (PDF) Published by IntechOpen, 2019
IntechOpen is the global imprint of INTECHOPEN LIMITED, registered in England and Wales, registration number: 11086078, The Shard, 25th floor, 32 London Bridge Street
London, SE19SG – United Kingdom
Printed in Croatia

British Library Cataloguing-in-Publication Data
A catalogue record for this book is available from the British Library

Additional hard and PDF copies can be obtained from orders@intechopen.com

Molecular Docking
Edited by Dimitrios P. Vlachakis

p. cm.

Print ISBN 978-1-78923-354-4

Online ISBN 978-1-78923-355-1

eBook (PDF) ISBN 978-1-83881-432-8

Meet the editor

Assist. Professor Dimitrios P. Vlachakis leads the Genetics and Computational Biology Group at the Genetics Laboratory, Biotechnology Department, Agricultural University of Athens. He is a medical biochemist with postgraduate, doctoral and postdoctoral studies in the eminent field of genetics, medicinal chemistry and drug discovery. He is also appointed as an associate researcher at the Clinical, Experimental Surgery and Translational Research, Biomedical Research Foundation of the Academy of Athens, as well as an adjunct investigator at the Faculty of Natural and Mathematical Sciences, King's College London. His main scientific interests are aligned in three distinct axes: the design of antiviral agents, immunoinformatics, and epigenetics of neoplastic and neurodegenerative diseases.

Contents

Preface

Scientists have hard time to keep up with the amount of information that is being generated and released to dedicated depositories by the minute. Techniques and scientific methodologies are now linked to their release date as due to the extremely fast developments in the field, they may only be synonymous to their earlier versions. Molecular docking is no exception to this rule. The first introduction of molecular docking, a few decades ago, can hardly be traced back to what molecular docking has become today.

The chapters of this book provide insights into a repertoire of recent developments, applications and breakthroughs in the field of molecular docking. All chapters have been carefully selected, adjusted and fine-tuned in a seamless way that help them achieve synergy and make it easier for both the novice and the expert readers to follow. A lot of effort has gone into providing the scientific basis underlying all different molecular docking applications, thus leaving no excuse for misinterpretation of quite complex use cases and research protocols described herein. In the postgenomic era, and during times of massive computational rearrangements as supercomputers have moved to the cloud and are now accessible to everyone via extremely user-friendly interfaces, molecular docking is bound to play a pivotal role in the eminent field of pharmacogenomics, medicinal chemistry, and the overall drug discovery process.

I would like to close this opening statement by the words of Bilbo Baggins, when he was stating that "it is not a bad thing to celebrate a simple life." That is also true for science and especially the world of biocomputing, where keeping it simple is integral to understanding and communicating the research pipeline. The chapters in this book have been accordingly curated to simplify quite complex elements of molecular docking, without any compromise in scientific quality. Finally, I would like to express my gratitude and to dedicate this book to the loving memory of my father, whose impact on the design and final form of this book was immense.

Prof. Dimitrios P. Vlachakis
Assist. Professor in Genetics
Leader of Genetics and Computational Biology Group
Genetics Laboratory, Department of Biotechnology
Agricultural University of Athens
Athens, Greece

Introduction

Chapter 1

Introductory Chapter: Molecular Docking - Overview, Background, Application and What the Future Holds

Dimitrios Vlachakis

Additional information is available at the end of the chapter

http://dx.doi.org/10.5772/intechopen.78266

1. Introduction

Molecular docking is on the frontline of computational biology and drug discovery. The explosion of structural and chemical information in recent years has rendered the use of efficient algorithms and large supercomputer facilities of uttermost importance in the drug discovery process. Medicinal chemists can now screen *in silico* hundreds of thousands of compounds on a repertoire of receptor molecules and putative pharmacological targets. It goes without saying that molecular docking comes in many shapes and sizes, thus allowing the researcher to balance out speed and exhaustiveness of calculation. Molecular docking can be performed online of freeware servers using just a web browser or it can be fully parameterized on a virtual machine on a cloud supercomputer for high resolution calculation. The main factor that changes here is the grid resolution and the rigidity and flexibility of both the ligand and the receptor.

2. Molecular docking in a nutshell

Let us start by setting the basis on molecular properties that are required to comprehend the molecular docking chapters that follow in this book. The geometry and the overall structure of a molecule are described by its bond distances, dihedral angles and bond angle [1]. This unique set of angles and distances create a set of coordinates that define the positioning of each atom in that molecular structure in three-dimensional (3D) space. The energy condition of this molecule can also be assessed and evaluated. The energy of a molecule includes all forms of energies, such as kinetic motion (described by vibration, rotation and translation) and forms of the potential energy of the molecule [2]. The potential energy of a molecule

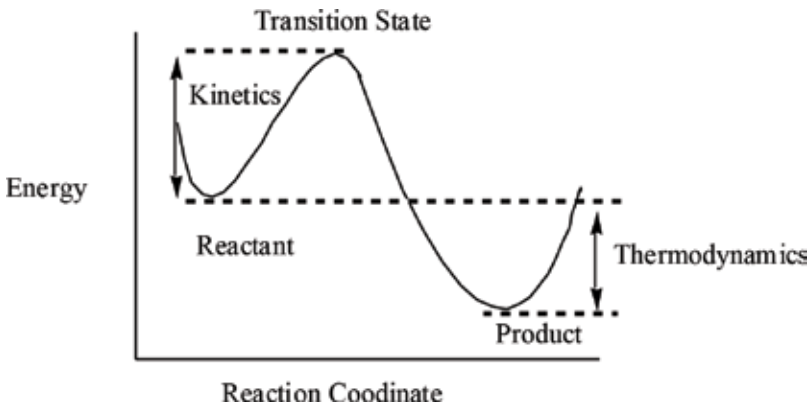

Figure 1. Energy changes during the course of a chemical reaction.

can be defined by the analysis of the electrostatic interaction between charges, the magnetic interactions between spinning charges and finally the potential energy of the bonds of the molecule. The total energy is indicative of the reactivity and stability of that a molecule or a system. **Figure 1** is depicts a reaction coordinate diagram that indicates the energy changes during the course of a chemical reaction [3].

Here the products are in the lowest or global minimum, the transition state is at energy maximum and the reactants are at an energy minimum. The dotted lines in the above diagram are indicative of the reactivity of the system (its kinetics) and the thermodynamic stability of the system. Through molecular modelling it is possible to quantify the above characteristics of the system and, for example, predict its reactivity. There are two fields in molecular modelling that attempt to do this: molecular mechanics and quantum mechanics [4].

The docking algorithm is basically split into two main parts: the searching algorithm and the scoring algorithm [5]. The searching algorithm will explore all conformations of the ligand within the space available [6]. Practically, it is impossible to perform all these calculations for every compound so most of the rotational and translational states of each compound will be explored within a given threshold of identical conformations. Each compound is not a rigid body but is a dynamic structure that exists in an ensemble of different conformations. The user can define how fine the docking algorithm will be by altering the various parameters of the task. Very fine calculations are much more accurate, but also much more time consuming. The most popular docking algorithm approaches can involve a coarse grained molecular dynamics simulation or a linear combination of many structures or a genetic algorithm that generates new conformations as it moves along.

The second feature of the docking algorithm is its scoring function [7]. The scoring function must be able to accurately evaluate each different conformation using certain forcefields and rules from physics and return a value that will describe the energy of the system at the given conformation. Low energies indicate better, more stable interactions.

http://dx.doi.org/10.5772/intechopen.78266

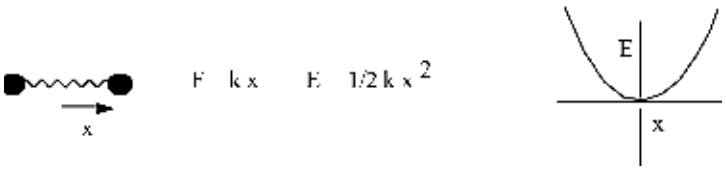

Molecular mechanics are based on the ball and spring representation of molecular systems. Here, the atoms are considered to be little balls, with varying properties according to the element, and the bonds are considered to be the springs that make the two interconnecting balls interact with each other. The ball and spring model is described by Hook's law, which evaluates and quantifies the energy of the stretching of the spring [8].

The force constant is the constant k. The energy that is contained in the spring and the restoring force of the spring are proportional to the force constant. The force constant will determine the strength of the bond that the spring represents [9]. The vibrational frequency of the spring is described as:

$$n = \frac{1}{2\pi}\sqrt{\frac{k}{\mu}} \tag{1}$$

The vibrational frequency (n) has been estimated to be proportional to the square root of the force constant (k) and inversely proportional to the reduced mass of the atoms that participate in a bond [10].

All of the above can be combined and through potential energy functions of various structural features, such as bond lengths, bond angles and non-bonded interactions, can describe a forcefield (**Figure 2**) [11]. There are many different ways to set a forcefield depending on the needs of the system under investigation. Usually the factors affecting the energy of a molecular system (bonds, angles, dihedrals, non-bonded, etc.), are evaluated separately and they will contribute to the value of the total energy of the system [12]. The most popular forcefields are the MM2, which is suitable for small molecules, hydrocarbons and some simple heteroatom

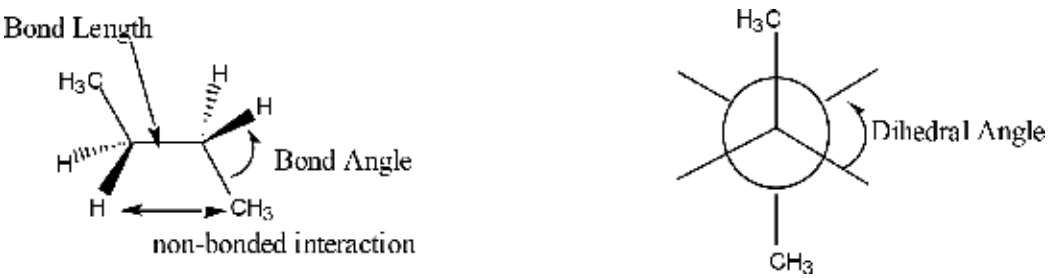

Figure 2. Total energy is affected by bond distances, bond angles, dihedral angles and finally non-bonded interactions.

functional groups, AMBER or CHARMM, which are parameterised to be used for peptides, nucleic acids and generic macromodels [13].

Overall through molecular mechanics the total energy of a molecule is described as a sum of all the contributions that may arise from loss of equilibrium in bond distances, also known as stretching contribution, bond angles, known as bending contribution, dihedral angles, the torsion contribution and finally non-bonded interaction contributions [14].

$$E^{total} = \sum_{i}^{bonds} E_i^{stretch} + \sum_{i}^{bond\ angles} E_i^{bend} + \sum_{i}^{dihedral\ angles} E_i^{torsion} + \sum_{i}\sum_{j}^{non\text{-}bonded\ atoms} E_{ij}^{non\text{-}bonded} \quad (2)$$

The energy that is stored in chemical bonds of a molecule can describe the stretch, bend, and torsion energy whereas it is the steric attraction or repulsion that represents the non-bonded energy [15]. The latter is broken down to two different categories: the van der Waals (VDW) and electrostatic interactions [16].

A very steep energy barrier is generated at the van der Waals radius of each atom. Moreover a very shallow energy well is produced at larger separations (**Figure 3**). The inherent steric size of atoms and elements is dictated by their VDW radii. The same metric is used to describe weak attractive forces between atoms in close proximity [17]. A trivial example of the weak van der Waals attractive forces is the condensation of a gas into liquids. Furthermore it is the van der Waals radii of each element that is used for its visualisation purposes in space filling models of the molecule they participate. Steric repulsion takes place only in the case where two atoms come closer than the sum distance of their VDW radii [18].

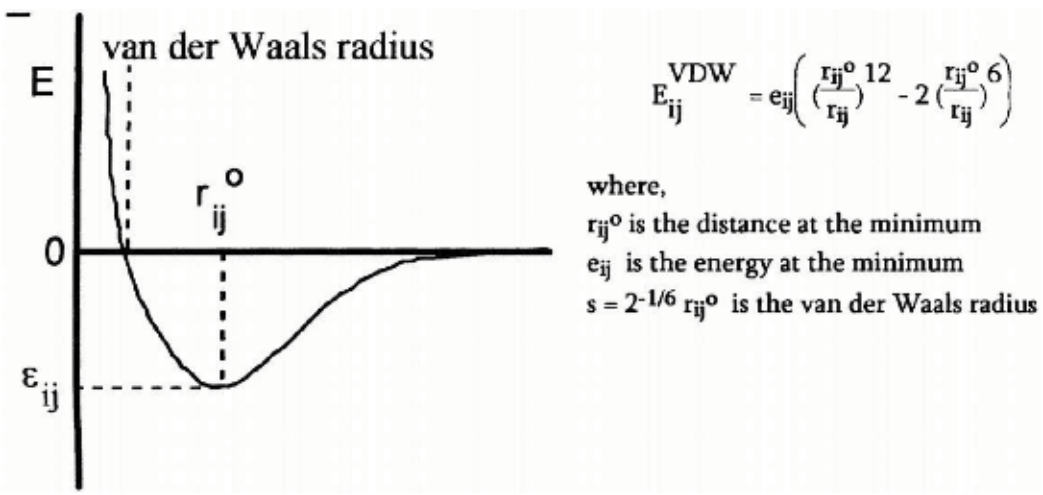

Figure 3. The van der Waals interactions plot and formula.

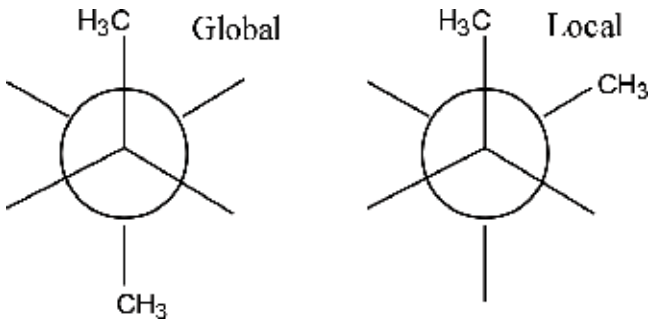

Figure 4. Two different conformations of butane.

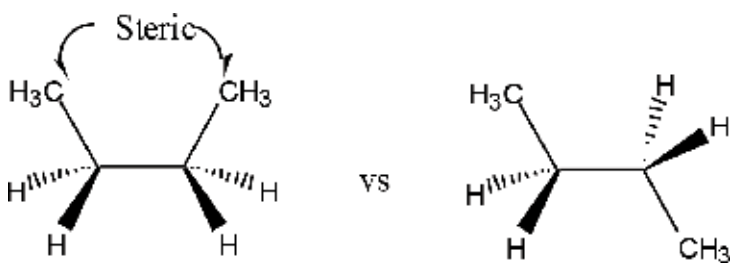

Figure 5. Steric hindrance of a small organic compound.

As soon as the set of the internal coordinates of a molecular system has been determined, computer algorithms can be used to help find those coordinates which will account for the lowest energy of the system [19]. All bond angles, lengths, dihedral angles and the relative energy between various different conformations of a given system will be evaluated in order to determine the minimum energy conformation [20]. It is crucial to understand that reducing the strain energy of a given molecular system does not mean that the system will reach energy minimum (also known as global minimum). An example is the following figure (**Figure 4**) with two different conformations of butane.

An energy minimisation algorithm will allow the rotation of groups, when their bonding allows. The rotation of the groups will give the molecule the opportunity to explore different conformations that will account for different energy values, thus allowing the compound to move towards its global minimum conformation [21].

Molecular modelling is very useful for investigating, comparing, analysing and visualising chemical structures and for giving qualitative and quantitative information about biological systems [22].

Figure 5 shows a characteristic example of steric hindrance. Two dimensional models like this only contain qualitative information. Quantitative information can arise through molecular mechanics and in conjunction with a computer, where the physical properties of the molecules can be evaluated and analysed based on a set of predefined criteria concerning various chemical

properties (such as bonding, charges, steric hindrance) [23]. Molecular Modelling can be used to study the geometry, the energy and the chemical properties *in silico* so efficiently that nowadays it is possible to predict the outcome of chemical reactions, design reactions, determine the unknown three-dimensional structures of proteins, screen and design new and effective drugs [23].

All in all, the future is bright for molecular docking. New technologies are being developed and employed in the race against drug discovery and lethal diseases. Data mining, machine or deep learning, hyper-computers and cloud computers are just few of the emerging technologies in modern molecular docking.

Author details

Dimitrios Vlachakis

Address all correspondence to: dimvl@aua.gr

Laboratory of Genetics, Department of Biotechnology, Agricultural University of Athens, Athens, Greece

References

[1] Branden C, Tooze J. Introduction to Protein Structure. 2nd ed. New York: Garland Publishing Inc; 1999

[2] Bratley P, Fox BL, Schrage LE. A Guide to Simulation. New York: Springer-Verlag; 1987

[3] BrooksIII CL, Karplus M, Pettitt BM. A Theoretical Perspective of Dynamics, Structure, and Thermodynamics. New York: Wiley Interscience; 1988

[4] Burkert U, Allinger NL. Molecular Mechanics. Washington D.C.: American Chemical Society; 1980

[5] Ryckaert JP, Ciccotti G, Berendsen HJC. Numerical integration of the Cartesian equations of motion of a system with constraints: Molecular dynamics of n-alkanes. Journal of Computational Physics. 1977;**23**:327-341

[6] Hess B, Bekker H, Berendsen HJC, Fraaije JGEM. LINCS: A linear constraint solver for molecular simulations. Journal of Computational Chemistry. 1997;**18**:1463-1472

[7] Ferguson DM, Raber DJ. A new approach to probing conformational space with molecular mechanics: Random incremental pulse search. Journal of the American Chemical Society. 1989;**111**:4371-4378

[8] Cantor CR, Schimmel PR. Biophysical Chemistry. Vol. 1-3. San Francisco: W.H. Freeman and Company; 1980

[9] Cohen NR, editor. Guidebook on Molecular Modeling in Drug Design. San Diego: Academic Press; 1996

[10] Deuflhard P, Hermans J, Leimkuhler B, Mark AE, Reich S, Skeel RD, editors. Computational Molecular Dynamics: Challenges, Methods, Ideas – Proceedings of the 2nd International Symposium on Algorithms for Macromolecular Modelling, Berlin, May 21-24, 1997. Vol. 4. Lecture Notes in Computational Science and Engineering. Berlin, Heidelberg: Springer-Verlag; 1999

[11] Creighton TE, editor. Protein Folding. New York: W.H. Freeman & Company; 1992

[12] Eisenberg D, Crothers D. Physical Chemistry with Applications to the Life Science. Menlo Park, California: Benjamin Cummings; 1979

[13] Fersht A. Structure and Mechanism in Protein Science: A Guide to Enzyme Catalysis and Protein Folding. New York: W. H. Freeman and Company; 1999

[14] Frenkel D, Smit B. Understanding Molecular Simulations. From Algorithms to Applications. San Diego, California: Academic Press; 1996

[15] Gierasch LM, King J, editors. Protein Folding, Deciphering the Second Half of the Genetic Code. Washington D.C.: AAAS; 1990

[16] Gould H, Tobochnik J. An Introduction to Computer Simulation Methods: Applications to Physical Systems. Part 1 and 2. Reading, MA: Addison-Wesley; 1988

[17] Grosberg AY, Khokhlov AR. Giant Molecules. Here, There, and Everywhere…. San Diego, California: Academic Press; 1997

[18] Haile JM. Molecular Dynamics Simulations: Elementary Methods. New York: Wiley; 1992

[19] Kalos M, Whitlock PA. Monte Carlo Methods. New York: John Wiley & Sons; 1986

[20] Leach AR. Molecular Modelling. Principles and Applications. Essex, England: Addison Wesley Longman; 1996

[21] Lipkowitz KB, Boyd DB, editors. Reviews in Computational Chemistry. New York: VCH Publishers; 1990

[22] Allen MP, Tildesley DJ. Computer Simulation of Liquids. New York: Oxford University Press; 1987

[23] Bates AD, Maxwell A. DNA Topology. In Focus Series. New York: Oxford University Press; 1993

Section 2

Molecular Docking for Enzymes

Chapter 2

Molecular Docking Studies of Enzyme Inhibitors and Cytotoxic Chemical Entities

Sadia Sultan, Gurmeet Kaur Surindar Singh, Kamran Ashraf and Muhammad Ashraf

Additional information is available at the end of the chapter

http://dx.doi.org/10.5772/intechopen.76891

Abstract

Docking is a powerful approach to perform virtual screening on large library of compounds, rank the conformations using a scoring function, and propose structural hypotheses of how the ligands inhibit the target, which is invaluable in lead optimization. Using experimentally proven active compounds, detailed docking studies were performed to determine the mechanism of molecular interaction and its binding mode in the active site of the modeled yeast α-glucosidase and human intestinal maltase-glucoamylase. All active ligands were found to have greater binding affinity with the yeast α-glucosidase as compared to that of human homologs, intestinal, and pancreatic maltase, by an average value of ~−1.3 and ~−0.8 kcal/mol, respectively. Thirty quinoline derivatives have been synthesized and evaluated against β-glucuronidase inhibitory potential. Twenty-four analogs, which showed outstanding β-glucuronidase activity, have IC_{50} values ranging between 2.11 ± 0.05 and 46.14 ± 0.95 μM than standard D-saccharic acid 1,4-lactone (IC_{50} = 48.4 ± 1.25 μM). Structure activity relationship and the interaction of the active compounds and enzyme active site with the help of docking studies were established. In addition, Small series of morpholine hydrazones synthesized to form morpholine hydrazones scaffold. The *in vitro* anti-cancer potential of all these compounds were checked against human cancer cell lines such as HepG2 (Human hepatocellular liver carcinoma) and MCF-7 (Human breast adenocarcinoma). Molecular docking studies were also performed to understand the binding interaction.

Keywords: docking studies, α-glucosidase inhibitors, cedryl acetate, quinoline, β-glucuronidase inhibitors, morpholine hydrazone

1. Introduction

Due to the current problems and complicated challenges faced by medicinal chemists docking is a most demanding and efficient discipline in order to rational design new therapeutic agents for treating the human disease. Previously, the strategy for discovering new drugs consisted of taking a lead structure and developing a chemical program for finding analog molecules exhibiting the desired biological properties, the whole process involved several trial and error cycles patiently developed and analyzed by medicinal chemists utilizing their experience to ultimately select a candidate analog for further development. The entire process when looked at today, conceptually inelegant. These days picture are quite reverse after the emergence of computational chemistry discipline in science world. The concepts used in three-dimensional (3D) drug design are quite simple. New molecules are conceived either on the basis of similarities with known reference structures or on the basis of their complementarity with the 3D structure of known active sites. Molecular modeling is a discipline that contributes to the understanding of these processes in a qualitative and sometimes quantitative way [1, 2].

In this chapter we have presented a brief introduction of the available molecular docking methods, and their development and applications in drug discovery especially for synthetic and bio-transformed derivatives.

2. Quantum mechanical calculations and molecular docking studies of α-glucosidase inhibitors

Inhibitors of a-glucosidase regarded as a convincing therapeutic target in the development of drugs against diseases such as obesity, diabetes, HIV, and cancer [3, 4]. In this connection, few synthetic a-glucosidase inhibitors (AGI's), such as acarbose, miglitol, and voglibose are in use since last two decades. Among the six drug classes for the management of diabetes mellitus (DM), α-glucosidase inhibitors are one of them. These inhibitors are quite target specific as they act in the intestine locally, in contrast to other oral anti-hyperglycemic drugs, which in addition, alter certain biochemical processes in the human body [5]. Therefore, discovery and development of novel α-glucosidase inhibitors are urgently needed.

2.1. Cedrol, cedryl acetate: microbial transformed metabolites

Development of novel α-glucosidase inhibitors requires screening of a large number of compounds. Cedryl acetate (**1**) and cedrol (**2**) are examples of newly identified α-glucosidase inhibitors that exhibit potent inhibitory activity. The most potent compound one was selected for microbial transformation and the transformed products were screened for the same activity. We successfully identified several α-glucosidase inhibitors that are more potent than acarbose [6]. However, this was the first report describing the α-glucosidase inhibitory activity of cedrol (**2**), cedryl acetate (**1**), [7] and some of the transformed products of cedryl acetate including 10β-hydroxycedryl acetate (**3**), 2α, 10β-dihydroxycedryl acetate (**4**), 2α-hydroxy-10-oxocedryl

http://dx.doi.org/10.5772/intechopen.76891

acetate (**5**), 3α,10β-dihydroxycedryl acetate (**6**), 3α,10α-dihydroxycedryl acetate (**7**), 10β,14α–dihydroxy cedryl acetate (**8**), 3β,10β-cedr-8(15)-ene-3,10-diol (**9**), and 3α, 8β, 10β -dihydroxycedrol (**10**) as mentioned in **Figure 1**. Compounds one, two, and four showed α-glucosidase inhibitory activity whereby one was more potent than the standard inhibitor, acarbose, against yeast α-glucosidase.

The structures have been also optimized computationally at Hartree-Fock (HF) level of theory using valence triple-zeta plus diffuse and polarization functions (6–311++G*) basis sets for H, C, N, and O atoms to get insight into the 3D structure of these metabolites. GAMESS package [8] has been used for all quantum chemical calculations. Molecular docking studies have been also performed to delineate the ligand-protein interactions at molecular level using autodock vina programs [9]. Avogadro [10], Gabedit [11], VMD [12], and Chimera [13] have been used for the structure building, analysis, and visualization for our calculations.

2.2. α-Glucosidase inhibitory activity

Compounds one, two, four, and six were tested for inhibition of the α-glucosidase enzyme. For the first time, the cedrol (**2**) and cedryl acetate (**1**) demonstrated α-glucosidase inhibitory with the latter being more potent than the former. This is possibly due to the presence of an Ac group at C (8). Overall compounds one, two, and four showed more than or comparable activity to the standard inhibitors (**Table 1**). Apparently, the polar OH group lowers the inhibitory activity toward the enzyme, as observed in compounds four and six (inactive) in comparison to one.

2.3. Geometry optimization

The biological activity of ligands is a function of their 3D structures. Thus, it is crucial to have an accurate description of the ligand in 3D space. Hartree-Fock (HF) approach have been used

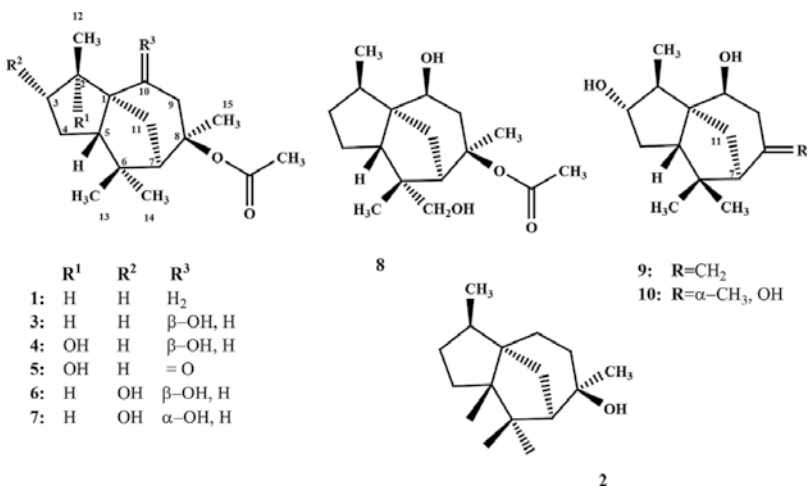

Figure 1. Structure of cedryl acetate and its microbial derivatives.

Compound	IC50* (in mM ± S.E.M)	Binding energy in kcal/mol (Yeast a-glucosidase)	Binding energy in kcal/mol (Human maltase glucoamylase)		Binding energy in kcal/mol (Human pancreatic amylase; 1 U33.pdb)
			C-terminal domain (3TOP.pdb)	N-terminal domain (3L4T.pdb)	
1	94 ± 15	−8.4	−6.9	−6.5	−7.9
2	130 ± 15	−7.4	−6.6	−6.2	−7.9
4	690 ± 16	−7.9	−6.3	−7.1	−7.6
6	Inactive	−8.2	−6.4	−6.5	−7.6
Acarbose	780 ± 20	—	—	—	—
Deoxynojirimycin	425.6 ± 8.14	—	—	—	—

Table 1. α-Glucosidase inhibitory activity of compounds **1**, **2**, **4** and **6** with their predicted binding energies in the active sites of yeast and mammalian α-glucosidases.

to obtain the structural details of all metabolites that were probed through the geometry optimization in the gaseous-phase with valence triple-zeta plus diffuse and polarization functions (6–311++G*) basis sets. We found in all the compounds studied, the distance of the bond between C and OH is 1.421 Å. The optimized geometry of these compounds also, showed a short length of carbonyl groups (C=O and COC=OCH3) distance of 1.208 Å. However, the bond order was slightly higher by a value of 0.11 in the case of C=O as expected. The carbon–oxygen bond in C-OCOCH$_3$ was slightly larger as compared to that in CO-COCH3 (1.402 and 1.338 Å, respectively) due to a lower bond order by a value of 0.233. The presence of acetate group (-O-CO-CH3) in the molecule was lowered the dipole moment of the molecule as could be seen in **Table 2**. These compounds with a low dipole moment seem to be most active. However, due to limited experimental inhibitory assay data, it was difficult to make a generalize conclusion.

Compound	Dipole (Debye)
1	2.03
2	3.03
3	2.87
4	3.87
5	5.07
6	3.90
7	4.09
8	3.93
9	2.65
10	6.01

Table 2. Dipole moment of metabolites calculated at HF/6–311++G* level of theory and basis sets.

2.4. Molecular docking studies

The most ideal is to obtain the orientation of ligand in 3D space into the protein binding site for determination of ligand activity. The ligand-protein binding mode and interaction are a very crucial to understand the catalytic activity. This modeled protein has been used as our target protein. In Addition, to elucidate their binding activity with mammalian α-glucosidase, we performed molecular docking studies of the human intestinal and pancreatic maltase glucoamylase with the active compounds. We found no significant difference in the binding affinity of active ligands with yeast α-glucosidase and the human pancreatic maltase glucoamylase. However, some differences in the binding energy were observed when ligands bind with the human intestinal maltase (**Table 1**). The structural changes in the binding sites of these proteins are

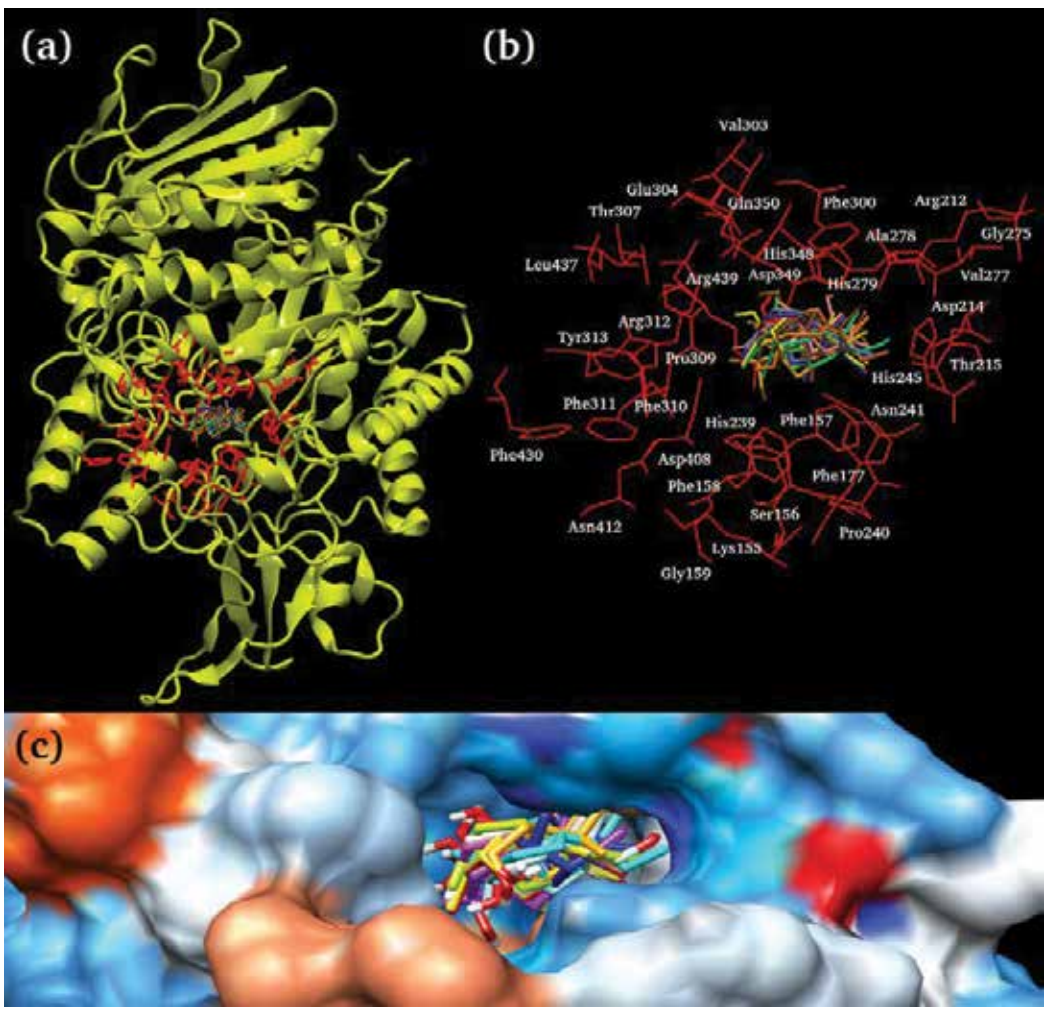

Figure 2. (a) Homology model of the yeast α-glucosidase (yellow color) showing the ligand cluster (variable color; licorice) into the binding site. The red color indicates the amino acid residues (labeled in white) surrounding the binding site (b). The lower picture (c) displays the binding site cavity with the ligand cluster.

postulated to be the cause of this less affinity of ligands toward intestinal maltase as compared to the yeast α-glucosidase. **Figure 2a** shows the homology model of the yeast α-glucosidase with the ligand cluster into the binding site. **Figure 2b** displays the close view of the binding site with the best predicted orientation of ligands **1–15,** obtained from the molecular docking studies, almost overlapping with each other to form a cluster. The amino acid residues forming the binding site cavity have been labeled in white. The cavity can be clearly visualized when the protein is shown with the surface model as depicted in **Figure 2c**.

Figure 3 displays the interactions of individual metabolites one, two, four, and six with the yeast α-glucosidase protein. Polar amino acid residues, that is, Asp349 and Arg439 have strong H-bonding with the acetate group of the ligand. Cedryl acetate (**1**) exhibits the strongest binding affinity with the protein as inferred by its lowest binding energy (−8.4 kcal/mol), the values are given in **Table 1**. Compound one had the lowest *IC50* of 94 ± 15 μM, which makes it

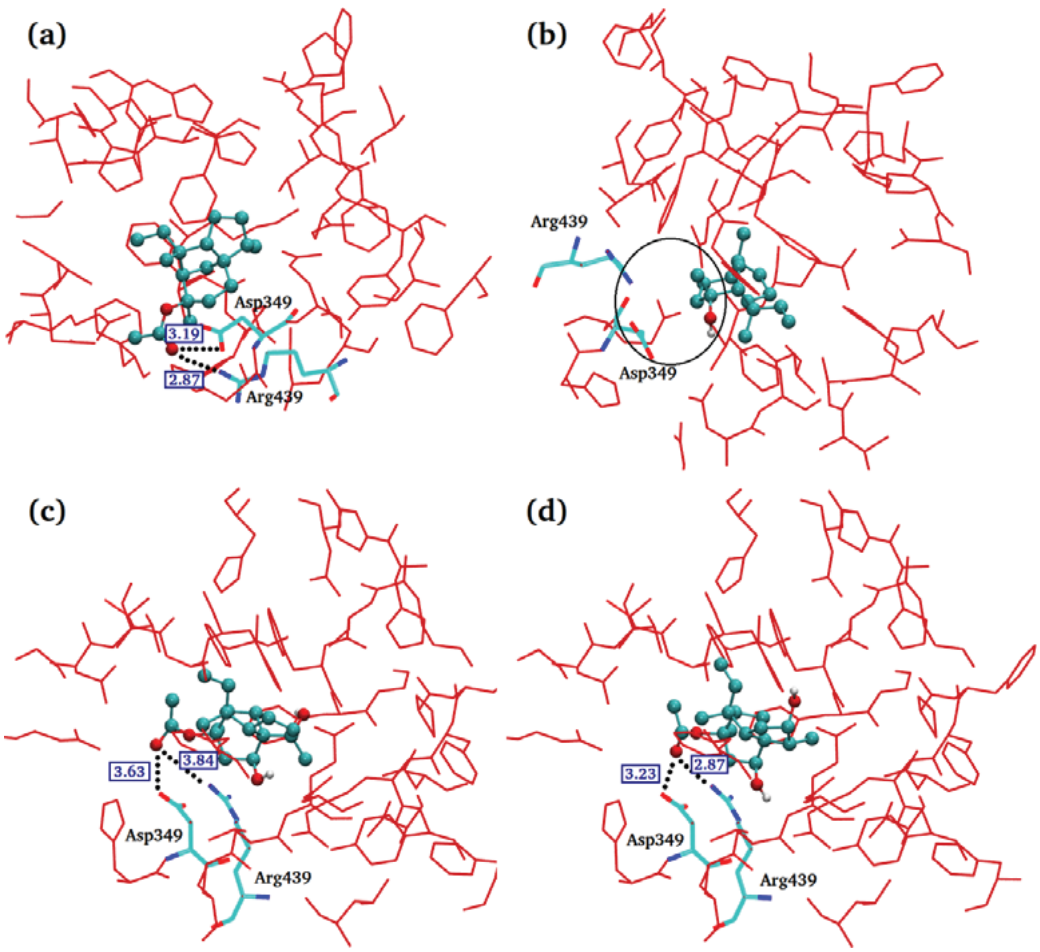

Figure 3. Ligand-protein interaction studies of compounds (a) 1, (b) 2, (c) 4, and (d) 6. The hydrogen bonds are shown as black dotted lines. The H-bond distances in Å are given in boxes. The amino acid residues in the binding pockets are indicated as red.

http://dx.doi.org/10.5772/intechopen.76891

in agreement with the enzymatic assay. The metabolite **2**, showed no interaction with the residues. The acetate group of metabolite two has been hydrolyzed to form hydroxyl group that may play a partial role in its low activity (**Figure 3b**) as compared to the compound one. Metabolites four and six are acetylated and they do form H-bonds with Asp349 and Arg439, thereby showing a good ligand-protein binding energy, however, their activity is dramatically lowered or diminished as compared to compound one. This attenuate activity of metabolites four and six may be associated with their high-polarity arising from the introduction of two hydroxyl groups into the rings, partially due to the fact that the neighboring residues around -OH are slightly hydrophobic in nature.

3. Molecular docking studies of novel quinoline derivatives as potent β-glucuronidase inhibitors

Glucuronidase has been used in numerous biotechnology and research applications. Glucuronidase as a gene has been studied as a positive selection marker for transformed plants, bacteria, and fungi carrying glucuronidase gene [14, 15]. It is also widely has been used for the structural investigations of proteoglycans and for research purposes in many diagnostic research laboratories [16].

3.1. Novel quinoline derivatives as potent β-glucuronidase inhibitors

Quinoline is an aromatic compound having an aza-heterocyclic ring. It possesses a weak tertiary base that can undergo both nucleophilic and electrophilic substitution reactions. The quinoline moiety is present in several pharmacologically active compounds as it does not harm humans, when it is orally absorbed or inhaled.

Various classes of compounds that showed considerable potential as β-glucuronidase inhibitors involved benzothiazole, bisindolylmethanes, bisindolylmethane-hydrazone, benzimidazole, unsymmetrical heterocyclic thioureas, 2,5-disubtituted-1,3,4-oxadiazoles with benzimidazole backbone, and benzohydrazone–oxadiazole [17]. In continuation of this work our study identified novel series of potent β-glucuronidase inhibitors of quinoline for further investigation [18].

3.2. β-Glucorinadase inhibitory activity

Thirty analogs of quinoline were synthesized, which have varied degree of β-glucorinadase inhibition ranging in between 2.11 ± 0.05 and 80.10 ± 1.80 μM, when compared with the standard inhibitor D-saccharic acid 1,4 lactone having IC_{50} value 48.4 ± 1.25 μM. Out of these thirty analogs, twenty four analogs 1–30 showed outstanding β-glucorinadase inhibitory potential with IC_{50} values (**Table 3**) analogs 17, 20, 21, and 27–29 showed good β-glucorinadase inhibitory potential. The structure–activity relationship studies suggested that the β-glucuronidase inhibitory activities of this class of compounds are mainly dependent upon the substitutions on the phenyl ring.

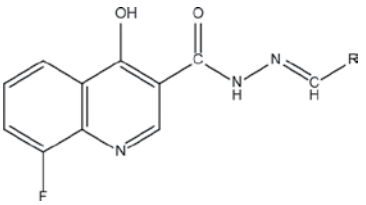

Quinoline hydrazones (1-30)

No	R	$IC_{50} \pm SEM^a$ [μM]	No	R	$IC_{50} \pm SEM^a$ [μM]
1	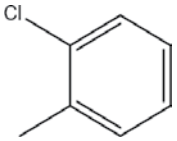	18.40 ± 0.45	16	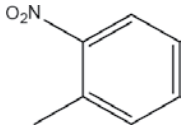	16.60 ± 0.55
2	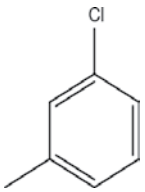	42.25 ± 0.80	17	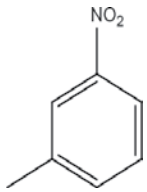	78.90 ± 1.50
3	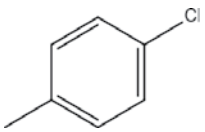	24.20 ± 0.40	18	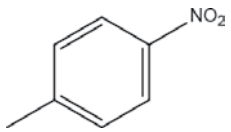	44.10 ± 0.70
4	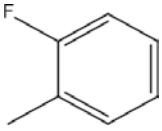	9.20 ± 0.30	19	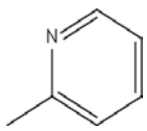	19.40 ± 0.90
5	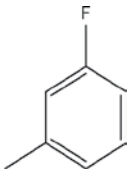	37.01 ± 0.70	20	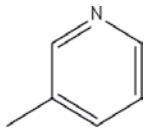	68.38 ± 1.25
6	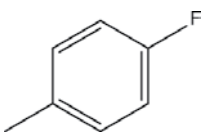	26.30 ± 0.50	21	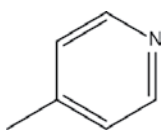	49.38 ± 0.90
7	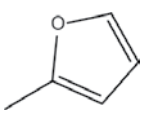	38.50 ± 0.80	22	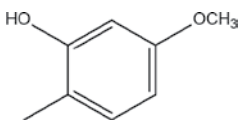	9.60 ± 0.20
8	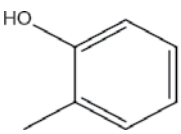	6.70 ± 0.25	23	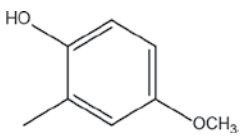	8.30 ± 0.20

9	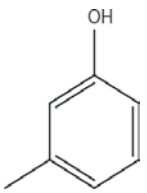	18.10 ± 0.40	24	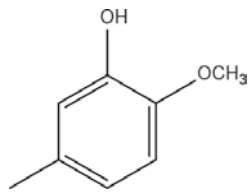	18.00 ± 0.30
10	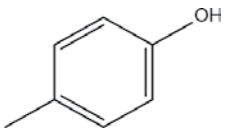	9.60 ± 0.20	25	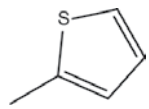	22.30 ± 0.45
11	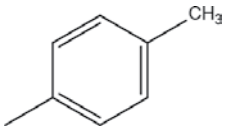	46.14 ± 0.95	26	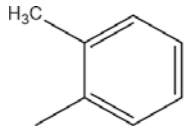	38.50 ± 0.80
12	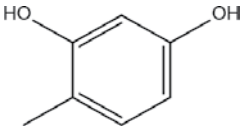	3.10 ± 0.10	27	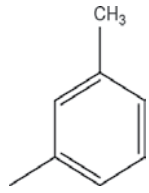	51.00 ± 1.25
13	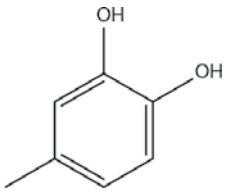	2.11 ± 0.05	28	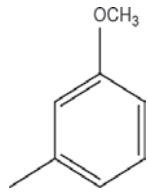	80.10 ± 1.80
14	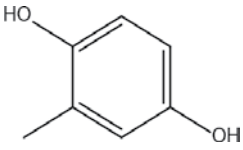	5.01 ± 0.20	29	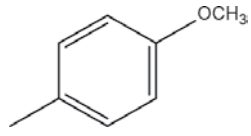	69.40 ± 1.30
15	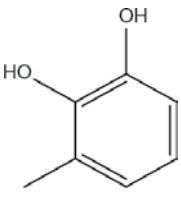	2.60 ± 0.05	30	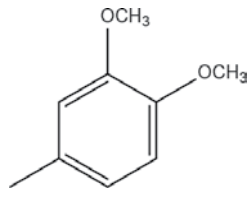	46.10 ± 0.85
	D-Saccharic acid 1,4-lactone	48.4 ± 1.25			

[a] IC50 values are expressed as mean ± standard error of mean.

Table 3. Different quinoline derivatives and their β-glucuronidase activity.

The most potent inhibition was noted in analog 13 that have hydroxy groups at 3, 4-positions on the phenyl part. Making comparison of analog 13 having IC_{50} value 2.11 ± 0.05 μM with other dihydroxy analogs such as 12, 14, and 15 having IC_{50} values 3.10 ± 0.10, 5.01 ± 0.20, and

2.60 ± 0.05 μM, respectively, analog 13 was found to be superior than other. In analog 13 the two hydroxy groups are present at *meta-para* position while in analog 12 the two hydroxy groups are present at *ortho-para* positions, in analog 14 the two hydroxy groups are present at *ortho-meta* positions, and in analog 15 the two hydroxy groups are present at *ortho-meta* positions. The little bit difference in the activity of these analogs may be due to the difference in position of the substituents on the phenyl part.

Similarly, effect of substituent position was also observed in other analogs such as 4, 5, and 6 having fluoro group. If we compare analog four, a *ortho* analog, having IC_{50} value 9.20 ± 0.30 μM with analog five, a *meta* analog, and six, a *para* analog having IC_{50} values 37.01 ± 0.70 and 26.30 ± 0.50 μM, respectively. In analog four the fluoro group is present at *ortho* position while in analog five the floro group is present at *meta* position and in analog six the floro group is present at *para* position. These three analogs demonstrated minute differences in their activity possibly due to the difference in the position of the substituents of the phenyl section. This was also observed in monohydroxy analogs. From these findings, we concluded that the factors that influence the inhibitory potentials of these analogs include the nature, position, and the number of substituents.

3.3. Docking studies

Molecular docking is a useful tool to obtain data on binding mode and to validate experimental results of active derivatives within the active site of β-D-glucuronidase. By using X-ray crystal structure of the human β-glucuronidase enzyme at 2.6 Å resolution (PDB ID: 1BHG) [19], it can be used to identify predict the binding modes involved in the inhibition activity.

Utilizing docking approach, we identified the stable binding mode of six most active compounds (8, 12–15, and 23) that was further used in characterizing their inhibitory activity. Compounds with the most stable binding conformation suggest to strongly alignment to the core of β-glucuronidase. In **Figure 4** shows that the quinolone moiety of these active compounds are oriented toward the active pocket and share some common interaction with catalytically important amino acids such as Glu450, Glu541, and Tyr504.

We predict that the hydrogen bonding interaction between the hydroxyl at C-4 of quinoline moiety and Glu451 plays a vital role. According to the docking result compound **13** (**Figure 5**),

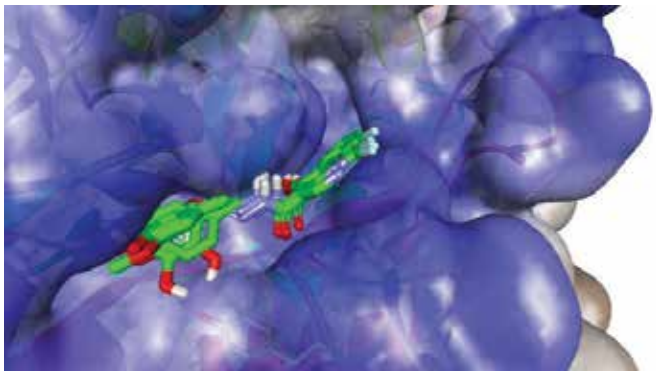

Figure 4. Active compounds aligned well into the binding cavity of β-glucuronidase enzyme.

http://dx.doi.org/10.5772/intechopen.76891

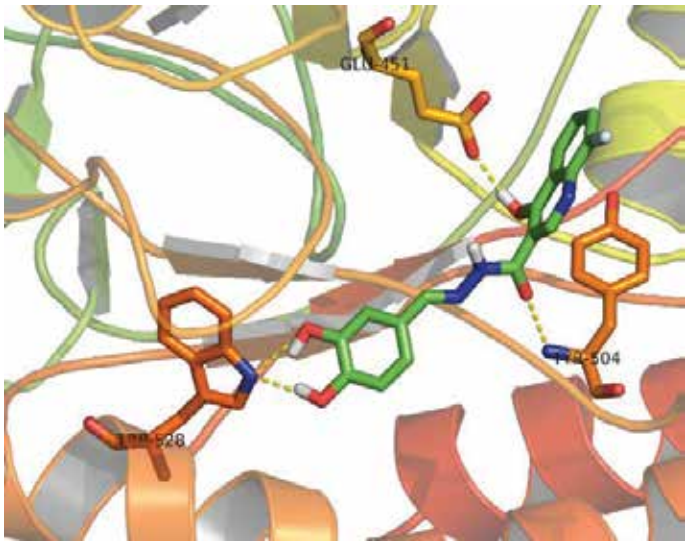

Figure 5. Best binding position of compound **13** in active pocket of β-glucuronidase enzyme.

was found to be to most active compound in this series, because of the hydroxyl (OH) at C-4 involved in hydrogen bonding with Oε2 of Glu451 side chain (1.99 Å). The complex is stabilized by π-donor hydrogen bond formation between the benzene ring on quinoline moiety and with hydroxyl (OH) of Tyr508 (3.73 Å). Two interactions were detected in hydrazone linkage between carboxamide and the surrounding residues. The hydrazone carbonyl (C=O) oxygen linked by a hydrogen bonding with the nitrogen on the backbone of Tyr504 (2.77 Å), another hydrogen bond forms between the NH group and the oxygen on side chain of Asn484 with a bond length of 3.10 Å. The two hydroxyls on the benzylidene moiety at *meta* positions also, involved in hydrogen bonds with indole nitrogen at Trp528 backbone having a distance of 2.11 and 1.99 Å, respectively.

Compound 15 showed that hydroxyl (OH) at C-4 of quinoline moiety for compound formed hydrogen bonding with Oε2 of Glu451 side chain at a longer distance (2.24 Å) as compared to previous compound (**Figure 6**). In this compound the quinoline benzene rings on forms a π-donor hydrogen bond with hydroxyl (OH) of Tyr508 at (3.96 Å). It was also observed that hydrazone linkage was oxygen of carbonyl (C=O) interacts with side chain of Tyr504 through a hydrogen bond at a distance of 2.80 Å. Both form hydrogen bonds were formed between hydroxyls at *ortho* and *meta* position on the benzylidene moiety and nitrogen of indole backbone of Tyr508 at a distance of 2.19 and 1.99 Å, respectively. Compound 15 was found to be a second most active inhibitor.

In third most active compound 12 (**Figure 7**), it was observed that hydroxyl (OH) at Carbon no 4 exhibited hydrogen bonding with Oε2 of Glu451 side chain with a distance of 2.11 Å. On the other hand we noted that a more stable π-donor hydrogen bond with hydroxyl (OH) of Tyr508 at (3.77 Å) and benzene ring on quinoline moiety when compared with derivative 14. Docking studies also showed the hydrazone linkage interaction of oxygen of carbonyl (C=O) with side chain of Tyr504 through a hydrogen bond with length of 2.99 Å. There is also a hydrogen

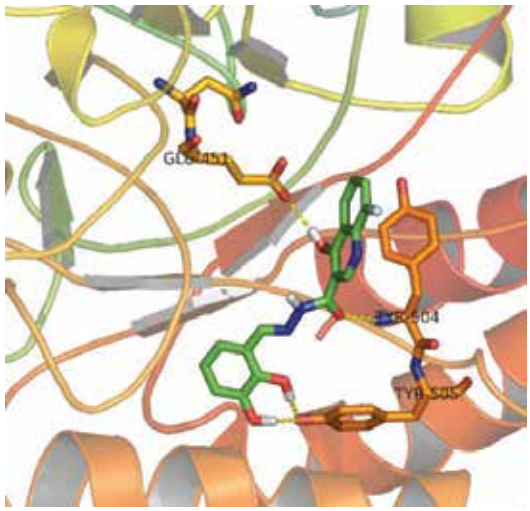

Figure 6. Binding positions of compound 15 in an active pocket of the β-glucuronidase enzyme.

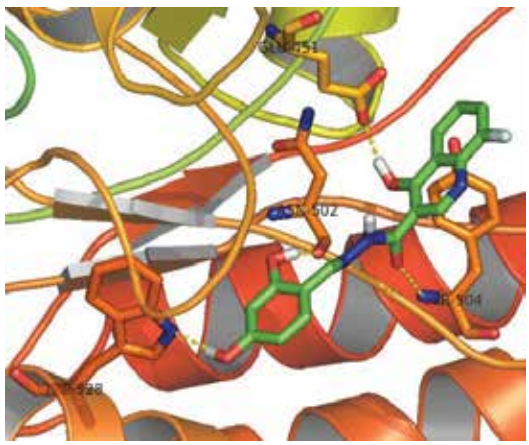

Figure 7. Binding position of compound 12 in an active pocket of the β-glucuronidase enzyme.

bonding of hydroxyl at *ortho* position on the benzylidene with the oxygen of Asn502 (1.87 Å), while the other another hydrogen bonding of hydroxyl at *para* position on the benzylidene with the nitrogen of indole backbone of Trp528 (1.89 Å).

4. Morpholine hydrazone scaffold: synthesis, anticancer activity, and docking studies

Cancer is a broad term to describe a disease that characterized by the uncontrolled proliferation of cells resulting from the disruption or dysfunction of regulatory signaling pathways that

are normally under tight control [20, 21]. In modern life, cancer is one of the big health killers. According to the American Association for cancer research (AACR) cancer progress report 2013, it expected that 580,350 Americans would die from the various type of cancer in the same year. Luckily, ultimate evolution has made against cancer. Approximately, from 1990 to 2012 almost 1,024,400 lives saved [22].

Currently chemotherapy is an ultimate clinic treatment to repel cancer [23]. Cisplatin drug has been commonly used in cancer treatment for decades [24, 25]. Though, its clinical value tends to be inadequate by the abrupt increase of drug resistance or new side effects [26]. Consequently, the exploration of unusual chemotherapeutic agents has sparked the great attention of scientists from varied disciplines.

The morpholine scaffold has been found to be an outstanding pharmacophore in medicinal chemistry and a number of molecules having morpholine skeleton are the clinically approved drugs [27]. *N*-substituted morpholines are used in the treatment of inflammatory diseases, such as migraine and asthma [28]. Morpholines derivatives have reported to possess activity such as platelet aggregation inhibitors, anti-eme-tics, and bronchodilators [29]. Morpholine analogs establish a new antifungal chemical entity not allied with other presently available medications with anti-fungal potential. The benefit in synthesizing morpholine analogs resides in the fact that these molecules offer chlorohydrates that are water soluble for pharmacological assays [30, 31].

Recently, we have reported synthesis, characterization, anti-cancer activity, and molecular docking studies of morpholine derivatives [32]. A small series of morpholine hydrazones synthesized by treating 5-morpholinothiophene-2-carbaldehyde with different aryl hydrazides to form morpholine hydrazones scaffold (**1–17**) (**Table 4**). The *in vitro* anti-cancer potential of all these compounds were checked against human cancer cell lines such as HepG2 (Human hepatocellular liver carcinoma) and MCF-7 (Human breast adenocarcinoma). Analogs **13** had similar substantial cytotoxic effects toward HepG2 with IC_{50} value 6.31 ± 1.03 μmol/L when compared with the standard doxorubicin (IC_{50} value 6.00 ± 0.80 μmol/L); while compounds five, eight, and nine showed potent cytotoxicity against MCF-7 with IC_{50} value 7.08 ± 0.42, 1.26 ± 0.34, and 11.22 ± 0.22 μmol/L, respectively, when compared with the standard Tamoxifen (IC_{50} = 11.00 ± 0.40 μmol/L). Molecular docking studies also performed to understand the binding interaction.

4.1. In vitro anti-cancer activity

All synthesized analogs (**1–17**) were screened against two human cancer cell lines, human breast carcinoma (MCF-7) and human liver carcinoma (HepG2). The potentials of these analogs calculated in IC_{50} value shown in **Table 5**. Among the series 10 compounds showed potential against HepG2 and six compounds showed potential against MCF-7.

Among them compound eight was found to be the excellent inhibitor against MCF-7 with IC_{50} value 1.26 ± 0.34 μmol/L, which is more potent than the standard inhibitor Tamoxifen (IC_{50} = 11.00 ± 0.40 μmol/L). Secondly, the compound five was found to be more potent with IC_{50} value 7.08 ± 0.42 μmol/L almost two fold better than the standard. The analogs such as

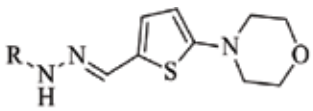

S.NO.	R	S.NO.	R
1	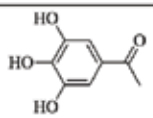	10	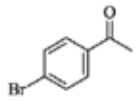
2	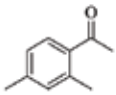	11	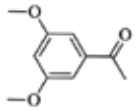
3	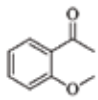	12	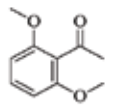
4	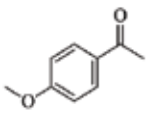	13	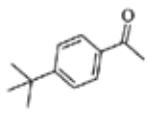
5	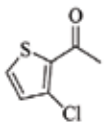	14	
6	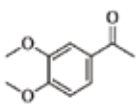	15	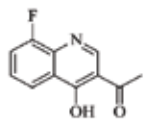
7	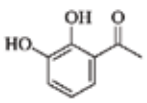	16	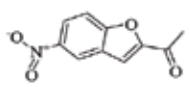
8	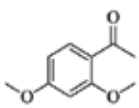	17	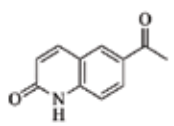
9	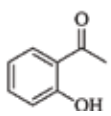		

Table 4. Various analogs of morpholine.

S. No.	HepG2	MCF-7	S. No.	HepG2	MCF-7
2	—	30.0 ± 1.00	9	40.0 ± 0.93	11.22 ± 0.22
4	7.94 ± 7.94	—	11	19.95 ± 1.31	41.67 ± 1.62
5	19.95 ± 0.63	7.08 ± 0.42	12	31.0 ± 2.26	—
6	12.59 ± 1.22	—	13	6.31 ± 1.03	—
7	20.0 ± 0.32	14.13 ± 1.42	14	56.23 ± 0.56	—
8	—	1.26 ± 0.34	15	15.85 ± 0.82	—
Doxorubicin	6.00 ± 0.80	—			
Tamoxifen	—	11.00 ± 0.40			
Cisplatin	12.00 ± 0.33	15.00 ± 0.80			

Table 5. Anti-cancer activity data (IC_{50} values in μmol/L) of morpholine derivatives (1–17).

two, seven, nine, and 11 also showed potent inhibition for this cell line, while remaining analogs found to be completely in active.

Compound 13 showed potent inhibition against HepG2 with IC_{50} value 6.31 ± 1.03 μmol/L when compared with the standard Doxorubicin (IC_{50} value 6.00 ± 0.80 μmol/L). Compound four and six were found second and third most active analogs among the series with IC_{50} value 7.94 ± 7.94 and 12.59 ± 1.22 μM, respectively. Other analogs such as five, seven, nine, 11, 12, 14, and 15 also showed good to moderate potential.

Molecular docking studies were performed to investigate the binding mode of the active compounds.

4.1.1. Molecular docking analysis of morpholinothiophene hydrazone compounds

The molecular docking procedure was widely used to predict the binding interaction of the compound in the binding pocket of the enzyme. The 3D crystal structure of the topoisomerase II enzyme (PDB id: 4FM9) was retrieved from the protein data bank. All the ions and water molecules removed and the hydrogen atoms added to the enzyme by the 3D protonation using the Molecular Operating Environment (MOE) software. The target enzymes were then energy minimized by the default parameters of the MOE for the stability and further assessment of the enzyme. The structures of the analogs of the morpholinothiophene hydrazone compounds built in MOE and energy minimized using the MMFF94x force field and gradient 0.05. The active site pocket of the enzyme found out by the site-finder implemented in the MOE software. The synthesized compounds docked into the active site of the target enzyme in MOE by the default parameters, that is, placement: Triangle matcher, Rescoring, and London dG. For each ligand, 10 conformations generated. The top-ranked conformation of each compound used for further analysis.

Molecular docking studies predicted the proper orientation of the compound five inside the binding pocket of topoisomerase II enzyme. From the docking conformation of this active compound, we have observed a docking score of **(−11.4975),** which correlates well to the biological activities (IC_{50} = 19.95 ± 0.63 μmol/L in HepG2 and **7.08** ± **0.42** μmol/L in MCF-7

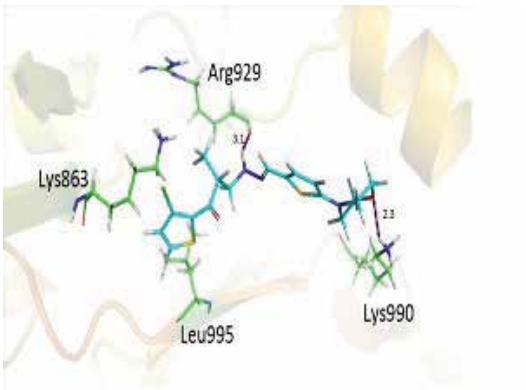

Figure 8. Docking conformations of compound five in the active site of topoisomerase II enzyme.

cell lines). The compound was observed making two interactions with active residues of the active site pocket of the enzyme. The oxygen atom of the morpholine moiety of the compound formed side chain acceptor interaction with the Lys 990 residue of the binding pocket. Arg 929 was observed making the hydrogen bond with the –NH group of the hydrazine moiety of the ligand as shown in the **Figure 8**. The electro-negative nature of Cl, O, and S of the substituent moiety may increase the polarizability of the ligand by electrons withdrawing inductive effect resulting in the enhanced potency and interactions.

5. Conclusion

The molecular docking is now fully recognized and integrated in the research process. In the past the emergence of this new discipline had occasionally encountered some opposition here and there. At presents, the science is mature and there are a growing number of success stories that continuously expand the armory of drug research. Several considerations that can greatly improve the success and enrichment of true bioactive hit compounds are commonly overlooked at the initial stages of a molecular docking study. In this chapter, we tried to cover several of these considerations, including few examples, of molecular docking studies of natural and synthetic analogs of potent α-glucosidase inhibitors, β-glucuronidase inhibitors, and cytotoxicity from our own findings. These molecular studies were performed for different classes of bioactive compounds in order to understand the binding interaction of the active compounds. It was concluded that the nature, position as well as the number of substituents affects the inhibitory potential of these analogs.

Acknowledgements

Sadia Sultan would like to acknowledge Universiti Teknologi MARA for the financial support under the reference number UiTM 600-IRMI/FRGS 5/3 (0119/2016), Ministry of Higher Education

Malaysia. One of our author Gurmeet Kaur Surindar Singh would also like to acknowledge Universiti Teknologi MARA for the financial support under the reference number UiTM 600-IRMI/FRGS 5/3 (28/2015), Ministry of Higher Education Malaysia. We also would like to highlight and acknowledge our previous published research under reference 7, 18, and 32.

Author details

Sadia Sultan[1,2,3]*, Gurmeet Kaur Surindar Singh[1,3], Kamran Ashraf[1] and Muhammad Ashraf[4]

*Address all correspondence to: sadiasultan301@yahoo.com; drsadia@puncakalam.uitm.edu.my

1 Faculty of Pharmacy, Universiti Teknologi MARA, Puncak Alam Campus, Bandar Puncak Alam, Selangor Darul Ehsan, Malaysia

2 Atta-ur-Rahman Institute for Natural Products Discovery (AuRIns), Universiti Teknologi MARA, Puncak Alam Campus, Bandar Puncak Alam, Selangor Darul Ehsan, Malaysia

3 Pharmaceutical and Life Sciences Core, Universiti Teknologi MARA, Shah Alam, Shah Alam, Selangor Darul Ehsan, Malaysia

4 Merck Pharmaceutical Private Limited, Karachi, Pakistan

References

[1] Meyer EF, Swanson MS, Williams JA. Pharmacology & Therapeutics. 2000;**85**:113-121

[2] Abraham DJ. Burger's Medicinal Chemistry Drug Discovery. 6th ed. Vol. 12003. pp. 847-900

[3] Pili R, Chang J, Partis RA, Mueller RA, Chrest FJ. A. Passaniti Cancer. Research. 1995;**55**:2920

[4] Zitzmann N, Mehta AS, Carrouée S, et al. Proceedings of the National Academy of Sciences of the United States of America. 1999;**96**:11878

[5] Hitoshi S, Nagao M, Harada T, Nakajima Y, Tanimura-Inagaki K, et al. Journal of Diabetes Investigation. 2014;**23**:206-212

[6] Choudhary MI, Atif M, Shah SAA, Sultan S, Erum S, Khan SN, Atta-ur-Rahman. International Journal of Pharmaceutical Science. 2014;**6**:375-378

[7] Sultan S, Choudhary MI, Nahar Khan S, Fatima U, Ali RA, Atif M, Atta-ur-Rahman, Fatmi MQ. European Journal of Medicinal Chemistry. 2013;**62**:764-770

[8] Trott O, Olson AJ. Journal of Computational Chemistry. 2010;**31**:455-461

[9] Hanwell MD, Curtis DE, Lonie DC, Vandermeersch T, Zurek E, Hutchison GR. Journal of Cheminformatics. 2012;**4**:17

[10] Allouche AR. Journal of Computational Chemistry. 2011;**32**:174-182

[11] Humphrey W, Dalke A, Schulten K. Journal of Molecular Graphics. 1996;**14**:33-38

[12] Pettersen EF, Goddard TD, Huang CC, Couch GS, Greenblatt DM, Meng EC, Ferrin TE. Journal of Computational Chemistry. 2004;**25**:1605-1612

[13] Smith RV, Rosazza J. Journal of Pharmaceutical Sciences. 1975;**64**:1737-1759

[14] Wenzl P, Wong L, Kwang-won K, Jefferson RA. Molecular Biology and Evolution. 2005;**22**: 308-316

[15] Basu C, Kausch AP, Chandlee JM. Biochemical and Biophysical Research Communications. 2004;**320**:7-10

[16] Kuroyama H, Tsutsui N, Hashimoto Y, Tsumuraya Y. Carbohydrate Research. 2001;**333**: 27-39

[17] Khan KM, Rahim F, Halim SA, Taha M, Khan M, Perveen S, Haq Z, Mesaik MA, Choudhary MI. Bioorganic & Medicinal Chemistry. 2011;**19**:4288

[18] Taha M, Sultan S, Nuzar HA, Imran S, Ismail NH, Rahim F, Ullah H. Bioorganic and Medicinal Chemistry. 2016;**4**:3596

[19] Taha M, Ismail NH, Imran S, Ali M, Jamil W, Uddin N, Kashif SM. RSC Advances. 2016;**6**: 3276

[20] Chen WS, Ou WZ, Wang LQ, et al. Dalton Transactions. 2013;**42**:15678-15686

[21] Rahman FU, Ali A, Guo R, et al. Dalton Transactions. 2015;**44**:2166-2175

[22] Sawyers CL, Abate-Shen C, Anderson KC, et al. AACR cancer progress report 2013. Clinical Cancer Research. 2013;**19**:S1-S98

[23] Robert NJ, Diéras V, Glaspy J, et al. Journal of Clinical Oncology. 2011;**29**:1252-1260

[24] Rosenberg B, Van Camp L, Krigas T. Nature. 1965;**205**:698-699

[25] Sak A, Grehl S, Engelhard M, et al. Clinical Cancer Research. 2009;**15**:2927-2934

[26] Galluzzi L, Senovilla L, Vitale I, et al. Oncogene. 2012;**31**:1869-1883

[27] Andrs M, Korabecny J, Jun D, et al. Journal of Medicinal Chemistry. 2015;**58**:41-71

[28] Dugave C, Demange L. Chemical Reviews. 2003;**103**:2475-2532

[29] Arrieta A, Oteagui D, Zubia A, et al. The Journal of Organic Chemistry. 2007;**72**:4313-4322

[30] Polak A. Annals of New York Academy of Sciences. 1988;**554**:221-228

[31] Kerkenaar A. Prous Science Publ., 1987;**1**:523-542. R.G.M.P

[32] Taha M, Shah SAA, Afifi M, Sultan S, Ismail NH. Chinese Chemical Letters. 2017;**28**:607-611

Chapter 3

Molecular Docking for Detoxifying Enzyme Studies

Rafael Trindade Maia and Vinícius Costa Amador

Additional information is available at the end of the chapter

http://dx.doi.org/10.5772/intechopen.73920

Abstract

In this chapter, we pointed some relevant results obtained by protein-ligand docking simulations in the context of insecticide and herbicide resistance performed by glutathione S-transferases (GSTs), a detoxifying superfamily enzyme. We present here some in silico evidences of GST binding against chemical insecticides in the malaria and dengue vectors (*Anopheles gambiae* and *Aedes aegypti* mosquitoes) and against chemical herbicides used on rice (*Oryza sativa*) culture. Our findings suggest that some members from epsilon class (GSTE2, GSTE5) can metabolize some insecticide compounds and that a tau class member (GSTU4) can metabolize some herbicides. The results reinforce the importance of docking studies for enzyme activity comprehension. These information can allow in the future the implementation of new strategies for mosquito control and herbicide management on rice culture through biotechnological improvements designed to specific GST targets. Induced mutations on catalytic binding sites of GSTU4 could improve rice herbicide resistance and minimize produce damage, while rational compounds can be designed to inhibit GSTE members to decline insecticide resistance on mosquito control. In both cases, biotechnological tools could be developed focusing on GSTs that would reduce environmental impact by the use of insecticide and herbicide.

Keywords: GSTs, insecticide resistance, herbicide resistance, AutoDock, detoxifying enzymes, mosquito control, rice culture, bioinformatics

1. Introduction

Mechanisms of resistance to chemical insecticides include the pathways of metabolization of toxic compounds, because of overexpression of detoxification enzymes or structural modifications in these enzymes. Glutathione S-transferases (GSTs) are one of the most important groups of enzymes involved in this type of resistance and comprise enzymes that catalyze reactions that transform various xenobiotic compounds into soluble products [1].

In eukaryotic organisms, these enzymes are classified into cytosolic GSTs, microsomal GSTs (associated with membranes), and mitochondrial GSTs [2, 3]. In insects, only two of these classes were found: cytosolic and microsomal [4]. In the present study, we found no GST of the mitochondrial class in insects to date [5, 6]. Microsomal GSTs catalyze reactions very similar to cytosolic ones, with trimeric structure and being associated with plasma membranes, although they have different structures and origins than cytosolic one [7, 8]. However, cytosolic GSTs have already been identified as important for resistance to chemical insecticides [5, 9, 10], while microsomal GSTs have not yet been related to resistance to insecticides [5].

In insects, cytosolic GSTs are represented, at least, by six classes: delta, epsilon, omega, sigma, theta, and zeta [5, 11, 12]. In the present study, it was found that these genes were found to be similar to those of other species, such as the *A. gambiae* malaria vector and the fruit fly *Drosophila melanogaster* [11]. The delta and epsilon classes are arthropod-specific and represent more than 65% of the total cytosolic GSTs found in these organisms [11]. Most GSTs found in insects and involved in the target (omega, sigma, theta, and zeta) have a much broader distribution between taxonomic groups, from bacteria to vertebrates [13, 14].

Members of delta, sigma, and epsilon classes were initially called class I, II, and III, respectively, and later, with the increase in the number of sequences deposited in databases and classification studies, the nomenclature was adopted based on the Greek alphabet in agreement with the system of nomenclature of GSTs of mammalians [15].

This classification was supported by phylogenetic analyses in both mammalian and insect GSTs [4, 13]. Currently the nomenclature of insect GSTs consists of three parts: the name of the species of which GST belongs, the specific class of GST, and the number that specifies the order in which the routine was discovered. In this way, the name AgGSTD1 is used to designate a GST of *A. gambiae*, member of delta class, being the first protein of this class to be discovered [12].

Cytosolic GSTs are composed of two subunits of approximately 25 kDa each, which may be homodimeric or heterodimeric. Each subunit has a specific glutathione binding site (G-site), near an electrophilic site (H-site). The G-site is located at the N-terminus of the protein and is a highly conserved region in the GSTs. However, the H-site residues that interact with the hydrophobic substrates are found at the C-terminus. The H-site diversity causes the GSTs to present different specificities in relation to the substrates they metabolize [16, 17]. The GST-catalyzed reaction consists of promoting the conjugation of the reduced glutathione tripeptide (GSH) to a specific and generally cytotoxic compound which, upon binding to such electrophilic grouping, will pass from the reduced state to the oxidized state and form a more soluble compound and easier to excrete from the cell. This phase of conjugation represents phase II of the cellular detoxification process, and the GSTs represent the most important enzymes of this phase, although others are involved. The GST enzymes display a big variety of substrate catalytic reactions. As multispecific and promiscuous proteins, the GSTs represent potential targets of inhibitors selection and design. In *Aedes aegypti*, hematin binds to GSTs resulting in activity inhibition [18].

Molecular docking is a computational technique that aims to predict the best orientation between two molecules. Usually, one of the compounds is small compound that is bounded to a macromolecule (protein). This powerful approach is an excellent tool that helps to understand relevant physiological processes in a wide range of organisms and systems, such as

insecticide and herbicide resistance. Molecular docking is based on molecular recognition and often is referred as a "lock-and-key" problem. In general, the best-fit orientation is obtained by shape complementarity and a score function based on binding energy affinity. In protein-ligand simulations, dockings generally are applied in a stochastic search algorithm to achieve the best binding complexes, and the energy can be estimated by molecular mechanic force fields.

2. Molecular docking between mosquitoes' GSTs and chemical insecticides

The atomic coordinates of AgGSTE2 and AgGSTE5 were from their respective PDB files, as well as their ligand, the tripeptide glutathione, or GSH (C10 H17 N3 O6 S). The geometry of the ligand was obtained from the PDB database.

An isoform of AgGSTE2 (AgGSTE2mut) with two mutations, I114T and F120L (isoleucine for threonine at residue 114, phenylalanine for leucine at amino acid 120) was also submitted to the simulations. The three proteins (AgGSTE2, AgGSTE2mut, and GSTE5) were simulated with and without the GSH linker. For the construction of the mutant (AgGSTE2mut), the nonmutant protein geometries (AgGSTE2) were used, and the residues in the PDB file were replaced manually in the two subunits.

The receptors used in the docking analyses were the crystallographic structure of AgGSTE2 and its mutant (AgGSTE2mut) and the structure of the model constructed for AgGSTE5. The ligands used were the insecticides DDT, carbaryl, cypermethrin, and malathion, being all these synthetic and commercially used organic insecticides normally used to control Culicidae vectors (**Table 1**). The atomic coordinates of the compounds were obtained from the ZINC database (http://zinc.docking.org/).

Molecular docking is a computational technique that aims to calculate atomic interactions between a small binding molecule and a macromolecule in search of the lower energy conformation. The AutoDock 4.2.2 program [18] was used to convert the files into PDB format for the form *pdbqt*, which is the file format used by AutoDock. The ligands were marked with *Gasteiger* load parameters and only the nonpolar hydrogens explicitly represented. The *Gasteiger* charge parameters provide charges properties of each atom, by the *SetPartialCharge* method, an algorithm that includes partial charges. In this algorithm, it

Singlet	Name	Access number
DDT	Dichlorodiphenyltrichloroethane	ZINC01530011
Carbaryl	1-Naphthyl methylcarbamate	ZINC00001090
Cypermethrin	Cypermethrin	ZINC71789490
Malathion	Malathion	ZINC1530800

Table 1. Compounds used as ligands for the calculation of docking.

is admitted that all hydrogens are explicitly represented and based on electronegativity equilibration. The *Kollman* set parameters were used to assign the receptor molecules. This force field uses values for each amino acid that was derived from the corresponding electrostatic potential. The simulations were performed with the Lamarckian genetic algorithm (LGA). The box was set in the 126×126×126 dimensions centered on the ligand and the active site, and the LGA was subjected to calculations of 10,000 replicates with populations of 150 individuals to a maximum of 27,000 generations and crossover mutation rates of 0.02 and 0.08, respectively.

The binding energies between the three proteins and the five different compounds studied were calculated and are available in **Table 2**. The lower energy conformations of each complex were visually analyzed (VMD, visual molecule dynamics) and was listed all residues in radius of 4.0 Å of the ligand (**Figures 1–4**).

The lowest energy was observed in the AgGSTE2muT-DDT complex, indicating a greater affinity between this enzyme and this insecticide. The observed distance between DDT and GSH (<4 Å) and position shows that this conformer is a potential candidate to metabolize DDT. The binding energy of this complex was the smallest among all comparisons. In the docking with the DDT, we observed a few higher energies for AgGSTE2 and AgGSTE5 when compared with the AgGSTE2mut values, but the values in both were negative. The distances between DDT and GSH in these conformers shows a value which allows for interactions, with AgGSTE5 being the shortest distance (2.91 Å) observed in complexes simulated with DDT. In all three enzymes, an approximation was observed between the trichloromethyl group of DDT and GSH, evidencing the ability of these enzymes to bind to this insecticide.

For carbaryl, the enzyme with the lowest binding energy was AgGSTE5, followed by AgGSTE2mut and AgGSTE2. However, it was the AgGSTE2mut that showed the conformation with the smallest distance between the ligands. The proximity of carbaryl to glutathione suggests that the three systems can form GSH conjugated with this insecticide.

In simulated complexes with cypermethrin that were observed, the lowest energy values were used, except for the AgGSTE2mut whose lowest energy score was for the DDT simulation. In the conformations of AgGSTE2 and AgGSTE2mut, the binding distances between cypermethrin and GSH were 3.39 and 2.74 Å, respectively, showing a potential of these enzymes to metabolize cypermethrin. In AgGSTE5, the distance between the ligands was 4.81 Å, indicating that although the enzyme has insecticide-binding affinity, the likelihood of the glutathione conjugation reaction is low.

Malathion, despite having demonstrated negative values when complexed with enzymes, was the compound that showed the highest energy values for all three systems. In addition, no

	DDT	Carbaryl	Cypermethrin	Malathion
AgGSTE2	−5.13	−5.85	−8.37	−3.37
AgGSTE2mut	−9.16	−6.09	−8.81	−3.67
AgGSTE5	−7.68	−6.42	−8.64	−3.24

Table 2. Binding energies (kcal/mol) for the best conformations of each complex.

http://dx.doi.org/10.5772/intechopen.73920

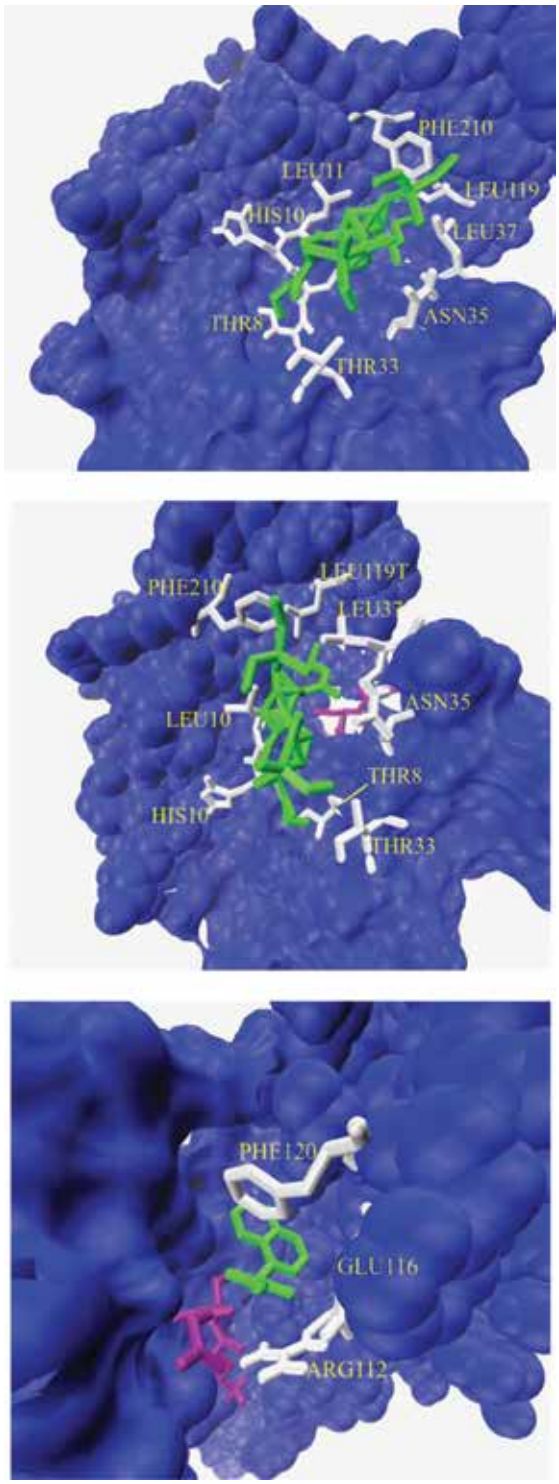

Figure 1. Representation of the best conformation of the AgGSTE2-carbaryl (top), AgGSTE2mut-carbaril (middle), and AgGSTe5-carbaryl (bottom) complexes. Residues are represented in rods and spheres. The GSH is represented in sticks (purple). In green the carbaryl.

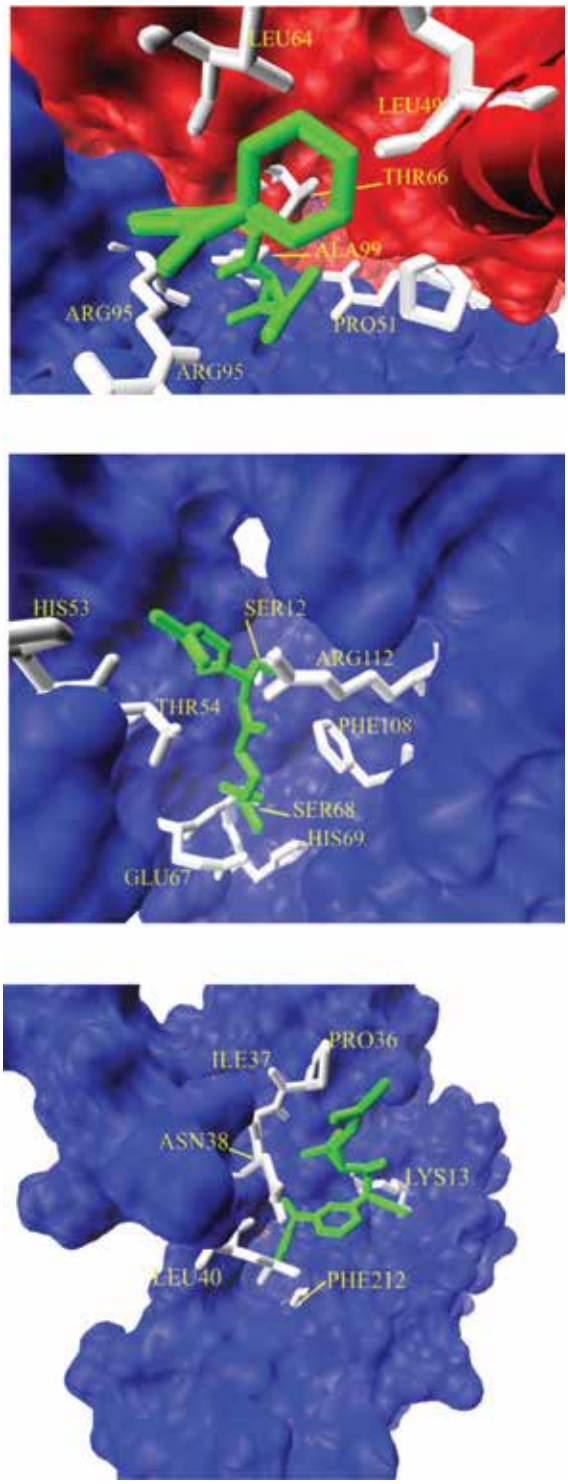

Figure 2. Representation of the best conformation of the AgGSTE2-cypermethrin (top), AgGSTE2mut-cypermethrin (middle), and AgGSTe5-cypermethrin (bottom) complexes. Residues are represented in rods and spheres. The GSH is represented in sticks. In green the cypermethrin.

http://dx.doi.org/10.5772/intechopen.73920

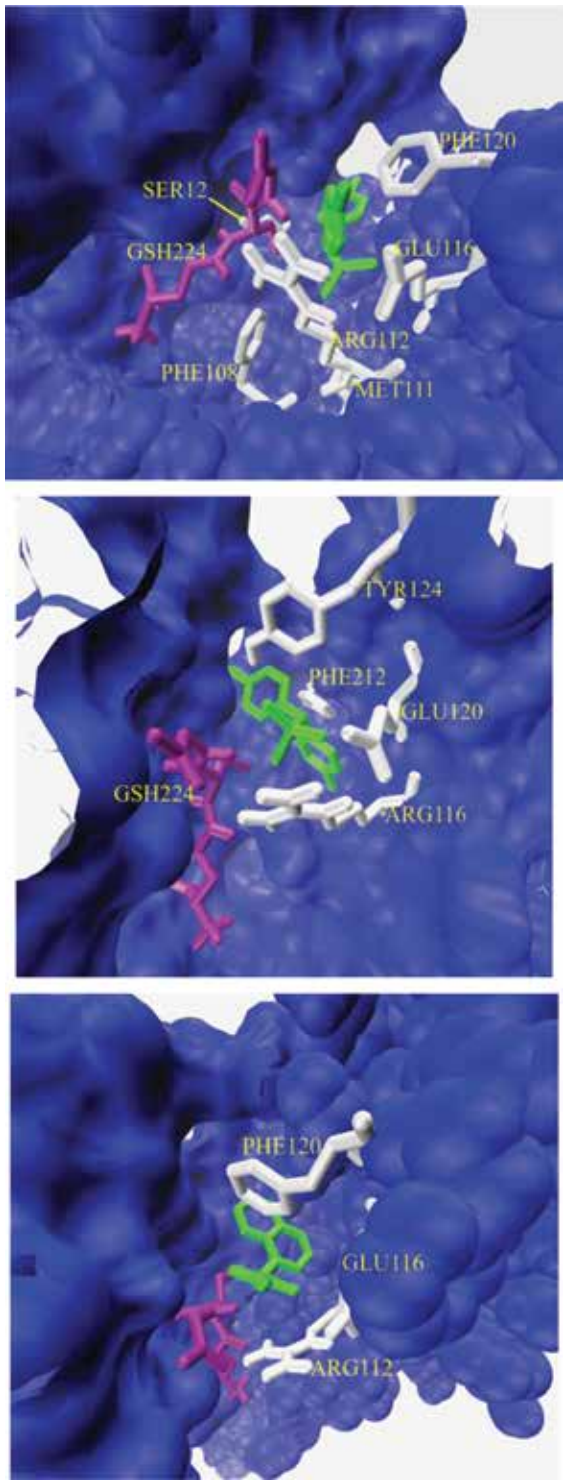

Figure 3. Representation of the best conformation of the AgGSTE2-DDT (top), AgGSTE2mut-DDT (middle), and AgGSTe5-DDT (bottom) complexes. Residues are represented in rods and spheres. The GSH is represented in sticks. In green the cypermethrin.

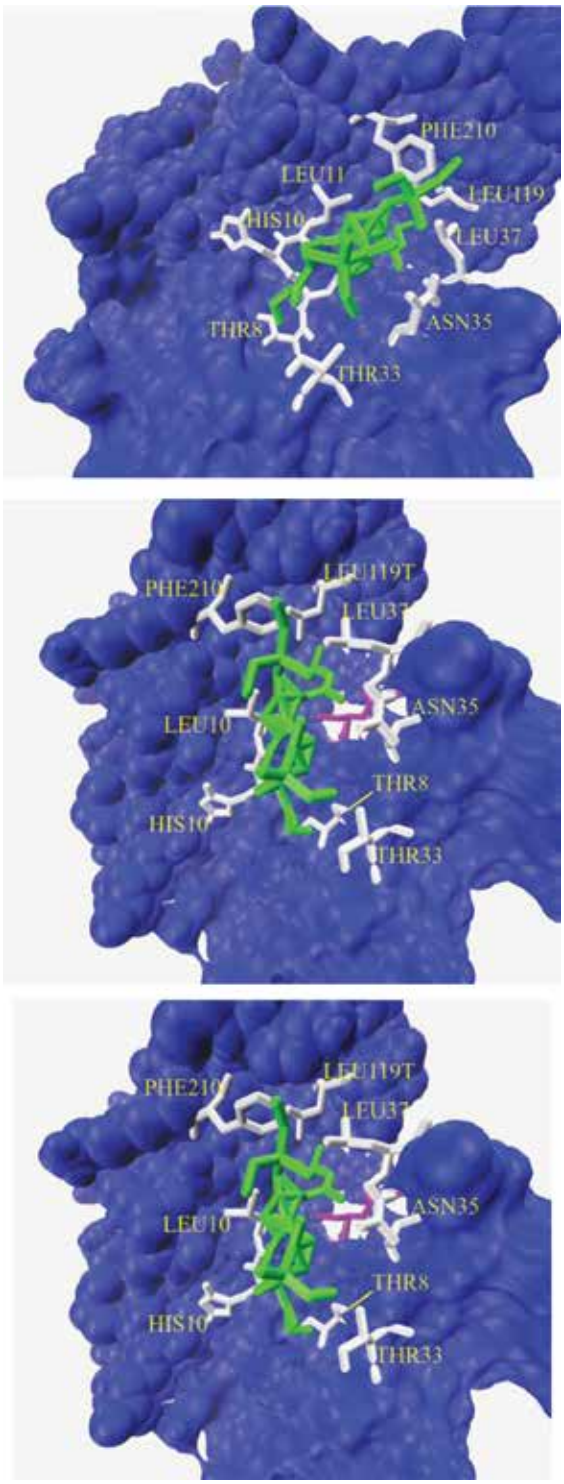

Figure 4. Representation of the best conformation of the AgGSTE2-malathion (top), AgGSTE2mut-malathion (middle), and AgGSTe5-malathion (bottom) complexes. Residues are represented in rods and spheres. The GSH is represented in sticks. In green the cypermethrin.

reasonable proximity of GSH (AgGSTE2 = 8.10 Å; AgGSTE2mut = 9.57 Å; AgGSTE5 = 5.26 Å) was observed in any of the conformers, which rule out the possibility that one of these enzymes could metabolize the malathion.

The docking results showed that the three enzymes have affinity for compounds of different nature. In fact, this represents an in silico that these enzymes show a remarkable functional promiscuity, resulting from a multi-specificity to the substrate. Although the AgGSTE2mut presented the lowest values for five of the seven compounds submitted to the docking calculation, the values did not differ much. When comparing the two isoforms, it was observed that for six of the seven compounds tested, the mutant enzyme had slightly more favorable energies than the wild type. The most plausible explanation for this result lies in the fact that AgGSTE2mut has a higher catalytic site resulting from the mutations in this enzyme, which probably allows a better accommodation of the compounds.

The docking results showed that the three enzymes have affinity for compounds of different nature. In fact, this represents in silico evidence that these enzymes show remarkable functional promiscuity, resulting from multi-specificity to the substrate. Although the AgGSTE2mut presented the lowest values for five of the seven compounds submitted to the docking calculation, the values did not differ much. When comparing the two isoforms, it was observed that for six of the seven compounds tested, the mutant enzyme had slightly more favorable energies than the wild type. The most plausible explanation for this result is that AgGSTE2mut has a larger catalytic site volume, resulting from the mutations in this enzyme, which probably allows a better accommodation of the compounds.

The multi-specificity presented by these enzymes, especially AgGSTE2mut, may represent an important aspect in the ability of *A. gambiae* to have populations resistant to chemical insecticides. This is a recent concept [19] and should be taken into account in future studies of the molecular evolution of enzyme superfamily. The use of chemical insecticides in this species needs to be rethought and reevaluated as a mode of control. A future perspective may be on the potential of development of specific inhibitors for these enzymes, in an attempt to decrease the response to the insecticides used, especially DDT. Another aspect that evidences the potential of the epsilon class GSTs as targets for inhibition is the fact that this class of enzymes is specific to arthropods, which enables the further development of inhibitory compounds that do not affect other species, such as mammals. Understanding the mechanisms of evolution and adaptation of these enzymes and details of their dynamics and functioning is indispensable when planning a rational and integrated control of a vector species. Another possible application is to use these enzymes as indicators of resistant populations and refractory to various insecticides and thus to choose the best type of compound to be used for each population.

3. Molecular docking between a rice GST and chemical herbicides

It is known that the superfamily of glutathione S-transferases (GSTs) gives rice (*Oryza sativa*) a catalytic action, protection against biotic and abiotic stress [20, 21]. The inactivation of the toxic effects of herbicides on plants has different defense systems [22]. Another study [23] has shown that the GST enzyme is associated with several crop herbicides' harmful effect tolerance,

promoting the resistance of grasses to its chemicals substances. In plants GST is also responsible through the metabolism of a huge name of commercial important herbicides [24] reducing damage that could occur through the toxically herbicides' action [25]. The reaction consists of the conjugation of the tripeptide glutathione to a hydrophobic compound, making it more soluble and less toxic [26], maintaining the cellular homeostasis. For this study two herbicides were selected, metsulfuron and bentazon sodium.

The herbicide metsulfuron-methyl belongs to the group of sulfonylureas and acts on the enzyme acetolactate synthase (ALS), consequently inhibiting the synthesis of the amino acids leucine, valine, and isoleucine, interfering in the protein synthesis and inducing the death of the plant by interfering in the cellular division. Among its properties, it is reported that metsulfuron-methyl has a systemic action and is rapidly absorbed by the whole plant, besides presenting selectivity to the crops for which its use is recommended. In susceptible plants, the absorption of this herbicide results initially in growth stoppage; due to the rapid translocation of this group of molecules to the meristems, apices, and later, death is inevitable, considering the impossibility of the essential amino acid biosynthesis to the plant. This mechanism inhibition of ALS was elucidated due to works done and published [27, 28].

Bentazon is a herbicide from the benzothiazinone class, which, after being absorbed, interferes in the photosynthesis process and is therefore a photosystem II photosynthesis inhibitor, affecting the carbohydrate synthesis in leaf areas that have received treatment, occasionally and may occasionally lead the plants to death, especially when they are in the early development stage. The photosynthesis inhibitors mechanism action is the removal or the inactivation of intermediary charge carriers from the electron transport process, and are considered to be inhibitors of electron transport [28]. The inhibitory mechanism of photosynthesis results in the blockade of the electron transport of the compound QB component of the photosynthetic system and, thus, makes impossible the occurrence of electron transport to plastoquinone B [29]. The aforementioned blockade occurs through the binding of the herbicides to the active site of QB in the D1 protein belonging to photosystem II, located on the membranes of the thylakoids of the chloroplasts. This process interrupts the fixation of CO_2 and interferes in the production of essential elements to the plant growth, such as ATP and $NADPH_2$; however, plant death usually occurs due to other factors. The interruption of the electron flow in photosystem II promotes a significant increase in the energy status of the chlorophyll, resulting in a state called "triplet," which causes an energy overload derived from the attenuation effect of the carotenoid pigments, and this characterizes the peroxidation process. In other study [30], lipid peroxidation due to excess triplet chlorophyll may occur through two mechanisms: direct formation of lipid radicals in unsaturated molecules of fatty acids constituting membranes and production of singlet oxygen through the reaction of chlorophyll triplet with oxygen. In both cases, the peroxidation process will corroborate with damage to cell membranes.

3.1. Molecular docking of rice GST and herbicides

The atomic coordinates of the compounds were obtained from the ZINC database (http://zinc.docking.org/) on *.mol2* file extension (**Table 3**).

Herbicide name	Molecular formula	2D structure	Access code
Bentazon-sodium	C10H12N2O3S	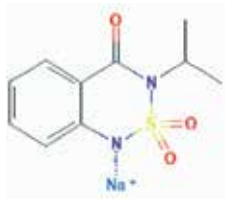	ZINC05442053
Metsulfuron-methyl	C14H15N5O6S		ZINC01532069

Source: ZINC database (http://zinc.docking.org/).

Table 3. Compounds used as ligands for the calculation of docking.

The *.mol2* files were converted to *.pdbqt* in AutoDock 1.5.6 (https://www.chpc.utah.edu/documentation/software/autodock.php) and had the polar hydrogens removed, and their molecules were flagged with the Gasteiger parameters [31]. The structure of OsGSTU4 was obtained from a *.pdb* file modeled using homology which was converted to *.pdbqt* file in AutoDock and added hydrogens and Kollman load parameters [32, 33]. For this step, glutathione was treated as a cofactor. The docking calculations were run in AutoDock 1.5.6 program, and the simulations were performed using the Lamarckian genetic algorithm (LGA). In this work, the LGA was used in conjunction with the Goodford method, allowing simultaneous sampling of the ligand configurational space and calculating the receptor and ligand atomic interaction energy [34, 35]. The grid parameters are established in 126×126×126 Å by the program Autogrid (http://autodock.scripps.edu/wiki/AutoGrid) and receiver-centered (GST). The parameters used for simulations were as follows: 10,000 replicates, energy analyzes per 1,500,000 and 27,000 generations, population size of 150, and mutation rates and crossing over of 0.02 and 0.08, respectively. Ten conformations were generated that were ranked based on the lowest energy and analyzed in the VMD (http://www.ks.uiuc.edu/Research/vmd/).

4. Results

The docking result for the herbicide metsulfuron-methyl, performed in the AutoDock program, ranked ten possible complexes; **Table 4** shows the best possible complex. This procedure is based on intermolecular energy, binding energy, and hydrogen bond scores, showing the atoms (and residues) of the protein and the ligand that present favorable interactions for the model.

Binding energy (kcal/mol)	Intermolecular energy (kcal/mol)	Hydrogen bond
–3.74	–5.53	B: LYS 111 HZ1-O2
		C: GTX1226 H11-N3
		B: LYS 111 HZ2-O6
		C: LYS 56 HZ1-O2

Source: Research data.

Table 4. Results of AutoDock-ranked complexes in the metsulfuron-methyl docking.

In metsulfuron-methyl, binding energies were lower than those of bentazon. The results revealed by the metsulfuron-methyl docking show that some residuals (LYS 111, LYS 56, GTX1226) were extremely favorable, being these possibly anchor residues for the binding, in combination with results evidenced by previous studies. The identification of the GTX1226 molecule as an anchor residue (**Table 5**) is evidence of a possible conjugation process [36] between metsulfuron-methyl and glutathione, evidencing the possibility of detoxification of metsulfuron-methyl by OsGSTU4. The best complex result ranked by the AutoDock for metsulfuron-methyl can be visualized in **Figure 5**. The image shows a zoom in a pocket where probably conjugation occurs by a hydrogen bond between bentazon and glutathione. The complex generated suggests that the OsGSTU4 displays a relevant role on the resistance for this herbicide (**Figure 5**).

The result of the docking performed for the herbicide bentazon sodium, also executed in the AutoDock program, is presented in **Table 6**. This procedure is the same used for metsulfuron-methyl and is also based on intermolecular energy, binding energy, and hydrogen bond scores, showing the atoms (and residues) of the protein and the ligand that present favorable interactions for the mode (**Figure 6**).

The results of **Table 6** also show the identified repeated residue (GLN 75) that presents the lowest binding energy, possibly showing as an anchor residue for the herbicide bentazon sodium, corroborating with the results obtained on previous studies [37].

Near residue atoms	Reference atoms (ligand)	Respective distance (Å)
ASP110: O	<0>0:C14	3.43
GLU69:OE2	<0>0:C5	2.95
LYS56:HZ1	<0>0:O2	1.91
LYS111:HZ1	<0>0:O2	1.91
GLN134:OE	<0>0:C10	2.87
HIS54:HE2	<0>0:C5	3.91

Source: Research data.

Table 5. Representation of the atoms of near residues belonging to metsulfuron-methyl, atoms used as corresponding in the ligand and their respective distances in angstroms in the output.

http://dx.doi.org/10.5772/intechopen.73920

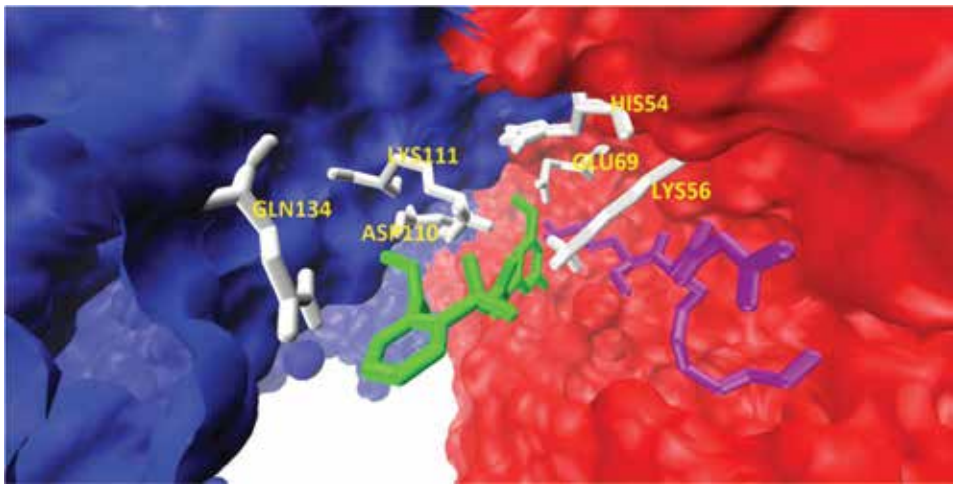

Figure 5. Deep view of catalytic site. In red, the chain A; in blue, the chain B. In green, the metsulfuron. Glutathione (purple) and residues (white) from H-binding-site, an interchain region. Source: Research data.

Binding energy (kcal/mol)	Intermolecular energy (kcal/mol)	Hydrogen bond
−0.86	−1.16	B: GLN 75 HE21-O3

Source: Research data.

Table 6. Results of AutoDock-ranked complexes in the bentazon sodium docking.

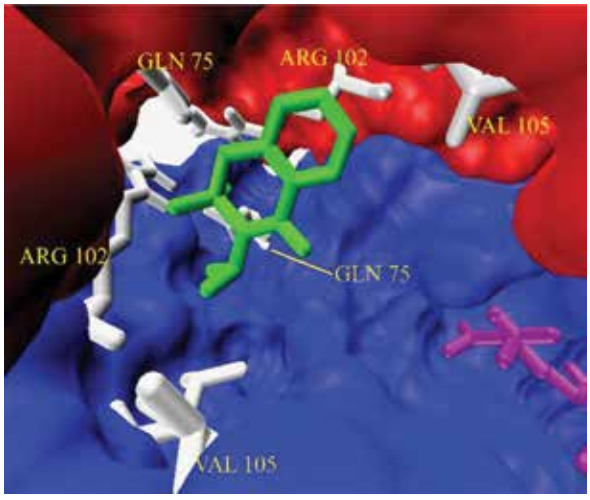

Figure 6. Deep view of catalytic site. In red, the chain A; in blue, the chain B. In green, the bentazon. Glutathione (purple) and residues (white) from H-binding-site, an interchain region. Source: Research data.

Near residue atoms	Reference atoms (ligand)	Respective distance (Å)
Val105:CG′	<0>0:C8	3.38
ALA106:HN	<0>0:C7	3.25
ARG102: O	<0>0:C7	2.79
VAL105:CG′	<0>0:C1	3.58
ALA106:HN	<0>0:C1	3.45
ARG102:HE	<0>0:O2	3.71
GLN75:2HE2	<0>0:N2	2.11
GLN75:1HE2	<0>0:O3	1.78

Table 7. Representation of the atoms of near residues belonging to bentazon sodium, atoms used as corresponding in the ligand and their respective distances in angstroms in the output.

Figure 6 depicts a catalytic cavity where a conjugation with metsulfuron may occur. In the image, the complex with lower binding energy was chosen. The interaction with glutathione is made by a hydrogen bond. This is evidence that OsGSTU4 is able to bind to metsulfuron in order to promote the conjugation reaction. Theoretically, this enzyme plays an important role in the resistance to this herbicide.

Complementing the information in the figure information, **Table 7** shows the atoms of surrounding amino acid residues at distances less than 4 Å and their respective distances to atoms of the ligand.

5. Conclusions

Molecular docking has proved to be an extremely useful technique for studying GSTs, especially in the context of resistance to chemical insecticides and herbicides. The methodology applied in these studies may be excused for other GSTs and other compounds. The complexes obtained provide a better understanding of the detoxification process performed by these enzymes.

However, although we find strong evidence of metabolization of these compounds, experimental studies should be undertaken to validate the in silico experiments. Site-directed mutation studies can be extremely providential to complement the information obtained here.

Not surprisingly, we notified that the GSTs here studied showed an affinity for more than one compound. This corroborates with the fact that members of this enzyme family display a multi-specificity on their H-binding-site.

As promiscuous proteins, these GSTs may be involved in metabolization of a wide range of toxic compounds, including other insecticides and herbicides. Further studies must be performed to investigate this.

Once the herbicide and insecticide resistance are multigenic, multi-enzymatic, and multifactorial process, the molecular docking technique can help to elucidate other pathways. Other computational techniques, such as molecular dynamics, can also give more insights about these systems.

Since herbicide and insecticide resistance is one of the major constraints of agriculture and mosquito control, the information from this study may be extremely useful for the development of specific inhibitors for these GSTs, thereby reducing the amount of herbicides and insecticides to be used and consequently reducing the environmental impact and other side effects.

New strategies of control can be applied too. The results point these enzymes as very promisor targets for iRNA technique.

The molecular docking is a powerful approach for understanding the interactions of molecules, and it is useful to elucidate biochemical processes. In the field of molecular modeling, this tool is an option of rapid, with low computational, requirements, to perform molecular simulations of many systems. Many software, including the commercial ones, have been developed, and new algorithms are quickly incorporated to the packages. In the fields of computational biology and bioinformatics, it has become one of the most popular tools, with a wide range of applications. The diffusion of this amazing technique is a great strategy on the advance of molecular studies and must be applied in many fields of knowledge.

Acknowledgements

We thank the Biomaterial Modeling group for the computational resources granted for research.

Author details

Rafael Trindade Maia[1]* and Vinícius Costa Amador[2]

*Address all correspondence to: rafael.rafatrin@gmail.com

1 Federal University of Campina Grande (UFCG), Sumé, Paraíba State, Brazil

2 Federal Rural University of Pernambuco (UFRPE), Recife, Pernambuco State, Brazil

References

[1] Hayes JD, Flanagan JU, Jowsey IR. Glutathione transferases. Annual Review of Pharmacology and Toxicology. **45**:51-88. DOI: 10.1146/annurev.pharmtox.45.120403.095857

[2] Robinson A et al. Modelling and bioinformatics studies of the human Kappa class glutathione transferase predict a novel third transferase family with homology to prokaryotic 2-hydroxychromene-2-carboxylate isomerases. Biochemistry Journal. **379**(Pt 3):541-552. DOI: 10.1042/BJ20031656

[3] Sheehan D. Structure, function and evolution of glutathione transferases: Implications for classification of 54 non-mammalian members of an ancient enzyme superfamily. Biochemistry Journal. **360**(Pt 1):1-16. DOI: 10.1590/S1984-29612008000200007

[4] Ding Y et al. The Anopheles gambiae glutathione transferase supergene family: Annotation, phylogeny and expression profiles. BMC Genomics. **4**(35):1-16. DOI: 10.1186/1471-2164-4-35

[5] Lumjuan N et al. The *Aedes aegypti* glutathione transferase family. Insect Biochemistry and Molecular Biology. **37**(10):1026-1035. DOI: 10.1016/j.ibmb.2007.05.018

[6] Enayati AA, Ranson H, Hemingway J. Insect glutathione transferases and insecticide resistance. Review. Insect Molecular Biology. 2005 Jan;**14**(1):3-8. DOI: 10.1111/j.1365-2583.2004.00529.x

[7] Prabhu KS et al. Characterization of a class alpha glutathione-S-transferase with glutathione peroxidase activity in human liver microsomes. Archives of Biochemistry and Biophysics. 2004;**424**(1):72-80

[8] Pearson WR. Phylogenies of glutathione transferase families. Methods in Enzymology. **401**:186-204. DOI: 10.1016/S0076-6879(05)01012-8

[9] Hemingway J, Hawkes NJ, McCarroll, Ranson H. The molecular basis of insecticide resistance in mosquitoes. Insect Biochemistry and Molecular Biology. **34**(7):653-665. DOI: 10.1016/j.ibmb.2004.03.018

[10] Ransom H, Hemingway J. Mosquito glutathione transferases. Methods in Enzymology. **401**:226-241. DOI: 10.1016/S0076-6879(05)01014-1

[11] Ranson H et al. Evolution of supergene families associated with insecticide resistance. Science. **298**:179-181. DOI: 10.1126/science.1076781

[12] Che-mendoza A, Penilla RP, Rodríguez DA. Insecticide resistance and glutathione S-transferases in mosquitoes. A review. 2009;**8**(8):1386-1397

[13] Board PG et al. Identification, characterization, and crystal structure of the Omega class glutathione transferases. Journal of Biological Chemistry. **275**:24798-24806. DOI: 10.1074/jbc.M001706200

[14] Wildenburg G, Liebau E, Henkle-Duhrsen K. Onchocerca volvulus: Ultrastructural localization of two glutathione S-transferases. Experimental Parasitology. **88**:34-42. DOI: 10.1006/expr.1998.4189

[15] Chelvanayagam G, Parker MW, Board PG. Fly fishing for GSTs: A unified nomenclature for mammalian and insect glutathione S-transferases. Chemico-Biological Interactions. 2001;**133**:256-260

[16] Mannervik B, Danielson UH. Glutathione transferases: Structure and catalytic activity. Critical Review in Biochemistry. 1988;**23**(3):283-337

[17] Ranson H, Collins FH, Hemingway J. The role of alternative mRNA splicing in generating heterogeneity within the Anopheles gambiae class I glutathione S transferase family. Proceedings of the National Academy of Sciences of United States of America. 1998;**95**(24):14284-14289

[18] Lumjuan N et al. The *Aedes aegypti* glutathione transferase family. Insect Biochemistry and Molecular Biology. **37**(10):1026-1035. DOI: 10.1016/j.ibmb.2007.05.018

[19] Morris GM et al. Automated docking using a Lamarckian genetic algorithm and empirical binding free energy function. Journal of Computational Chemistry. **19**:1639-1662. DOI: 10.1002/(sici)1096-987x(19981115)19:14<1639::aid-jcc10>3.0.co;2-b

[20] Tokuriki N, Tawfik DS. Protein dynamism and evolvability. Science. **324**(5924):203-207. DOI: 10.1126/science.1169375

[21] Frova C. The plant glutathione gene family: Genomic structure, functions, expression and evolution. Physiologia Plantarum, Lund. 2003;**119**(4):469-479

[22] Frova C. Glutathione transferases in the genomics era: New insights and perspectives. Biomolecular Engineering. Amsterdam. **56**(31):4073-4083. DOI: 10.1016/j.bioeng.2006.05.020

[23] Bor M, Özdemir F, Türkan I. The effect of salt stress on lipid peroxidation and antioxidants in leaves of sugar beet Beta vulgaris L. and wild beet Beta maritima L. Plant Science. **164**:77-84. DOI: 10.1016/S0168-9452(02)00338-2

[24] Edwards R et al. Chemical manipulation of antioxidant defenses in plants. Advances in Botanical Research. London. 2005;**42**:1-32

[25] Edwards R, Dixon DP, Walbot V. Plant gluthatione S-transferases: Enzymes with multiple functions sockness and in health. Trends in Plant Science. **47**:127-158

[26] Radetski CM, Cotelle S, Ferrard JF. Classical and biochemical endpoints in the evaluation of phytotoxic effects caused by herbicide trichloroacetate. Environmental and Experimental Botany. 2000;**44**:221-229

[27] Marrs KA. The functions and regulation of glutathione S-transferases in plants. Annual Review of Plant Physiology and Plant Molecular Biology. DOI: 10.1146/annurev.arplant.47.1.127

[28] Durner J, Gailus V, Böger P. New aspects on inhibition of plant acetolactate synthase depend on flavin adenine dinucleotide. Plant Physiol. 1991;**95**:1144-1149

[29] Oliveira Jr RS. Mecanismo de ação de herbicidas. In: Oliveira Jr RS, Constantin J, Inoue MH. (Coord.). Biologia e Manejo de Plantas Daninhas. Curitiba, PR: Omnipax, 2011. p. 141-184

[30] Balke NE. Herbicide effects on membrane functions. In: Duke SO, editor. Weed Physiology, v. II. Boca Raton, EUA: CRC Press; 1985. pp. 113-139

[31] Christoffoleti PJ, López-Ovejero RF. Resistência das plantas daninhas a herbicidas: Definições, bases e situação no Brasil e no mundo. Aspectos de resistência de plantas daninhas a herbicidas. 2008;**3**:9-34

[32] Dan HF. Mode of action of photosynthesis inhibitors. In: Purdue University, editor. Herbicide Action Course. West Lafayette, EUA: CRC Press; 1994. pp. 85-102

[33] Weiner SJ et al. A new force field for molecular mechanical simulation of nucleic acids and proteins. Journal of the American Chemical Society. 1984;**106**:765-784

[34] Gasteiger J, Masili M. Iterative partial equalization of orbital electronegativity—A rapid access to atomic charges. Tetrahedron. 1980;**36**:3219-3228

[35] Goodford PJ. A computational procedure for determining energetically favorable binding sites on biologically important macromolecules. Journal of Computational Chemistry. 1985;**28**:849-857

[36] Kilili K et al. Differential roles of tau class glutathione S-transferases in oxidative stress. The Journal of Biological Chemistry. **279**:24540-2451. DOI: 10.1074/jbc.M309882200

[37] Rigo MM. Estudo in silico da reatividade cruzada entre epitopos de hantavírus [Mestrado Tese]. Rio Grande do Sul: Instituto de Biociências da UFRS; 2011. 91 p

Section 3

Molecular Docking for Medicinal Chemistry

Chapter 4

A Click Chemistry Approach to Tetrazoles: Recent Advances

Ravi Varala and Bollikolla Hari Babu

Additional information is available at the end of the chapter

http://dx.doi.org/10.5772/intechopen.75720

Abstract

Introduction to tetrazole and click chemistry approaches was briefed in a concise way in order to help the readers have a basic understanding. Tetrazole and its derivatives play very important role in medicinal and pharmaceutical applications. The synthesis of tetrazole derivatives can be approached in ecofriendly approaches such as the use of water as solvent, moderate conditions, nontoxic, easy extractions, easy setup, low cost, etc. with good to excellent yields.

Keywords: click chemistry, tetrazoles, biological activity, synthesis and molecular docking

1. Introduction

1.1. Chemistry of tetrazoles

1*H*-Tetrazole (**1**) is a crystalline light yellow powder and odorless. Tetrazole shows melting point temperature at 155–157°C. On heating, tetrazoles decomposed and emit toxic nitrogen fumes. These are burst vigorously on exposed to shock, fire, and heat on friction.

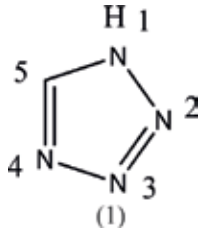

(1)

Tetrazoles easily react with acidic materials and strong oxidizers (acidic chloride, anhydrides, and strong acids) to liberate corrosive and toxic gases and heat. It undergoes reaction with few active metals and produces new compounds which are explosives to shocks. It involves exothermic reactions with reducing agents. On heating or burning, it releases carbon monoxide, carbon dioxide, and harmful nitrogen oxide. Tetrazole dissolves in water, acetonitrile, etc. Generally, dilute 1*H*-tetrazole in acetonitrile is used for DNA synthesis in biochemistry.

The presence of free N-H causes the acidic nature of tetrazoles and forms both aliphatic and aromatic heterocyclic compounds. Heterocycles of tetrazoles can stabilize the negative charge by delocalization and show corresponding carboxylic acid pKa values. Tetrazole nitrogen electron density results in the formation of so many stable metallic compounds and molecular complexes. This compound shows strong negative inductive effect (−I electron withdrawing) and weak positive mesomeric effect (+M electron releasing).

The tetrazole is a five-membered aza compound with 6π electrons, and 5-substituted tetrazole reactivity is similar to aromatic compounds. The Huckel 6π electrons are satisfied by four π electrons of ring and one loan pair of electrons of nitrogen. The acidic nature of tetrazole is similar to corresponding carboxylic acids, but there is a difference in annular tautomerism of ring tetrazoles to carboxylic acids. The acidic nature of tetrazole is mainly affected by substitution compound nature at C-5 position. 5-Phenyltetrazole anion shows high acidic nature like benzoate due to resonance stabilization. A simple method to produce tetrazole anion is the reaction of tetrazole with metal hydroxides and can be stable in aqueous and alcoholic solution at high temperature.

1.2. Introduction to click chemistry

Click chemistry is called as tagging in synthesis of chemicals. It is in the category of non-harmful reactions, proposed initially to unite the base materials of choice with certain bimolecular substance. It also can be termed as a non-peculiar reactive process. Indeed it explains a way of generating products that follow examples in nature. At the same time, it can produce the variety of materials by consolidating small compatible units. Usually, click reactions join a biomolecule and a reporter molecule. Click chemistry is not limited to the state of survival. It is the concept of a "click" reaction that has been used in pharmacological and various biomedical applications. It also can be described as non-single specific reaction etic application. Nevertheless, it is observed to be highly functional in the diagnosis of localization and qualification of bimolecular material.

Click reactions occur in one pot and generally make an evidence of being uninterrupted by water. They produce negligible and innocuous corollary and are spring-loaded. In addition to this, they are distinguished by a high thermodynamic driving force that pushes them rapidly and irrevocably to supply a single reaction product, with high reaction specificity. In few cases, they are created with both regio- and stereospecificity. These click reactions are specifically adaptable in the case of segregating and navigating the molecules in composite biological environments. In such conditions, items in like manner should be physiologically steady, and any side effects should be nonlethal.

Researchers have opened up the likelihood of hitting specific focuses in complex cell lysates, by developing specific and controllable bio-orthogonal reactions. Recently, they have adjusted snap science for use in live cells, for instance, utilizing little atom tests that find and append to their objectives by click reactions. In spite of difficulties of cell porousness, bio-orthogonality, foundation naming, and response effectiveness, click responses have officially demonstrated valuable in another era of pull-down tests and fluorescence spectrometry. All the more as of late, novel strategies have been utilized to fuse click response accomplices onto and into biomolecules, including the joining of unnatural amino acids containing receptive gatherings into proteins and the change of nucleotides. These strategies speak to a piece of the field of compound science, in which click science assumes a central part by deliberately and particularly coupling secluded units to different finishes.

This refresh outlines the developing use of "click" science in various zones, for example, bioconjugation, sedate disclosure, materials science, and radiochemistry. It additionally talks about snap science responses that continue quickly with high selectivity, specificity, and yield. Two essential qualities make click science so appealing for collecting mixes, reagents, and biomolecules for preclinical and clinical applications. To begin with, click reactions are bio-orthogonal. First of all, they are neither reciprocal nor their functional gatherings of different products connect with functionalized biomolecules. Secondly, the responses continue effortlessly under gentle nontoxic conditions. Example is their reaction at the room temperature and, for the most part, in water. The copper-catalyzed Huisgen cycloaddition, azide-alkyne [3+2] dipolar cycloaddition, Staudinger ligation, and azide-phosphine ligation all have these interesting qualities. These responses can be utilized to change one cell part while leaving others unharmed or untouched.

Click chemistry has discovered expanding applications in all parts of medication revelation in restorative science, for example, for producing lead mixes through combinatorial strategies. Through bioconjugation click chemistry is thoroughly utilized in proteomics and nucleic exploration. In radiochemistry, specific radiolabeling of biomolecules in cells and living creatures for imaging and treatment has been acknowledged by this innovation. Bifunctional chelating operators for a few radionuclides are valuable for positron discharge tomography and single-photon emanation processed tomography. They have additionally been set up by click chemistry. This survey reasons that click chemistry is not the ideal conjugation, and gathering innovation for all applications, however, gives a capable, appealing another option to ordinary science. This science has turned out to be prevalent in fulfilling numerous criteria, e.g., biocompatibility, selectivity, yield, stereospecificity, etc. In this way, one can expect that it will subsequently turn into a more normal procedure soon for an extensive variety of uses.

1.3. Introduction to molecular docking

Molecular docking (hereafter, MD) is the study of fitting together by two or more molecular components (e.g., drug and enzyme or protein). It is something like a problem of "lock and key" (**Figure 1**). It is an optimization issue which clearly explains how best a ligand and protein bind based on orientation. As both ligand and protein are flexible, a "hand-in-glove"

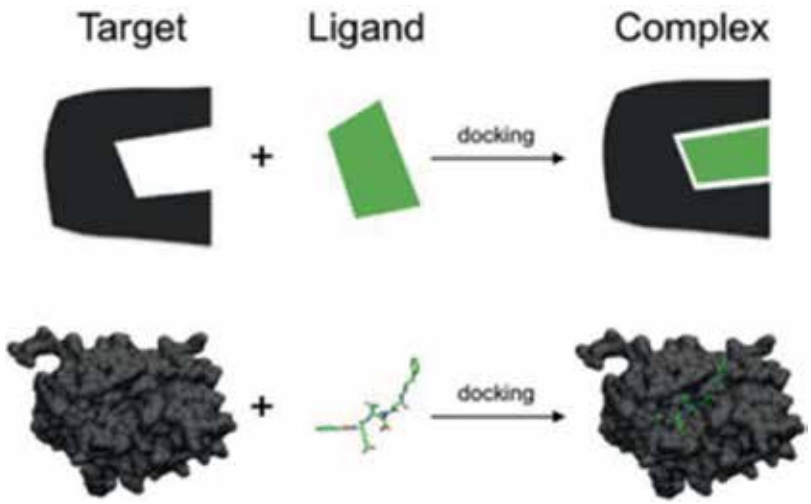

Figure 1. Lock and key models for Ligand-Target fitting.

word suit more effective compared to "lock and key" model. Both ligand and protein adapt their confirmation for overall binding, known as "induced effect."

MD research depends mostly on computationally simulating the molecular recognition process by decreasing the free energy of overall system. Basic awareness on the preferred orientation in turn may be used to predict the binding affinity between two molecules used. Molecular docking is an invaluable tool in the field of molecular biology, computational structural biology, computer-aided drug designing, and pharmacogenomics.

There are two ways of docking approaches, namely, the first matching methodology which explains ligand-enzyme as complementary surfaces and the other simulated docking methodology of protein and ligand pairwise interaction energies. The application of docking in a targeted drug-delivery system is a huge benefit. One can study the size, shape, charge distribution, polarity, hydrogen bonding, and hydrophobic interactions of both ligand (drug) and receptor (target site).

1.4. Aims and significance

The investigation of tetrazoles centers the most imperative organic exercises like antihypertensive, against inflammatory, antibacterial, antifungal, anticancer, antidiabetic, and hypoglycemic activity. Different strategies for synthesis and characterization techniques were discussed.

Throughout the previous couple of years, investigation of tetrazole chemistry has been rapidly expanded in view of its huge applications, for the most part because of the pretended by this heterocyclic usefulness in restorative chemistry. This provides more support to pharma field and metabolically stable swap for carboxylic acid functionalities, particularly, joining of the tetrazole exercises into angiotensin II rival structures, sartans (2–4) [1–4].

http://dx.doi.org/10.5772/intechopen.75720

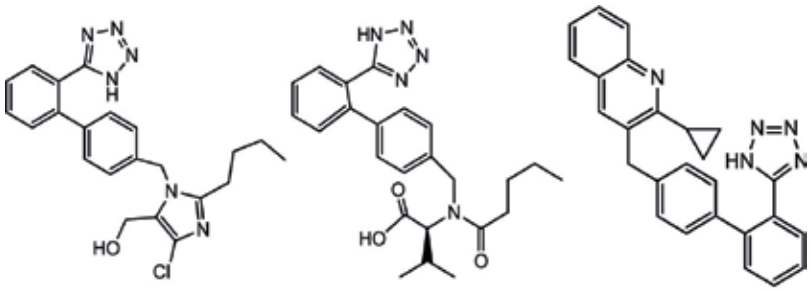

LOSARTAN (2) VALSARTAN (3) BMS-183920 (4)

Irbesartan (5), one of the essential tetrazole subsidiaries, has a place with the sort of medication called angiotensin II receptor enemy antihypertensives. This medication is utilized for the treatment of high blood pressure (hypertension) and for kidney issues because of Type 2 diabetes (noninsulin-dependent).

Tetrazolo quinoline has an imminent and empowering new structure for the novel against the anti-inflammatory (6) and antibacterial (7) agents [3, 4].

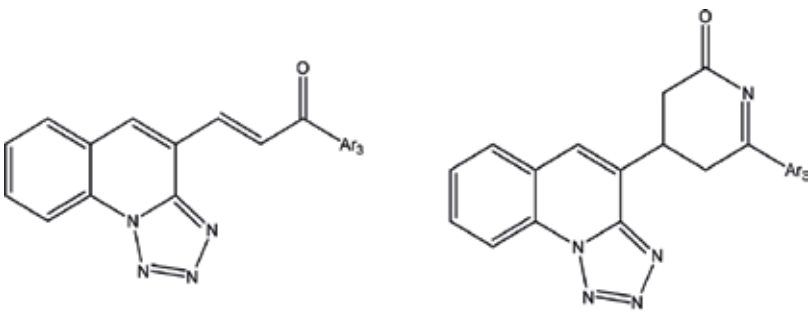

$Ar_3 = C_6H_5$, p-BrC_6H_4, p-ClC_6H_4 (6)

$Ar_3 = C_6H_5$, p-BrC_6H_4, p-ClC_6H_4 (7)

Piperidine-substituted tetrazoles (**8**) showed antifungal activity.

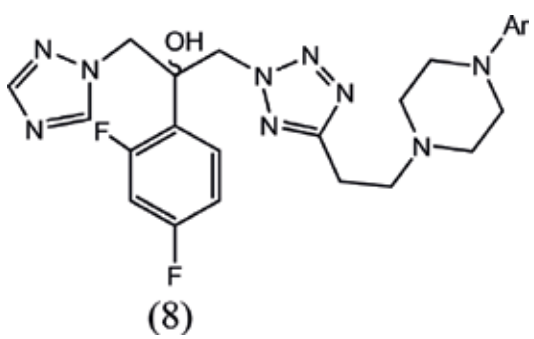

(8)

Tetrazole derivatives (**9**) have been chosen and enhanced for their anticancer action on the majority of various human tumor cell lines separated from nine neoplastic disease sorts. The capable anticancer compound was observed to be dynamic with specific impact on ovarian cancer [1–4].

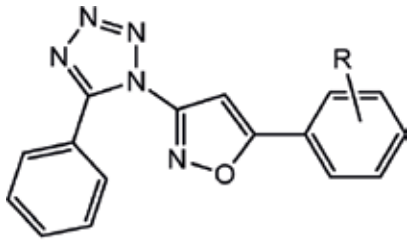

(9)

The 2,4 thiazolidinedione by-products (**10**) comprise tetrazole loop for their antidiabetic movement. The greater part of the mixes indicated great antidiabetic action when contrasted to glibenclamide [1–4].

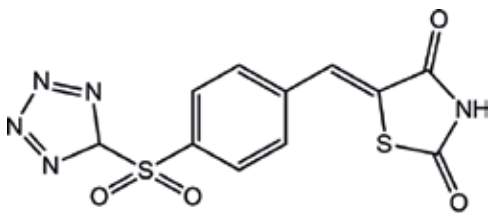

(10)

The in vivo hypoglycemic action of tetrazole bears *N*-glycosides as SGLT2 inhibitors. A progression of 5-[(5-aryl-1*H*-pyrazol-3-yl)methyl]-1*H*-tetrazoles (**11–13**) has been assessed for their in vivo antihyperglycemic action. A portion of the mixture have indicated critical glucose bringing down the movement [1–4].

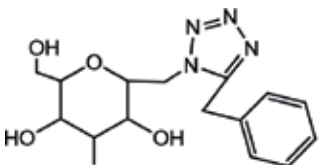

(11)

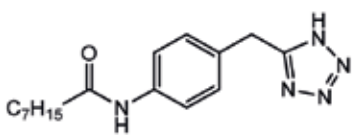

(12)

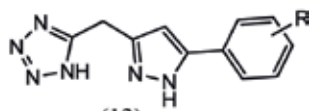

(13)

1.5. Motivation of the chapter

Powerful drugs in opposition to hypertension, cancer, and bacterial and fungal infections have to fulfill a number of requirements like toxicity to tumor cells and are capable of being

dissolved for efficient delivery. This makes necessary full-fledged characterization of drug position, comprising achieved synthetic strategies. In this chapter we directed on tetrazole biological activities. As a consequence, the need of synthetic routes to prepare tetrazole derivatives that are selective toward specific malfunctioning enzyme connects with illness. The study of good approaches of tetrazoles and medicinal applications will definitely allow to propose more useful drugs.

1.6. History of tetrazoles

Since 1901, regular synthesis of 5-switched-1*H*-tetrazoles (16) has been accounted for to continuation of [3+2] cycloaddition of azide (**14**) with nitriles (**15**). This strategy experiences various disadvantages including utilization of costly and poisonous metal natural azide, exceedingly dampness touchy response conditions, solid Lewis corrosive, and hydrazoic corrosive. The "click" chemistry approach using metal catalysis in fluid arrangement is an outstanding evolution over last strategies, however every so often still requires the monotonous and tedious expulsion of metal salts from the acidic items.

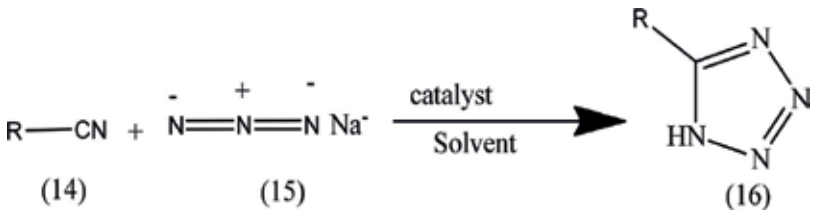

Tetrazoles as a gathering of heterocyclic compounds are accounted for having an expansive range of organic exercises, for example, antibacterial, antifungal, antiviral, pain-relieving, mitigating, antiulcer, and antihypertensive exercises. Likewise, 5-substituted-1*H*-tetrazoles can work as lipophilic spacers and carboxylic corrosive surrogates, forte explosives and data recording frameworks in materials ligands, and forerunners of an assortment of nitrogen-containing heterocycles in coordination science.

2. Synthesis of tetrazole and its analogues

2.1. Synthesis and crystal structures of copper(II), zinc(II), lead(II), and cadmium(II)

2.1.1. Tetrazole-5-carboxylate mixtures produced via in situ hydrolysis reaction

A facile method to synthesize Cu(II), Zn(II), Pb(II), and Cd(II) complexes with di-anionic tetrazole-5-carboxylate (ttzCOO2−) ligands (18), involving an in situ hydrolysis of 1*H*-tetrazole-5-carboxylic acid ethyl ester sodium salt (17) was described [5–8].

2.2. Synthesis, characterization, and anti-inflammatory activity of novel *N*-substituted tetrazoles

5-Phenyl tetrazole (**19**) responds with acidic anhydride to produce 5-phenyl 1-acetyl tetrazole (**20**), which can be additionally served with various electronically or structurally divergent aldehydes to shape chalcones (**21**). Chalcones additionally respond with isonicotinic acid hydrazide to produce pyrazolines (**22**) [9–12].

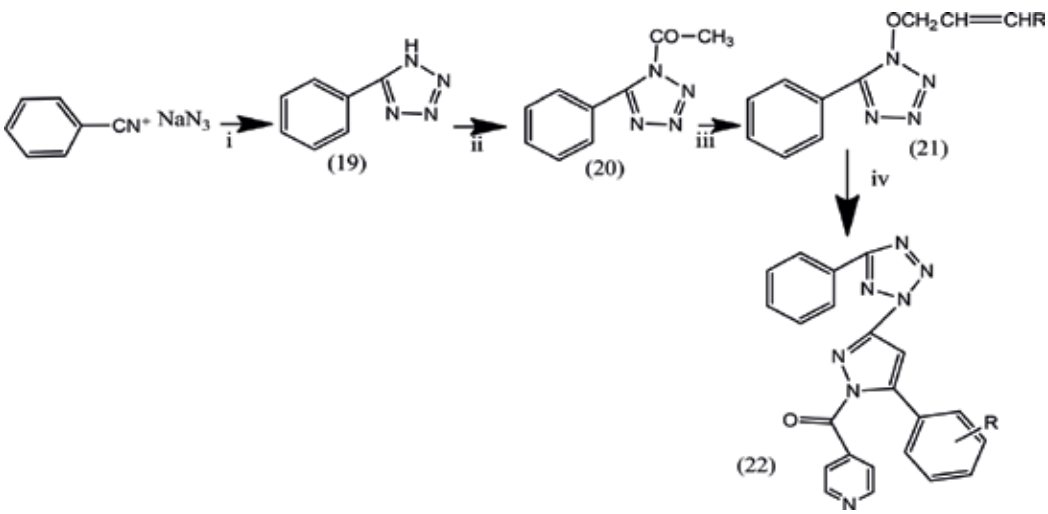

Reagent conditions: (i) DMF/ammonium chloride; (ii) acetic anhydride, 20 min; (iii) R-CHO, 50% KOH, ethanol; (iv) isonicotinic acid hydrazide/GAA.

2.3. Synthesis of 5-substituted 1*H*-Tetrazole using nano-ZnO/Co_3O_4 catalyst

5-Phenyl, 1*H*-tetrazole (24) is synthesized by reacting 1 mmol benzonitrile (23) and 1.5 mmol NaN_3 in the presence of nano-ZnO/Co_3O_4 catalyst and 3 mL DMF for 12 h at 120–130°C [13–16].

2.4. Advances in the synthesis of tetrazoles coordinated to metal ions

2.4.1. Reactions of tetrazoles with metal bases and salts

Tetrazoles (**25**) react with metal bases or salts to synthesize tetrazole-containing metal derivatives (**26**) [17–21].

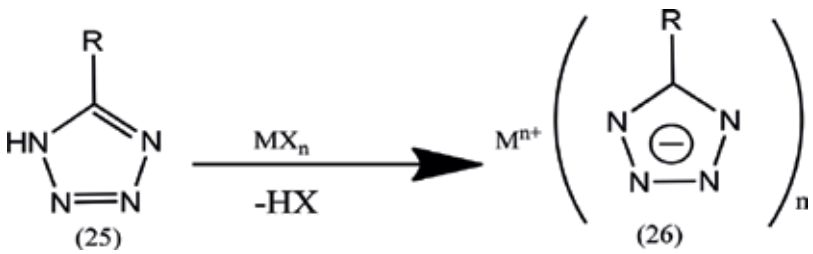

2.4.2. Responses of N1-substituted tetrazoles with metal salts

N1-substituted tetrazoles (**27**) due to the absence of the labile hydrogen iota in the ring, so they don't display acidic properties. In this way, the N1- and N2-substituted tetrazoles (**28**) are associated with the development of metal subsidiaries only in the unbiased frame [22, 23].

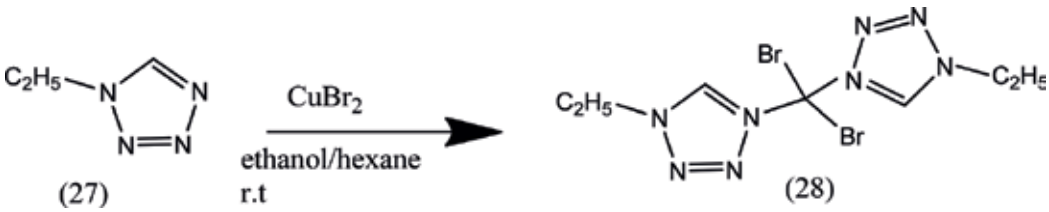

2.4.3. Substitution of ligands for tetrazoles in coordination compounds

To synthesize tetrazole-containing complexes with anionic ligands (29), tetrazole reacts with another ligand in a coordination compound [24, 25].

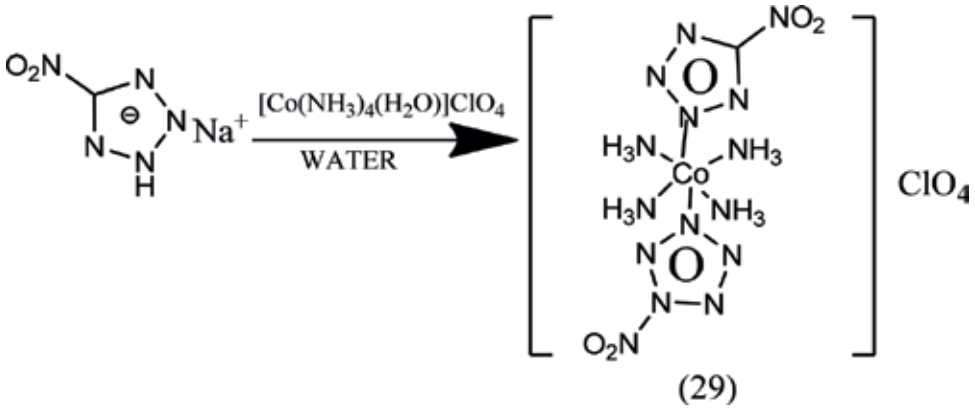

(29)

2.4.4. Metal-promoted cycle formation

The synthetic protocol involves reaction of inorganic azides and organic nitriles in the presence of Zn(II) salts under hydrothermal conditions to afford 5-substituted-1*H*-tetrazoles via 1,3-dipolar cycloaddition [26].

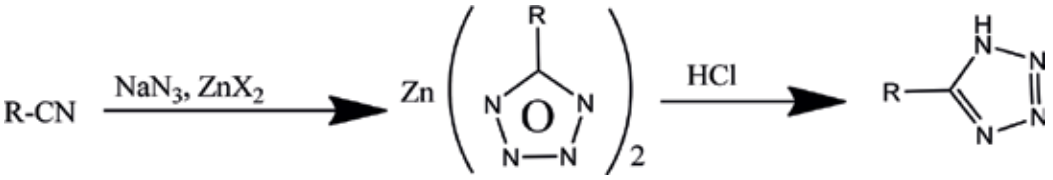

2.5. Synthesis of chosen 5-thio-substituted tetrazole subordinates and assessment of their antimicrobial exercises

To union of 5-thio replaced tetrazole subordinates and assessment of their antibacterial and antifungal properties, industrially accessible benzyl isothiocyanate (**30**) and sodium azide respond in presence of water to create 1-benzyl-1*H*-tetrazole-5-thiol (**31**) in great yield. The untouched mix is served with 1,3-dibromopropane with tetrahydrofuran to give a moderate 1-benzyl-5-[(3-bromopropyl)thio]-1*H*-tetrazole (**32**). The synthon is another compound and revealed here for the first time. This compound is treated with relating amines or thiols to manage the cost of the 5-thio-substituted tetrazole derivatives (**33**) [27–31].

2.6. Synthesis of novel 1*H*-tetrazoles: spectral characterization and antibacterial activities

The tetrazoles (35, 37) were orchestrated in outstanding reactiveness by the response of sodium azide and triethyl orthoformate with relating amines, viz., 1-[3-(2-amino ethyl)-1*H*-

http://dx.doi.org/10.5772/intechopen.75720

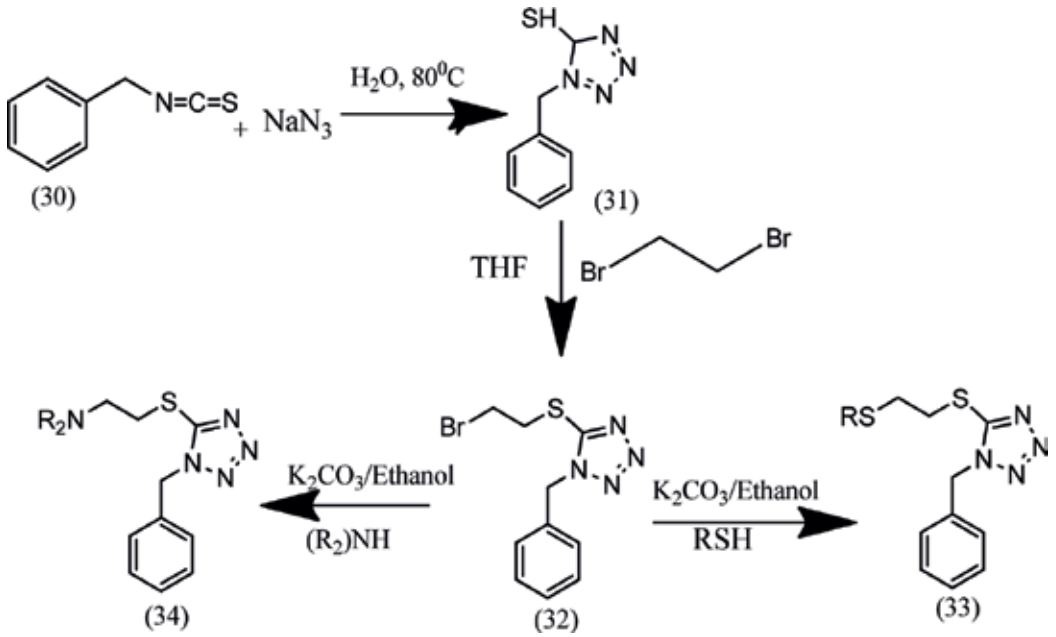

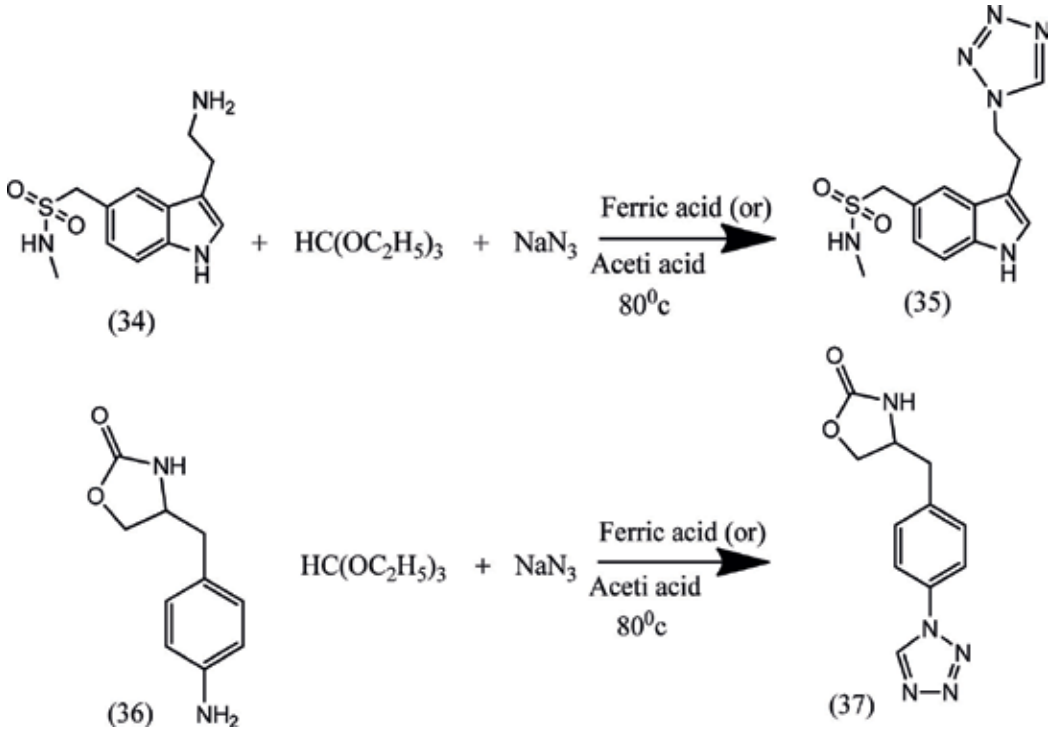

indol-5-yl]-*N*-methyl methanesulfonamide (**34**) or 4-(4-aminobenzyl)-1,3-oxazolidin-2-one (**36**) in acidic corrosive or formic corrosive [32–36].

2.7. Synthesis of tetrazole-containing 1,2,3-thiadiazole subordinates through U-4CR and their opposition of TMV movement

To prepare tetrazole-containing 1,2,3-thiadiazole derivative (**39**), take 4-methyl-1,2,3-thiadiazole-5-carbaldehyde (**38**), and substituted amine is mixed in methanol at room temperature. The imine was precondensated for 0.5–1 h, and afterward cyclohexyl isocyanide and TMSN3 were included. The response blend was mixed for 12–24 h at room temperature until the point when the response was finished (demonstrated by TLC). At that point the natural dissolvable was dissipated in vacuum. The unrefined items were decontaminated by a silica gel segment utilizing ethyl acetic acid derivation/oil ether (1:2–1:3 (v/v), 60–90°C) as an eluent to give the corresponding products as white or light yellow solids in direct yields [37–41].

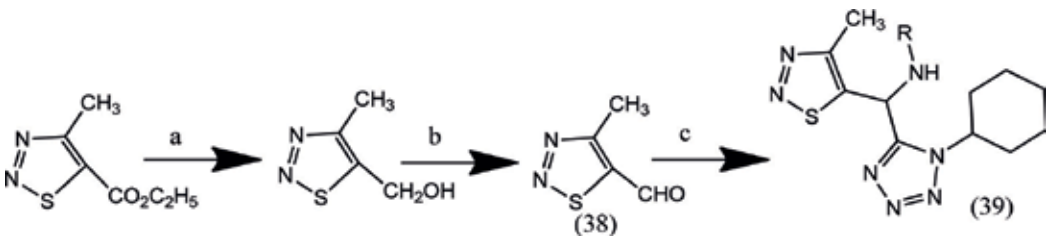

Reagents and conditions: (a) $NaBH_4$ (2.0 equiv.), EtOH, 0°C for 1 h, r.t. for 6 h; (b) pyridinium chlorochromate (2.0 equiv.), CH_2Cl_2, r.t. for 8 h; (c) (i) R-NH2 (1.0 equiv.), CH_3OH, r.t. for 0.5–1 h; and (ii) cyclohexyl isocyanide (1.2 equiv.), $TMSN_3$ (1.5 equiv.), r.t. for 12–24 h.

2.8. Synthesis of 2-{[2-(1*H*-tetrazole-5-yl)ethyl]sulfanyl}-1,3-benzimidazole (3) as antioxidants

10 mmol of 3-(1,3-benzimidazole-2-yl-sulfanyl)propanenitrile, 10 mmol sodium azide (**40**), 10 mL of DMF, and 10 mmol of zinc chloride were accepted in a flask, and the substances were warmed in an oil bath for 6 h at 125°C. After the routine workup, it was recrystallized from equimolar DMF-ethanol blend to get compound (**41**) [42, 43].

2.9. Single-leap synthesis of sterically hindered b1,5-disubstituted tetrazoles from bulky secondary *N*-benzoyl amides: usage of triazidochlorosilane (TACS)

A mixture of 1-(2-trifluoromethane phenyl)-5-phenyl-1*H*-tetrazole (**42**), sodium azide, and tetrachlorosilane in dry acetonitrile was refluxed under dry conditions to give the corresponding tetrazole **43** [44, 45].

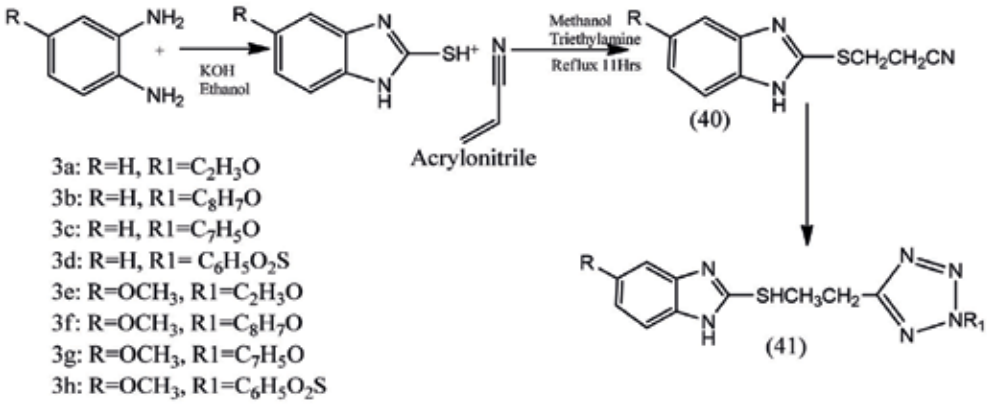

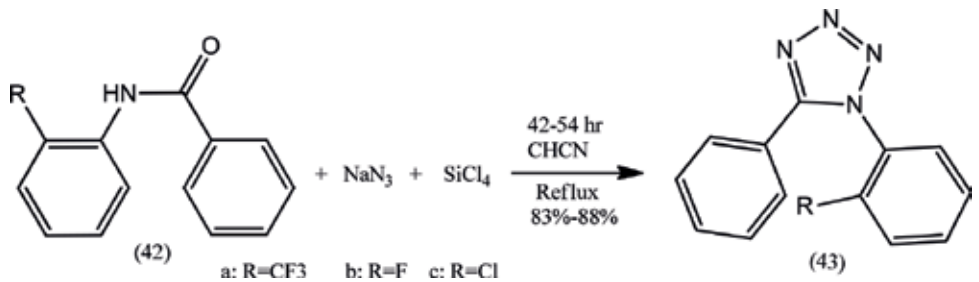

2.10. Synthesis of 1-substituted-1*H*-1,2,3,4-tetrazoles catalyzed by methanesulfonic acid under neat conditions

A blend of chosen amine (**44**), triethyl orthoformate (0.4 ml), and sodium azide (0.13 g) was added to methanesulfonic acid (20 mol%). The blend was mixed for adjusted time, and the advance of the response was checked by TLC. The mixture was stirred for the specified time to obtain 1-substituted 1*H*-1,2,3,4-tetrazole (**45**) [46–50].

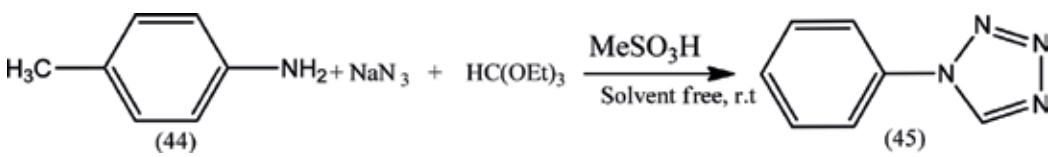

The above experiments yield very good result in the presence of various catalysts especially with silica sulfuric acid.

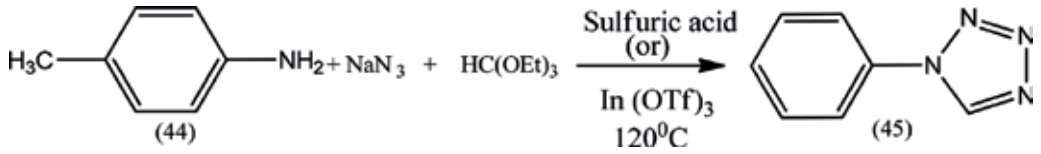

2.11. Productive synthesis of 1,5-disubstituted-1*H*-tetrazoles through an Ugi-azide procedure

The readiness of 1,5-disubstituted-1*H*-tetrazoles (**47**) was achieved in no catalyst conditions, optimized Ugi-azide process. The addition of aryl-ethanamine derivatives (**46**), aldehydes, isocyanides, and $TMSN_3$ in MeOH under mild conditions to give corresponding tetrazole (**47**) at room temperature [51–56].

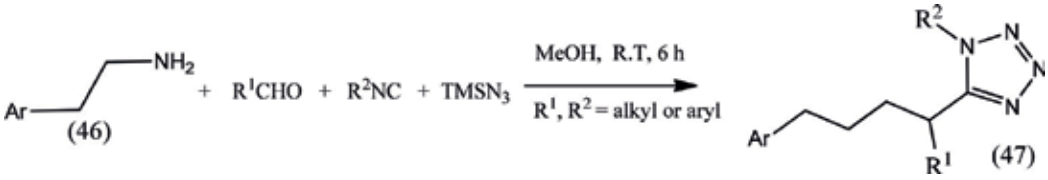

2.12. Straightforward and proficient strategy for the synthesis of novel tetrazole derivatives and its antibacterial exercises

A progression of novel 5-phenyl-1-acyl-1,2,3,4-tetrazoles (**53**) has been combined by buildup of 5-phenyl-1,2,3,4-tetrazoles (**49, 51**) with different acylating reagents. The union of tetrazoles by the response of amines (**48, 50**) with sodium azide and triethyl orthoformate in acidic medium [34, 36, 57–59].

2.13. Synthesis and characterization of new 5-supplemented 1*H*-tetrazoles in water: a greener approach

A blend of carbonyl compound, malononitrile, and sodium azide in the presence of H_2O was mixed at 50°C for proper time to outfit the required tetrazole [34, 60–63].

*2.13.1. Synthesis of (1*H*-tetrazole-5-yl) acrylonitrile (NPTA)*

3-Nitro benzaldehyde (**54**) reacts with malononitrile in the presence of sodium azide to give NPTA (**55**).

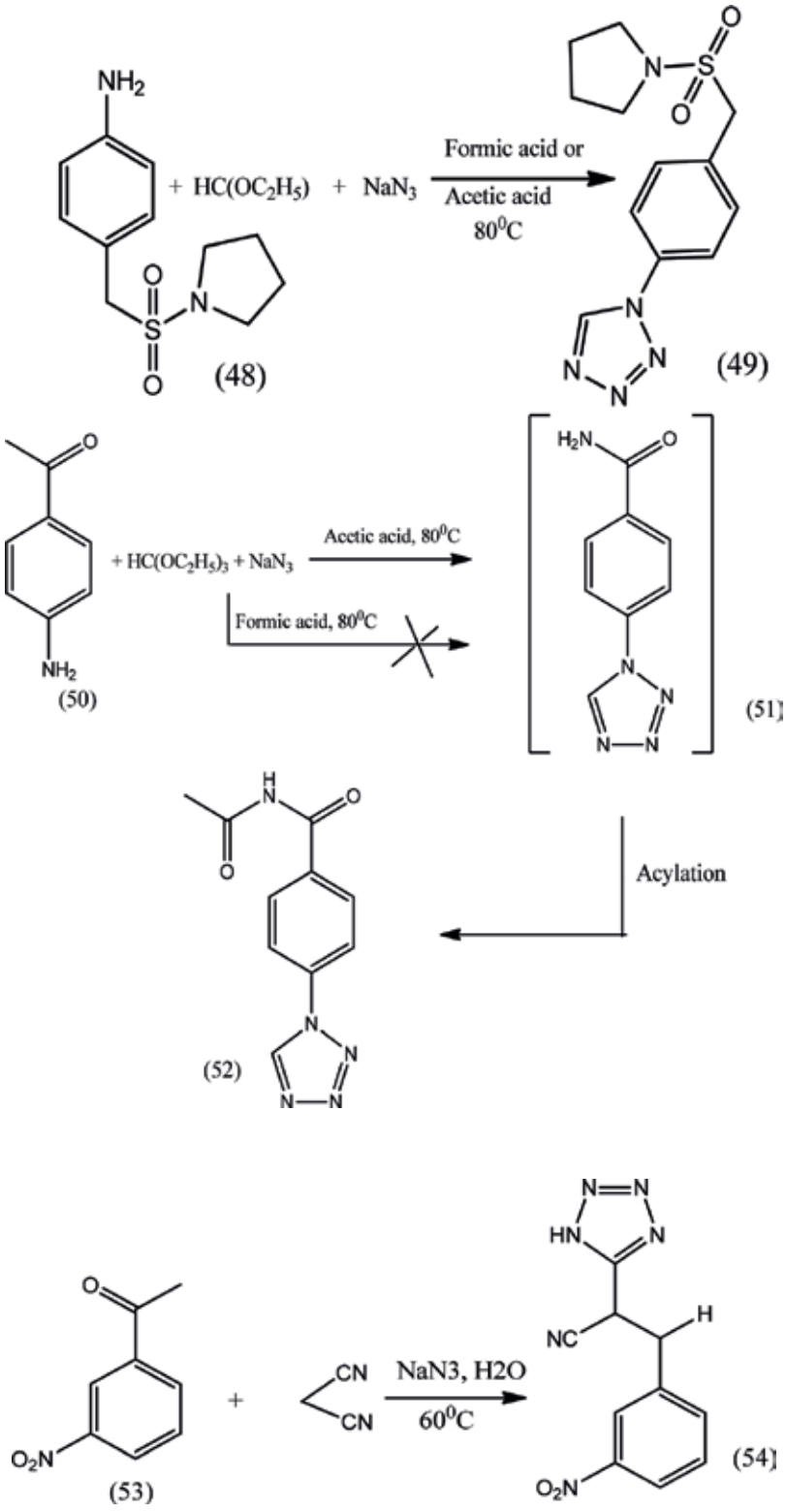
NH2
+ HC(OC2H5) + NaN3
Formic acid or
Acetic acid
80⁰C
(48)
(49)
+ HC(OC2H5)3 + NaN3
Acetic acid, 80⁰C
Formic acid, 80⁰C
(50)
(51)
Acylation
(52)
(53)
CN
CN
NaN3, H2O
60⁰C
(54)

2.13.2. Synthesis of (E)-3,3′-(phenyl)-bis (1,4(2-(1H-tetrazole-5-yl)) acrylonitrile) (PBTA)

Aryl dicarbonyl compound (**55**) reacts with malononitrile in the presence of sodium azide to give PBTA (**56**).

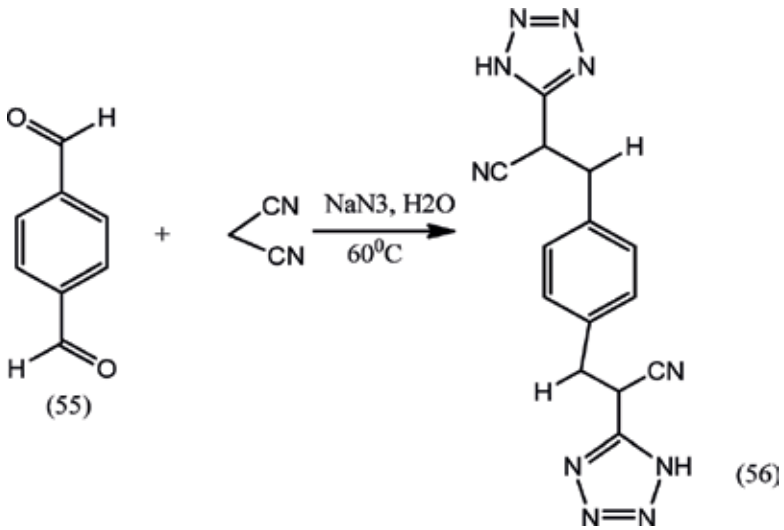

2.13.3. Synthesis of (z)-3-(hexahydro-2,4,6-trioxopyrimidine-5-yl)2-(1H-tetrazole-5-yl)-2-butane nitrile (BTBN)

2,4,6-Trioxo derivative-5-yl compound (**57**) reacts with malononitrile in presence of sodium azide to give BTBN (**58**).

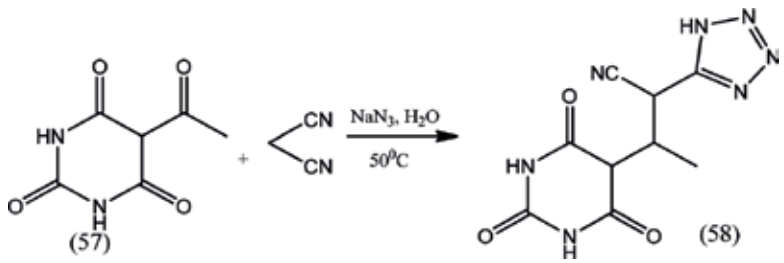

2.14. Preparation of 5-phenyltetrazole and its *N*-methyl derivatives

Azidation of benzonitrile (**59**) with dimethylammonium azide passive 5-phenyltetrazole dimethylammonium salt (**60**) was executed under microreactor setting. The energy of azidation of benzonitrile in DMF was examined at the range 80–95°C. The thermodynamic parameters of azidation under the microreactor conditions relate to the component of the 1,3-dipolar cycloaddition of azides to nitriles [17, 64–67].

http://dx.doi.org/10.5772/intechopen.75720

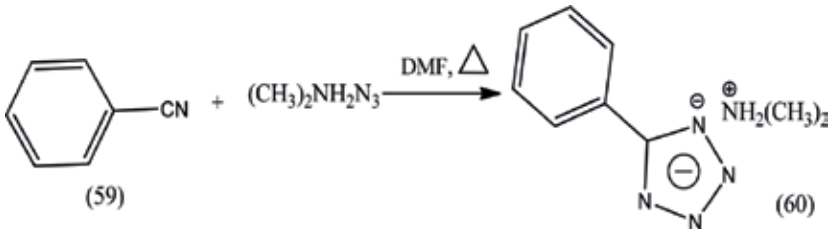

2.15. Synthesis, characterization, and biological examination of novel thiazole outcomes carrying indole moiety bearing tetrazole

A mixture of indole-3-carbaldehyde (**62**) and chloroethyl acetic acid was mixed in DMF. To this, anhydrous K_2CO_3 is included, and the response reaction mixture is mixed at room temperature (35°C) for 8 hours, to manage the effective yield of 2-(3-formyl-1*H*-indol-1-yl) acetate (**63**).

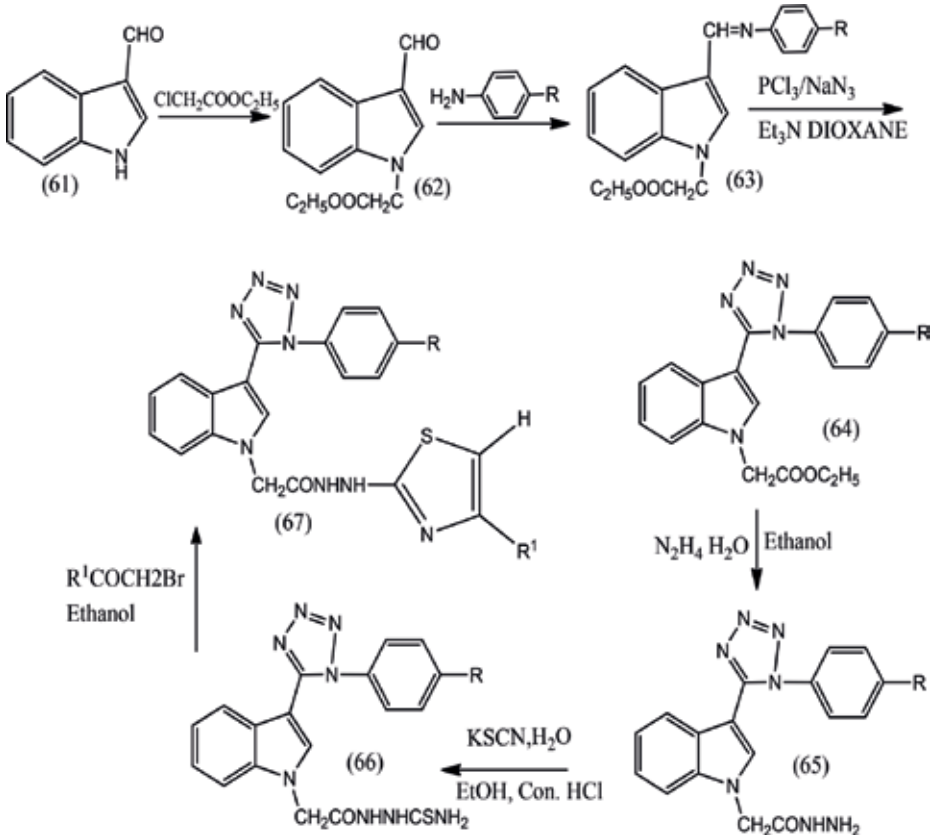

To this mixture, aniline, EtOH, and three drops of acidic corrosive are included and after that a warmed steam shower for 5–6 h to obtain the compound (**64**) ethyl 2-(3-phenyl amino)methyl-1*H*-indole-1-yl-acetic acid. Compound (**64**) is changed over into ethyl2-(3-(1-phenyl-1*H*-tetrazol-5-yl)-1*H*-indol-1-yl)acetate (**65**) by utilizing of conditions. Schiff base combination of thiazole subsidiaries containing indole moiety bearing tetrazole ring (**66**) was incorporated by the buildup of 2-(3-(3-chloro-1-(4-substituted phenyl)-4-tetrazole-2-yl)-1*H*-indole-1-yl) acetohydrazide with potassium thiocyanide and substituted ketones. At that point 1-(2-(3-(3-chloro-1-(4-substituted phenyl)-4-tetrazole-2-yl)-1*H*-indol-1-yl)acetyl)-4-(2-(4-substituted phenyl)hydrazono)-3-(trifluoromethyl)-1*H*-pyrazol-5(4*H*)-one (**67**) is obtained [68–72].

2.16. A fast metal-free union of 5-substituted-1*H*-tetrazoles utilizing cuttlebone as a characteristic high compelling and minimal effort heterogeneous catalyst

Cuttlebone has a characteristic minimal effort heterogeneous impetus with high porosity. It carries high flexural firmness, high compressive quality, and high thermal solidness. Cuttlebone was taken out from cuttlefish (*Sepia esculenta*), which is ordinarily found in saltwater shorelines like Persian Gulf in Iran. This specimen can be found in a genuinely decent condition with negligible outer destruction. So as to evacuate contamination on the surface of cuttlebone, the catalyst has been powdered, washed with refined water, and dried at 100°C for 2 h [52, 73, 74]. The SEM image of cuttlebone was shown in **Figure 2**.

An advantageous, fast, and metal-free synthesis of 5-substituted-1*H*-tetrazoles (**70**) is depicted by [3+2] cycloaddition response of nitriles (**68**) with sodium azide (**69**).

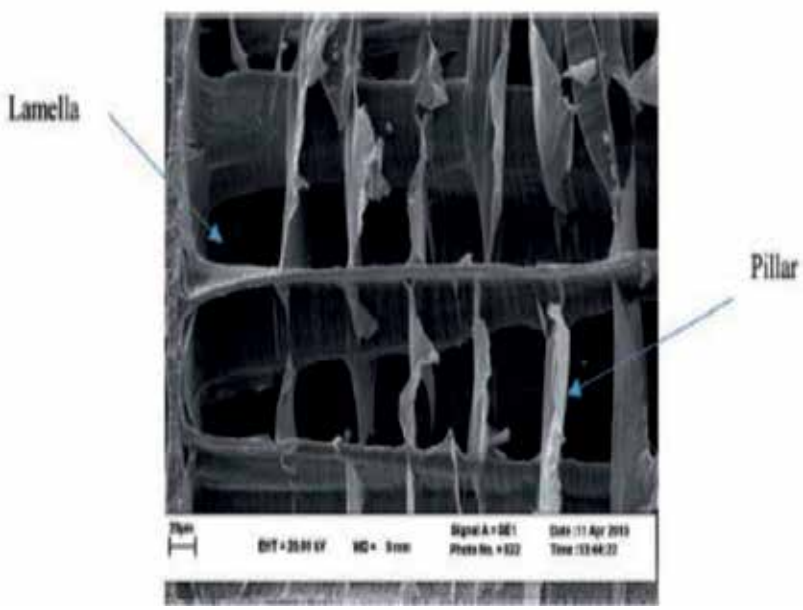

Figure 2. SEM image of cuttlebone.

http://dx.doi.org/10.5772/intechopen.75720

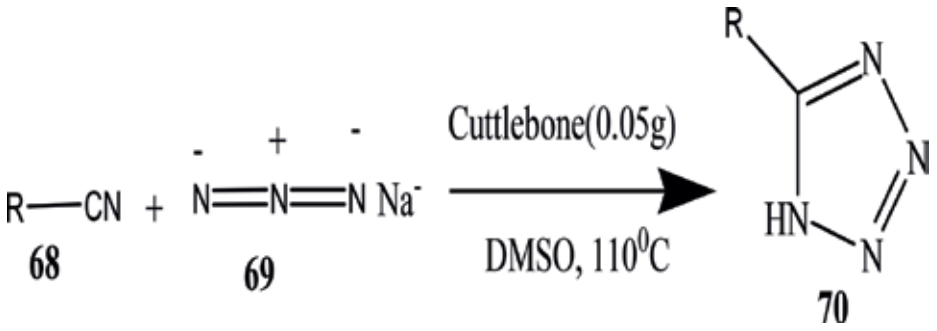

Figure 3 describes the system for the synthesis of 5-substituted-1*H*-tetrazoles within the sight of cuttlebone [30, 75].

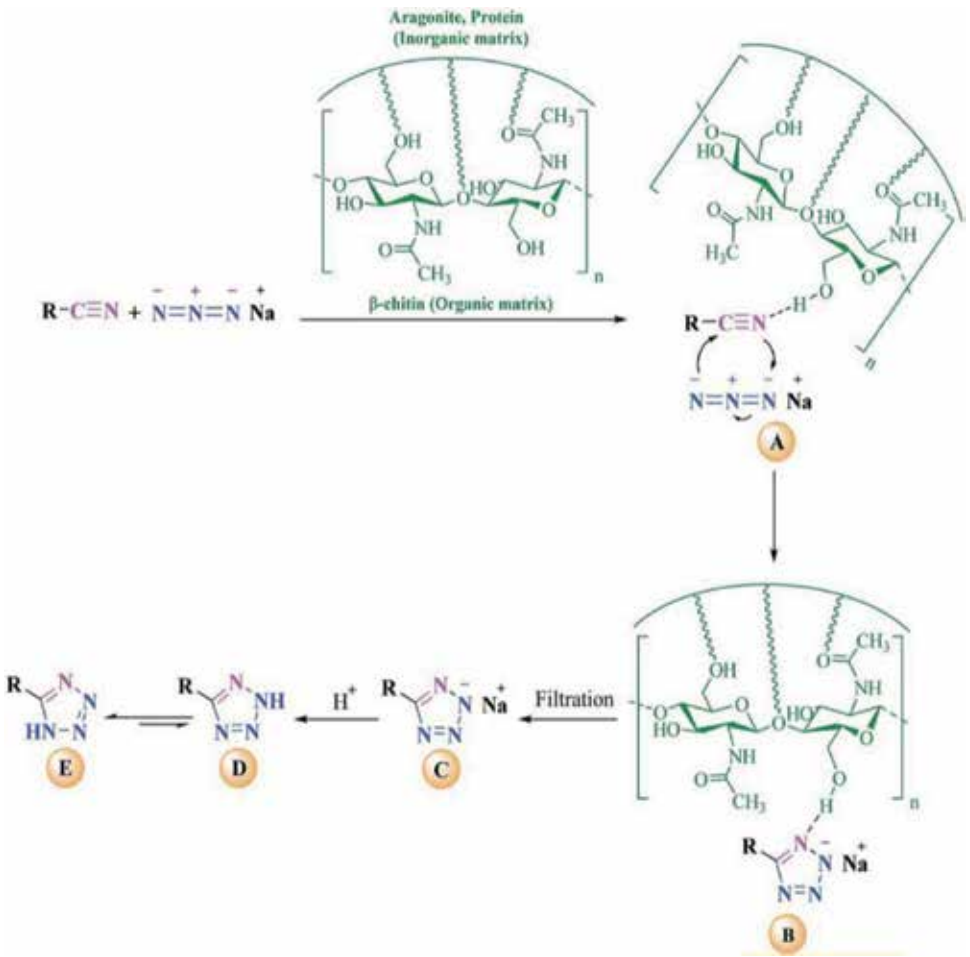

Figure 3. Synthesis of 5-substituted-1*H*-tetrazoles in the sight of cuttlebone.

3. Molecular docking-tetrazole derivatives

There are several literature reports pertaining to molecular docking studies of divergent tetrazole derivatives. We are citing a few for basic understanding of the readers who can explore this field a lot.

Very recently, Jonnalagadda et al. have synthesized some tetrazole-linked benzochromene derivatives and had their molecular docking study as well [76]. 5-Substituted 5-styryl terazolo [1,5-c]quinazoline derivatives were studied for their cytotoxicity and molecular docking by Parbhoo et al. [77]. In a similar fashion, several tetrazole derivatives were synthesized and subject to molecular docking in recent years [78–82].

4. Conclusion

The synthesis of tetrazole derivatives can be approached in various methods like ecofriendly, water solvent, moderate conditions, nontoxic, easy extractions, easy setup, low cost, etc. with good to excellent yields. The structural analysis was done by thermal and spectroscopic methods. Tetrazole and its derivatives play very important role in medicinal and pharmaceutical applications. Molecular docking studies play a vital role to decide the synthesis of pharmacologically relevant tetrazole derivatives in the near future. This facilitates, in fact, for new researchers to choose this topic as an apt and relevant research topic to explore.

Acknowledgements

Dr. Ravi Varala thanks honorable Vice Chancellor, Sri Dr. A. Ashok, IAS, RGUKT Basar, and T. N. Venkata Swamy, administrative officer, for his kind support and encouragement.

Author details

Ravi Varala[1]* and Bollikolla Hari Babu[2]

*Address all correspondence to: ravivarala@rgukt.ac.in

1 Department of Chemistry, Rajiv Gandhi University of Knowledge Technologies, Basar, Nirmal, Telangana, India

2 Department of Chemistry, Acharya Nagarjuna University, Guntur, Andhra Pradesh, India

References

[1] Joule JA, Mills K. Heterocyclic Chemistry. 4th ed. Germany: Blackwell Publishing House; pp. 507-511

[2] Rossi S, editor. Australian Medicines Handbook. Adelaide: Australian Medicines Handbook Pty Ltd. 2011

[3] Dahlof B, Deveruex RB, Kjeldsen SE. Cardiovascular morbidity and mortality in the Losartan Intervention for endpoint reduction in hypertension study (LIFE): A randomised trial against atenolol. Lancet. 2002;**359**(9311):995-1003

[4] Bhalla Y, Puri E, Monga P, Sapra S. Medicinal and chemical aspects of tetrazoles: An overview. Innovations in Pharmacy Plane. Synthesis and biological evaluation of New 4-amino tetrazole [1,5-9] quinoline. 2013;**1**(1):20-30

[5] Butler RN. In: Katritzky AR, Rees CW, Scriven EFV, editors. Comprehensive Heterocyclic Chemistry II. Vol. 4, 17. New York: Elsevier; 1996. Chapter 4. p. 621

[6] Singh H, Chawla AS, Kapoor VK, Paul D, Malhotra R. In: Ellis GP, West GB, editors. Progress in Medicinal Chemistry. Vol. 17. North Holland: Elsevier/North-Holland Biomedical Press; 1980. Chapter 4. p. 151

[7] Ostrovskii VA, Pevzner MS, Kofman TP, Shcherbinin MB, Tselinskii IV. In: Attanasi OA, Spinelli D, editors. Targets in Heterocyclic Systems – Chemistry and Properties. Vol. 3. Rome: Italian Society of Chemistry; 1999. p. 467

[8] Jiang C, Yu Z, Wang S, Jiao C, Li J, Wang Z, Cui Y. Rational design of metal-organic frameworks based on 5-(4-Pyridyl)tetrazolate: From 2D grids to 3D porous networks. European Journal of Inorganic Chemistry. 2004;**43**:3662-3667

[9] Bhaskar VH, Mohite PB, Pandhare RB, Khanage SG. Acta Pharmaceutica Sciencia. 2010;**52**:504

[10] Mulwad VV, Pawar Rupesh B, Chaskar Atul C. Journal of the Korean Chemical Society. 2008;**52**(3):249-256

[11] Upadhayaya RS, Jain S, Sinha N, Kishore N, Chandra R, Arora SK. European Journal of Medicinal Chemistry. 2004;**39**:579

[12] Bachar SC, Lahiri SC. Pharmazie. 2004;**59**:435

[13] Bladin JA. Berichte der Deutschen Chemischen Gesellschaft. 1885;**18**:1544

[14] Hantzsch A, Vagt A. Justus Liebigs Annalen der Chemie. 1901;**314**:339

[15] Butler RN. In: Katritzky AR, Rees CW, Scriven EFV, editors. Comprehensive Heterocyclic Chemistry. Vol. 4. Oxford, UK: Pergamon; 1996

[16] Moderhack DJ. Journal für praktische Chemie. 1988;**340**:687

[17] Ostrovskii VA, Koldobskii GI, Trifonov RE. In: Katritzky AR, Ramsden CA, Scriven EFV, Taylor RJK, editors. Comprehensive Heterocyclic Chemistry III. Vol. 6. Oxford: Elsevier; 2008. p. 257

[18] Gaponik PN, Voitekhovich SV, Ivashkevich OA. Russian Chemical Reviews. 2006;**75**:507

[19] Anacona JR, Alvarez P. Transition Metal Chemistry. 2002;**27**:856

[20] Chohan ZH, Supuran CT, Scozzafava A. Journal of Enzyme Inhibition and Medicinal Chemistry. 2004;**19**:79

[21] Ostrovskii VA, Zubarev VY, Putis SM, Trifonov RE, Popova EA, Pinchuk LS. Khimicheskaya Promyshlennost. 2005;**82**:605

[22] Andreeva NP, Kazanskiy LP, Seljaninov IA, Kuznetzov YI, Ostrovskii VA. Korroziya: Materialy, Zashchita. 2008;**12**:1

[23] Voitekhovich SV, Gaponik PN, Koldobskii GIR. The Journal of Organic Chemistry. 2005; **41**:1565

[24] Bhandari S, Mahon MF, Molloy KC, Palmer JS, Sayers SF. Thallium(I)- and organothallium (III)-substituted mono-, bis- and tris-tetrazoles: Synthesis and supramolecular structures. Journal of the Chemical Society Dalton Transactions. 2000;**7**:1053-1060

[25] Brubaker CH. Journal of the American Chemical Society. 1960;**82**:82

[26] Daugherty NA, Brubaker CH. Journal of Inorganic and Nuclear Chemistry. 1961;**22**:193

[27] Bergmans S, Hunt J, Roach A, Goldsmith P. Epilepsy Research. 2007;**75**:18

[28] Myznikov LV, Hrabalek A, Koldobskii GI. Chemistry of Heterocyclic Compounds. 2007;**43**:1

[29] Klaubert HD, Sellstedt JH, Guinosso CJ, Bell SC, Capetola RJ. Journal of Medicinal Chemistry. 1981;**24**:748

[30] Toney JH, Fitzgerald PMD, Grover Sharma N, Olson SH, May WJ, Sundelof JG, Venderwall DE, Cleary KA, Grant SK, Wu JK, Kozarich JW, Pompliano DL, Hammond GG. Chemistry & Biology. 1998;**5**:185

[31] Butter RN, Katritzky AR, Rees CW. The structure, reactions, synthesis and uses of heterocyclic compounds. Comprehensive Heterocyclic Chemistry. 1984;**5**:791

[32] Beattie DT, Connor HE, Feniuk W, Humphrey PPA. Reviews in Contemporary Pharmacotherapy. 1994;**5**:285-294

[33] Humphrey PPA, Feniuk W. Trends in Pharmacological Sciences. 1991;**12**:444-446

[34] Okabayashi T, Kano H, Makisumi Y. Chemical & Pharmaceutical Bulletin. 1960;**8**:157

[35] Sangal SK, Ashok Kumar A. Journal of the Indian Chemical Society. 1986;**63**:351

[36] Witkowski JK, Robins RK, Sidwell RW, Simon LN. Journal of Medicinal Chemistry. 1972; **15**:1150-1154

[37] Tripathy R, Ghose A, Singh J, et al. 1,2,3-Thiadiazole substituted pyrazolones as potent KDR/VEGFR-2 kinase inhibitors. Bioorganic & Medicinal Chemistry Letters. 2007;**17**: 1793-1798

[38] Dong WL, Liu ZX, Liu XH, Li ZM, Zhao WG. Synthesis and antiviral activity of new acrylamide derivatives containing 1,2,3-thiadiazole as inhibitors of hepatitis B virus replication. European Journal of Medicinal Chemistry. 2010;**45**:1919-1926

[39] Fan ZJ, Yang ZK, Zhang HK, et al. Synthesis, crystal structure, and biological activity of 4-methyl-1,2,3-thiadiazole- containing 1,2,4-triazolo[3,4-b][1,3,4]thiadiazoles. Journal of Agricultural and Food Chemistry. 2010;**58**:2630-2636

[40] Zuo X, Mi N, Fan ZJ, et al. Synthesis of 4-methyl-1,2,3-thiadiazole derivatives via Ugi reaction and their biological activities. Journal of Agricultural and Food Chemistry. 2010; **58**:2755-2762

[41] Padmavathi V, Mahesh K, Nagendra Mohan AV, Padmaja A. Synthesis and bioassay of oxazolyl/thiazolyl selenadiazoles, thiadiazoles and diazaphospholes. Chemical & Pharmaceutical Bulletin. 2009;**57**:561-566

[42] Tripathi KD. Essentials of Medicinalpharmacology. 5th ed. New Delhi: Jaypee brothers medical publishers Pvt Ltd.; 2008. p. 627

[43] Ueda I, Ishii K, Sinozaki K, Htanaka M. Antiulcer Agents. II. Synthesis and gastric acid antisecretory activity of N-[3-(3-(piperidinomethyl)phenoxy)propyl]-4-(1-methyl-1H-tetrazol-5-ylthio)butanamide and related compounds. Chemical & Pharmaceutical Bulletin (Tokyo). 1991;**39**:1430-1435

[44] Butler RN. In: Katritzky AR, Rees CW, editors. Comprehensive Hetrocyclic Chemistry. One step synthesis of sterically hindered 1,5-di substituted tetrazoles from Bulky secondary N-benzoyl amides using triazidochloro silane. (TACS). Vol. 5 (part 4A). Oxford: Pergamon; 1984. pp. 791-838

[45] Abe T, Goto T, Hattori Y, Ito S, Kido K, Kurahashi Y, Dr. Maurer F, Otsu Y, Sawada H, Shibuya K, Tanaka K. 1-Phenyl-5-anilinotetrazoles derivatives, their preparation and their use as microbiocides, insecticides and/or herbicides. Publication number EP 0855394 A1, Application number EP19980100673, Published as US5981438. 1998

[46] Butler RN. In: Alan RK, Charles WR, Scriven EFV, editors. Comprehensive Heterocyclic Chemistry II. Oxford: Pergamon; 1996. pp. 621-678

[47] Bhat MR, Jeddi NM, Walikar AB, Patil MB. A novel synthesis and characterization of 5-substituted tetrazole derivatives. Asian Journal of Biomedical and Pharmaceutical Sciences. 2011;**1**:13-17

[48] Su WK, Hong Z, Shan WG, Zhang XX. A facile synthesis of 1-substituted-1 *H*-1,2,3,4-tetrazoles catalyzed by ytterbium triflate hydrate. European Journal of Organic Chemistry. 2006;**12**:2723-2726

[49] Singh H, Chawla AS, Kapoor VK, Paul D, Malhotra RK. Progress in Medicinal Chemistry. 1980;**17**:151-183

[50] Muraglia E, Kinzel OD, Laufer R, Miller MD, Moyer G, Munshi V, Orvieto F, Palumbi MC, Pescatore G, Rowley M. Bioorganic & Medicinal Chemistry Letters. 2006;**16**:2748-2752

[51] García G, Rodríguez-Puyol M, Alajarín R, Serrano I, Sánchez- Alonso P, Griera M, Vaquero J, Rodríguez-Puyol D, Alvarez-Builla J, Díez-Marques MJ. Medicinal Chemistry. 2009;**52**:7220-7227

[52] Herr RJ. Bioorganic & Medicinal Chemistry. 2002;**10**:3379-3393

[53] a) Chu SS. Drugs of the Future. 1985;**10**:632-635

[54] Davulcu A, Mc Leod D, Li J, Katipally K, Littke A, Doubleday W, Xu Z, McConlogue C, Lai C, Gleeson M, Schwinden M, Parsons R. The Journal of Organic Chemistry. 2009;**74**: 4068-4079

[55] Koldovskii GI, Kharbash RB. Russian Journal of Organic Chemistry. 2003;**39**:453-470

[56] Cannon JR, Eacho PI. Biochemical Journal. 1991;**280**:387-391

[57] Sangal SK, Ashok Kumar A, Indian J. Chemical Society. 1986;**63**:351

[58] Tsov KC, Su HCF. Journal of Medicinal Chemistry. 1963;**6**:693

[59] Bary VC, Conalty MC, O'Sllivan JP, Twomey D. Chemotherapy. 1977;**8**:103

[60] Jakhar K, Makrandi JK. Green Chemistry Letters and Reviews. 2008;**1**:219

[61] Jiang B, Tu SJ, Kaur P, Wever W, Li G. Journal of the American Chemical Society. 2009; **131**:11660

[62] Enders D, Huttl MRM, Grondal C, Raabe GJ. Nature. 2006;**441**:861

[63] Genin MJ, Allwine DA, Anderson DJ, Barbachyn MR, Emmert DE, Garmon SA, Graber DR, Grega KC, Hester JS, Hutchinson DK, Morris J, Reischer RJ, Ford CW, Zurenko GE, Hamel JC, Schaadt RD, Stapert D, Yagi BH. Journal of Medicinal Chemistry. 2000;**43**:953

[64] Palde PB, Timothy F, Jamison TF. Angewandte Chemie, International Edition. 2011; **50**:3525

[65] Abiev RS. Russian Journal of General Chemistry. 2012;**82**:2019

[66] Popova EA, Pavlyukova YN, Popov EV, Ostrovskii VA, Trifonov RE. Russian Journal of Organic Chemistry. 2009;**45**:890

[67] Ostrovskii VA, Poplavskii VS, Koldobskii GI, Erusalimskii GB. Khimiya Geterotsiklicheskikh Soedinenii. 1992:1214

[68] Bulmer GS. Introduction to Medical Mycology. 2nd ed. London: Benjamin cumiimmgs publishing; 2002. pp. 80-100

[69] Cruick, Shank R, Duguid JP, Marmion BP, Swain RT. Medicinal Microbiology. 12th ed. Vol. 26. London: Churchill Livingstone, Elsevier; 1975. p. 196

[70] Iro A, Athina G, Paola V, Franca Z. Synthesis and biological evalution of sulfonamide thiazole derivatives as antimicrobial agents. Journal of Chemistry. **3**(13):267-273

[71] Janssen AM, Scheffer JC, Svendsen AB. Antimicrobial activity of essential oils. Journal of Medicinal Plants. 2002;**53**(5):395-398

[72] McEvoy GK. Drug information. American society of health-system pharmacists. J. Inc., USA. 2006, Vol. 5, No. 1, pp. 91-96

[73] Ford RE, Knowles P, Lunt E, Marshal SM, Penrose AJ, Ramsden CA, Summers AJH, Walker JL, Wrigth DE. Journal of Medicinal Chemistry. 1986;**29**:538

[74] Hallinan EA, Tsymbalov S, Dorn CR, Pitzele BS, Hansen DW Jr. Journal of Medicinal Chemistry. 2002;**45**:1686

[75] Inada Y, Wada T, Shibouta Y, Ojima M, Sanada T, Ohtsuki K, Itoh K, Kubo K, Kohara Y, Naka T. The Journal of Pharmacology and Experimental Therapeutics. 1994;**268**:1540

[76] Sridevi G, Maddila S, Maddila SN, Naicker K, Singh M, Parvesh S, Jonnalagadda SB. Anti-Cancer Agents in Medicinal Chemistry. 2017;**17**(3):464-470

[77] Mphahlele MJ, Gildenhuys S, Parbhoo N. Molecules. 2017;**22**:1719-1732

[78] Al-Hourania BJ, McDonaldb R, El-Barghouthic MI, Al-Awaidaa W, Sharmad SK, Wuestd F. Jordan Journal of Chemistry. 2015;**10**(1):34-40

[79] Reddivari CKR, Subba Rao Devineni SR, Venkateshwarulu JKM, Baki VB, Chippada AR, Wudayagiri R, Venkata RRY, Chamarthi NR. European Journal of Chemistry. 2017;**8**(1): 66-75

[80] Navarrete-Vázquez G, Palacios AA, Hidalgo-Figuero S, González-Acevedo C, Ávila-Villarreal G, Estrada-Soto S, Webster SP, Medina-Franco JL, López-Vallejo F, Guerrero-Álvarez J, Tlahuext H. Bioorganic & Medicinal Chemistry Letters. 2013;**23**:3244-3247

[81] Al-Hourani BJ, Sharma SK, Kaur J, Wuest F. Medicinal Chemistry Research. 2015;**24**(1):78-85

[82] Al-Hourani BJ, Al-Awaida W, Matalka KZ, Musa I, El-Barghouthi MI, Alsoubani F, Wuest F. Bioorganic & Medicinal Chemistry Letters. 2016;**26**(19):4757-4762

Chapter 5

Docking Studies on Novel Analogues of 8-Chloro-Quinolones against *Staphylococcus aureus*

Lucia Pintilie and Amalia Stefaniu

Additional information is available at the end of the chapter

http://dx.doi.org/10.5772/intechopen.72995

Abstract

Molecular docking studies have been carried out for a better understanding of the drug-receptor interactions. All the synthesized compounds have been subjected to molecular docking against targets that have been chosen based on the specific mechanism of action of the quinolones used in the antibacterial activity screening. A study of the characteristics and molecular properties of the small molecule known as ligand has been realized. In the first stage of the study, the 2D and 3D structures have been generated. The most stable conformer for each structure was obtained by geometry optimization and energy minimization. A series of topological, conformational characteristics and QSAR properties, important to assess the flexibility and the ability of the studied conformer to bind to the protein receptor, were determined and analyzed. These properties were discussed in order to assess the flexibility and the binding ability of studied conformers to bind to the receptor protein. The docking studies have been carried out. The score and hydrogen bonds formed with the amino acids from group interaction atoms are used to predict the binding modes, the binding affinities and the orientation of the docked quinolones in the active site of the protein receptor.

Keywords: molecular docking, antimicrobial activity, fluoroquinolones, quinolones

1. Introduction

An important parameter in the development of a new drug is the drug's affinity to the identified target (protein/enzyme). Predicting the ligand binding to the target (protein/enzyme) by molecular simulation would allow the synthesis to be restricted to the most promising compounds [1–9]. Molecular docking can be accomplished by two interdependent steps [7–9]. The first step consists in sampling the ligand conformations in the active site of the protein receptor. The second step is to classify these conformations by a scoring function. The sampling algorithms

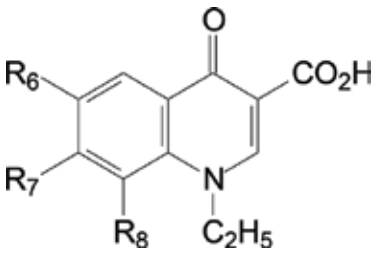

Figure 1. The structure of the quinolone compounds.

should be able to reproduce experimental binding mode. Various algorithms used for docking analysis are molecular dynamics, Monte Carlo methods, genetic algorithms, fragment-based methods, point complementary methods and distance geometry methods, systematic searches. The scoring function should classify the highest among all the generated conformations. These mathematical models are used to predict the strength of binding affinity called noncovalent interaction between two molecules after they have been docked. They have also developed scoring function to predict the strength of other types of intermolecular interactions, for example, between two proteins or between proteins and DNA or protein and drug. These configurations are evaluated using the scoring functions to distinguish experimental binding modes of all other ways explored by the search algorithm. The goal of molecular docking is to predict the ligand-receptor complex structure by computation method to identify new active molecules that bind to a biological target [10–14]. The main methods used for docking are Lock and Key/Rigid Docking and Induced Fit/Flexible Docking. In rigid docking, the internal geometry of the receptor and ligand is kept fixed and docking is performed. In flexible docking, enumeration on the rotations of one of the molecules (usually smaller one) is performed. Every rotation, the surface cell occupancy and energy are calculated; later, the most optimum pose is selected.

This chapter presents design and molecular docking studies about 8-chloro-quinolone compounds. The influence of the presence of chlorine atom in the eighth position of the quinolone ring (**Figure 1**, where R_8 = Cl) on the antimicrobial activity against *Staphylococcus aureus* has been studied. The predicted activity has been correlated with the experimental activity who has been determined by agar dilution method [15, 16].

Drugs belonging to the quinolone compound are characterized by a quicker biological activity and a larger antibacterial spectrum. They are active on both gram-positive and gram-negative bacteria, as well as on recently discovered bacteria with intercellular development (Legionella, Mycoplasma, etc.), or even on acid-resistant bacteria (*M. tuberculosis* and *M. leprae*). The area of use of quinolones has expanded from urinary infections to systemic acute and chronic infections (lung and bronchus infections, osteitis, septicemia and endocarditis, chronic infections [chronic bronchitis, purulent osteoarthritis, chronic prostatite, cystitis and chronic sinusitis]) [15, 16].

2. Materials and methods

Molecular docking studies have been performed with CLC Drug Discovery Workbench Software in order to achieve accurate predictions on optimized conformation for both the quinolone (as

ligand) and their target receptor protein to form a stable complex. Molecular docking studies have been performed on topoisomerase II DNA gyrase with 32 quinolone compounds to understand the binding affinity of all quinolones with DNA gyrase. The crystal structure of topoisomerase II was downloaded from Protein Data Bank (PDB ID: 2XCT) [17]. The quinolone compounds have been synthesized in our laboratory [16], and their structures are shown in **Figure 1** and **Table 1**.

2.1. Ligand preparation

The ligands have been prepared using SPARTAN'14 software package [18]. In this study, the DFT/B3LYP/6–31G* level of basis set has been used for the computation of molecular structure, vibrational frequencies and energies of optimized structures (**Figure 2**). In order to perform structure–activity relationship (SAR) studies, some electronic properties (**Table 2**) such as highest occupied molecular orbital (HOMO) and lowest unoccupied molecular orbital (LUMO) energy values, HOMO and LUMO orbital coefficient distribution, molecular dipole moment, polar surface area (PSA), the ovality, polarizability, the octanol water partition coefficient (logP), the number of hydrogen-bond donors (HBDs) and ad acceptors (HBAs) and acceptor sites (HBAs) and positive and negative ionizable sites are derived from CFD assignments. HBA/HBD and ±Centers, Hydrophobe Centers including aromatic centers, can be viewed in **Figure 2**, for the quinolones FPQ 28 and 6ClPQ 28 (compounds that showed good activity against MRSA [19]). The polarizability is useful to predict the interactions between nonpolar atoms or groups and other electrically charged species, such as ions and polar molecules having a strong dipole moment.

2.1.1. Molecular polar surface area (PSA)

Molecular polar surface area (PSA) [20] is a descriptor that has been shown to correlate well with passive molecular transport through membranes and therefore allows the prediction of transport properties of the drugs. Log P is estimated according to the method of Ghose, Pritchett and Crippen [21]. A number of important graphical quantities resulted from quantum chemical calculations were displayed, manipulated and interrogated. Another indicator of electrophilic addition local map is provided by the ionization potential, an overlapping of the energy of electron removal (ionization) on the electron density. In addition, the *electrostatic potential map*, an overlay of the electrostatic potential (the attraction or repulsion of a positive charge for a molecule) on the electron density, is valuable for describing the overall distribution of molecular charge, as well as to predict the sites of electrophilic addition. Another indicator of the electrophilic addition is supplied by the *local ionization potential map*, an overlapping of the energy of electron removal (ionization) on the electron density. In the end, an indicator of nucleophilic addition is offered by the $|LUMO|$ *map*, an overlap of the absolute value of the lowest unoccupied molecular orbital (LUMO).

2.1.2. Frontier molecular orbital analysis

The molecular orbital analysis of the Frontier molecular orbitals (FMOs) plays an essential role in the chemical stability of a molecule and in the interactions between atoms. They provide information that can be used to predict the characteristics of molecules such as optical properties and biological activities. Between them, the most important are the highest occupied molecular orbital (HOMO) and the lowest unoccupied molecular orbital (LUMO). The

Compounds	R_6	R_7	R_8
NF:1-Ethyl-6-fluoro-7-(piperazin-1-yl)-1,4-dihydro-4-oxo-quinoline-3-carboxylic acid	F	Piperazinyl	H
FPQ50:1-Ethyl-6-fluoro-7-(piperazin-1-yl)-8-chloro-1,4-dihydro-4-oxo-quinoline-3-carboxylic acid [20]	F	Piperazinyl	Cl
PF:1-Ethyl-6-fluoro-7-(4-methyl-piperazin-1-yl)-1,4-dihydro-4-oxo-quinoline-3-carboxylic acid	F	4-Methyl-piperazinyl	H
FPQ51:1-Ethyl-6-fluoro-7-(4-methyl-piperazin-1-yl)-8-chloro-1,4-dihydro −4-oxo-quinoline-3-carboxylic acid	F	4-Methyl-piperazinyl	Cl
FPQ27:1-Ethyl-6-fluoro-7-(3-methyl-piperazin-1-yl)-1,4-dihydro-4-oxo-quinoline-3-carboxylic acid	F	3-Methyl-piperazinyl	H
FPQ29.HCl:1-Ethyl-6-fluoro-7-(3-methyl-piperazin-1-yl)-8-chloro-1,4-dihydro-4-oxo-quinoline-3-carboxylic acid . hydrochloride	F	3-Methyl-piperazinyl	Cl
FPQ35:1-Ethyl-6-fluoro-7-(pyrrolidin-1-yl)-1,4-dihydro-4-oxo-quinoline −3-carboxylic acid	F	Pyrrolidinyl	H
FPQ36:1-Ethyl-6-fluoro-7-(pyrrolidin-1-yl)-8-chloro-1,4-dihydro-4-oxo-quinoline-3-carboxylic acid	F	Pyrrolidinyl	Cl
FPQ32:1-Ethyl-6-fluoro-7-(piperidin-1-yl)-1,4-dihydro-4-oxo-quinoline-3-carboxylic acid	F	Piperidinyl	H
FPQ33:1-Ethyl-6-fluoro-7-(piperidin-1-yl)-8-chloro-1,4-dihydro-4-oxo-quinoline-3-carboxylic acid	F	Piperidinyl	Cl
Q83:1-Ethyl-6-fluoro-7-(4-methyl-piperidin-1-yl)-1,4-dihydro-4-oxo-quinoline-3-carboxylic acid	F	4-Methyl-piperidinyl	H
Q85:1-Ethyl-6-fluoro-7-(4-methyl-piperidin-1-yl)-8-chloro-1,4-dihydro-4-oxo-quinoline-3-carboxylic acid	F	4-Methyl-piperidinyl	Cl
FPQ24:1-Ethyl-6-fluoro-7-(3-methyl-piperidin-1-yl)-1,4-dihydro-4-oxo-quinoline-3-carboxylic acid	F	3-Methyl-piperidinyl	H
FPQ30:1-Ethyl-6-fluoro-7-(3-methyl-piperidin-1-yl)-8-chloro-1,4-dihydro-4-oxo-quinoline-3-carboxylic acid	F	3-Methyl-piperidinyl	Cl
FPQ25:1-Ethyl-6-fluoro-7-(morpholin-1-yl)-1,4-dihydro-4-oxo-quinoline-3-carboxylic acid	F	Morfolinyl	H
FPQ28:1-Ethyl-6-fluoro-7-(morpholin-1-yl)-8-chloro-1,4-dihydro-4-oxo-quinoline-3-carboxylic acid	F	Morfolinyl	Cl
NClX:1-Ethyl-6-chloro-7-(piperazin-1-yl)-1,4-dihydro-4-oxo-quinoline-3-carboxylic acid	Cl	Piperazinyl	H
6ClPQ50:1-Ethyl-6,8-dichloro-7-(piperazin-1-yl)-1,4-dihydro-4-oxo-quinoline-3-carboxylic acid	Cl	Piperazinyl	Cl
PClX:1-Ethyl-6-chloro-7-(4-methyl-piperazin-1-yl)-1,4-dihydro-4-oxo-quinoline-3-carboxylic acid	Cl	4-Methyl-piperazinyl	H
6ClPQ51:1-Ethyl-6,8-dichloro-7-(4-methyl-piperazin-1-yl)-1,4-dihydro −4-oxo-quinoline-3-carboxylic acid	Cl	4-Methyl-piperazinyl	Cl
6ClPQ27:1-Ethyl-6-chloro7-(3-methyl-piperazin-1-yl)-1,4-dihydro-4-oxo-quinoline-3-carboxylic acid	Cl	3-Methyl-piperazinyl	H

Compounds	R_6	R_7	R_8
6ClPQ29:1-Ethyl-6,8-dichloro-7-(3-methyl-piperazin-1-yl)-1,4-dihydro-4-oxo-quinoline-3-carboxylic acid	Cl	3-Methyl-piperazinyl	Cl
6ClPQ35:1-Ethyl-6-chloro-7-(pyrrolidin-1-yl)-1,4-dihydro-4-oxo-quinoline-3-carboxylic acid	Cl	Pyrrolidinyl	H
6ClPQ36:1-Ethyl-6,8-dichloro-7-(pyrrolidin-1-yl)-1,4-dihydro-4-oxo-quinoline-3-carboxylic acid	Cl	Pyrrolidinyl	Cl
6ClPQ32:1-Ethyl-6-chloro-7-(piperidin-1-yl)-1,4-dihydro-4-oxo-quinoline-3-carboxylic acid	Cl	Piperidinyl	H
6ClPQ33:1-Ethyl-6,8-dichloro-7-(piperidin-1-yl)-1,4-dihydro-4-oxo-quinoline-3-carboxylic acid	Cl	Piperidinyl	Cl
Q80:1-Ethyl-6-chloro-7-(4-methyl-piperidin-1-yl)-1,4-dihydro-4-oxo-quinoline-3-carboxylic acid	Cl	4-Methyl-piperidinyl	H
Q87:1-Ethyl-6,8-dichloro-7-(4-methyl-piperidin-1-yl)-1,4-dihydro-4-oxo-quinoline-3-carboxylic acid	Cl	4-Methyl-piperidinyl	Cl
6ClPQ24:1-Ethyl-6-chloro-7-(3-methyl-piperidin-1-yl)-1,4-dihydro-4-oxo-quinoline-3-carboxylic acid	Cl	3-Methyl-piperidinyl	H
6ClPQ30:1-Ethyl-6,8-dichloro-7-(3-methyl-piperidin-1-yl)-1,4-dihydro-4-oxo-quinoline-3-carboxylic acid	Cl	3-Methyl-piperidinyl	Cl
6ClPQ25:1-Ethyl-6-chloro-7-(morpholin-1-yl)-1,4-dihydro-4-oxo-quinoline-3-carboxylic acid	Cl	Morfolinyl	H
6ClPQ28:1-Ethyl-6,8-dichloro-7-(morpholin-1-yl)-1,4-dihydro-4-oxo-quinoline-3-carboxylic acid	Cl	Morfolinyl	Cl

Table 1. The structure of the quinolone compounds.

HOMO represents the ability of a molecule to donate an electron, while the LUMO represents the ability to accept an electron [22, 23]. The HOMO and LUMO, calculated at the B3LYP/6-31G* level, can be seen in **Figure 3** for the gas phase, for the quinolones FPQ 28 and 6ClPQ 28 (compounds that showed good activity against MRSA [19]). The graphic has 'blue and red' regions. These correspond to positive and negative values of the orbital.

For the HOMO of 7-piperazinyl-8-unsubstituted-quinolones, electron density of NF, PF and FPQ27 is localized on piperazine heterocyclic, on aromatic ring and on 4-oxo group. For the HOMO of 7-piperazinyl-8-chloro-quinolones, electron density of FPQ 50 and FPQ 51 is localized on piperazine heterocyclic; for FPQ29 compound, electron density is localized on piperazine heterocyclic and C6, C8 and C10 atoms from aromatic ring. For the HOMO of 7-piperidinyl-8-unsubstituted-quinolones, electron density of Q 83, FPQ 24 and FPQ 32is localized on piperidine heterocyclic, and on C6, C7 and C8 atoms from aromatic ring. For the HOMO of 7-piperidinyl-8-chloro-quinolones, electron density of Q 85, FPQ 30 and FPQ 33is localized on piperidine heterocyclic, on C6, C7 and C8 atoms from aromatic ring and on chlorine atom. For the HOMO of 7-morpholinyl-8-unsubstituted-quinolone, FPQ 25 electron density is localized on morpholine heterocyclic, on aromatic ring and on 4-oxo group. For the HOMO of 7-morpholinyl-8-chloro-quinolone, FPQ 28 electron density is localized on

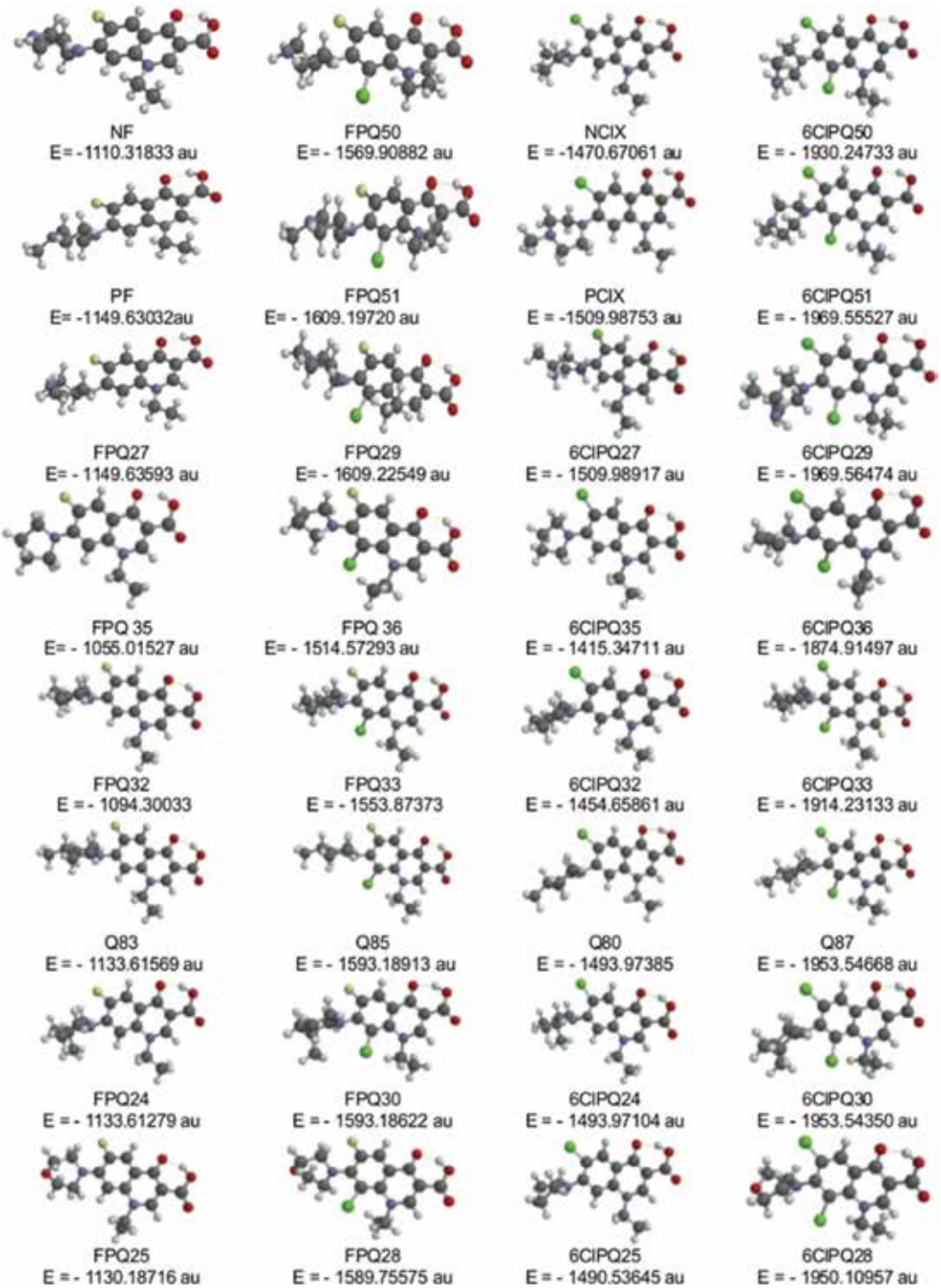

Figure 2. Optimized geometry of quinolone compounds.

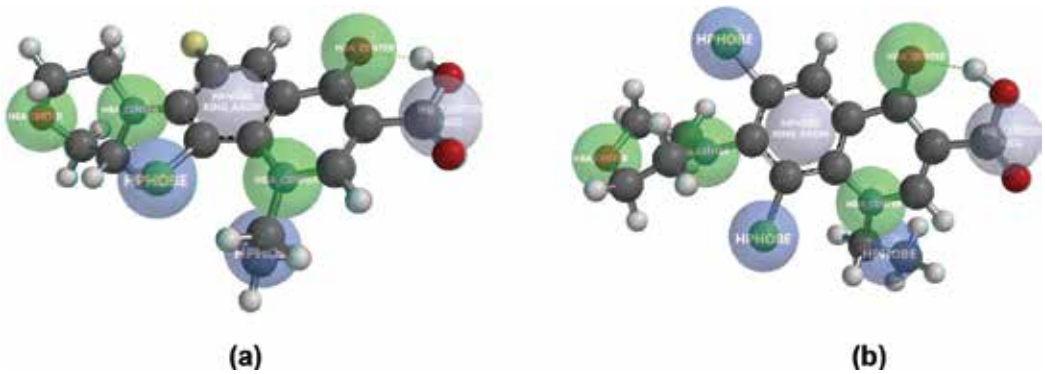

Figure 3. HBA/HBD and ±Centers, Hydrophobe centers of 8-chloro-quinolone compounds: (a) FQ28 (b) 6ClPQ28.

morpholine heterocyclic, on aromatic ring, on 4-oxo group and on chlorine atom. For the HOMO of 7-pyrrolidinyl-8-unsubstituted-quinolone, FPQ 35 electron density is localized on pyrrolidine heterocyclic, on aromatic ring and on 4-oxo group. For the HOMO of 7-pyrrolidinyl-8-chloro-quinolone, FPQ 36 electron density is localized on pyrrolidine heterocyclic, on aromatic ring, on 4-oxo group and on chlorine atom. For the LUMO of 7-substituted-8-unsubstituted-quinolones, NF, PF, FPQ27, O 83, FPQ 24, FPQ 32, electron density of FPQ 25 and FPQ 35 is localized on 4-piridinona ring and on aromatic ring. For the LUMO of 7-substituted-8-chloro-quinolones, electron density of FPQ 50, FPQ 51, FPQ29, O 85, FPQ 30, FPQ 33, FPQ 28 and FPQ 36 is localized on 4-piridinona ring, on aromatic ring B and on chlorine atom. For the 6-cloroqinolones, the electron density is located in the same manner as the corresponding fluoroquinolones.

The *frontier orbital gap* helps to characterize chemical reactivity of the molecule (**Table 2**). HOMO and LUMOs determine the way in which it interacts with other species. The introduction of the electron-withdrawing substituent (chlorine) at position C 8 in quinolone compounds decreases the HOMO-LUMO gap as compared to their corresponding 8-unsubstituted quinolone compounds (**Figure 4**).

2.1.3. Molecular electrostatic potential (MEP)

Molecular electrostatic potential (MEP) has been evaluated using B3LYP method with the basis set 6-31G* to investigate the chemical reactivity of a molecule. The MEP is especially important for the identification of the reactive sites of nucleophilic or electrophilic attack in hydrogen-bonding interactions and for the understanding of the process of biological recognition [21, 22]. An electrostatic potential map for quinolone compounds shows hydrophilic regions in red (negative potential) and blue (positive potential) and hydrophobic regions in green. In **Figure 5** can be viewed the MEP of the quinolones FPQ28 and 6ClPQ28.

The **local ionization potential map** provides another indicator of electrophilic addition; the local ionization map is an overlay of the energy of electron removal (ionization) on the

Compounds	Molecular properties									
	Dipole moment (debye)	E HOMO (eV)	E LUMO (eV)	HOMO-LUMO GAP	Polarizability (10^{-30} m^3)	PSA(Å^2)	Ovality	Log P	HBA count	HBD count
NF	12.76	−5.76	−1.41	4.35	65.09	56.587	1.45	1.37	5	1
FPQ50	8.71	−6.00	−2.02	3.98	66.33	57.344	1.46	1.92	5	1
PF	12.36	−5.77	−1.43	4.34	66.65	46.369	1.48	1.74	5	1
FPQ51	8.91	−5.79	−1.97	3.82	67.92	46.808	1.49	2.30	5	1
FPQ27	12.86	−5.76	−1.40	4.36	66.57	56.053	1.48	1.68	5	1
FPQ29	9.10	−6.01	−1.96	4.05	67.80	56.717	1.49	2.24	5	1
FPQ35	12.50	−5.77	−1.39	4.38	64.18	44.034	1.43	2.30	4	1
FPQ36	8.83	−6.14	−1.97	4.17	65.44	44.405	1.45	2.86	4	1
FPQ32	9.49	−6.63	−1.82	−4.81	65.58	45.402	1.46	2.72	4	1
FPQ33	8.28	−6.33	−2.05	4.28	66.75	44.781	1.47	3.28	4	1
Q83	9.49	−6.36	−1.82	4.54	67.06	45.389	1.49	3.05	4	1
Q85	8.29	−6.33	−2.05	4.58	68.23	44.785	1.50	3.61	4	1
FPQ24	9.48	−6.34	−1.82	4.52	67.07	45.295	1.48	3.12	4	1
FPQ30	8.23	−6.33	−2.06	4.27	68.24	44.768	1.50	3.68	4	1
FPQ25	10.15	−6.02	−1.58	4.44	64.87	51.758	1.44	1.59	5	1
FPQ28	8.26	−6.24	−1.97	4.97	66.00	51.859	1.45	2.15	5	1
NClX	8.80	−6.08	−1.93	4.15	65.98	57.537	1.47	1.77	5	1
6ClPQ50	7.81	−6.06	−2.11	3.95	67.11	56.756	1.48	2.32	5	1
PClX	11.84	−5.84	−1.59	4.25	67.42	46.688	1.49	2.14	5	1
6ClPQ51	8.69	−5.77	−2.07	3.07	68.72	46.277	1.51	2.70	5	1
6ClPQ27	8.56	−6.13	−1.93	4.20	67.46	57.339	1.59	2.08	5	1
6ClPQ29	8.00	−6.04	−2.10	3.94	68.60	56.469	1.51	2.64	5	1
6ClPQ35	12.16	−5.92	−1.54	4.38	64.92	44.303	1.44	2.70	4	1
6ClPQ36	8.51	−6.05	−2.09	3.96	66.27	43.934	1.47	3.26	4	1
6ClPQ32	9.48	−6.25	−1.89	4.36	66.39	44.937	1.47	3.12	4	1
6ClPQ33	8.26	−6.19	−2.11	4.08	67.57	44.194	1.49	3.68	4	1
Q80	9.47	−6.26	−1.89	5.07	67.86	44.979	1.50	3.45	4	1
Q87	8.26	−6.19	−2.12	4.07	69.04	44.205	1.51	4.01	4	1
6ClPQ24	9.47	−6.24	−1.89	4.35	67.88	44.863	1.50	3.52	4	1
6ClPQ30	8.27	−6.19	−2.12	4.07	69.05	44.304	1.51	4.08	4	1
6ClPQ25	7.85	−6.26	−1.97	4.29	65.69	52.427	1.46	1.99	5	1
6ClPQ28	6.68	−6.20	−2.20	−4.00	66.86	51.596	1.48	2.55	5	1

Table 2. Molecular properties for CPK model computations for quinolone compounds using Spartan'14 V1.1.4 software.

http://dx.doi.org/10.5772/intechopen.72995

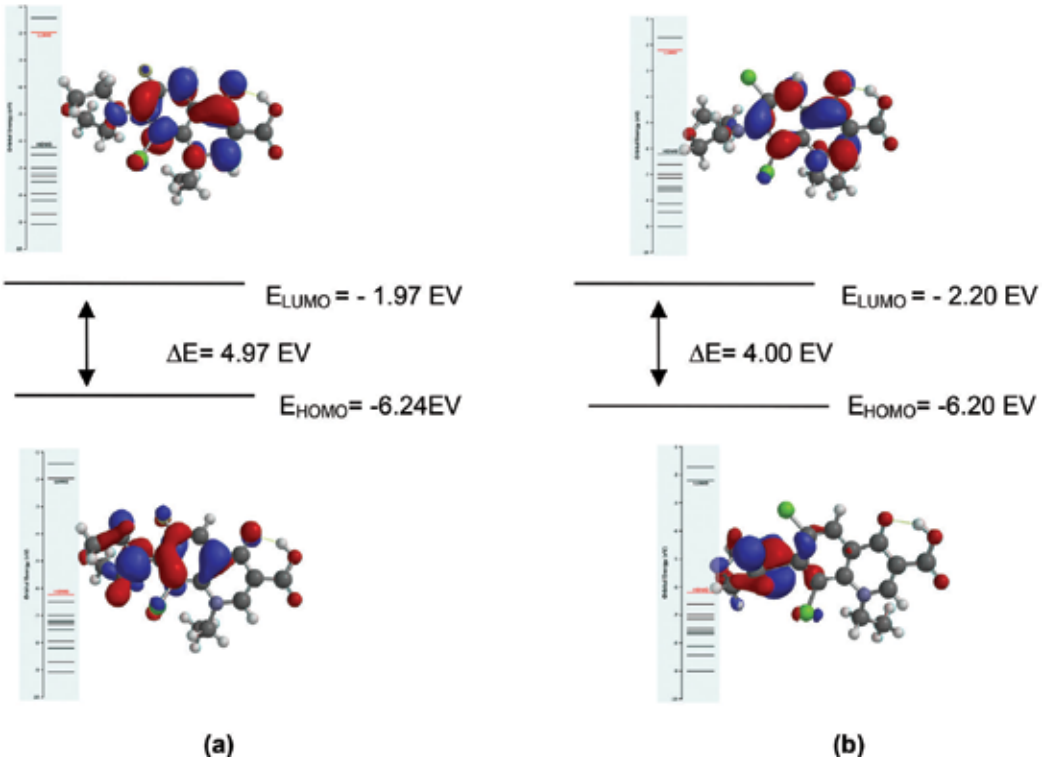

Figure 4. HOMO, LUMO surfaces of 8-chloro-quinolone compounds: (a) FQ28 (b) 6ClPQ28.

electron density (**Figure 6**). **|LUMO| map**, map that represents a superposition of the absolute value of the lowest unoccupied molecular orbital (the LUMO) on the electron density, provides another indicator of the nucleophilic addition (**Figure 7**).

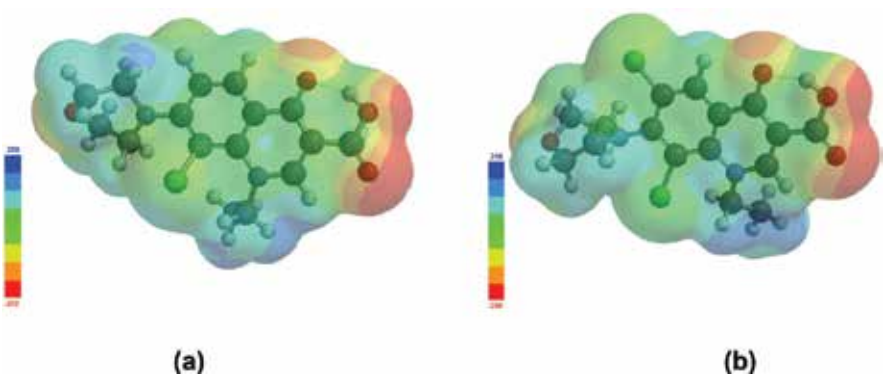

Figure 5. The optimized geometry and electrostatic potential pattern of the surface of (a) FPQ 28 and (b) 6ClPQ 28 (red—negative, high electron density, blue—positive area, low electron density).

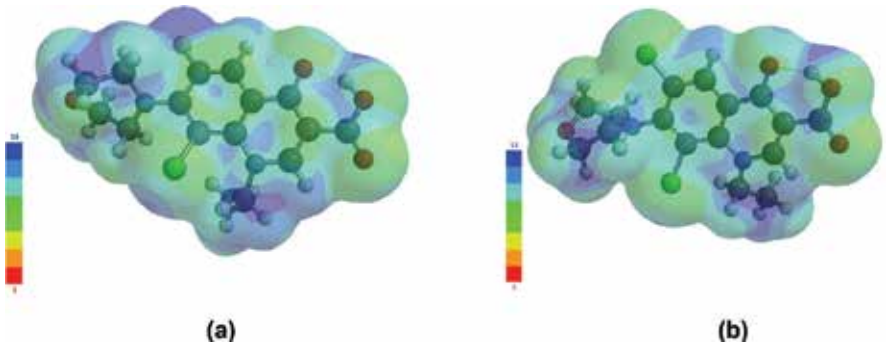

Figure 6. The optimized geometry and local ionization potential map of (a) FPQ 28 and (b) 6ClPQ 28.

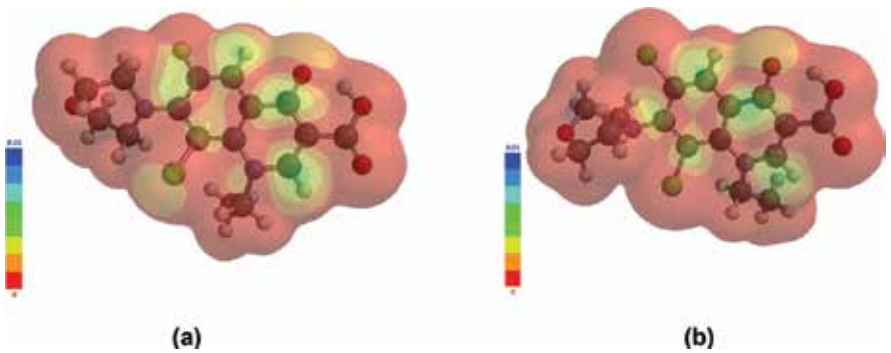

Figure 7. The optimized geometry and ILUMOI map of (a) FPQ 28 and (b) 6ClPQ 28.

2.2. Molecular docking

The steps to go through to explore protein-ligand interaction using docking are as follows: set up the binding site in a Molecule Project, import the dock ligands to a Molecule Table and inspect the docking results. The docking studies have been carried out using CLC Drug Discovery Workbench Software. The score and hydrogen bonds formed with the amino acids from group interaction atoms are used to predict the binding modes, the binding affinities and the orientation of the docked quinolone compounds (**Figure 8a–c**, **e**, **f**, **h**) in the active site of the protein receptor (**Table 3**). The docking score used in the Drug Discovery Workbench is the $PLANTS_{PLP}$ score [24]. The protein-ligand complex has been realized based on the X-ray structure of *S. aureus* DNA GYRASE, who was downloaded from the Protein Data Bank (PDB ID: 2XCT) [17].

2.2.1. Docking method validation

It ensures that the ligand orientations and position obtained from the molecular docking studies are valid and reasonable potential binding modes of ligands; the docking methods and parameters used have been validated by redocking (**Figure 8d**, **f**).

http://dx.doi.org/10.5772/intechopen.72995

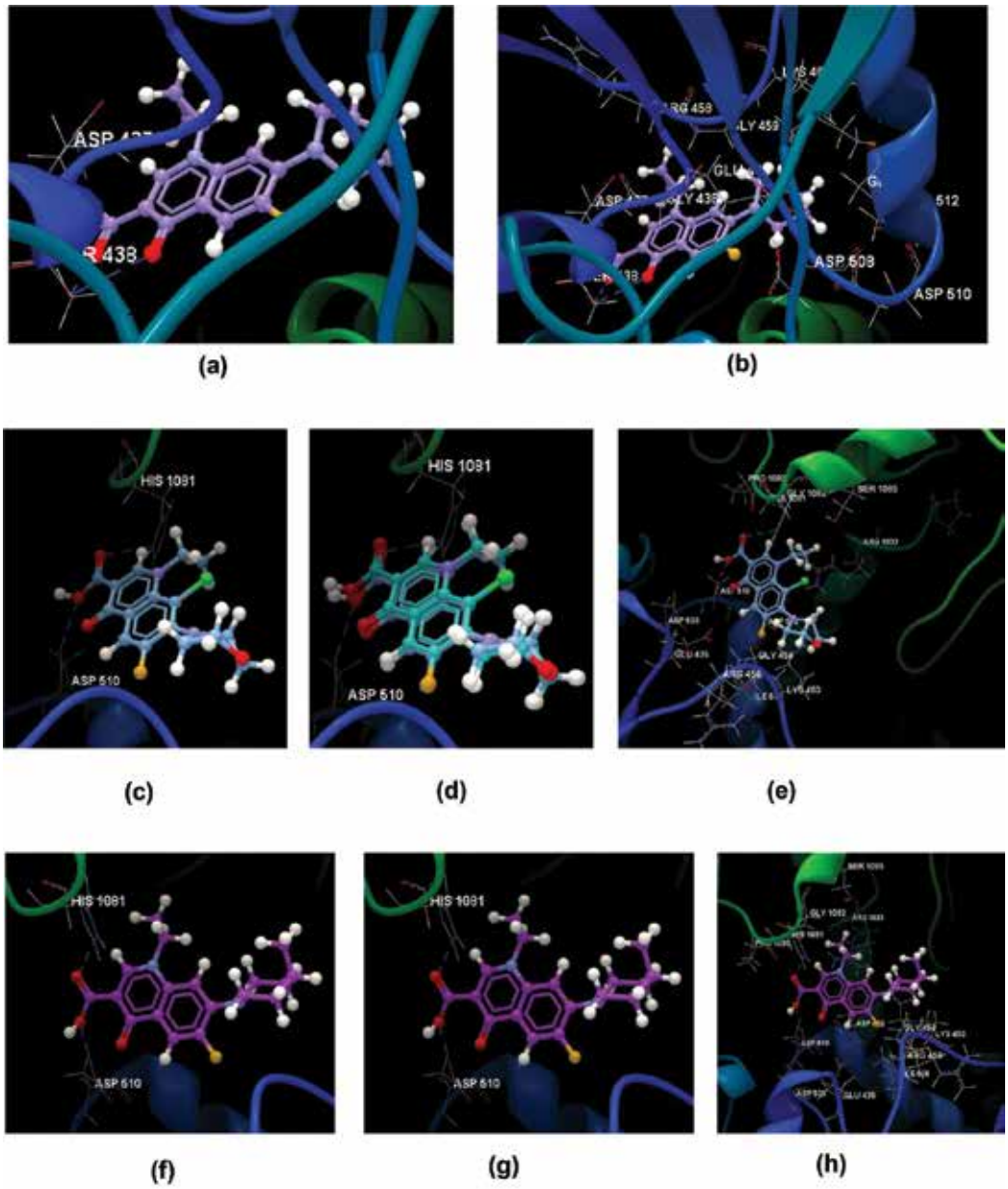

Figure 8. Molecular docking studies with 2XCT receptor. (a) Docking pose of the co-crystallized ligand CP. (b) Docking pose of the co-crystallized ligand CP interacting with residues in the binding site. (c) Docking pose of FPQ 28. (d) Docking validation of FPQ 28. (e) Docking pose of the FPQ 28 interacting with residues in the binding site. (f) Docking pose of Q 83. (g) Docking validation of Q 83. (h) Docking pose of the Q 83 interacting with residues in the binding site.

2.2.2. Determining molecular properties

Using the "Calculate Molecular Properties" tool it have been calculated important molecular properties such as logP, number of hydrogen bond donors, number of hydrogen bond acceptors

Ligand	Score/ RMSD (Å)	Group interaction/hydrogen bond	Bond length (Å)
CP	−37.27/ 0.79	*ASP510, ASP508, ASP512, GLY513, LYS460, GLY459,ARG458, GLU435, GLY436, ASP437, SER438*	
		–O sp^2 from CO–O sp^3 from SER 438	3.065
		–O sp^2 from COOH(CO)–O sp^2 from SER 438	2.816
		–O sp^3 from COOH(OH)–O sp^2 from ASP 437	2.872
ClCP	−36.63/ 0.10	*GLU477, ASP512, ASP437, ARG458,LYS460, ASN475, GLY459, ASN476, ILE461*	
		–O sp^3 from COOH(OH)–O sp^2 from GLU 477	2.933
		–O sp^2 from COOH(CO)–N sp^2 from ARG 458	3.125
NClX	−34.82/ 0.06	*ASP512, ILE 516, LYS459, ILE461, ARG458, GLU477*	
		–O sp^2 from COOH(CO)–Nsp^3 from LYS 460	3.036
NF	−39.79/ 0.11	*LYS460, GLY459, ARG458, ILE516, GLU435, ASP512, ASP510, ASP508, ARG1033, SER1085, GLY1082, HIS1081, PRO1080*	
		–O sp^2 from COOH(CO)–N sp^2 from HIS 1081	2.765
		–O sp^3 from COOH(OH)–O sp^2 from ASP 510	2.802
6ClPQ50	−33.63/ 0.07	*ASP437, ARG458, GLY459, LYS460, ILE477, LEU462*	
		–N $sp^3$from piperazine–O sp^2 from ASP 437	2.840
		–O sp^3 from COOH(OH)–O sp^2 from LYS 460	3.149
		–O sp^3 from COOH(OH)–O sp^2 from ILE 461	3.818
FPQ 50	−38.33/ 0.19	*GLY582, GLY584, LEU583, ASP508, ASP510 ASP512,LYS460, ILE516, GLY459, ARG458, LEU457, ASP437, GLY36, GLU435, SER438, ALA439*	
		–N sp^3 from piperazine–N sp^3 from LYS 460	3.195
		–O sp^3 from COOH(OH)–O sp^2 from ASP 508	3.036
		–O sp^2 from COOH(CO)–N sp^2 from ALA 439	3.027
PClX	−36.00/ 0.04	*ASP437, ARG458, GLU477,ILE461, LYS460, GLY459,TYR1025*	
		–O sp^2 from COOH(CO)–Nsp^3 from LYS 460	2.809
		–O sp^2 from CO–Nsp^3 from LYS 460	2.919
PF	−39.89/ 0.65	*ASP512, LYS460, ILE461,GLU477 GLY459, ARG458, ARG1033*	
		–O sp^2 from CO–N sp^3 from LYS 460	2.732
		–O sp^2 from COOH(CO)–N sp^3 from LYS 460	2.934
		–O sp^3 from COOH(OH)–O sp^2 from ASP 512	2.948
6ClPQ51	−34.98/ 0.10	*ASP437, ASP512,GLY459, ARG458,GLU477, ASN476,ASN475, ILE461, LYS460*	
		–O sp^3 from COOH(OH)–O sp^2 from GLU 477	2.821
		–O sp^2 from COOH(CO)–N sp^2 from ARG 458	2.929
FPQ 51	−36.50/ 0.44	*TYR1025, ASP512, HIS515, LYS460, ILE461, LEU519, LEU462, ASN463, LYS466, VAL464, ALA467, ARG471*	
		–O sp^3 from COOH(OH)–N sp^3 from LYS 460	2.888
		–O sp^2 from COOH(CO)–N sp^3 from LYS 460	2.722

Ligand	Score/ RMSD (Å)	Group interaction/hydrogen bond	Bond length (Å)
6ClPQ27	−35.72/ 0.02	*SER438, ASP437, GLY436, GLU435, SP508, LEU457, ASP510, ILE516, ASP512, LYS460, GLY459, ARG458*	
		–O sp^3 from COOH(OH)–O sp^2 from ASP 437	2.854
		–O sp^2 from COOH(CO)–O sp^3 from SER 438	2.746
		–O sp^2 from CO–O sp^3 from SER 438	3.073
FPQ 27	−37.06/ 1.50	*ASP508, GLU435, ASP510, ASP512, ILE516, LYS460,ARG458, ARG1033, GLY459, PRO1080, HIS1081, GLY1082, SER1085*	
		–O sp^3 from COOH(OH)–O sp^2 from ASP510	3.081
		–O sp^2 from COOH(CO)–N sp^2 from HIS 1081	2.726
6ClPQ29	−32.01/ 0.16	*ASP437, ARG58, GLU477, LYS460, GLY459*	
		–O sp^3 from COOH(OH)–O sp^2 from ASP 437	2.714
		–O sp^3 from COOH(OH)–O sp^2 from ASP 437	3.389
FPQ 29	−39.67/ 0.21	*SER185, ARG1033, GLY1082, HIS1081, PRO1080, LYS460, GLY459, ASP512, ARG458, ILE516, ASP508, GLU435,ARG458*	
		–O sp^2 from COOH(CO)–N sp^2 from HIS 1081	2.768
		–O sp^3 from COOH(OH)–O sp^2 from ASP510	2.804
6ClPQ25	−35.08/ 0.32	*GLU477, ARG458, LYS460, GLY459, GLU435, ASP512*	
		–O sp^3 from COOH(OH)–Nsp^3 from LYS 460	2.978
FPQ25	−39.55/ 0.04	*LYS460, ARG458, GLY459, ILE516, GLU435, ASP512,ASP510, PRO1080, HIS1081, GLY1082, SER1084, SER1085*	
		–O sp^2 from COOH(CO)–N sp^2 from HIS 1081	2.905
		–O sp^3 from COOH(OH)–O sp^2 from ASP 510	2.632
6ClPQ28	−35.65/ 0.22	*ILE516, LYS460, GLY513, ASP512, GLY459, ARG458, GLU435, ASP510, ASP508,GLY436, ASP437, SER438, ALA439*	
		–O sp^3 from COOH(OH)–O sp^2 from ASP 437	2.968
		–O sp^2 from COOH(CO)–O sp^3 from SER 438	2.641
		–O sp^2 from CO–O sp^3 from SER 438	2.915
FPQ28	−39.63/ 0.17	*LYS460, ARG458, GLY459, ILE516, GLU435, ASP508,ASP512, ASP510, ARG1033, PRO1080, HIS1081, GLY1082, SER1085*	
		–O sp^2 from COOH(CO)–N sp^2 from HIS 1081	2.863
		–O sp^3 from COOH(OH)–O sp^2 from ASP 510	2.671
6ClPQ35	−34.10/ 0.02	*SER438, ASP437, ALA439, GLY584, GLY436, GLU435, LEU457, ARG458, GLY459, LYS460, ASP512, ILE516*	
		–O sp^2 from COOH(CO)–O sp^3 from SER 438	3.174
		–O sp^2 from COOH(CO)–N sp^2 from SER 438	3.017
		–O sp^2 from COOH(CO)–N sp^2 from ASP 437	2.995
FPQ35	−39.13/ 0.18	*GLY582, ASP508, GLY584, LEU583, ALA439,SER438, ASP437,GLY436, GLU435, ASP510, ASP510, ASP512,LEU457, ARG458, GLY459, LYS460*	
		–O sp^3 from COOH(OH)–O sp^2 from ASP 508	2.642

Ligand	Score/ RMSD (Å)	Group interaction/hydrogen bond	Bond length (Å)
6ClPQ36	−35.59/ 0.23	*ASP437, ARG458, GLU477,ILE461, LYS460, GLY459,TYR1025*	
		–O sp^2 from COOH(CO)–Nsp^3 from LYS 460	3.070
		–O sp^2 from CO–Nsp^3 from LYS 460	3.040
FPQ36	−37.23/ 0.54	*LYS460, GLY459, ILE516, GLU435, ASP508, ASP512, ASP510, ARG1033, PRO1080, HIS1081, GLY1082, SER1085*	
		–O sp^2 from COOH(CO)–N sp^2 from HIS 1081	2.896
		–O sp^3 from COOH(OH)–O sp^2 from ASP 510	2.614
Q80	−38.37/ 0.02	*ASP437, ARG458, GLU477, ILE461, LYS460, GLY459*	
		–O sp^3 from COOH(OH)–Nsp^3 from LYS 460	2.935
Q83	−42.73/ 0.07	*PRO1080, HIS1081, GLY1082, SER1085, ARG1033, ASP510, ASP508, GLU435, ASP12, ILE516, ARG458, LYS460 GLY459*	
		–O sp^3 from COOH(OH)–Osp^2 from ASP 510	2.855
		–O sp^2 from COOH(CO)–N sp^2 from HIS 1081	2.761
Q87	−34.72/ 0.04	*ASP512, ASP510, GLY513, ASP508, ILE516, LYS460, GLY459, ARG458, LEU457,GLY436, GLU435, ASP437, SER438,ALA439*	
		–O sp^3 from COOH(OH)–Osp^2 from ASP 437	2.645
		–O sp^2 from COOH(CO)–Osp^3 from SER 438	2.778
		–O sp^2 from CO–Osp^3 from SER 438	2.792
		–O sp^2 from CO–Nsp^2 from SER 438	3.239
Q85	−42.07/ 0.08	*LYS460, GLY459, ARG458, ILE516, GLU435, ASP512, ASP510, SER1084, SER1085, GLY1082, HIS1081, PRO1080*	
		–O sp^3 from COOH(OH–N sp^2 from HIS 1081	2.981
		–O sp^3 from COOH(OH)–O sp^2 from PRO1080	2.411
6ClPQ24	−37.07/ 0.27	*ASN475, ASN476, GLU477,ARG458,SER437, ILE461, LYS460, GLY459*	
		–O sp^3 from COOH(OH)–O sp^2 from GLU 477	2.962
		–O sp^2 from COOH(CO)–N sp^2 from ARG 458	2.821
FPQ24	−40.64/ 0.18	*ASP510, ASP512, GLY582, ASP508, LEU583 GLU435, ILE516, LYS460, GLY459, ARG458, GLY436, ALA439, SER438, SP437 LEU457*	
		–O sp^3 from COOH(OH)–O sp^2 from ASP 508	2.644
6ClPQ30	−37.66/ 0.0063	*ARG458, GLY459, GLU477, LYS460, ILE461, ASN475*	
		–O sp^3 from COOH(OH)–N sp^3 from LYS 460	3.060
FPQ30	−41.90/ 0.32	*ARG458, GLY459, LYS460, ILE461,LEU462, ASN463, LEU519, LYS466, MET622, HIS515, ASP512, TYR1025*	
		–O sp^3 from CO–N sp^3 from LYS 460	3.060

Ligand	Score/ RMSD (Å)	Group interaction/hydrogen bond	Bond length (Å)
6ClPQ32	−33.86/ 0.03	*SER438, ASP437, ALA439, GLY436,GLU435, LEU457, ASP510, ASP512, LYS460, ASP508, ARG458, ILE516, GLY459*	
		–O sp^2 from COOH(CO)–O sp^3 from SER 438	2.852
		–O sp^2 from CO–O sp^3 from SER 438	2.897
FPQ32	41.85/ 0.07	*SER1085, ARG458, GLY459, LYS460,ILE516, GLU435, SP508, ASP512, ARG1033, LYS462, PRO1080, HIS1081, GLY1082*	
		–O sp^2 from COOH(CO)–N sp^2 from HIS 1081	2.775
		–O sp^3 from COOH(OH)–O sp^2 from ASP 510	2.817
6ClPQ33	−35.28/ 0.57	*LYS460, ILE461, ARG458, GLU477, ASN476*	
		–O sp^2 from COOH(CO)–N sp^3 from LYS 460	3.073
FPQ33	−42.53/ 0.11	*ARG458, LYS460, GLY459, ILE516, GLU435, ASP508,ASP512, ASP510, ARG1033, PRO1080, HIS1081, GLY1082, SER1085*	
		–O sp^2 from COOH(CO)–N sp^2 from HIS 1081	2.759
		–O sp^3 from COOH(OH)–O sp^2 from ASP 510	2.830

Table 3. The list of intermolecular interactions between the ligand molecules docked with 2XCT using CLC drug discovery workbench software.

Compounds	Atoms	Weight (Daltons)	Flexible bonds	Lipinski violations	Hydrogen donors	Hydrogen acceptors	Log P
NF	41	319.33	3	0	2	6	0.68
FPQ50	41	353.78	3	0	2	6	1.31
PF	44	333.36	3	0	1	6	1.15
FPQ51	44	367.80	3	0	1	6	1.77
FPQ27	44	333.36	3	0	2	6	1.11
FPQ29	44	367.80	3	0	2	6	1.74
FPQ35	39	304.32	3	0	1	5	3.90
FPQ36	39	338.76	3	0	1	5	4.53
FPQ32	42	318.34	3	0	1	5	4.26
FPQ33	42	352.79	3	0	1	5	4.89
Q83	45	332.37	3	0	1	5	4.70
Q85	45	366.81	3	1	1	5	5.32
FPQ24	45	332.37	3	0	1	5	4.70
FPQ30	45	366.81	3	1	1	5	5.32
FPQ25	40	320.32	3	0	1	6	3.04

Compounds	Atoms	Weight (Daltons)	Flexible bonds	Lipinski violations	Hydrogen donors	Hydrogen acceptors	Log P
FPQ28	40	354.76	3	0	1	6	3.67
NClX	41	335.79	3	0	2	6	0.66
6ClPQ50	41	370.23	3	0	2	6	1.28
PClX	44	349.81	3	0	1	6	1.12
6ClPQ51	44	384.26	3	0	1	6	1.75
6ClPQ27	44	349.81	3	0	2	6	1.09
6ClPQ29	44	384.26	3	0	2	6	1.72
6ClPQ35	39	320.77	3	0	1	5	3.88
6ClPQ36	39	355.22	3	0	1	5	4.51
6ClPQ32	42	334.80	3	0	1	5	4.24
6ClPQ33	42	369.24	3	0	1	5	4.86
Q80	45	348.82	3	0	1	5	4.67
Q87	45	383.27	3	1	1	5	5.30
6ClPQ24	45	348.82	3	0	1	5	4.67
6ClPQ30	45	383.27	3	1	1	5	5.30
6ClPQ25	40	336.77	3	0	1	6	3.02
6ClPQ28	40	371.22	3	0	1	6	3.64

Table 4. Ligands with properties.

and molecular weight, parameters that can be used to evaluate if a molecule has properties that would make it a likely orally active drug, according to the Lipinski's rule of five [25].

- Number of hydrogen bond donors less than 5 (the total number of nitrogen-hydrogen and oxygen-hydrogen bonds);
- Number of hydrogen bond acceptors less than 10 (the total number of nitrogen and oxygen atoms);
- The molecular weight less than 500 Daltons;
- Log P (octanol–water partition coefficient) less than 5. The calculation of the log P is based on the XLOGP3-AA method [26].

The number of violations of the Lipinski rules gives an indication of how *drug-likeness* for a molecule is. In general, orally active drugs have fewer than two violations.

These properties can be useful for identifying potential drug-like molecules, or for removing nondrug-like molecules from a compound library before starting a large virtual screening experiment (**Table 4**).

http://dx.doi.org/10.5772/intechopen.72995

3. Results and discussions

Molecular docking study has been performed relating to some quinolone compounds known in medical therapeutics: ciprofloxacin, norfloxacin and pefloxacin. For a correct interpretation of the data has been used in the study the corresponding compound of ciprofloxacin, ClCp.

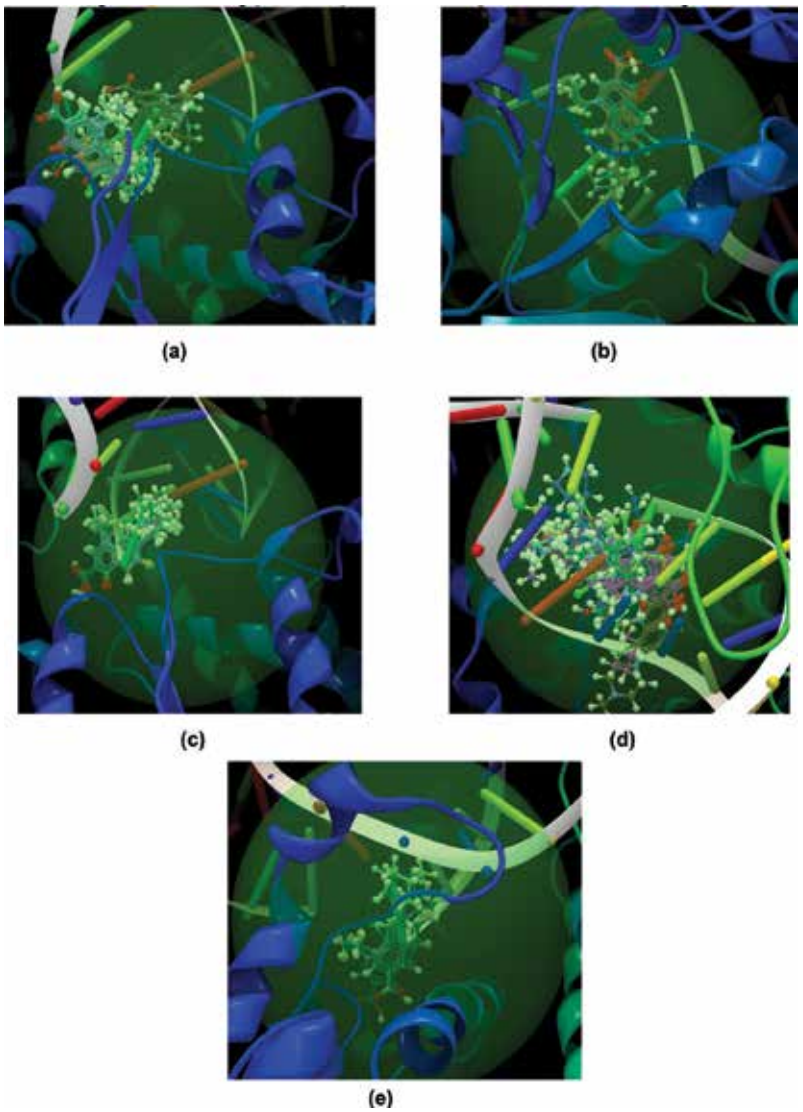

Figure 9. Docking pose of quinolone compounds in the binding site. (a) The quinolones with the similar binding mode of the co-crystallized ligand Cp. (b) The quinolones with the similar binding mode of the ClCp. (c) The quinolones with the similar binding mode of the ligand NF. (d) The quinolones with the similar binding mode of the ligand PF. (e) The quinolones with the similar binding mode of the ligand FPQ 35.

ClCp is the compound having a chlorine atom in 6-position of quinolone ring in place of fluorine atom.

The result of molecular docking study for quinolone FPQ 28, compound with a good activity '*in vitro*' against *Staphylococcus aureus* ATCC 6538 (MIC = 0.32 μg/ml) and with a good activity against MRSA [19], reveals docking score −39.63 (RMSD 0.17) and shows the occurrence of two hydrogen bonds with HIS 1081 (2.863 Å) and ASP 510 (2.671 Å) (**Figure 8c**). The orientation of the FPQ 28 is the same of NF (norfloxacin). Same orientation shows also the compounds: FPQ 32, FPQ 33, Q 83, Q 85, FPQ 27, FPQ 29, FPQ24 and FPQ 25 (**Figure 9c**). Docking score of NF compound is −39.79 (RMSD 0.11). NF shows the occurrence of two hydrogen bonds with HIS 1081 (2.863 Å) and ASP 510 (2.671 Å). The better score docking has been obtained from quinolone Q83: −42.73 (RMSD 0.07). Q83 shows the occurrence of two hydrogen bonds with HIS 1081 (2.761 Å) and ASP 510 (2.855 Å), and its orientation is the same of NF. Compound Q83 shows also a good activity '*in vitro*' against *Staphylococcus aureus* ATCC 6538 (MIC <0.125 μg/ml).

Results of the docking showed that quinolones have adopted various orientations. The same orientation with the co-crystallized ligand Cp (ciprofloxacin) shows the compound 6 ClPQ 27, 6ClPQ 28, 6ClPQ35 and Q 87. Co-crystallized Cp shows the occurrence of three hydrogen bonds with SER 438 (3.065 Å), SER 438 (2.816 Å) and ASP 437 (2.872 Å) (**Figure 9a**). The quinolones with the similar binding mode of the ClCp are 6ClPQ 51 and 6ClPQ 24 (**Figure 9b**). The quinolones with the similar binding mode of the ligand PF (pefloxacin) are 6ClPQ50, NClX, 6ClPQ 25, Q 80, FPQ 30, 6 ClPQ 33, PClX, FPQ 51, 6 ClPQ 36 and 6ClPQ 30.Docking score of PF is −39.89 (RMSD 0.65).PF shows the occurrence of three hydrogen bonds with LYS 460 (2.732 Å), LYS 460 (2.934 Å) and ASP 512 (2.948 Å) (**Figure 9d**). Same orientation shows the compounds FPQ 35, FPQ 24 and FPQ 50 (**Figure 9e**).

3.1. Drug-likeness of the quinolone compounds

According to the data presented in **Table 4**, four quinolones (Q 85, Q 87, FPQ 30 and 6ClPQ30) failed to respect one parameter (Log P > 5) of the Lipinski rules (Lipinski violation is 1). It was observed that 30 compounds of the study have zero violation of all the parameters involved in Lipinski's rule of five.

4. Conclusions

In silico molecular docking, simulation was performed to position all quinolone compounds into the preferred binding site of the protein receptor *S. aureus* DNA GYRASE, to predict the binding modes, the binding affinities and the orientation. The docking studies revealed that the all compounds showed good docking score. The docking score is a measure of the antimicrobial activity of the studied compounds. A correlation of the predicted data was observed which is obtained by molecular docking study (score docking) with the experimental data obtained from the evaluation of the antimicrobial activity against *Staphylococcus aureus* ATCC 6538 [16] of the quinolone compounds (**Figure 10a**, **b**, and **11a**, **b**).

The studies presented in this chapter show the importance of the design and the molecular docking in the discovery of new compounds with biological activity. The prediction of the

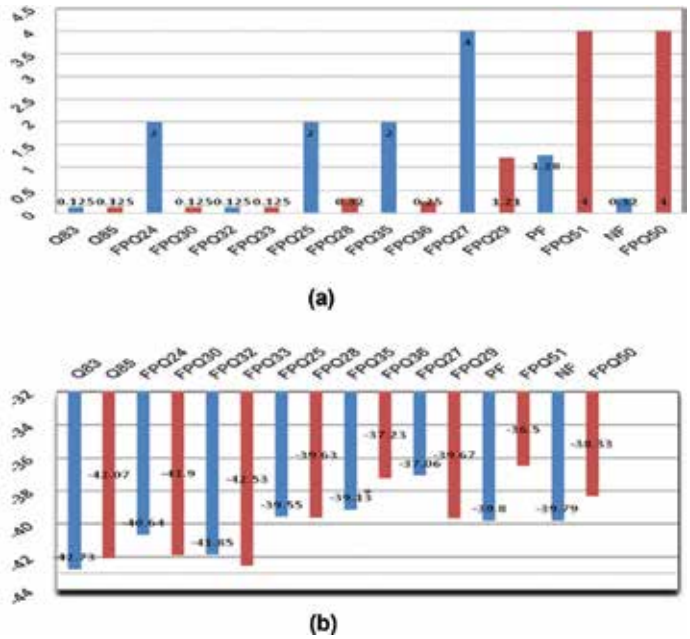

Figure 10. (a) MIC histogram of 6-fluoro-quinolone compounds. *Minimum inhibitory concentration* (MIC) of quinolone compounds against *St. aur.* ATCC 6538 (8-H-fluoroquinolones-blue, 8-Cl-fluoroquinolones-red). (b) Score docking of 6-fluoro-quinolone compounds (8-H-fluoroquinolones-blue, 8-Cl-fluoroquinolones-red).

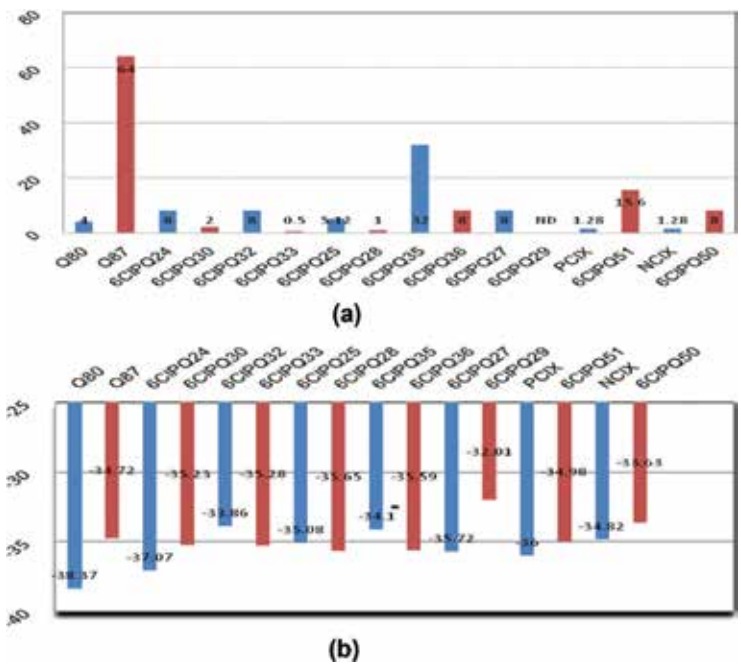

Figure 11. (a) MIC histogram of 6-chloro-quinolone compounds. Minimum inhibitory concentration (MIC) of quinolone compounds against *St. aur.* ATCC 6538 (8-H-chloroquinolones-blue, 8-Cl-chloroquinolones-red). (b). Score docking of 6-chloro-quinolone compounds (8-H-chloroquinolones-blue, 8-Cl-chloroquinolones-red).

binding affinity of a new compound (ligand) to an identified target (protein/enzyme) is a significant parameter in the development of a new drug. The prediction of the binding mode of a ligand (a new compound) to the target (protein/enzyme) by molecular simulation would allow restricting the synthesis to the most promising compounds.

Acknowledgements

This chapter has been financed through the NUCLEU Program, which is implemented with the support of ANCSI (project no. PN 09-11 01 01 and PN 09-11 01 09).

Author details

Lucia Pintilie* and Amalia Stefaniu

*Address all correspondence to: lucia.pintilie@gmail.com

National Institute of Chemical-Pharmaceutical Research and Development, Bucharest, Romania

References

[1] Meng X-Y, Zhang H-X, Mezei M, Cui M. Molecular docking: A powerful approach for structure-based drug discovery. Current Computer-Aided Drug Design. 2011;**7**:146-157. PMCID: PMC3151162 NIHMSID: NIHMS308746

[2] Ferreira FG, dos Santo RNS, Oliva G, Andricopulo AD. Molecular docking and structure-based drug design strategie. Molecules. 2015;**20**:13384-13421. DOI: 10.3390/molecules 200713384

[3] Trager E, Giblock P, Soltani S, Upadhyay AA, Rekapalli B, Peterson YK. Docking optimization, variance and promiscuity for large-scale drug-like chemical space using high performance computing architectures. Drug Discovery Today. 2016;**21**:1672-1680. DOI: 10.1016/j.drudis.2016.06.023

[4] Chen Y, Pohlaus DT, In silico docking and scoring of fragments. Drug Discovery Today Technologies. 2010;**7**:e149-e156. DOI: 10.1016/jddtec.2010.11.02

[5] Xu M, Lill MA. Induced fit docking, and the use of QM/MM methods in docking. Drug Discovery Today Technologies. 2013;**7**:e411-e418. DOI: 10.1016/jddtec.2013.02.003

[6] Alonso H, Bliznyuk AA, Gready JE. Combining docking and molecular dynamic simulations in drug design. Medicinal Research Reviews. 2006;**26**:531-568. DOI: 101002/med.20067

[7] Agarwal S, Mehrotra R. An overview of molecular docking. JSM Chemistry. 2016; **4**:1024-1027

[8] Dar AM, Mir S. Molecular docking: Approaches, types, applications and basic challenges. Journal of Analytical and Bioanalytical Techniques 2017;**8**:2. DOI: 10.4172/2155-9872.1000356

[9] Kroemer RT. Structure-based drug design: Docking and scoring. Current Protein and Peptide Science. 2007;**8**:312-328

[10] Pagadala NS, Syed K, Tuszynski J. Software for molecular docking: A review. Biophysical Reviews. 2017;**9**:1-102. DOI: 10.1007/s12551-016-0247-1

[11] Cerra B, Mostarda S, Custodi C, Macchiarulo A, Gioiello A. Integrating multicomponent flow synthesis and computational approaches for generation of a tetrahydroquinoline compound based library. Medicinal Chemical Communications. 2016;**7**:439-446. DOI: 10.1039/c5md00455a

[12] Mafud AC, Ferreira GL, Mascarenhas YP, Andricopulo AD and de Moraes J. Discovery of novel antischistomal agents by molecular modeling approaches. Trends in Parasitology. 2016;**32**:874-885. DOI: 101016/j.pt.2016.08.002

[13] Zhang X, Wang X, Liu C. Molecular docking and 3-D-QSAR study of pyranmycin derivatives against 16S rRNA a site. Journal of Molecular Structure: Theochem. 2005;**730**:85-94. DOI: 10.1016/j.theochem.2005.05.039

[14] Zhao H, Caflish A. Molecular dynamics in drug design. European Journal of Medicinal Chemistry. 2015;**91**:4-14. DOI: 10.1016/j.ejmech.2014.08.004

[15] Pintilie L. Quinolones: Synthesis and antibacterial activity. In: Bobbarala V, editor. Antimicrobial Agents. Croatia: Intech; 2012. pp. 255-272. DOI: 10.5772/33215 . Available from: https://www.intechopen.com/books/antimicrobial-agents/quinolones-synthesis-and-antibacterial-activity

[16] Pintilie L. Quinolone compounds with activity against multidrug-resistant gram-positive microorganisms. In: Bobbarala V, editor. Concepts, Compounds and the Alternatives of Antibacterials. Croatia: Intech; 2015. pp. 45-80. DOI: 10.5772/60948. Available from: https://www.intechopen.com/books/concepts-compounds-and-the-alternatives-of-antibacterials/quinolone-compounds-with-activity-against-multidrug-resistant-gram-positive-microorganisms

[17] Bax DB, Chan PF, Eggleston DS, Fosberry A, Gentry DR, Gorrec F, Giordano I, Hann M, Hennessy A, Hibbs M, Huang J, Jones E, Jones J, Brown KK, Lewis CJ, May EW, Saunders MR, Singh O, Spitzfaden CS, Shen C, Shillings A, Theobald AT, Wohlkonig A, Pearson ND, Gwynn MN. Type II A topoisomerase inhibition by a new class of antibacterial agents. Nature. 2010;**466**:935-940. DOI: 10.1038/nature09197

[18] Spartan'14 Wavefunction, Inc. Irvine, CA. Available from: www.wavefun.com

[19] Pintilie L, Dorobat O, Caproiu MT, Maganu M. Quinolone derivatives with activity against multi-drug resistant gram-positive microorganisms. Revista de Chimie. 2014;**65**: 1176-1181

[20] Martin YC. A bioavailability score. Journal of Medicinal Chemistry. 2005;**48**:3164-3170. DOI: 10.1021/jm0492002

[21] Arup K, Ghose AK, Pritchett A, Crippen GM. Atomic physicochemical parameters for three dimensional structure directed quantitative structure-activity relationships III: Modeling hydrophobic interactions. Journal of Computational Chemistry. 1988;**9**:80-90

[22] Gautam BP, Dani RK, Prasad R, Srivastava M, Yadav RA, Gondwal M. Synthesis, characterization, single crystal structural studies, antibacterial activity and dft investigations of 2-chloro-5-ethoxy-3,6-bis(methylamino)-1,4-benzoquinone. Pharmaceutica Analytica Acta. 2015;**6**. DOI: 10.4172/2153-2435.1000418

[23] Lasri J, Eitayeb NE, Ismail AI. Experimental and theoretical study of crystal and molecular structure of 1,2-di(9*H*-fluoren-9-ylidene)hydrazine. Journal of Molecular Structure. 2016;**1121**:35-45. DOI: 10.1016/j.molstruc.2016.05.044

[24] Korb O, Stützle T, Exner TE. Empirical scoring functions for advanced protein-ligand docking with PLANTS. Journal of Chemical Information and Modeling. 2009;**49**:84-96. DOI: 10.1021/ci800298z

[25] Lipinski CA, Lombardo F, Dominy BW, Feeney PJ. Experimental and computational approaches to estimate solubility and permeability in drug discovery and devel opment settings. Advanced Drug Delivery Reviews. 2001;**46**:3-26. DOI: 10.1016/S0169-409X(00)00129-0

[26] Cheng T, Zhao Y, Li X, Lin F, Xu Y, Zhang X, Li Y, Wang R. Computation of octanol-water partition coefficients by guiding an additive model with knowledge. Journal of Chemical Information and Modeling. 2007;**47**:2140-2148. DOI: 10.1021/ci700257y

Chapter 6

Molecular Docking in Halogen Bonding

Abel Suárez-Castro, Mario Valle-Sánchez,
Carlos Jesús Cortés-García and Luis Chacón-García

Additional information is available at the end of the chapter

http://dx.doi.org/10.5772/intechopen.72994

Abstract

Molecular modeling applies several computational chemistry tools as molecular docking; this latter has been useful in medicinal chemistry for prediction of interactions between small ligands and biological targets measuring angles, enthalpy and other physical-chemical properties involved in the supramolecular entities. In this chapter, we present molecular docking advances with a perspective to the improvement of parameterization including halogen bonding interactions (XB) and the modification of scoring functions based on halogen sigma-hole polarization. At the same time, we have included the current computational methods to study halogen bonding that increased the accuracy of predicted entities. Finally, we present examples of the main force fields including electronic distribution and modifications for halogen atoms.

Keywords: molecular docking, scoring functions, force fields, halogen bonding, molecular modeling, σ-hole

1. Introduction

Molecular docking is a powerful computational method to predict the pose and intermolecular interactions between a small ligand and a specific receptor (in most of the cases), using algorithms and scoring functions to obtain numerical scores or thermodynamic properties from the most favorable molecular interactions through predicted supramolecular entities. The molecular docking is a useful tool for the medicinal chemist who wants to know with certain accuracy the outcomes for each project; it involves a low computational cost in the quest of utility for predicted compounds in several ligands, i.e., virtual screening. The accuracy of the molecular docking predictions came up from the algorithm and the scoring function that needs to be adequate for each objective. In recent years, it has been a goal to improve the

analysis and prediction of the halogen bonding interactions (XB) that several halogenated small compounds can perform and have a huge relevance in drug discovery.

The molecular interactions generated from a halogenated compound with a specific receptor could be addressed with molecular docking studies using quantum mechanics/molecular mechanics (QM/MM) approaches, combining a specific force field that could predict the chemical interactions of halogenated ligands based in their electronic distribution when they are close to an electronegative or electropositive atom. Here, we present some of current scoring functions (SF) used in molecular docking and some examples of works starting with the XB potential of mean force (XBPMF) that is a knowledge-based SF, following with the VinaXB, which is an implementation of the halogen bonding scoring function (XBSF) classified into the empirical-based SF. In order to improve molecular docking experiments regarding the XB interaction, in the lasts years, some force fields presented with high detail in here have been implemented and have been used by numerous researchers with fine performance and high accuracy; these are the optimized potentials for liquid simulations-all atoms (OPLS-AA), which is applied to biological macromolecules and the force field for biological halogen bonds (ffBXB) that implemented the anisotropic effect to investigate the XB between small compounds as ligands and specific receptors in molecular modeling.

1.1. Halogen bonding (XB)

The XB is defined as the interaction where a halogen is an electrophilic species and can be described as D ··· X-Y, where X is the electrophilic halogen atom (Lewis acid, XB donor), D is the donor of electron density (Lewis base, XB acceptor) and Y is a carbon, nitrogen or halogen atom, and in this context, the X electrophilic halogen atoms are iodine, bromine and chlorine (**Figure 1**), and the fluorine halogen atom is not considered under this description because this atom does not have the capacity to form the σ-hole effect [1]. The ability of halogens to form interactions with electron donor species was reported unequivocal the first time by Guthrie in 1896 [2] where he reported the formation of ammoniac-iodine complex and described the properties and the necessary conditions to obtain this unusual interaction now. In the subsequent years, there are reports about the interactions between amines and the bromine and chlorine halogens. In 1970, Odd Hassel explained the similarities in halogen and hydrogen bonding and remarked the importance of this kind of interactions and the opportunity to understand the atomic arrangements in donor-acceptor complexes [3]. The study of XB interaction has become interesting to be studied in many fields including rational drug design under the basis

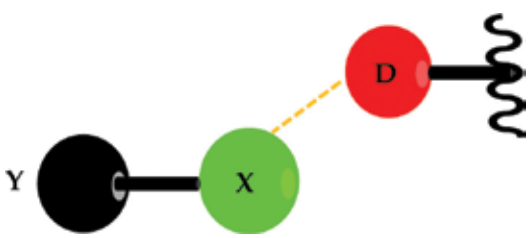

Figure 1. Schematic representation of a XB interaction, X = Lewis acid donor, halogen (I, Br, Cl); D = Lewis base acceptor; Y = carbon, nitrogen.

of medicinal chemistry and theoretical chemistry calculations using ab initio approaches [4]. Here, we describe the XB and their importance in biological systems, the theoretical and chemical bases, the computational methods that have been used to study this interaction to improve the drug design process and the recent applications in the computer drug design research.

1.2. Halogen bonding in drug design: an emerged non-covalent interaction

The importance of XB in drug design research has emerged from the past decade with the discovery of its importance in biological systems as potent stabilizing non-covalent interaction between ligand and receptor complexes. Although the first successful application of the XB concept was in 1996 by the optimization of an inhibitor of clotting factor Xa stressing, the importance of this kind of interaction started since the past decade with the discovery of a four-stranded DNA and aldose reductase complexes with halogens [5, 6]. As an example, one of the first applications of the XB interaction was the development of a compound that contains iodine atom in a pyridinone derivative identified as R221239 as inhibitor of reverse transcriptase in human immunodeficiency virus 1 [7] where the authors compare the reported angles between C—X··· O and their findings in the complex interaction between this inhibitor and the reverse transcriptase receptor. For 2009, around 25% was reported that the brand name drugs possess halogen atoms in their chemical structure becoming this type of atoms in important molecular scaffold fragments in drug design [8]. The insights about the XB concept have led to its implementation into the principal approaches of drug design process being the computational methods of the most useful approaches to predict this kind of interactions to improve the predictions through the computer calculations to generate accurate results that can help for the best design of compounds as drug candidates for many diseases [4]. The importance of XB in drug design has been compared with the hydrogen bonding (XB) interactions but with the difference that the first ones have some chemical properties in the strength and short distances between the atoms that form them [9].

1.3. Importance of halogen bonding in biological systems

Biological systems are composed of few elements from the periodic table, being based on carbon, oxygen, nitrogen, hydrogen, phosphorus and sulfur, but at the same time, few biological compounds contain halogens as iodine in the thyroid hormones functions [10], fluorine in bone-specific structures as teeth [11] and the chloride that has an anionic effect [12]. This type of elements is very important because they are not abundant in the cellular or subcellular structures, which means that they have specific interactions. In the human body, the presence of some biological compounds and ions that are halogenated starting with the thyroid hormones, the fluoride and chloride ions and its effect as anions playing an important role keeping the homeostasis of some important physiological mechanisms is well known. The beginning of the importance about the XB in biological systems started in 2003 with the discovery of a four-stranded DNA Holliday Junction that contains a bromine atom that played an important role in this type of macromolecular interaction [5] and the discovery of the complex aldolase reductase and a halogenated inhibitor at high resolution [6] where a bromine interaction was found as unusual showing short bromine-oxygen contact around 12% less

than their van der Waals radii of both atoms. These findings attracted the attention of medicinal chemists and theoretical chemists to search deeply the characteristics of these interactions. The thyroid hormones are the most studied and understood halogen compounds in biological systems where the iodine atom forms a halogen bonding with the oxygen atom in the binding site for the thyroxine with short I—O interactions that play essential roles for the highly recognition of these types of hormones. Also, the thyroxine hormone binds to RNA sequences through halogen bonds [13]. Although the fluoride is not considered as a halogen bond, its molecular mechanisms are the more studied in the aspect of the toxicity of this halogen that explains the high negative effect of this halogen in the cellular respiration, generation of reactive oxygen species, necrosis and apoptosis between others [14]. The halogen bonding has the effect of stabilizing inter- and intramolecular interactions that can stabilize ligand interactions and can affect molecular folding [15]. In drug design, the pharmacological research has included many halogenated molecules that are inhibitors (some of them approved), but only few times, this interaction is considered as important for the rational drug design process. There are many X-ray crystal structures in the PDB that contain halogen bonding interactions.

2. Halogenated drugs in medicinal chemistry

At present, the insertion of halogen atoms to improve the biological profile of a candidate compound has become an important strategy in drug development, and it is quite common in analogue-based drug discovery [16, 17]. Consequently, in medicinal chemistry the halogenation benefits include (a) increased membrane permeability, facilitating the blood-brain barrier crossing; (b) lower metabolic degradation, prolonging the lifetime of the drug; and (c) the addition of specific effects that enhance its binding to target macromolecules [18–20]. However, it was only recently that heavy halogen atoms are recognized to play an important role in the pharmacological activity through an interaction now defined as the halogen bond [21]. For this reason, it should not be surprising to find a greater presence of halogenated compounds at all stages of drug development.

In this context, the FDA has approved over 1582 new molecular entities (NME), of which approximately 20% are halogenated [22, 23]. On the other hand, 35% of the top 15 best-selling drugs between 2010 and 2016 were halogenated [24–26]. What is more interesting is that the pharmaceuticals called "blockbuster drugs" are mostly halogenated compounds (some examples are shown in **Figure 2**) [27, 28]. Additionally, a detailed analysis about the halogen atoms and statistical analysis of organohalogens and halogen bonds in medicinal chemistry were performed by Njardarson et al. [29], Hernandes et al. [18] and Zhu et al. [30], respectively.

2.1. Optimization of the halogenated drugs

The objectives to optimizing a drug are to increase their oral bioability and pharmacological pharmacodynamics and improve its metabolism. In the case of halogenated drugs, the influence of a halogen atom or substituents improves the thermodynamic parameters of the system (ligand-receptor pair), and the dissociation constant (*Kd*) is positively modified [18].

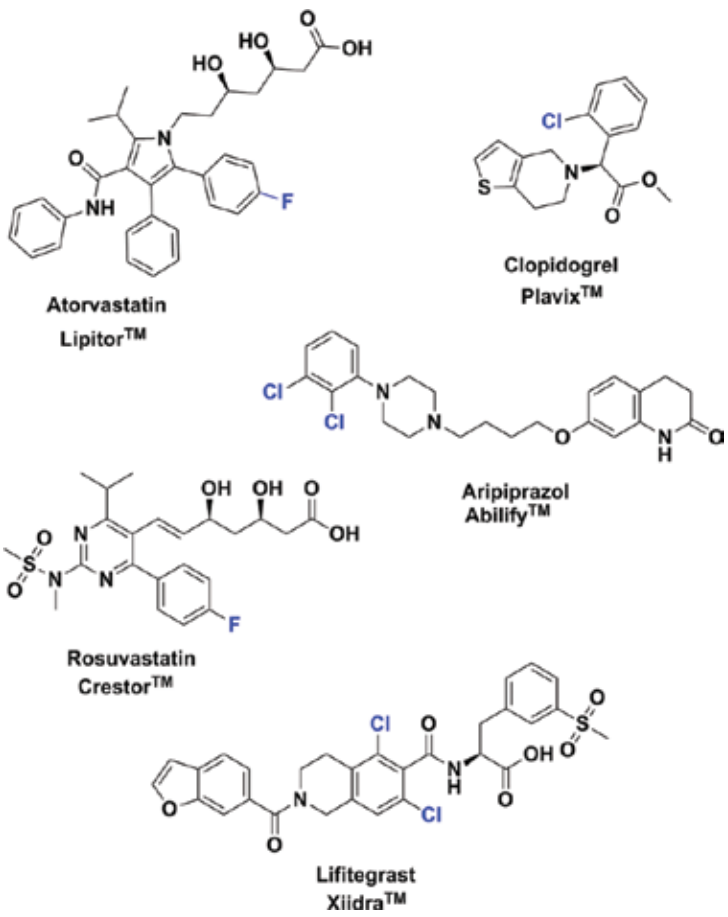

Figure 2. Some halogenated drugs considered as "blockbuster" drugs.

The XB is an important approach in lead optimization of drug development and increases the binding affinity and binding selectivity [31].

3. Theory and concepts of halogen bonding

Considered as the first event in a chemical process, molecular recognition is a fundamental but complex step in the building of supramolecular entities [32]. Molecular recognition involves the synergy of a vast number of weak interactions, such as hydrogen bonding, and electrostatic, hydrophobic and other nonconventional interactions [33]. In this context, we can mention anion-π stacking, hyper-coordination of carbon atoms and the σ-hole deformation that originates from the halogen bonding interactions [34–36].

Halogen bonding (XB) is a non-covalent interaction classified into Lewis acid-base bonding, where particularly in this species, halogen acts as the Lewis acid in front of neutral or anionic

Lewis base entities. This interaction was first reported by Guthrie in the middle of the nineteenth century; nonetheless, it has attracted attention after its "rediscovery" in the 1990s as a strong interaction even compared with hydrogen bonding [37].

The halogen bonding interaction is defined as pre-reactive complexes formed between species with a type Y-X----D, where X is a halogen atom that can behave as an electron acceptor, D is a neutral or anionic nucleophile and Y could be nitrogen, oxygen, carbon, halogen, etc. Also, n and π electron pairs can form interactions as XB acceptors. It is well known that alkenes and arenes can form complexes with dihalogen molecules prior to formation of addition or substitution products [15].

Theoretical and experimental data about this phenomenon prove that the four halogens can act as XB formers marking a tendency in strength from the strongest I > Br > Cl > F to the weakest interaction. Charge transfer, polarization, concentration, temperature, solvent properties and the nature of A play an important role in the ability of halogen.

The XB interaction energy spans from 5 to 180 KJ/mol, giving stability to formed complexes and a typical interaction angle of ~180°, leading to linear or slightly bended architectures in crystallographic data of available complexes, which correlates with the calculations that propose a deformation in the halogen σ^* molecular orbital. This phenomenon is called "the sigma hole" [15, 38].

Applications of XB properties are wide, covering crystal engineering design, improvement of conductor materials and the design of drugs.

The employment of halogen bonding in biomedical tasks is a new and interesting trend as the halogen can afford a short-range interaction (smaller to van der Waals interaction length) with electron-rich atoms involved in biological receptors and enzyme's active sites [38].

The electron acceptor stage of a halogen atom is a fashion research topic due to its outstanding properties. The preferred complexes that are subject of study are those where B is a tertiary amine. For example, García-Garibay's group recently reported the dynamics of a supramolecular rotor where the axle is based on this interaction between DABCO as an acceptor and 1,4-diiodotetrafluorobenzene as the halogen donor [39].

Applications of XB properties are wide, covering crystal engineering design, development of drugs and improvement of conductor materials.

Computational calculations help to explain, correlate and predict behavior of halogen donors and acceptors. The most accurate methods involve the use of quantum mechanics (QM) to calculate geometry and architecture of halogen bonding, but most of them are just available for small molecules. The development of different algorithms and methods is a useful tool to generate indirect experimental measurements of halogen bonding involving biological targets [38–40].

Interactions between proteins and drugs can be predicted by molecular docking; this method analyzes two crystallographic structures: one about biological target and the other about drug's molecule. This computational experiment uses classic mechanic's collisions, potential energy surfaces and some electrostatic and geometrical descriptors to correlate assemblies and enthalpy of the supramolecular complexes; the best methods will be treated further in this chapter.

4. Current computational methods to study the halogen bonding

As we have described so far in this chapter, the XB is relevant in drug design, and it requires to be studied and implemented by the current auxiliary computational tools and methods for drug design, and for this propose, the simulations of the σ-hole effect is a challenging task because not all the computational methods can achieve the accuracy to predict the distance, angle and strength of the interaction. There are references addressing algorithms to describe this phenomenon [41, 42], and the main parameters employed have been the charge-transfer (CT) complex, the electrostatic interactions (EI) and the polarization of the halogen atoms when they are in an environmental where their behavior is as a Lewis acid. The XB interactions arise from a combination of EI, CT and dispersion interactions. Other important considerations are the net attractive Coulomb interactions that play a key role in the σ-hole interactions. One of the deepest methods to simulate the XB came from the coupled clusters with single and double (CCSD) substitution method which came from the Hartree-Fock determinant, and the CCSD (T) provides better results in the type of interaction; the lighter Moller-Plesset truncated at the second order (MP2) is valid for XB interactions [43].

It is important to consider that to apply computational methods in drug design, it is necessary to consider the use of those that are accessible and reliable for simulating. The docking experiments can help us to process a big amount of information through virtual screening where many compounds are halogenated, and in this sense, this calculation is more efficient to know how the halogenated ligand can bind in some specific target, but almost all the docking scoring functions are not capable to model the XB in a correct way, leading to some errors that we can interpret as false positives or vice versa. To address this point, there are some methods and approaches that allow us to model, search and know the best rank poses into a binding site, and this type of calculations is based on ab initio calculations and, in some cases, is modified as scoring functions into the docking algorithms with the software that are well known. The ab initio calculations can be performed with the evaluation of quantum mechanics/molecular mechanics (QM/MM) approaches. Therefore, some accurate methods play a key role in the prediction of binding free energy that rescores the best docking poses; the most useful method to do that is the molecular mechanics/generalized-born/surface area (MM/GBSA) [44]. Molecular docking is in some cases improved by this type of calculations, but now we described the molecular docking scoring functions as improved tools to get accurate predicted results in XB.

5. Molecular docking and halogen bonding

Molecular docking is classified into the structure-based drug design methods and is a good and extensively medicinal chemistry tool to predict the pose of a ligand in a specific region of the receptor structure. As is well known, molecular docking has two main components: scoring functions and search algorithms. The scoring functions can predict the affinity energy between the ligand and the receptor by calculations of the all possible interactions being the best ranked those that have the minimum energy (ΔG). One of the most used applications of molecular docking is virtual screening to find probable lead compounds against some specific receptor, because this method has the capability to do this and presents a less consuming time

of the calculations during the process, but we may say that not all of the scoring functions have the capacity to identify and predict the best XB interactions, and for this task, many scoring functions have emerged in molecular docking to improve and try to solve this problem.

5.1. Scoring functions to study the halogen bonding

There are some scoring functions to predict and model the XB in molecular docking and now are well known and designed knowledge- and empirical-based methods.

5.1.1. Knowledge-based method

This type of scoring functions is based in pairwise interactions that came from experimental properties of molecular interactions of high-resolution X-ray crystal structures and most of the times came from the Protein Data Bank (PDB). The particularity of this type of scoring functions is that it improves the computational efficiency but lacks enough accuracy. In the case of XB scoring functions of this type, we can cite to Zhu et al. [45] who developed a scoring function named XBPMF (halogen bonding potential of mean force) that was developed from two high-quality training datasets of protein-ligand complexes. The XB and the hydrogen binding (HB) were characterized by two-dimensional potentials for taking the energetic and geometric preferences for ligand-receptor interactions. The authors establish that this scoring function was evaluated to have moderate power of predicting ligand-receptor interactions in terms of docking power that shows the ability of the scoring function to identify the original ligand conformation from a set of decoys and is reflected in the root-mean-square deviation (RMSD) of the best conformation of the ligand with the minimum free energy. At the same time, ranking power that is the ability to rank a set of ligands against a receptor by affinity, was obtained and is described as scoring power being good scoring function for high-throughput virtual screening.

5.1.2. Empirical-based method

This type of scoring functions has been designed to estimate the free energy between ligand and its receptor when it is possible to know the structure information or it can be approximated [46]. This scoring function uses some parameterized functions based in physical or chemical properties, and the most important consideration is that this method is parameterized against training sets derived from experimental data [47]. One of the first empirical-based scoring functions was described by Watts et al., which considers local cooperative effects from the interaction between ligand and receptor [48] using a "small network" approach to describe how the environment affects to the non-covalent interactions as XB. The capability to predict with accuracy the binding affinities is when occurred small local changes in a ligand configuration, leading to obtaining the best affinity values.

More recently, Koebel et al. developed a new empirical-based scoring function that has been added to the most widely free used docking tool as AutoDock Vina (AutoDock VinaXB) that is an implementation of the halogen bonding score function (XBSF) [49]. This scoring function is derived on the X ··· A distance and C—X ··· A angle; other important parameters that are considered are the size and the anisotropic charge of the halogen atoms; and to define the halogen bonding term, an angle term was included to account for the varying positive charge on the atom (Eq. (1)):

$$E = W\phi D \quad (1)$$

where W is the weight, φ is the angle factor and D is the distance factor.

To validate the implementation of this scoring function, 106 halogenated ligand-protein complexes were evaluated with Vina and VinaXB finding that XB scoring function was closer to the original poses below 2 Å deviation twice than Vina.

6. Achievements and advances in the study of halogen bonding with modified and improved docking scoring functions

Derived from the development and implementation of scoring functions in XB in the past early years, there are few researches that apply this new scoring function. More relevant, we describe the most useful empirical-based scoring function VinaXB so far. As is well known, AutoDock Vina is a free docking tool, and the addition of the XB can be added to it. One of the first researches reported that the empirical-based scoring functions were used in the work developed by Pal et al. [50] where they reported the application of VinaXB scoring function in molecular docking experiments with an aberrant expression of Notch-1 in aldehyde dehydrogenase (ALDH) in cancer stem cells in breast cancer. The aim of using molecular docking was to search for the binding ability of psoralidin with gamma secretase where the best pose ranked with a value of free energy of −8.5 kcal/mol was found suggesting that psoralidin binds to nicarstin in the micromolar concentrations. The docking studies let them know the main chain residues in the binding pocket with accuracy. Šeflová et al. [51] reported the effect of halogenated phenylquinolines specifically 5,6,7,8-tetrafluoro-3-hydroxy-2-phenylquinolin-4(1H)-one (**TFHPQ**) (**Figure 3a**) on Na+/K+-ATPase (NKA) where the experimental observations with the results from molecular docking using the VinaXB scoring function correlated. An important observation for these studies is that the compounds investigated firstly were optimized using density functional theory at the B3P86/631 + G (dp) level (289 K and 1 atm) and then were submitted to docking experiments to the open and closed NKA enzyme. The docking was performed in two steps: first, in a general screening with the whole protein, exhaustiveness was set to 400, and the number of modes was 9999; afterwards, they carried out redocking in the most favorable regions using the AutoDock VinaXB extension. The finding in this study that came from molecular docking was that the results provided a clue to the question why only **TFHPQ** inhibited in the in vitro studies to NKA, while other analogues can bind in the TFHPQ binding pose but were less active despite that all of molecules have similar chemical structure because the free energies were different by 1–3 kcal/mol, and in addition, they can bind in several sites of the NKA enzyme being different for **TFHPQ**.

Another well application of VinaXB soring function is in the work developed by Enkhtaivan et al. [52] where they researched the ability of berberine-based derivatives (**BDs**) as anti-influenza agents against the neuraminidase using the VinaXB scoring function finding that **BD-5** (**Figure 3b**) has better affinity energies than oseltamivir that was used as a control in the utilized neuraminidase receptor.

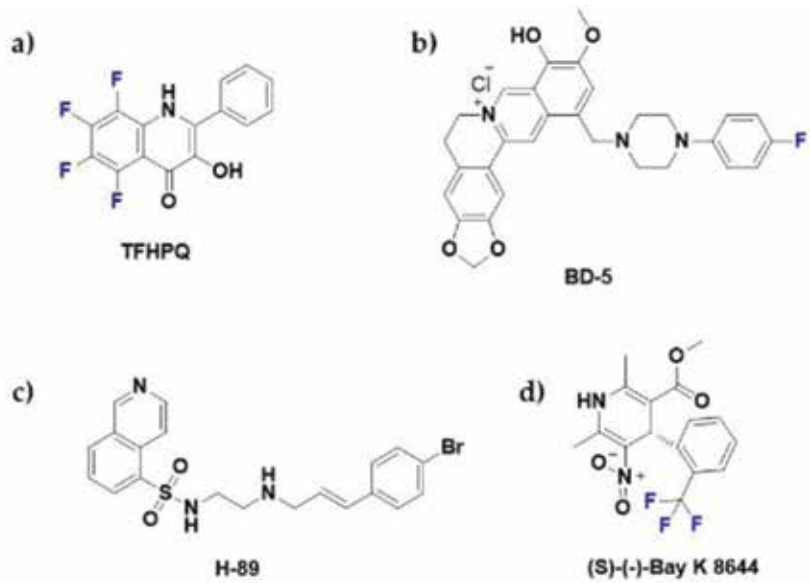

Figure 3. Compounds analyzed in recent drug design projects using molecular docking with XB scoring functions.

The other most representative studies are the use of VinaXB scoring function by Fusi et al. [53] where they investigated the block of the vascular Ca_{2+} channel by the PKA inhibitor **H-89** (N-[2-[[3-(4-bromophenyl)-2-propen-1-yl] amino] ethyl]-5-isoquinolinesulfonamide) (**Figure 3c**) and the compound named **(S)-(−)-Bay K 8644** (S)-(−)-Bay ((S)-(−)-methyl-1,4-dihydro-2,6-dimethyl-3-nitro-4-(2-trifluoromethylphenyl) pyridine-5-carboxylate) (**Figure 3d**) in rat artery myocytes. These docking experiments were carried out with a flexible docking in AutoDock with the VinaXB. The findings in this research established the differences between the poses of the analyzed compounds where the compounds positioned at the same binding region but in different binding pockets.

7. Quantum mechanics-derived scoring functions

In a normal docking experiment, the atoms are described by an atom type and a partial charge that fails when we want to describe the characteristic of anisotropic electron distribution in XB. In 2012, Jorgensen and Schyman described the additional positive charge in the σ-hole region using their optimized potentials for liquid simulations-all atom (OPLS-AA) that is a force field applied to biological macromolecules [54]. This force field has the ability to predict thermodynamic and physical-chemical properties of biomolecules in aqueous phase with high accuracy for organic liquid compounds and for 20 neutral peptide residues that were investigated first by Monte Carlo simulations where intramolecular terms for bond stretches, angle bending and torsions, as well as the intermolecular and intramolecular nonbonded interactions were taken for the final calculations similar to AMBER or CHARMM force fields, for example, that represent electrostatic interactions with a single partial charge on each atom.

To study the XB interactions with this useful force field at the quantum calculation level, one of the key modifications to the original force field was the inclusion of the X-site term to refer the XC, XB and XI for chlorine-, bromine- and iodine-halogenated compounds being a OPLS-AAx as the new term for the general force field where this X-sites have a stretching bond bringing constants for angle bending except for the fluorine atom. On the other hand, in 2015 as well, Rappé et al. reported the creation of force field named force field for biological halogen bonds (*ffBXB*) that implemented the anisotropic effect of the σ-hole in the bromine atom [55]. In this force field, the calculations are performed based on the anisotropic structure-energy relationships, calorimetric data and ab initio calculations specifically in bromine; in addition, the result was consistent with a charge-dipole electrostatic potential that could calculate and predict properly the XB interaction. Finally, Zimmerman et al. reported in 2015 a development of a scoring function named XB scoring function (XBScore) that includes the force fields described above and the next parameters based in the study of each XB property: σ-hole score that includes the angle, interaction geometry, tuning effects, the interaction partner and the type of halogen [56]. The spherical score comes from the MP2/TZVPP theory level. At least, Zimmerman et al. concluded that using a quantum mechanics calculation they could predict energies with high accuracy and that based in their scoring function quantum mechanics derived, it is possible to apply this term to improve the docking experiments.

8. Conclusions

One of the main objectives in computational medicinal chemistry is to generate useful predictions employing different tools that could be achieved through molecular modeling using computational approaches. This fact is very important during the implementation of strategies in the projects or protocols for drug development due to the different tasks and challenges in the quest of hit compounds. Molecular docking is an important part of this area bringing consistent advantages. It is a nice tool that decreases consuming time by allowing calculations with several compounds simultaneously, with the use of an appropriated scoring function, and including a suitable force field, the researcher could obtain positive results in many cases. Nevertheless, it is important to recognize that the halogenated compounds have no chemical behavior that is studied in most of docking programs; thus, it is necessary to take in account the scoring functions or force fields showed here if it is a need to carry out molecular docking with halogenated ligands. The concepts and fundamental aspects of XB are well known, their importance in the drug design and discovery processes, thereby, the non-covalent interactions involving halogens as Lewis acid donors and the Lewis base acceptors have become in an important issue during pharmacophore design suiting halogenated ligand or drugs using computational approaches and methods. Here, we have described the main aspects about the computational considerations, specifically in molecular docking because it remains the tool to investigate the type of ligand-receptor interactions, and the XB represents a challenge due to its electronic anisotropic effects that we need to define and select for the best scoring function to achieve accurate results and to predict good results about the interactions in the supramacromolecular chemistry leading to the improvement of some techniques and methods in the computer-aided drug discovery field.

Author details

Abel Suárez-Castro[1]*, Mario Valle-Sánchez[1], Carlos Jesús Cortés-García[2] and Luis Chacón-García[1]

*Address all correspondence to: belypat@hotmail.com

1 Instituto de Investigaciones Químico-Biológicas, Universidad Michoacana de San Nicolás de Hidalgo, Morelia, Michoacán, México

2 Apotex, API Toluca, Toluca, Edo. Mex., México

References

[1] Politzer P, Murray JS, Clark T. Halogen bonding and other σ-hole interactions: A perspective. Physical Chemistry Chemical Physics. 2013;**15**:11178-11189. DOI: 10.1039/C3CP00054K

[2] Guthrie F. XXVIII—On the iodide of iodammonium. Journal of the Chemical Society. 1863; **16**:239-244. DOI: 10.1039/JS8631600239

[3] Hassel O. Structural aspects of interatomic charge-transfer bonding. Science. 1970;**170**: 497-502. DOI: 10.1126/science.170.3957.497

[4] Ho PS. Halogen bonding in medicinal chemistry: From observation to prediction. Future science. Medicinal Chemistry. 2017;**9**:637-640. DOI: 10.4155/fmc-2017-0052

[5] Hays FA, Vargason JM, Ho PS. Effect of sequence on the conformation of DNA Holliday Junctions. Biochemistry. 2003;**42**:9586-9597. DOI: 10.1021/bi0346603

[6] Howard EI, Sanishvili R, Cachau RE, Mitschler A, Chevrier B, Barth P, Lamour V, Van Zandt M. Ultrahigh resolution drug design I: Details of interactions in human aldose reductase-inhibitor complex at 0.66 Å. Proteins: Structure, Function, and Bioinformatics. 2004;**55**:792-804. DOI: 10.1002/prot.20015

[7] Himmel DM, Das K, Clark AD Jr, Hughes SH, Benjahad A, Oumouch S, Guillemont J, Coupa S, Poncelet A, Csoka I, Meyer C, Andries K, Nguyen H, Grierson DS, Arnold E. Crystal structures for HIV-1 reverse transcriptase in complexes with three pyridinone derivatives: A new class of non-nucleoside inhibitors effective against a broad range of drug-resistant strains. Journal of Medicinal Chemistry. 2005;**48**:7582-7591. DOI: 10.1021/jm0500323

[8] Xu Z, Liu Z, Chen T, Chen TT, Wang Z, Tian G, Shi J, Wang X, Lu Y, Yan X, Wang G, Jiang H, Chen K, Wang S, Xu Y, Shen J, Zhu W. Utilization of halogen bond in lead optimization: A case study of rational Design of Potent Phosphodiesterase Type 5 (PDE5) inhibitors. Journal of Medicinal Chemistry. 2011;**54**:5607-5611. DOI: 10.1021/jm200644r

[9] Lu Y, Shi T, Wang Y, Yang H, Yan X, Luo X, Jiang H, Zhu W. Halogen bondings—A novel interaction for rational drug design? Journal of Medicinal Chemistry. 2009;**52**:2854-2862. DOI: 10.1021/jm9000133

[10] Chung HR. Iodine and thyroid function. Annals of Pediatric Endocrinology & Metabolism. 2014;**19**:8-12. DOI: 10.6065/apem.2014.19.1.8

[11] Everett ET. Fluoride's effects on the formation of teeth and bones, and the influence of genetics. Critical Reviews in Oral Biology & Medicine. 2011;**90**:552-560. DOI: 10.1177/0022034510384626

[12] Kunz W. Specific ion effects in colloidal and biological systems. Current Opinion in Colloid & Interface Science. 2010;**15**:34-39. DOI: 10.1016/j.cocis.2009.11.008

[13] Lévesque D, Beaudoin J, Roy S, Perreault J. In vitro selection and characterization of RNA aptamers binding thyroxine hormone. Biochemical Journal. 2007;**403**:129-138. DOI: 10.1042/BJ20061216

[14] Barbier O, Arreola-Mendoza L, Del Razo LM. Molecular mechanisms of fluoride toxicity. Chemico-Biological Interactions. 2010;**188**:319-333. DOI: 10.1016/j.cbi.2010.07.011

[15] Metrangolo P, Meyer F, Pilati T, Resnati G, Terraneo G. Halogen bonding in supramolecular chemistry. Angewandte Chemie International Edition. 2008;**47**:6114-6127. DOI: 10.1002/anie.200800128

[16] Zhou Y, Wang J, Gu Z, Wang S, Zhu W, Aceña JL, Soloshonok VA, Izawa K, Liu H. Next generation of fluorine-containing pharmaceuticals, compounds currently in phase II-III clinical trials of major pharmaceutical companies: New structural trends and therapeutic areas. Chemical Reviews. 2016;**116**:422-518. DOI: 10.1021/acs.chemrev.5b00392

[17] Fischer J, Ganellin CR. Analogue-based Drug Discovery. 2nd ed. Germany: Wiley-VCH; 2010. 564 p. DOI: 978-3-527-32549-8

[18] Hernandes MZ, Cavalcanti SMT, Moreira DRM, Azevedo Junior WF, Leite CL. Halogen atoms in the modern medicinal chemistry: Hints for the drug design. Current Drug Targets. 2013;**11**:303-314. DOI: 10.2174/138945010790711996

[19] Kosjek T, Heath E. Halogenated Heterocycles as pharmaceuticals. Topics in Heterocyclic Chemistry. 2012;**27**:219-246. DOI: 10.1007/7081_2011_61

[20] Purser S, Moore PR, Swallow S, Gouverneur V. Fluorine in medicinal chemistry. Chemical Society Reviews. 2008;**37**:320-330. DOI: 10.1039/B610213C

[21] Ho PS. Halogen bonding in medicinal chemistry: From observation to prediction. Future Medicinal Chemistry. 2017;**9**:637-640. DOI: https://doi.org/10.4155/fmc-2017-0052

[22] Kinch MS, Haynesworth A, Kinch SL, Hoyer D. An overview of FDA-approved new molecular entities: 1827-2013. Drug Discovery Today. 2014;**19**:1033-1039. DOI: https://doi.org/10.1016/j.drudis.2014.03.018

[23] FDA. Novel Drug Approvals for 2017 [Internet]. 2017. Available from: https://www.fda.gov/Drugs/DevelopmentApprovalProcess/DrugInnovation/ucm537040.htm [Accessed: 2017-09-01]

[24] Genetic Engineering & Biotechnology News. 15 Top-Selling Drugs Launched in 2015 [Internet]. 2016. Available from: http://www.genengnews.com/the-lists/15-top-selling-drugs-launched-in-2015/77900625?page=1 [Accessed: 2017-09-01]

[25] Genetic Engineering & Biotechnology News. The Top 25 Best-Selling Drugs of 2014 [Internet]. 2015. Available from: http://www.genengnews.com/the-lists/the-top-25-best-selling-drugs-of-2014/77900383?page=1 [Accessed: 2017-09-01]

[26] Genetic Engineering & Biotechnology News. The Top 25 Best-Selling Drugs of 2013 [Internet]. 2014. http://www.genengnews.com/the-lists/the-top-25-best-selling-drugs-of-2013/77900053?page=1 [Accessed: 2017-09-01]

[27] Forbes. The Best-Selling Drugs of All Time; Humira Joins the Elite [Internet]. 2013. https://www.forbes.com/sites/simonking/2013/01/28/the-best-selling-drugs-of-all-time-humira-joins-the-elite/#7b2249d75110 [Accessed: 2017-09-01]

[28] Clarivate Analytics. The Blockbuster Drugs of 2016 [Internet]. 2017. https://clarivate.com/blog/the-blockbuster-drugs-of-2016/ [Accessed: 2017-09-01]

[29] Smith BR, Eastman CM, Njardarson JT. Beyond C, H, O, and N! Analysis of the elemental composition of U.S. FDA approved drug architectures. Journal of Medicinal Chemistry. 2014;**57**:9764-9773. DOI: 10.1021/jm501105n

[30] Xu Z, Yang Z, Liu Y, Lu Y, Chen K, Zhu W. Halogen bond: Its role beyond drug–target binding affinity for drug discovery and development. Journal of Chemical Information and Modeling. 2014;**54**:69-78. DOI: 10.1021/ci400539q

[31] Lu Y, Liu Y, Xu Z, Li H, Liu H, Zhu W. Halogen bonding for rational drug design and new drug discovery. Expert Opinion in Drug Discovery. 2012;**7**:375-383. DOI: 10.1517/17460441.2012.678829

[32] Anslyn EV, Dougherty DA, editors. Modern Physical Organic Chemistry. USA: University Science Books; 2006. 1095 p. Chapter 4: Molecular Recognition and Supramolecular Chemistry, 222-251

[33] McConnell A, Beer PD. Heteroditopic receptors for ion-pair recognition. Angewandte Chemie—International Edition. 2012;**51**:5052-5061. DOI: 10.1002/anie.201107244

[34] Martinez CR, Iverson BL. Rethinking the term "pi-stacking". Chemical Science. 2012; **3**:2191-2201. DOI: 10.1039/c2sc20045g

[35] McKee WC, Agarwal J, Schaefer HF, Schleyer P. Covalent hypercoordination: Can carbon bind five methyl ligands? Angewandte Chemie—International Edition. 2014;**53**:7875-7878. DOI: 10.1002/anie.201403314

[36] Mele A, Metrangolo P, Neukirch H, Pilati T, Resnati G. A halogen-bonding-based heteroditopic receptor for alkali metal halides. Journal of the American Chemical Society. 2005;**127**:14972-14973. DOI: 10.1021/ja054862h

[37] Metrangolo P, Neukirch H, Pilati T, Resnati G. Halogen bonding based recognition processes: A world parallel to hydrogen bonding. Accounts of Chemical Research. 2005; **38**:386-395. DOI: 10.1021/ar0400995

[38] Scholfield MR, Vander CM, Carter M, Ho PS. Halogen bonding (X-bonding): A biological perspective. Protein Science. 2013;**22**:139-152. DOI: 10.1002/pro.2201

[39] Catalano L, Pérez-Estrada S, Wang H, Ayitou A, Khan S, Terraneo G, Metrangolo P, Brown S, Garcia-Garibay MA. Rotational dynamics of diazabicyclo [2.2.2] octane in isomorphous halogen-bonded co-crystals: entropic and enthalpic effects. Journal of the American Chemical Society. 2017;**139**:843-848. DOI: 10.1021/jacs.6b10780

[40] Coates M, Ho P. Computational tools to model halogen bonds in medicinal chemistry. Journal of Medicinal Chemistry. 2016;**59**:1655-1670. DOI: 10.1021/acs.jmedchem.5b00997

[41] Wolters LP, Schyman P, Pavan MJ, Jorgensen WL, Bickelhaupt FM, Kozuch S. The many faces of halogen bonding: A review of theoretical models and methods. WIREs Computational Molecular Science. 2014;**4**:523-540. DOI: 10.1002/wcms.1189

[42] Cavallo G, Metrangolo P, Milani R, Pilati T, Priimagi A, Resnati G, Terraneo G. The halogen bond. Chemical Reviews. 2016;**116**:2478-2601. DOI: 10.1021/acs.chemrev.5b00484

[43] Řezáč J, Šimová L, Hobza P. CCSD[T] describes noncovalent interactions better than the CCSD(T), CCSD(TQ), and CCSDT methods. Journal of Chemical Theory and Computation. 2012;**9**:364-369. DOI: 10.1021/ct3008777

[44] Kurczab R. The evaluation of QM/MM-driven molecular docking combined with MM/GBSA calculations halogen-bond scoring strategy. Structural Science Crystal Engineering Materials. 2016;**B73**:1-7. DOI: 10.1107/S205252061700138X

[45] Liu Y, Xu Z, Yang Z, Chen K, Zhu W. A knowledge-based halogen bonding scoring function. Journal of Molecular Modelling. 2013;**19**:5015-5030. DOI: 10.1007/s00894-013-2005-7

[46] Eldridge MD, Murray CW, Auton TR, Paolini GV. Empirical scoring functions: I. The development of a fast-empirical scoring function to estimate the binding affinity of ligands in receptor complexes. Journal of Computer-Aided Molecular Design. 1997;**11**:425-445. DOI: 10.1023/A:1007996124545

[47] Kitchen DB, Decornez H, Furr JR, Bajorath J. Docking and scoring in virtual screening for drug discovery: Methods and applications. Nature Reviews Drug Discovery. 2004;**3**:935-949. DOI: 10.1038/nrd1549

[48] Kuhn B, Fuchs JE, Reutlinger M, Stahl M, Taylor NR. Rationalizing tight ligand binding through cooperative interaction networks. Journal of Chemical Information and Modeling. 2011;**51**:3180-3198. DOI: 10.1021/ci200319e

[49] Koebel MR, Schmadeke G, Posner RG, Sirimulla S. AutoDock VinaXB: Implementation of XBSF, new empirical halogen bond scoring function, into AutoDock Vina. Journal of Cheminformatics. 2016;**8**:2-8. DOI: 10.1186/s13321-016-0139-1

[50] Pal D, kolluru V, Chandrasekaran B, Baby BV, Aman M, Suman S, Sirimulla S, Sanders MA, Alatassi H, Ankem MK, Damodaran C. Targeting aberrant expression of Notch-1 in ALDH cancer stem cells in breast cancer. Molecular Carcinogenesis. 2017;**56**:1127-1136. DOI: 10.1002/mc.22579

[51] Šeflová J, Cechov P, Biler M, Hradil P, Kubala M. Inhibition of Naþ/Kþ-ATPase by 5,6,7,8-tetrafluoro-3-hydroxy-2-phenylquinolin-4(1H)-one. Biochimie. 2017;**138**:56-61. DOI: 10.1016/j.biochi.2017.04.009

[52] Enkhtaivan G, Muthuraman P, Kim DH, Mistry B. Discovery of berberine based derivatives as anti-influenza agent through blocking of neuraminidase. Bioorganic and Medicinal Chemistry. 2017;**25**:5185-5193. DOI: 10.1016/j.bmc.2017.07.006

[53] Fusi F, Trezza A, Spiga O, Sgaragli G, Bova S. Cav1.2 channel current block by the PKA inhibitor H-89 in rat tail artery myocytes via a PKA-independent mechanism: Electrophysiological, functional, and molecular docking studies. Biochemical Pharmacology. 2017;**140**:53-63. DOI: 10.1016/j.bcp.2017.05.020

[54] Jorgensen WL, Schyman P. Treatment of halogen bonding in the OPLS-AA force field: Application to potent anti-HIV agents. Journal of Chemical Theory and Computation. 2012;**8**:3895-3901. DOI: 10.1021/ct300180w

[55] Schilfield MR, Ford MC, Vander Zanden CM, Billman MM, Ho PS, Rappé AK. Force field model of periodic trends in biomolecular halogen bonds. Journal of Physical Chemistry B. 2015;**119**(29):9140-9149. DOI: 10.1021/ip509003r

[56] Zimmermann MO, Lange A, Boeckler FM. Evaluating the potential of halogen bonding in molecular design: Automated scaffold decoration using the new scoring function XBScore. Journal of Chemical Information and Modeling. 2015;**55**(3):687-699. DOI: 10.1021/ci5007118

Chapter 7

A Combined Molecular Docking and Electronic Structure Study for a Breast Cancer Drug Design

Linda-Lucila Landeros-Martinez,
Daniel Glossman-Mitnik,
Erasmo Orrantia-Borunda and
Norma Flores-Holguin

Additional information is available at the end of the chapter

http://dx.doi.org/10.5772/intechopen.72895

Abstract

The molecular docking of tamoxifen's metabolites, 4-hydroxy-tamoxifen, N-desmethyl-tamoxifen, and 4-hydroxy-N-desmethyl-tamoxifen, in estrogen and progesterone hormone receptors was studied in aqueous solution. The metabolites 4-hydroxy-tamoxifen, N-desmethyl-tamoxifen, and 4-hydroxy-N-desmethyl-tamoxifen exhibit a binding energy in the estrogen receptor cavity of −10.69 kcal/mol, −10.9 kcal/mol, and −11.35 kcal/mol, respectively, and −1.45 kcal/mol, −9.29 kcal/mol, and −0.38 kcal/mol in the progesterone receptor. This indicates a spontaneous interaction between the metabolites and the active sites in the hormone receptors. Docking has an adequate accuracy for both receptors, and from this calculation the active site residues were defined for the different metabolites and the estrogen and progesterone receptors. Also, the chemical reactivity of the amino acids of the active sites of each metabolite was determined. These reactivity properties were obtained within the framework of density functional theory, using the functional M06 with the basis set 6-31G (d). The results indicate that in the estrogen receptor, the highest charge transfer of the three analyzed metabolites is in the union of the metabolite and the Leu346-Thr347 residue. The progesterone receptor shows minor tendency to react with higher hardness values than the estrogen receptor. The hydrogen bonds are three for the estrogen receptor in two different metabolites, while in progesterone only one is formed with the N-desmethyl-tamoxifen metabolite.

Keywords: molecular docking, tamoxifen, binding energy, charge transfer, hydrogen bond, hormone receptors

1. Introduction

Breast cancer is the leading cause of cancer death in women. A prognosis of breast cancer can be issued because there are parameters that predict the evolution or aggressiveness of the cancer, such as lymph nodes, tumor size, and histological grade of cancer [1–4]. In mammary cells there are hormone receptors (estrogen receptors (ERs) and progesterone receptors (PRs)) that function as "switches," activating or deactivating a particular function in the mammary cell.

Over the last two years a number of drugs have been developed with specific properties for the treatment of breast cancer. Fulvestrant is a steroid-based selective estrogen receptor downregulator (SERD) that antagonizes and degrades ER-α and is active in patients who have progressed to antihormonal agents [5]. Also, the selective ER modulators (SERMs)/SERD hybrids (SSHs) have been used to facilitate the first-line treatment for ER 1 degradation in breast cancer cells [6].

Another important piece of research by Srinivasan et al. presents the discovery of a series of SERDs lacking a prototypical side chain. This absence improves the mechanism called "indirect antagonism" [7]. The latest developments have found the optimal design of antiestrogen cores and side chains with the middle structures of the original SERMs class, such as tamoxifen (TAM), raloxifene, lasofoxifene, and bazedoxifene. Also, current studies of SERDs have been made by GlaxoSmithKline(GSK), Genentech, and AstraZeneca. In these studies the side chain is modified to a simple adamantyl core [8].

In addition, for several years, have been used antibodies as cancer drugs, and some examples are trastuzumab and pertuzumab, which are used in breast cancer as the only component. In fact, efforts have been made to use the antibodies conjugated with a variety of substances with the aim of improving their effect. Research on cancer therapy is still in progress [9].

TAM is a SERM [10, 11] and is used for the treatment of hormone receptors expressing breast cancer [12]. This drug is metabolized in the liver, producing three different metabolites: 4-hydroxy-tamoxifen (4OHTAM), N-desmethyl-tamoxifen (NDTAM), and 4-hydroxy-N-desmethyl-tamoxifen, also known as endoxifen (END) [13, 14]. These metabolites show a range of agonist and partial antagonist activities of ER-mediated effects [15]. In vivo studies have shown that TAM competes against estrogens to dock to the receptors, resulting in an attenuation of the cellular response measured by estrogen [16]. Therefore, the clinical response to TAM therapy will depend on the total effect of the resulting metabolites on the patient, their affinity for receptors, and their agonist/antagonist profile [15].

Recently, a number of theoretical studies on TAM and some of its active metabolites have described its interaction with ERs. Calculations of molecular dynamics have been used to model dynamic fluctuations in structures of ERs (ER-α following the binding to estradiol and the metabolite 4OHTAM) [17]. Recently, in an article written by the authors, the molecular docking of TAM in ER and PR was presented in which the active site of the hormone receptors was determined, as well as the charge transfer of the drug to the amino acids of the active sites of the receptors [18]. Other theoretical studies analyzed the chirality of TAM using density

functional theory (DFT) with functional B3LYP and BLYP with a basis set 6-311++G(2d, 2p) [12]. In addition, there was a reported analysis of the amount of charge transfer and the direction of the flow of charge of alkylating drugs in the presence of DNA bases allowing prediction among its bases of which one is the main target of these antitumor drugs [19].

Another technique is molecular docking, which is a computational procedure that attempts to predict noncovalent binding of macromolecules (receptor) and small molecules (ligands) efficiently [20]. In detail, docking consists of an operation in which one molecule is brought into the vicinity of another while calculating the interaction energies of the many mutual orientations and conformations of the two interacting species. A docking procedure is used as a guide to identify the preferred orientation of one molecule relative to the other [21]. This method plays a key role in promoting fundamental biomolecular events such as enzyme–substrate, drug–protein, and drug–nucleic acid interactions [22]; it is also widely used in drug design [23]. Some authors have used the molecular docking of macromolecules to define the energy and bonding affinity in ER-α and ER-β with estrogen [24]. It has also been used in the analysis of a maltogenic amylase of *Bacillus lehensis* G1, which provides a view of the substrate and specificity in the macromolecule [25], and in the DNA docking analysis of natural products such as methyltransferase inhibitors, which have become an alternative for cancer therapies [26].

The objective of this research is to develop molecular docking of the metabolites of TAM with the macromolecules ER and PR, to obtain an active site of the hormone receptors. To perform computational protein–ligand docking experiments, a 3-D structure of the target protein at atomic resolution must be available. The most reliable sources are crystal and solution structures provided by the Protein Data Bank (PDB) [26, 27]. The hormone receptors selected for this work are the 1A52 ER-α ligand-binding domain complexed to estradiol, and the 1A28 hormone-bound human progesterone receptor ligand-binding domain. Both belong to the organism *Homo sapiens* and are present in breast cancer cells. Molecular docking has the advantage of working on a large scale, as well as determining the important sites of the macromolecule (active sites) [27, 28]. Once the active site is defined, an accurate calculation of electronic structure can be developed with methods such as DFT, which is the most popular, efficient, and versatile tool for obtaining precise information of molecular systems. For both receptors, the amino acids (residues) forming the active site were analyzed in an attempt to obtain their electronic properties such as ionization potential, electron affinity, electrophilicity, chemical hardness, chemical potential, and electronegativity. A transfer and charge flow direction analysis was also performed.

2. Computational details

2.1. Molecular docking

Molecular docking is calculated with the specially tailored software AutoDock 4.2 with the Lamarckian Genetic Algorithm (LGA) [28, 29] to explore how ER and PR bond with the metabolites. AutoDock uses a semiempirical free energy force field to predict binding free energies of

small molecules to macromolecule targets [29]. The force field is based on a comprehensive thermodynamic model that allows incorporation of intramolecular energies into the predicted free energy of binding. It also incorporates a charge-based method for evaluation of desolvation designed to use a typical set of atom types [30]. The use of LGA allows individual conformations to search their local conformational space, find local minima, and then pass this information to later generations [29]; also LGA can handle ligands with more degrees of freedom and is efficient, reliable, and successful [31].

The water molecules in the receivers are eliminated and only the polar H atoms are added. The docking area is selected by constructing a grid box, size 52 × 36 × 34 points, centered at x, y, and z coordinates of 89.304, 14.745, and 70.512, respectively, for ER, and a grid box, size 20 × 18 × 26 points, centered at x, y, and z coordinates of 36.999, 31.767, and 42.694, respectively, for PR using in both receptors a grid spacing of 0.375 Å in AutoGrid [28, 29]. The docking parameters used for the LGA-based conformational searches are: docking trials—150; population size—150; maximum number of energy evaluations—25,000,000; maximum number of top individuals to survive to next generation—1; rate of gene mutation—0.02; rate of crossover —0.8; mean of Cauchy distribution for gene mutation—0.0; variance of Cauchy distribution for gene mutation—1.0; and number of generations for picking the worst individual—10.

2.2. Electronic structure calculations

The energy calculations of the amino acids that make up the active site on ER, PR, and TAM metabolites are calculated with the functional hybrid meta-GGA M06 [32, 33] developed by the Truhlar Group from the University of Minnesota, combined with the basis set 6-31G (d) proposed by Pople [34] and the conductor-like polarizable continuum model (CPCM) [35] using water as a solvent. All calculations were made using DFT [35–38] with the Gaussian program 09 [39]. The charge distribution for amino acids and metabolites was obtained with the population analysis of Hirshfeld charges [40].

Equations	
$$\eta = \frac{(I - AE)}{2}$$	(1)
$$\chi = \frac{(I + AE)}{2}$$	(2)
$$\omega = \frac{\mu^2}{2\eta}$$	(3)
$$\mu = -\chi$$	(4)
$$\Delta N = \frac{\mu_B - \mu_A}{2(\eta_A + \eta_B)}$$	(5)

Table 1. Global reactivity and charge transfer parameters.

http://dx.doi.org/10.5772/intechopen.72895

The chemical reactivity descriptors of the studied molecular systems were calculated using the DFT conceptual framework. These parameters include ionization potential (I), electron affinity (EA), chemical hardness (η) [41], electronegativity (χ) [41], electrophilicity (ω) [42], and chemical potential (μ) [42]. The overall interaction between metabolites and the amino acids that make up the active site on ER and PR can be identified by the charge transfer. This parameter determines the behavior of the different molecular systems as a donor or as an acceptor system. In this case, the electrons transferred from the metabolites to the amino acids of the active site of receptors or vice versa. The global interactions between two constituents can been determined using the charge transfer parameter (ΔN) [43].

The equations of the reactivity and charge transfer descriptors are shown in **Table 1**.

3. Results and discussion

3.1. Validation docking

Validation docking was performed for each hormone receptor using the PyMOL program [44]. **Figure 1** shows the structure of the native co-crystallized TAM bond and its metabolites. The root mean square deviation (RMSD) between TAM and the metabolites was calculated for each

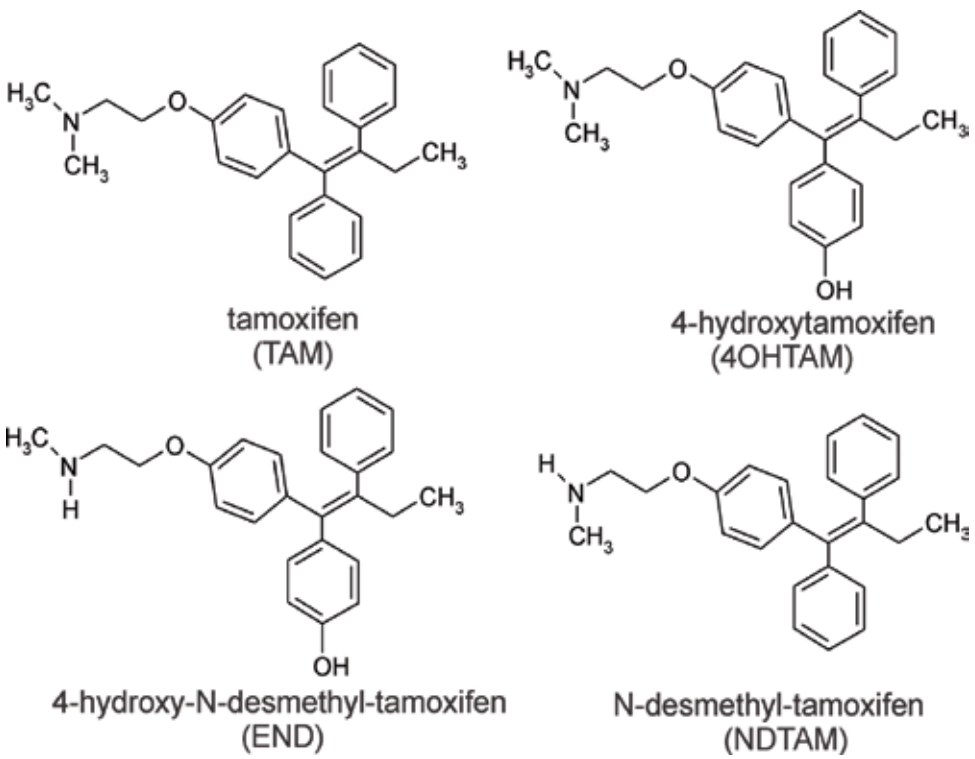

Figure 1. Chemical structures of tamoxifen and metabolites.

of the hormone receptor dockings. An RMSD value is considered a measurement of the accuracy of the docking results. The optimal position is recognized if the RMSD value is less than 2 Å [45]. In the case of metabolite dockings, TAM was used as the template for molecular overlap, as it is known that this drug is metabolized into the metabolites analyzed in this study. The metabolites were aligned by rotation and translation to obtain the RMSD using the "Align" option in PyMOL. Therefore, the RMSD in ER obtained between TAM with 4OHTAM, END, and NDTAM is 0.672, 1.106, and 1.461, respectively. For PR the RMSD obtained between TAM and 4OHTAM, END, and NDTAM is 1.387, 2.006, and 0.953, respectively. **Figure 2** shows the alignment between TAM (black) and 4OHTAM, END, and NDTAM (gray).

3.2. Analysis of the estrogen receptor with the metabolites

An analysis of molecular docking of the metabolites in ER was carried out, revealing the active site of the ER, followed by its description, the analysis of the chemical reactivity parameters of the residues and the metabolites, as well as the description of the hydrogen bonds between the metabolites and the ER active site.

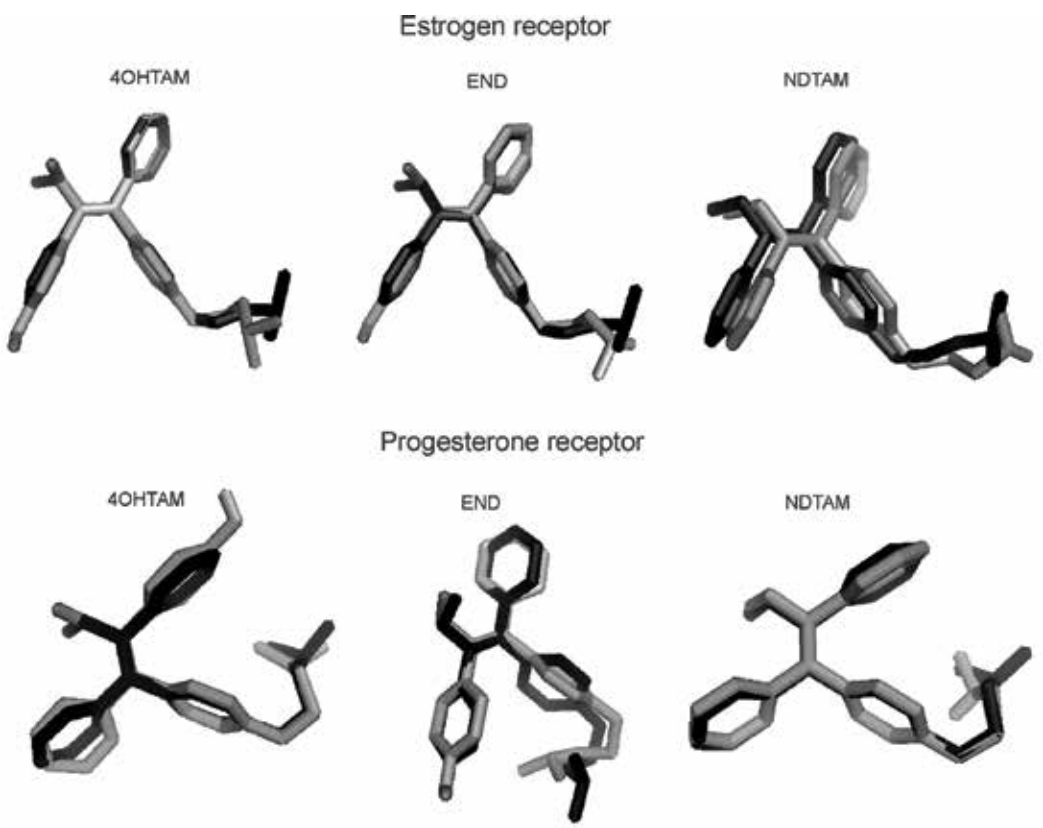

Figure 2. Conformation of tamoxifen and metabolites after docking in hormone receptors.

3.2.1. Molecular docking

The binding energy of the metabolites with the ER active site was predicted with molecular docking calculations. The negative value of the binding energy (affinity) in the docking indicates that the system is stable and that there is an interaction between ER and the metabolites in the active site: −10.69 kcal/mol for 4OHTAM, −11.35 kcal/mol for END, and − 10.90 kcal/mol for NDTAM. It was observed that the binding affinity was lower in 4OHTAM; this is due to the effect of the orientation of the metabolite within the active site caused by the influence of the tertiary amine functional group containing the 4OHTAM.

Finally, the binding energy shows that END, which exhibits −11.35 kcal/mol, is the metabolite with the highest affinity with the active site. It even shows a better affinity than TAM at −10.38 kcal/mol [18]. This coincides with previous information reported by Clarke [46] who says that END has an affinity for ERs higher than NDTAM or TAM itself. As can be observed, all the metabolites have a high affinity to the receptor. According with Gareth [47], the greater the affinity of the ligand for the receptor, the more easily it binds to that receptor. This is important because the binding of a drug to a receptor stimulates the physiological response that characterizes the action of the drug, which means that release of a series of biochemical events results in a biological or pharmacological effect [47].

The schematic structure of the active site and the binding energies are shown in **Figure 3**.

3.2.2. Active site

The conformational coupling of the active site with each metabolite is described below.

4OHTAM. There are 14 residues in contact with the metabolite 4OHTAM at the active site of the ER. Nine of them are linked forming an amino acids sequence: leucine346-threonine347 (Leu346-Thr347), tryptophan383-leucine384 (Trp383-Leu384), glutamic acid353-leucine354 (Glu353-Leu354), and leucine349-alanine350-aspartic acid351 (Leu349-Ala350-Asp351). The other five are: glycine residue (Gly521)—glycine is the smallest of the amino acids. It is ambivalent, which means that the amino acid can be inside or outside of the protein molecule; lysine529 (Lys529)—this residue contains a protonated amino group that provides a positive charge to proteins as acetyltransferases; histidine524 (His524)—this residue has a positively charged imidazole functional group. This group participates in enzyme-catalyzed reactions; phenylalanine404 (Phe404)—an essential amino acid, it is a derivative of alanine with a phenyl substituent on the β carbon. Due to its hydrophobicity, phenylalanine is nearly always found buried within a protein. The π electrons of the phenyl ring can stack with other aromatic systems and often do so within folded proteins, adding stability to the structure; and finally, methionine388 (Met 388), which has a hydrophobic thiol ether in its lateral chain. According to the results obtained by theoretical calculations, in the metabolite 4OHTAM the active site of estrogen coincides with that reported by Shiau et al. [48].

END. The active site of END is formed by the following residues: leucine346-threonine347 (Leu346-Thr347), leucine387-methionine388 (Leu387-Met388), tryptophan383-leucine384 (Trp383-Leu384), glycine521 (Gly521), and histidine524 (His524). The last two residues are highly hydrophilic.

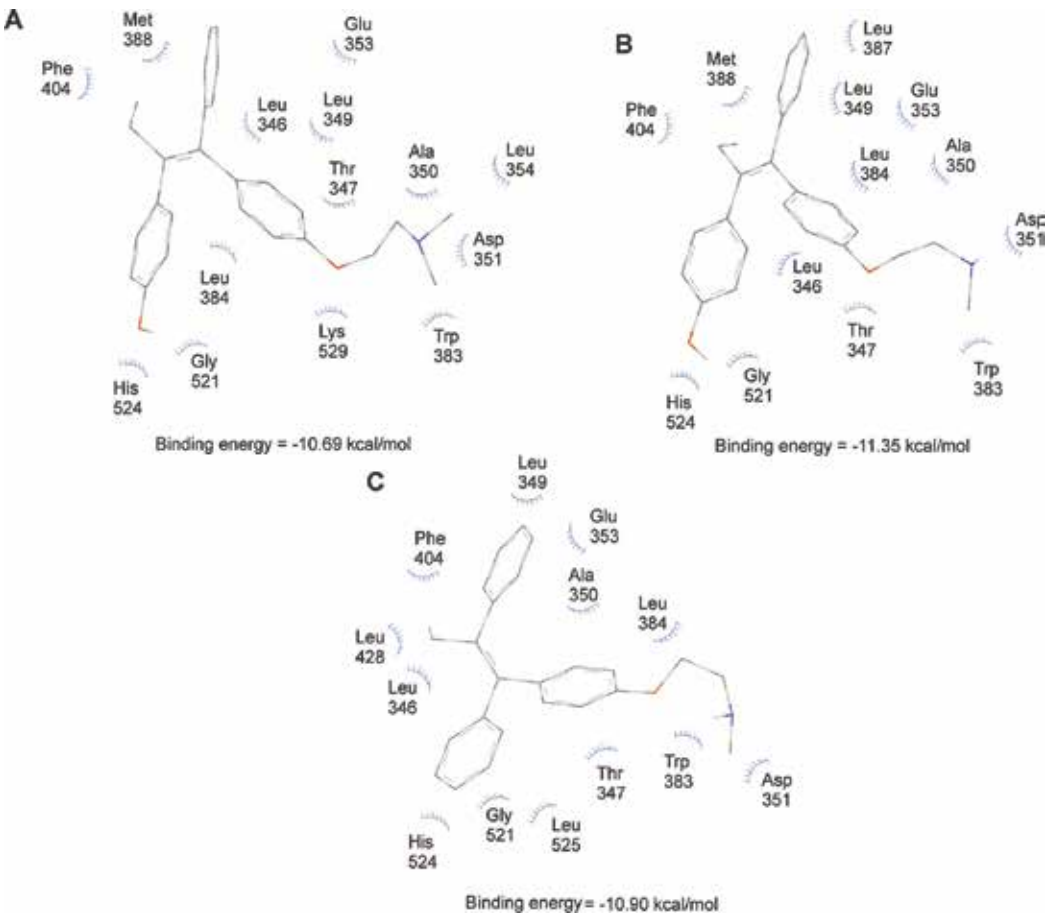

Figure 3. Amino acids of the active site of the estrogen receptor with (A) 4OHTAM, (B) END, and (C) NDTAM.

NDTAM. The active site in NDTAM consists of the following residues: leucine346-threonine347 (Leu346-Thr347), histidine524-leucine525 (His524-Leu525), tryptophan383-leucine384 (Trp383-Leu384), and (Leu349-Ala350-Asp351),and hydrophilic residue glycine521 (Gly521) and hydrophobic residues phenylalanine404 (Phe404), glutamic acid (Glu353), and leucine428 (Leu428).

Most of the residues are situated over the planar core of the ligand. The others surround the functional groups amine and hydroxyl. These interactions contribute to binding energies of up to −10 kcal/mol.

The metabolites act by blocking the activation domain AF-2 of ER found in the ligand bond domain or LBD of the active site. Therefore, the metabolites act as estrogen antagonists over the genes that require only the activation domain AF-2 [49, 50].

The residues for the metabolites in ER are shown in **Figure 3**.

3.2.3. Chemical reactivity

Once the most stable structure of the active site of TAM's metabolites were defined, an analysis of the reactivity of ER residues was performed using descriptors such as ionization potential (I), electron affinity (EA), chemical potential (μ), chemical hardness (η), and electrophilicity (ω). Calculated results for the reactivity parameters of the drug and residues of the ER are shown in **Table 2**.

The electron affinities of the residues fluctuate from 0.21 eV to 0.91 eV. The highest value of electron affinity is for the Trp383-Leu384 residue, which is present in the active site of the three different metabolites analyzed in this work. According to the ionization potential results, the residue with the greatest possibility of losing electrons is Leu346-Thr347 with 7.74 eV. This residue is present in the active site of the three metabolites.

Metabolite	Active site	EA (eV)	I (eV)	hη(eV)	μ = −χ (eV)	ω (eV)
4OHTAM	Gly521	0.21	7.03	3.41	3.62	1.92
	Met388	0.46	6.11	2.82	2.39	1.91
	His524	0.43	6.2	2.89	3.31	1.9
	Lys529	0.83	7.22	3.19	4.02	2.54
	Phe404	0.51	6.4	2.95	3.46	2.03
	Trp383-Leu384	0.91	6.04	2.56	3.47	2.35
	Glu353-Leu354	0.66	5.59	2.47	3.13	1.98
	Leu346-Thr347	0.88	7.74	3.43	4.31	2.71
	Leu349-Ala350-Asp351	0.73	5.79	2.53	3.26	2.1
END	Gly521	0.21	7.03	3.41	3.62	1.92
	His524	0.43	6.2	2.89	3.31	1.9
	Leu387-Met388	0.51	6.25	2.87	3.38	1.99
	Leu346-Thr347	0.88	7.74	3.43	4.31	2.71
	Trp383-Leu384	0.91	5.79	2.53	3.26	2.1
NDTAM	Gly521	0.21	7.03	3.41	3.62	1.92
	Phe404	0.51	6.4	2.95	3.46	2.03
	Glu353	0.2	5.62	2.71	2.91	1.57
	Leu428	0.47	7	3.23	3.73	2.14
	His524-Leu525	0.81	6.1	2.65	3.46	2.25
	Trp383-Leu384	0.91	6.04	2.56	3.47	2.35
	Leu346-Thr347	0.88	7.74	3.43	4.31	2.71
	Leu349-Ala350-Asp351	0.73	5.79	2.53	3.26	2.1

Table 2. Parameters of chemical reactivity of the active site residues of the estrogen receptor.

Chemical hardness ranges from 2.53 eV to 3.43 eV; this parameter measures the resistance to change in the electronic configuration. The Glu353-Leu354 residue with 2.47 eV will react more easily in the presence of 4OHTAM, the Leu349-Ala350-Asp351 residue with 2.53 eV will react more easily in the presence of NDTAM, and the Trp383-Leu384 residue with 2.56 eV will react more easily in the presence of END. The chemical potential ($\mu = -\chi$) represents the average effect between the tendency among molecules to attract and transfer electrons. This parameter is an important part in the description of the charge transfer descriptor. The electronegativity shows that the Leu346-Thr347 residue has the greatest tendency to attract electrons with 4.31 eV. This trend is repeated with the three different metabolites. Electrophilicity ω represents the stabilization energy of the systems when it becomes saturated with electrons coming from the surroundings. In this case, in the active site of 4OHTAM, value decreases in the following order: Leu346-Thr347 > Lys529 > Trp383-Leu384 > Leu349-Ala350-Asp351 > Phe404 > Glu353-Leu354 > Gly521 > Met388 > His524. In END the decreasing order is Leu346-Thr347 > Trp383-Leu384 > Leu387-Met388 > Gly521 > His524 and in NDTAM the decreasing order is Leu346-Thr347 > Trp383-Leu384 > His524-Leu525 > Leu428 > Leu349-Ala350-Asp351 > Phe404 > Gly521 > Glu353.

3.2.4. Charge transfer descriptor

The chemical reactivity descriptors mentioned above are intramolecular parameters, whose values are calculated from the electronic properties of the molecule. To understand a chemical reaction in depth an intermolecular parameter that represents the fractional number of electrons transferred from one system to another should also be considered. This parameter is called charge transfer and is described as Eq. 5 in **Table 1**. In this formula, μA is TAM's metabolites and μB is the chemical potential for the residues of the active site. ηA, ηB represent the chemical hardness of TAM's metabolites and its residues of the active site, respectively [43]. The significance of these kinds of interactions lies in the fact that they are the primary directors of specificity, rate control, and reversibility in many biochemical reactions. Furthermore, it represents a first step in understanding oxidative damage in the active site produced by the TAM's metabolites and leads to identify their functioning and biological activity. Some authors use charge transfer to describe the oxidative damage of DNA bases [51, 52].

The interpretation of the value ΔN is as follows: for $\Delta N < 0$ the charge flows from A to B (A acts as an electron donor). For $\Delta N > 0$ the charge flows from B to A (A acts as an electron acceptor). Therefore, in the presence of Glu353-Leu354, Leu349-Ala350-Asp351, and His524 residues, ΔN of 4OHTAM accepts electrons, while for the rest of the residues it acts as an electron donor. END is an electron acceptor in the presence of the Trp383-Leu384 residue and with the remainder of the residues it acts as an electron donor. Finally, NDTAM acts as an electron acceptor in the presence of Glu353 and Leu349-Ala 350-Asp351 residues, and as an electron donor with the remainder of the residues. The values are shown in **Table 3**.

The charge transfer descriptor is one of the noncovalent interactions that are present in biological systems in a macromolecule–ligand complex. In this case, the highest charge transfer value is in the same residue, Leu346-Thr347, for all the metabolites, which acts as a donor with amounts of −0.080, −0.086, and –0.073 for 4OHTAM, END, and NDTAM, respectively. Therefore, oxidative damage in the active site decreases in the order 4OHTAM > NDTAM > END.

Metabolite	Residue	ΔN
4OHTAM	Gly521	−0.022
	Met388	0.089
	His524	0.004
	Lys529	−0.058
	Phe404	−0.010
	Trp383-Leu384	−0.012
	Glu353-Leu354	0.022
	Leu346-Thr347	−0.080
	Leu349-Ala350-Asp351	0.009
NDTAM	Gly521	−0.016
	Phe404	−0.004
	Glu353	0.047
	Leu428	−0.026
	His524-Lue525	−0.004
	Trp383-Leu384	−0.005
	Leu346-Thr347	−0.073
	Leu349-Ala350-Asp351	0.015
END	Gly521	−0.029
	His524	−0.004
	Leu387-Met388	−0.010
	Leu346-Thr347	−0.086
	Trp383-Leu384	0.001

Table 3. Charge transfer descriptor in the estrogen receptor.

3.2.5. Electrostatics interactions

Other noncovalent interactions between the ligand and hormone receptor are the hydrogen bond and π–π interactions. An analysis of these bonds between the ER and each of TAM's metabolites was done. The results are as follows.

4OHTAM. This residue has one hydrogen bond (C=O----O-H) between the donor group (O-H) and the acceptor group (C=O) of the Gly521 residue. Also, there is a π–π interaction between residue Trp383 and the planar core of the ligand.

END. There are two hydrogen bonds: first (C=O----OH) between the acceptor group (C=O) of Gly521 and the donor group (O-H) belonging to one of the rings and second (C=O----HN) between the accepting group (C=O) of Asp351 and the secondary amine (NH). The π–π interaction was found among residue Trp383 and the planar core of the ligand.

NDTAM. In this metabolite was found one hydrogen bond (C=O----HN) between the accepting group (C=O) of Asp351 and the amine group of the ligand. No π–π interactions were found in this ligand–receptor complex.

In all cases the metabolites analyzed followed the Lipinski et al. rule of five, which states: when there are five or fewer hydrogen bonds the drug will not present poor absorption or permeation and will be more active [53]. **Figure 4** shows the metabolites as a ball and stick and the residues of the active site as a tube. The hydrogen bonds are shown as green dots and π–π interactions are the areas marked in yellow.

3.3. Analysis of the progesterone receptor with the metabolites

Analysis of molecular docking between PR and the metabolites is characterized by the active site of PR: the active site was described and the calculation and analysis of chemical reactivity

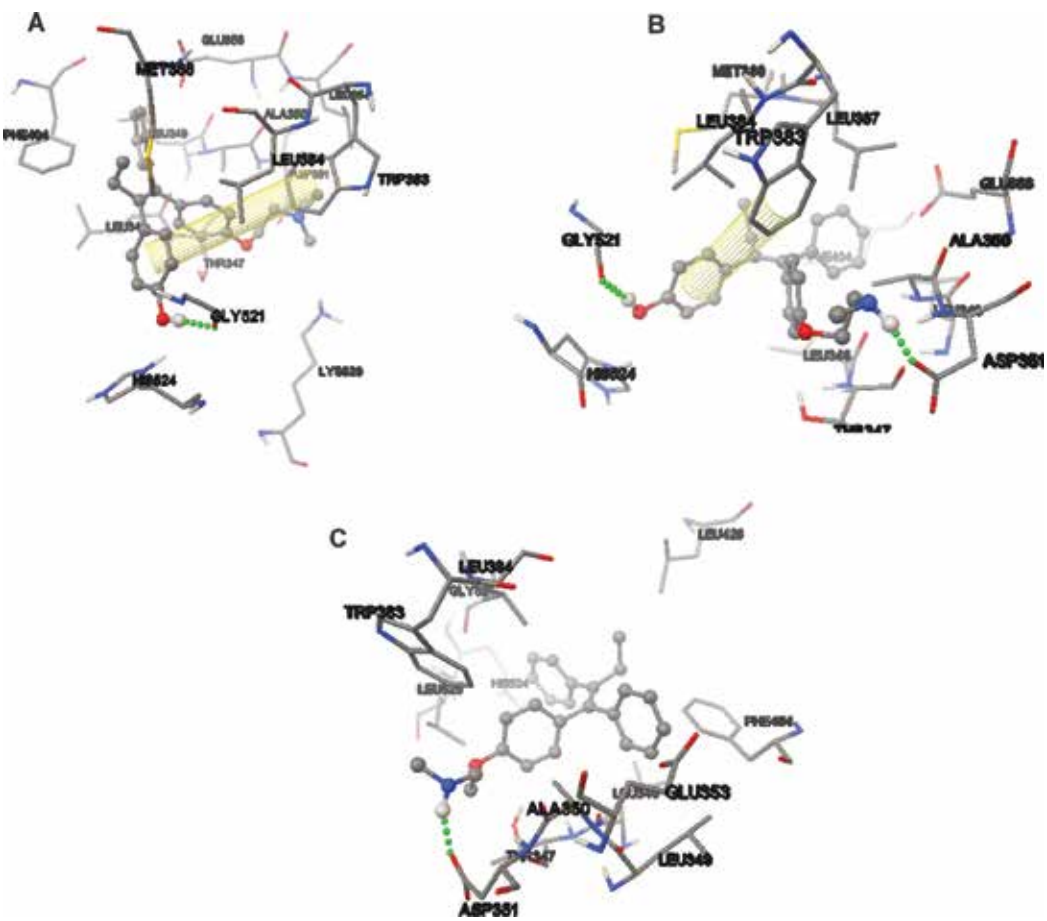

Figure 4. Hydrogen bond (green) and π–π interactions (yellow) at the active site of the estrogen receptor with (A) 4OHTAM, (B) END, and (C) NDTAM.

http://dx.doi.org/10.5772/intechopen.72895

parameters of the residues and metabolites were carried out, as well as the description of the hydrogen bond formed between the metabolites and the PR active site.

3.3.1. Molecular docking

The binding energy of TAM's metabolites at the active site of PR has been predicted by carrying out molecular docking calculations. The schematic structure of the active site and the binding energies are shown in **Figure 5**. The negative value of the binding energy in the

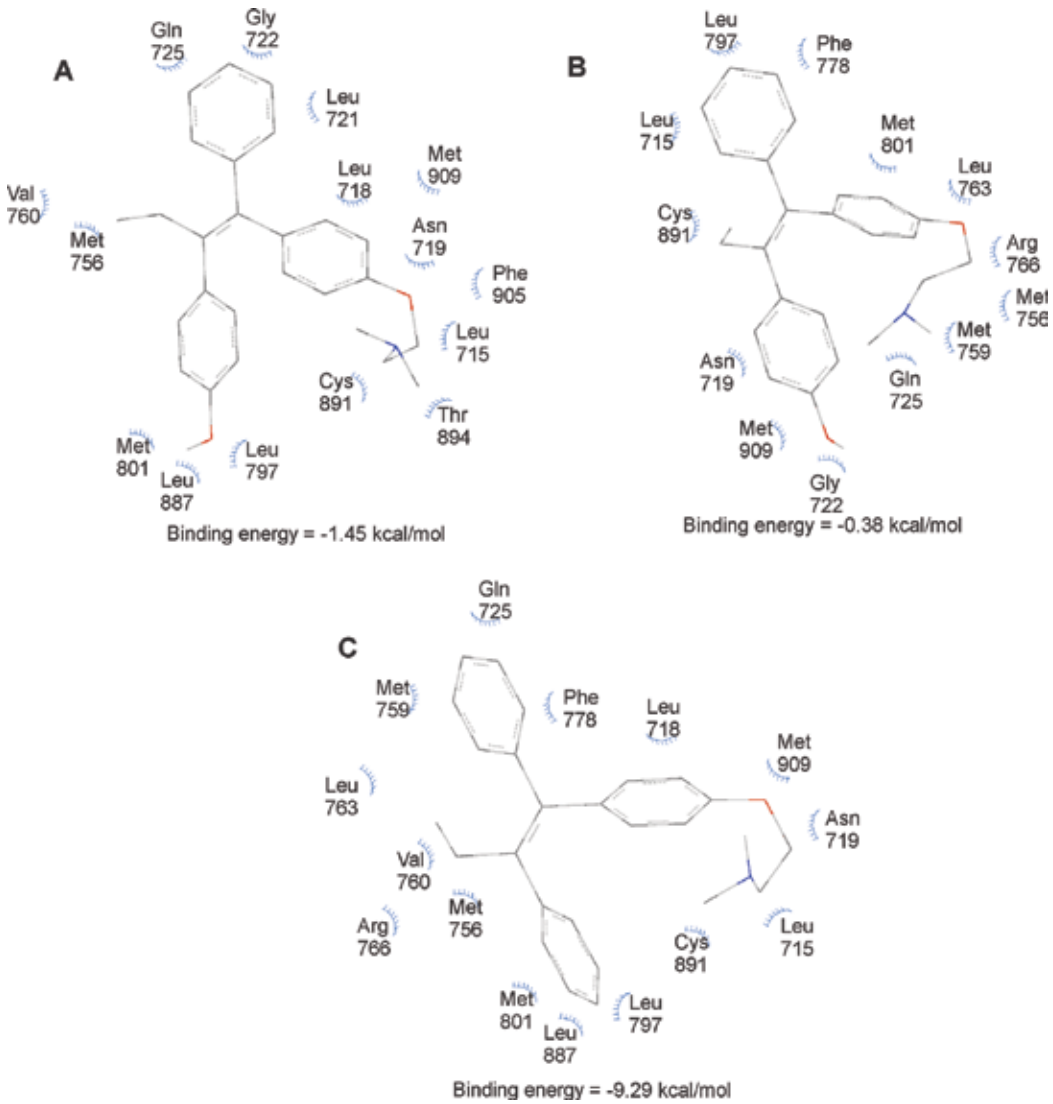

Figure 5. Amino acids of the active site of the progesterone receptor with (A) 4OHTAM, (B) END, and (C) NDTAM.

docking indicates that the system is stable and that there is an interaction between PR and metabolites at the site: –1.45 kcal/mol for 4OHTAM, –0.38 kcal/mol for END, and –9.29 kcal/mol for NDTAM.

Although the metabolites END and 4OHTAM have a negative bond energy, their values remain very low compared to TAM, which has –9.38 kcal/mol [13]. Therefore, these two metabolites will have very low biological activity in PRs.

3.3.2. Active site

The active site of PR obtained by theoretical analysis is as follows.

4OHTAM. There are 15 residues in contact with the metabolite 4OHTAM at the active site of PR. Four of them are linked, forming an amino acids sequence, leucine718-aspartic acid719 (Leu718-Asn719) and leucine721-glycine722 (Leu721-Gly722). The other 11 residues are highly hydrophilic: glutamine725 residue (Gln725), cysteine891 (Cys891), threonine894 (Thr894), and phenylalanine905 (Phe905); and seven are hydrophobic residues: methionine756, methionine801, and methionine909 (Met756, Met801, and Met909), valine760 (Val760), and leucine715, leucine797, and leucine887 (Leu715, Leu797, and Leu887).

END. The active site in END is formed by the following residues: glutamine725 (Gln725), cysteine891 (Cys891), glycine722 (Gly722), asparagine719 (Asn19), and arginine766 (Arg766), which are hydrophilic. The hydrophobic residues are phenylalanine778 (Phe778), tryptophan755 (Trp755), methionine756, methionine759, methionine801, and methionine909 (Met756, Met759, Met801, and Met909), and leucine715, leucine763, and leucine797 (Leu715, Leu763, and Leu797).

NDTAM. The active site for NDTAM consists of the following residues: leucine718-aspartic acid719 (Leu718-Asn 719) and methionine759-valine760 (Met759-Val760). Hydrophilic residues are glutamine725 (Gln725), arginine766 (Arg766), and cysteine891 (Cys891). Hydrophobic residues are phenylalanine778 (Phe778), methionine756, methionine801, and methionine909 (Met756, Met801, and Met909), and leucine715, lucine763, leucine797, and leucine887 (Leu715, Leu763, Leu797, and Leu887).

Most of the residues of the active site of 4OHTAM and END surround the planar core of the ligand and over the functional group amine. The steric hindrance of this amine group produces minor binding energy.

When the metabolites bind, there is a conformational change and they are recognized by the amino acids of the active site. This has to do with the coupling energies. In PR, NDTAM has a higher amount of binding energy exceeding –9 kcal/mol.

Even when PR is more labile than ER, the binding energies indicate that the receptor is not sufficiently labile to recognize the metabolites 4OHTAM and END, which present binding energies lower than –1.5 kcal/mol.

The residues for the metabolites in PR are shown in **Figure 5**.

3.3.3. Chemical reactivity

As soon as the most stable structure of the active site of TAM's metabolites was obtained, an analysis of the chemical reactivity of progesterone residues was performed by means of the reactivity descriptors. Results for these calculations are shown in **Table 4**.

Metabolite	Active site	EA (eV)	I (eV)	η (eV)	μ = − χ (eV)	ω (eV)
4OHTAM	Phe905	0.93	6.58	2.82	3.76	2.50
	Leu797	0.67	6.86	3.09	3.74	2.36
	Leu887	0.43	7.01	3.29	3.72	2.10
	Thr894	0.49	6.57	3.04	3.53	2.05
	Val760	0.76	6.92	3.08	3.84	2.40
	Met756	0.75	6.3	2.77	3.52	2.54
	Leu715	0.60	7.02	3.21	3.81	2.26
	Gln725	0.70	7.10	3.20	3.90	2.38
	Cys891	0.55	6.89	3.17	3.72	2.18
	Met801	0.64	6.27	2.82	3.45	2.12
	Met909	0.50	6.21	2.85	3.36	1.97
	Leu721-Gly722	−0.33	7.13	3.73	3.40	1.55
	Leu718-Asn719	1.06	7.06	3.00	4.06	2.74
END	Arg766	0.21	7.03	3.41	3.62	1.92
	Leu763	0.43	6.2	2.89	3.31	1.90
	Gly722	0.51	6.25	2.87	3.38	1.99
	Met759	0.88	7.74	3.43	4.31	2.71
	Gln725	0.70	7.10	3.20	3.90	2.38
	Trp755	0.86	5.85	2.50	3.35	2.25
	Asn719	0.76	7.16	3.20	3.96	2.45
	Leu797	0.67	6.86	3.09	3.74	2.36
	Met756	0.75	6.30	2.77	3.52	2.54
	Phe778	0.86	6.60	2.87	3.73	2.42
	Leu715	0.60	7.02	3.21	3.81	2.26
	Cys891	0.55	6.89	3.17	3.72	2.18
	Met801	0.64	6.27	2.82	3.45	2.12
	Met909	0.73	5.79	2.85	3.26	2.10
NDTAM	Leu763	0.35	7.17	3.41	3.76	2.07
	Leu797	0.67	6.86	3.09	3.74	2.36
	Leu887	0.43	7.01	3.29	3.72	2.10

Metabolite	Active site	EA (eV)	I (eV)	η (eV)	μ = – χ (eV)	ω (eV)
	Phe778	0.86	6.6	2.87	3.73	2.42
	Leu715	0.60	7.02	3.21	3.81	2.26
	Arg766	0.78	6.70	2.96	3.74	2.36
	Gln725	0.70	7.10	3.20	3.90	2.38
	Cys891	0.55	6.89	3.17	3.72	2.18
	Met756	0.75	6.30	2.77	3.53	2.24
	Met801	0.64	6.27	2.82	3.45	2.12
	Met909	0.50	6.21	2.85	3.36	1.97
	Met759-Val760	1.05	6.26	2.61	3.65	2.56
	Leu718-Asn719	1.06	7.06	3	4.06	2.74

Table 4. Parameters of chemical reactivity of the active site residues of the progesterone receptor.

The electron affinities of the residues fluctuate from −0.33 eV to 1.06 eV. The highest value of electron affinity is for the Leu718-Asn719 residue, which is present in the active site of 4OHTAM, NDTAM, and the Met759 residue of END. The ionization potential results show that the greatest possibility of losing electrons is: Leu721-Gly722 with 7.13 eV in 4OHTAM, Leu763 with 7.17 eV in NDTAM, and Met759 with 7.74 eV in END.

Chemical hardness, the parameter that measures the resistance to change in the electronic configuration, exhibited amounts from 2.50 eV to 3.73 eV. In 4OHTAM, the lowest value and therefore the one that will react more easily in the presence of the metabolites is 2.77 eV for Met756. For END it is 2.50 eV in Trp755 and 2.61 eV in Met759-Val760. Met801 had a value of 2.82 eV in the NDTAM metabolite.

According to chemical potential, Met759 residue at –4.31 eV presents the highest value in END. The electronegativity ($\mu = -\chi$) shows that the Met759 residue has the greatest tendency to attract electrons at 4.31 eV in END. Electrophilicity ω is the measure of the stabilization energy when systems become saturated by electrons from the surroundings. In this case in the active site of 4OHTAM value decreases in the following order: Leu718-Asn719 > Met756 > Phe905 > Val760 > Gln725 > Leu797 > Leu715 > Cys891 > Met801 > Leu887 > Thr894 > Met909 > Leu721-Gly722. In END the decreasing order is Met759 > Met756 > Asn719 > Phe778 > Gln725 > Leu797 > Leu715 > Trp755 > Cys891 > Met801 > Met909 > Gly722 > Arg766 > Leu763 and in NDTAM the decreasing order is Leu718-Asn719 > Met759-Val760 > Phe778 > Gln725 > Leu797 > Arg766 > Leu715 > Met756 > Cys891 > Met801 > Leu887 > Leu763 > Met909.

3.3.4. Charge transfer descriptor

Considering the high importance of this parameter in the formation of complexes in biological systems, the highest values in the different metabolites were defined. The charge transfer between metabolites and PR residues was calculated using Eq. 5. The results show that Met909 in 4OHTAM, Met909 and Leu763 in END, and Met909, Met756, Arg766, and Leu763

in NDTAM act as donor acceptors, namely, these residues are oxidized in the presence of the metabolites. The remainder of the residues act as electron acceptors. The values are shown in **Table 5**.

For 4OHTAM and NDTAM the maxima values are in Leu718-Asp719 with −0.064 and −0.057, respectively. For END the maxima value is in Met759 with −0.088. Thus, the calculations

Metabolite	**Residue**	**Δ*N***
4OHTAM	Leu718-Asn719	−0.064
	Leu721-Gly722	−0.002
	Phe905	−0.037
	Leu797	−0.033
	Leu887	−0.03
	Thr894	−0.014
	Val760	−0.043
	Met756	−0.014
	Leu715	−0.039
	Gln725	−0.047
	Cys891	−0.031
	Met801	−0.007
	Met909	0.002
END	Arg766	−0.027
	Leu763	0.001
	Gly722	−0.006
	Met759	−0.088
	Trp755	−0.003
	Asn719	−0.06
	Leu797	−0.04
	Met756	−0.020
	Gln725	−0.058
	Phe778	−0.041
	Leu715	−0.046
	Cys891	−0.037
	Met801	−0.013
	Met909	0.006
NDTAM	Leu763	0.615
	Leu797	−0.027
	Leu887	−0.024
	Phe778	−0.027

Metabolite	Residue	ΔN
	Leu715	−0.033
	Arg766	0.665
	Gln725	−0.041
	Cys891	−0.025
	Met756	0.669
	Met801	−0.001
	Met909	0.008
	Met759-Val760	−0.021
	Leu718-Asn719	−0.057

Table 5. Transfer of charge between metabolites and progesterone receptor residues.

indicate that oxidative damage in the active site decreases in the following order: NDTAM > END > 4OHTAM.

3.3.5. Electrostatics interactions

An analysis of the hydrogen bond and π–π interactions between the active site on PR and TAM's metabolites was performed. In the case of 4OHTAM and END metabolites no hydrogen bonds were generated, nor were there any π–π interactions, whereas with NDTAM only a

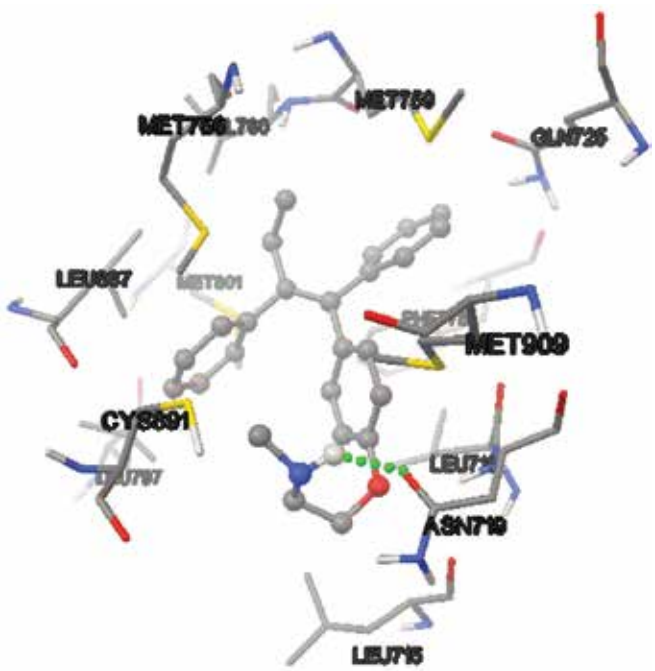

Figure 6. Hydrogen bond (green) at the active site of the progesterone receptor with the NDTAM metabolite.

hydrogen bond (C=O----H-N) was formed between the Asn719 residue and the amino group. The unique electrostatic interaction is shown with green dots in **Figure 6**. Also, it was found that the rule of five by Lipinski et al. [52, 53] was fulfilled.

4. Conclusions

In this chapter the molecular docking of ER and PR with TAM's metabolites, 4OHTAM, NDTAM, and NDTAM, was analyzed. The amino acids sequence of the active site for each ligand–macromolecule complex was examined. The residues that constituted each active site were analyzed separately to find the charge transfer parameter, the hydrogen bond, and the π–π interaction between the ligand and the receptor.

According to the binding energy obtained from docking, ER has greater stability than PR with the metabolites analyzed. However, in both cases there is a coupling between the receptor and the ligand, even when two of the binding energies in PR–ligand coupling are very small.

This coupling plays an important part in avoiding the transcription factor cascade reported by Leehy et al. [54].

This information agrees with the results of the chemical reactivity parameters, where it was found that the average of the chemical hardness values are lowest in active site residues of ER than in PR.

The charge transfer descriptor shows that TAM's metabolites mostly act as electron acceptors in their interaction with the hormone receptors. The hydrogen bonds in ER with END agree with the highest binding energy of this ligand. There are two hydrogen bonds, one π–π interaction, and a ΔN of –0.086. While in PR, there is only one hydrogen bond with NDTAM and the value of ΔN is –0.057.

This work described the successful combination of the methods of molecular mechanics and electronic structure. It also explored the different conformational spaces and binding modes that allow smaller systems to work with them at the electronic level.

In addition to the above a significant conclusion is that the molecular modeling and simulations are an important improvement tool for any laboratory in many industries. Currently, many sectors are moving toward using more modeling and simulations in their laboratories. As Bernard Charlès, Dassault Systèmes CEO, states: "digitalization will mean big changes for everyday lab activities down the road." Two key solutions for all industries (such as pharmaceutical, chemical, life sciences, energy, and consumer goods) are collaboration and the ability to predict using simulation and modeling [55].

Patrick Bultinck et al. in their preface to the book *Computational Medicinal Chemistry for Drug Discovery* [21] wrote: "Nowadays, one can safely state that the computational chemist has become a respectable member of a drug design team." And we can add that the docking tool is essential for most techniques for structure-based drug design.

Author details

Linda-Lucila Landeros-Martinez, Daniel Glossman-Mitnik, Erasmo Orrantia-Borunda and Norma Flores-Holguin*

*Address all correspondence to: norma.flores@cimav.edu.mx

NANOCOSMOS Virtual Lab, Department of Environment and Energy, Advanced Materials Research Center (CIMAV), Miguel de Cervantes 120, Complejo Industrial Chihuahua, Chihuahua, México

References

[1] Weidner N, Cady B, Goodson 3rd W. Pathologic prognostic factors for patients with breast carcinoma. Which factors are important. Surgical Oncology Clinics of North America. 1997;**6**(3):415-462

[2] Veronesi U, Paganelli G, Galimberti V, Viale G, Zurrida S, Bedoni M, et al. Sentinel-node biopsy to avoid axillary dissection in breast cancer with clinically negative lymph-nodes. The Lancet. 1997;**349**(9069):1864-1867

[3] Singletary SE, Allred C, Ashley P, Bassett LW, Berry D, Bland KI, et al. Revision of the American Joint Committee on Cancer staging system for breast cancer. Journal of Clinical Oncology. 2002;**20**(17):3628-3636

[4] Molina M, Reigosa A, Nobrega D, Molina Y. Receptores de estrógeno y progesterona en cáncer de mama. Asociacion con variables clinicopatologicas. Revista Salus Online Facultad de Ciencias de la Salud Universidad de Carabobo (Valencia-Venezuela). 2001;**5**:34-42

[5] Lai A, Kahraman M, Govek S, Nagasawa J, Bonnefous C, Julien J, et al. Identification of GDC-0810 (ARN-810), an orally bioavailable selective estrogen receptor degrader (SERD) that demonstrates robust activity in tamoxifen-resistant breast cancer xenografts. Journal of Medicinal Chemistry. 2015;**58**(12):4888-4904

[6] Wardell SE, Nelson ER, Chao CA, Alley HM, McDonnell DP. Evaluation of the pharmacological activities of RAD1901, a selective estrogen receptor degrader. Endocrine-related Cancer. 2015;**22**(5):713-724

[7] Srinivasan S, Nwachukwu JC, Bruno NE, Dharmarajan V, Goswami D, Kastrati I, et al. Full antagonism of the estrogen receptor without a prototypical ligand side chain. Nature Chemical Biology. 2016;**13**:111

[8] Min J, Guillen VS, Sharma A, Zhao Y, Ziegler Y, Gong P, et al. Adamantyl antiestrogens with novel side chains reveal a spectrum of activities in suppressing estrogen receptor mediated activities in breast cancer cells. Journal of Medicinal Chemistry. 2017;**60**(14):6321-6336

[9] Papageorgiou L, Cuong NT, Vlachakis D. Antibodies as stratagems against cancer. Molecular BioSystems. 2016;**12**(7):2047-2055

[10] Altmeyer C, Karam TK, Khalil NM, Mainardes RM. Tamoxifen-loaded poly(L-lactide) nanoparticles: development, characterization and in vitro evaluation of cytotoxicity. Materials Science and Engineering: C. 2016;**60**:135-142

[11] Khan MM, Wakade C, de Sevilla L, Brann DW. Selective estrogen receptor modulators (SERMs) enhance neurogenesis and spine density following focal cerebral ischemia. Journal of Steroid Biochemistry and Molecular Biology. 2015;**146**:38-47

[12] Gao L, Tu Y, Wegman P, Wingren S, Eriksson LA. Conformational enantiomerization and estrogen receptor α binding of anti-cancer drug tamoxifen and its derivatives. Journal of Chemical Information and Modeling. 2011;**51**(2):306-314

[13] Irarrázaval OME. Tamoxifeno y antidepresivos: ¿Antagonistas en la prevención del cáncer de mama? Revista médica de Chile. 2011;**139**:89-99

[14] Sanyakamdhorn S, Agudelo D, Bekale L, Tajmir-Riahi HA. Targeted conjugation of breast anticancer drug tamoxifen and its metabolites with synthetic polymers. Colloids and Surfaces B: Biointerfaces. 2016;**145**:55-63

[15] Johnson MD, Zuo H, Lee K-H, Trebley JP, Rae JM, Weatherman RV, et al. Pharmacological characterization of 4-hydroxy-N-desmethyl tamoxifen, a novel active metabolite of tamoxifen. Breast Cancer Research and Treatment. 2004;**85**(2):151-159

[16] Beverage JN, Sissung TM, Sion AM, Danesi R, Figg WD. CYP2D6 polymorphisms and the impact on tamoxifen therapy. Journal of Pharmaceutical Sciences. 2007;**96**(9):2224-2231

[17] Ng HL. Simulations reveal increased fluctuations in estrogen receptor-alpha conformation upon antagonist binding. Journal of Molecular Graphics and Modelling. 2016;**69**:72-77

[18] Landeros-Martínez LL, Orrantia-Borund E, Flores-Holguín N. Predicción de la reactividad química de Tamoxifeno en receptores hormonales. Memorias Congreso de Investigación Científica Multidisciplinaria. 2016;**4**(1):24-38

[19] Kumar V, Jain G, Kishor S, Ramaniah LM. Chemical reactivity analysis of some alkylating drug molecules—a density functional theory approach. Computational and Theoretical Chemistry. 2011;**968**(1):18-25

[20] Trott O, Olson AJ. AutoDock Vina: improving the speed and accuracy of docking with a new scoring function, efficient optimization, and multithreading. Journal of Computational Chemistry. 2010;**31**(2):455-461

[21] Bultinck P, De Winter H, Langenaeker W, Tollenare JP. Computational Medicinal Chemistry for Drug Discovery. CRC Press; 2003

[22] Mohan V, Gibbs AC, Cummings MD, Jaeger EP, DesJarlais RL. Docking: successes and challenges. Current Pharmaceutical Design. 2005;**11**(3):323-333

[23] Kitchen DB, Decornez H, Furr JR, Bajorath J. Docking and scoring in virtual screening for drug discovery: methods and applications. Nature Reviews Drug Discovery. 2004;**3**(11): 935-949

[24] DeLisle RK, Yu S-J, Nair AC, Welsh WJ. Homology modeling of the estrogen receptor subtype β (ER-β) and calculation of ligand binding affinities. Journal of Molecular Graphics and Modelling. 2001;**20**(2):155-167

[25] Manas NHA, Bakar FDA, Illias RM. Computational docking, molecular dynamics simulation and subsite structure analysis of a maltogenic amylase from Bacillus lehensis G1 provide insights into substrate and product specificity. Journal of Molecular Graphics and Modelling. 2016;**67**:1-13

[26] Maldonado-Rojas W, Olivero-Verbel J, Marrero-Ponce Y. Computational fishing of new DNA methyltransferase inhibitors from natural products. Journal of Molecular Graphics and Modelling. 2015;**60**:43-54

[27] Berman HM, Westbrook J, Feng Z, Gilliland G, Bhat TN, Weissig H, et al. The Protein Data Bank. Nucleic Acids Research. 2000;**28**(1):235-242

[28] Norgan AP, Coffman PK, Kocher J-PA, Katzmann DJ, Sosa CP. Multilevel parallelization of AutoDock 4.2. Journal of Cheminformatics. 2011;**3**(1):1

[29] Morris GM, Ruth H, Lindstrom W, Sanner MF, Belew RK, Goodsell DS, et al. Software news and updates AutoDock4 and AutoDockTools4: automated docking with selective receptor flexibility. Journal of Computational Chemistry. 2009;**30**(16):2785-2791

[30] Huey R, Morris GM, Olson AJ, Goodsell DS. A semiempirical free energy force field with charge-based desolvation. Journal of Computational Chemistry. 2007;**28**(6):1145-1152

[31] Morris GM, Goodsell DS, Halliday RS, Huey R, Hart WE, Belew RK, et al. Automated docking using a Lamarckian genetic algorithm and an empirical binding free energy function. Journal of Computational Chemistry. 1998;**19**(14):1639-1662

[32] Zhao Y, Truhlar D. The M06 suite of density functionals for main group thermochemistry, thermochemical kinetics, noncovalent interactions, excited states, and transition elements: two new functionals and systematic testing of four M06-class functionals and 12 other functionals. Theoretical Chemistry Accounts. 2008;**120**(1-3):215-241

[33] Zhao Y, Truhlar DG. Density functionals with broad applicability in chemistry. Accounts of Chemical Research. 2008;**41**(2):157-167

[34] Rassolov VA, Ratner MA, Pople JA, Redfern PC, Curtiss LA. 6-31G* basis set for third-row atoms. Journal of Computational Chemistry. 2001;**22**:976-984

[35] Tomasi J, Persico M. Molecular interactions in solution: an overview of methods based on continuous distributions of the solvent. Chemical Reviews. 1994;**94**(7):2027-2094

[36] Hohenberg P, Kohn W. Inhomogeneous electron gas. Physical Review. 1964;**136**:B864-B871

[37] Kohn W, Sham LJ. Self-consistent equations including exchange and correlation effects. Physical Review. 1965;**140**(4A):A1133-A1138

[38] Robert G, Parr YW. Density-Functional Theory of Atoms and Molecules. New York, NY, USA: Oxford University Press; 1989

[39] Frisch MJT, Trucks GW, Schlegel HB, Scuseria GE, Robb MA, Cheeseman JR, Scalmani G, Barone V, Mennucci B, Petersson GA, et al. Gaussian 09; Gaussian, Inc.: Wallingford, CT, USA; 2009

[40] Hirshfeld FL. Bonded-atom fragments for describing molecular charge densities. Theoretica Chimica Acta. 1977;**44**(2):129-138

[41] Pearson RG. Absolute electronegativity and hardness correlated with molecular orbital theory. Proceedings of the National Academy of Sciences of the United States of America. 1986;**83**(22):8440-8441

[42] Parr RG, von Szentpály L, Liu S. Electrophilicity index. Journal of the American Chemical Society. 1999;**121**(9):1922-1924

[43] Padmanabhan J, Parthasarathi R, Subramanian V, Chattaraj P. Electrophilicity-based charge transfer descriptor. Journal of Physical Chemistry A. 2007;**111**(7):1358-1361

[44] DeLano WL. The PyMOL molecular graphics system. DeLano Scientific; Palo Alto, CA, USA; 2002

[45] Samanta PN, Das KK. Prediction of binding modes and affinities of 4-substituted-2,3,5,6-tetrafluorobenzenesulfonamide inhibitors to the carbonic anhydrase receptor by docking and ONIOM calculations. Journal of Molecular Graphics and Modelling. 2016;**63**:38-48

[46] Clarke R, Liu MC, Bouker KB, Gu Z, Lee RY, Zhu Y, et al. Antiestrogen resistance in breast cancer and the role of estrogen receptor signaling. Oncogene. 2003;**22**(47):7316-7339

[47] Thomas G. Fundamentals of Medicinal Chemistry. Weinheim, Germany; 2003

[48] Shiau AK, Barstad D, Loria PM, Cheng L, Kushner PJ, Agard DA, et al. The structural basis of estrogen receptor/coactivator recognition and the antagonism of this interaction by tamoxifen. Cell. 1998;**95**(7):927-937

[49] Dávila JT, Garrán ADT. Moduladores selectivos de los receptores estrogénicos (SERMs): bioquímica, farmacología y aplicación clínica en ginecología. Ginecología y Obstetricia de México. 2005;**73**(08):424-435

[50] Hall JM, McDonnell DP. The estrogen receptor β-isoform (ERβ) of the human estrogen receptor modulates ERα transcriptional activity and is a key regulator of the cellular response to estrogens and antiestrogens. Endocrinology. 1999;**140**(12):5566-5578

[51] Wan C, Fiebig T, Schiemann O, Barton JK, Zewail AH. Femtosecond direct observation of charge transfer between bases in DNA. Proceedings of the National Academy of Sciences. 2000;**97**(26):14052-14055

[52] Kanvah S, Schuster GB. The sacrificial role of easily oxidizable sites in the protection of DNA from damage. Nucleic Acids Research. 2005;**33**(16):5133-5138

[53] Lipinski CA, Lombardo F, Dominy BW, Feeney PJ. Experimental and computational approaches to estimate solubility and permeability in drug discovery and development settings. Advanced Drug Delivery Reviews. 2001;**46**(1-3):3-26

[54] Leehy KA, Truong TH, Mauro LJ, Lange CA. Progesterone receptors (PR) mediate STAT actions: PR and prolactin receptor signaling crosstalk in breast cancer models. Journal of Steroid Biochemistry and Molecular Biology. 2018;**176**:88-93

[55] Tulsi BB. A new generation. Lab Manager 2016;**11**(1):1-100

Section 4

Molecular Docking for Medicine

Chapter 8

Has Molecular Docking Ever Brought us a Medicine?

Mark Andrew Phillips, Marisa A. Stewart,
Darby L. Woodling and Zhong-Ru Xie

Additional information is available at the end of the chapter

http://dx.doi.org/10.5772/intechopen.72898

Abstract

Molecular docking has been developed and improving for many years, but its ability to bring a medicine to the drug market effectively is still generally questioned. In this chapter, we introduce several successful cases including drugs for treatment of HIV, cancers, and other prevalent diseases. The technical details such as docking software, protein data bank (PDB) structures, and other computational methods employed are also collected and displayed. In most of the cases, the structures of drugs or drug candidates and the interacting residues on the target proteins are also presented. In addition, a few successful examples of drug repurposing using molecular docking are mentioned in this chapter. It should provide us with confidence that the docking will be extensively employed in the industry and basic research. Moreover, we should actively apply molecular docking and related technology to create new therapies for diseases.

Keywords: computational drug design, molecular docking, drug repurposing

1. Introduction

Molecular docking is one of many computational tools that can be used in drug discovery [1–4]. It is a form of structure-based drug discovery that quantifies the binding affinities between small molecules and macromolecular targets (proteins). The first step in molecular docking is choosing a drug target. Any macromolecule can be used as a target; some very common targets include enzymes and regulatory elements. Next, the three-dimensional structure must be determined or predicted; high resolution structures can be determined using X-rays, NMR, or electron microscopy (EM). Thousands of popular targets have solved structures available on the protein data bank (PDB) [5]. Many drug targets have known binding sites; if not, software that can predict potential binding sites for different ligands have been developed. Docking

studies can be performed using known ligands (naturally occurring molecules or known drugs) or novel ligands. Virtual screening (i.e. identifying novel ligands with molecular docking) provides an extremely useful (but time consuming) method of drug discovery because molecules can be designed to have high binding affinity to a very specific site. Docking studies are often validated using further computational methods, such as molecular dynamic simulation. The most successful candidates from computational trials can be tested *in vitro* or *in vivo*, and eventually progress to clinical trials (**Figure 1**).

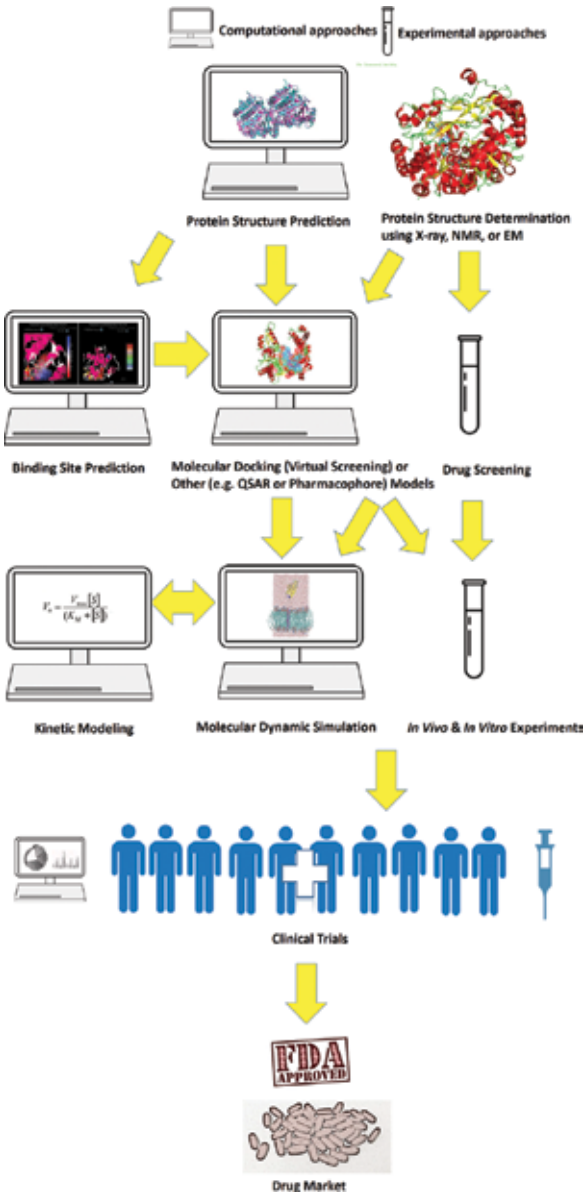

Figure 1. A brief flowchart of novel drug discovery procedure.

It is believed that a searching algorithm, which assists in thoroughly and efficiently exploring possible positions, orientations and conformations of potential drugs and the target proteins, and a scoring function, which assists in precisely and correctly identifying the most energetically favorable binding poses, are two most important components of a molecular docking programs. However, some other factors will affect the effectiveness and accuracy of molecular docking, such as the availability and quality of a determined or predicted structure of the target protein, the conformational changes of the target proteins after the drug binding, and the identification of potential binding sites. As those mentioned in previous chapters, many commercial and academic docking search algorithms, scoring functions, and software packages have been developed and improved in the past decades. However, it is still questioned if there are any successful stories in which molecular docking have helped to bring a drug to the market.

Although many molecular docking algorithms have been developed and improved for many decades, biomedical laboratories or pharmaceutical companies used to be hesitant to apply this technology to drug screening. Here are some possible reasons:

1. The "force fields" which describe the intra- and inter-molecular interaction energies were not accurate and precise enough to estimate or calculate the binding affinities between proteins and potential binding drugs.

2. The computer was not "fast" enough to calculate the interacting energy of many possible binding "conformations" of one or many possible binding compound(s) using a sophisticated model taking account into all the factors, components, and conditions of molecular interactions.

3. The number of binding complex structures was not large enough and the resolution of available structures was not good.

4. The searching/sampling algorithms to explore the possible binding orientations and conformations were not efficient to identify possible binding poses with reasonable time.

These reasons and concerns are all tightly cross-linked together, and, fortunately, have been dramatically improved in the past years. For example, the number of structures on PDB has increased from 47,605 to 133,759 since 2007 [6]. The resolution of determined structures has significantly improved. Therefore, the accuracy of both physics-based and knowledge-based scoring functions which assist researchers in identifying the most energy favorable binding poses and estimating binding affinities have been improved. The substantial improvement in both computer hardware and software also make it possible to screen a large number of natural and artificial compounds and search the best binding poses efficiently.

When we attempt to dock a compound to a target protein, often we need to use other computational methods before docking or in parallel. For instance, we may need to do structure prediction if the structure of the target protein has not yet been determined. The accumulated PDB structures with good resolution and the accurate structure prediction algorithms make it possible for researchers to obtain reliable structural models to perform molecular docking experiments. The enhanced quantity, quality, and diversity of protein-compound complex structures provide solid basis for creation of accurate binding site

prediction methods, and they help reduce the searching surface area on the target proteins for docking algorithms [7–9]. Other computational methods such as pharmacophore and quantitative structure-activity relationship (QSAR) models can be used prior to the molecular docking to reduce computational load and time [10–12]. In summary, the technology of molecular docking has matured and been applied in different stages of the drug discovery process. The successful stories have not been mentioned often and are not widely known. They will be introduced in this chapter.

2. Identification of medicine for HIV

The human immunodeficiency virus (HIV) epidemic around the world has pushed massive amounts of money into research that looks for ways to help treat and prevent this virus. Because bringing a drug into the market can take many years and cost astronomical amounts of money, it is of the utmost importance of researchers to use a cost effective ways to find these new therapeutics. Computational methods have been gradually becoming commonplace in drug design research. These methods have been either confirming established research, discovering new compounds, binding sites or conformations, and even allowing for the repurposing of the drug to treat other illnesses. HIV research has seen an influx of multiple computational methods being used to confirm discoveries of previous studies and establish new ones. Methods such as docking and molecular dynamics are saving researchers valuable time. These methods are also allowing research to make accurate and precise predictions of what is going on at the molecular level. While computational drug design methods are nowhere near replacing *in vitro* and *in vivo* testing, *in silico* testing is becoming increasingly popular for researchers to validate their research or act as a starting point for *in vitro* testing. This section will introduce how researchers used computational methods to help identify drugs for HIV-1 Protease and HIV-1 Integrase. It will also discuss how these methods are being utilized for future developments in this area of research, and how researchers were able to use the drugs Saquinavir and Nelfinavir toward treating a disease unrelated to HIV—Chagas.

2.1. Human immunodeficiency virus

Acquired immunodeficiency syndrome (AIDS) is acquired in humans by the retrovirus HIV [13]. HIV infects important helper T cells in the human immune system—specifically CD4+ T cells [14]. HIV is transmitted as positive-sense, single-stranded, enveloped RNA virus. There are currently two types of HIV that have been characterized as HIV-1 and HIV-2. HIV-1 was the first HIV virus discovered and it is more virulent and more infective than HIV-2 [15]. After the viral capsid has entered the cell, an enzyme called reverse transcriptase liberates the positive-sense RNA from the viral proteins and copies it into a complimentary DNA molecule [16]. The reverse transcriptase process is very prone to errors. This characteristic results in many mutations that make this component of HIV likely to encounter drug resistance. For this reason, HIV reverse transcriptase is an unlikely target for HIV therapeutics. The newly formed circular DNA strand and its complement form a double-stranded

viral DNA that is transported to the nucleus. The integration of the viral DNA into the host's genome is carried out by the integrase enzyme [16]. The HIV virus then may remain dormant or continue to assemble new HIV-1 virions. The plasma membrane of the host cell is the site for the production of new HIV-1 virions. The virion buds that are produced at the plasma membrane are cleaved by HIV-1 protease enzyme. Once the bud has been cleaved by HIV-1 protease, the internal components can assemble, and in turn create a virion capable of infecting other cells. The two targets that computational drug researchers have focused on significantly are HIV-1 integrase and HIV-1 protease.

2.2. HIV-1 integrase

Integrase (IN) is a retrovirus enzyme not exclusive to only HIV. This protein allows the genetic material of the virus to be integrated into the DNA of the host cell. Integration occurs after the double-stranded viral DNA is produced by reverse transcriptase. Once integration has commenced for a cell, there is no turning back. The cell is now considered a pro-virus, and it is now a permanent carrier of the virus. In general, retroviral integrases catalyze two reactions. Both reactions are catalyzed by the same active site on the enzyme and occur via transesterification.

2.2.1. HIV-1 integrase inhibitor—Raltegravir and its ensuing analogs

The most common inhibitors for integrase are referred to as integrase strand transfer inhibitors (INSTIs). Mg^{2+} and Mn^{2+} are critical cofactors in the integration phase [17], and inactivating these cofactors causes functional impairment of integrase. Most HIV-1 INSTIs contain a structural motif that coordinates the two divalent magnesium ions in the enzyme's active site [17]. Researchers screen over 250,000 compounds to yield potent inhibitors [18]. The most active inhibitors seemed to contain a distinct beta-diketo acid (DKA) moiety [19]. This moiety had the ability to coordinate metal ions within the IN active site. There was similar antiviral activity when the DKA pharmacophore was transferred to a naphthyridine carboxamide core [20]. A class of N-alkyl hydroxypyridinone carboxylic acids was the result of the success with the diketo acid structural analogs. These new analogs had a good pharmacokinetic profile in rats [21]. The drug, MK-0518, also known as Raltegravir, became the most promising pyrimidinone carboxamide derivative. Raltegravir was the first integrase inhibitor to progress to Phase III clinical trials. While there have been multiple resistant mutations for both treatment-experienced and treatment-naïve patients, Raltegravir still proved to be an effective IN inhibitor [22]. In October 2007, Raltegravir became the first FDA-approved IN inhibitor (**Table 1**).

To bring a single drug to the market, it can cost upwards of $2 billion [23]. Even with this, only one in three drugs will generate enough revenue to cover the cost of the research and development of the drug [24]. Pharmaceutical researchers and executives can see the allure of modifying current leads on drugs, rather than trying to design a new drug. "Me-too" drugs [18] can create an optimized drug and create vital marketplace competition, but many argue that slight modifications are producing negligible improvements [25]. "Me-too" drug emergence has seen a surge in the HIV-1 integrase inhibitor market. While Raltegravir has become the known and widely used anti-HIV drug, amino acid mutations have already conferred robust viral resistance of the drug [26]. This viral drug resistance normally occurs when one

Table of various HIV-1 integrase and HIV-1 protease inhibitors

Drug	Type of inhibitor	Affected residues	Structure
Raltegravir	HIV-integrase	D64 T66 E92 D116 Y143 Q148 E152 N155	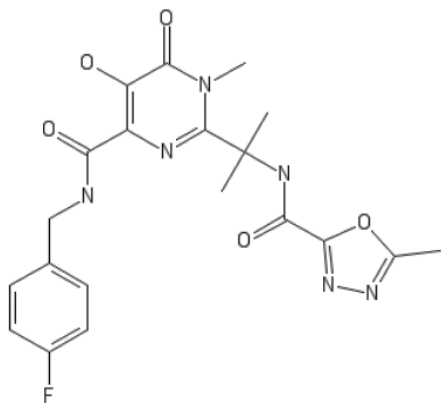
S-1360	HIV-1 integrase	D64 T66 D116 Y143 Q148 E152 N155	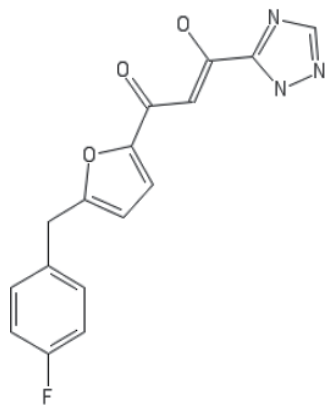
Saquinavir	HIV-1 protease	G84 I84 L90	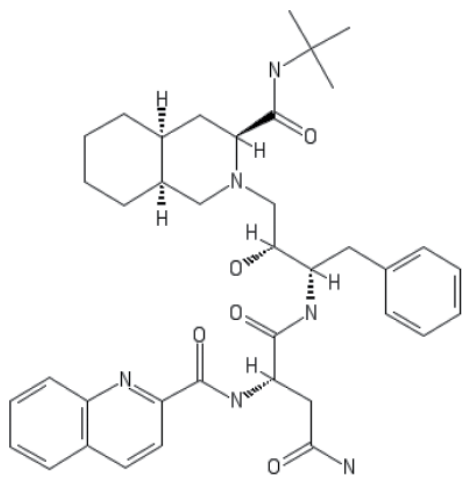

Table of various HIV-1 integrase and HIV-1 protease inhibitors

Drug	Type of inhibitor	Affected residues	Structure
Nelfinavir	HIV-1 protease	D30 I84 L90	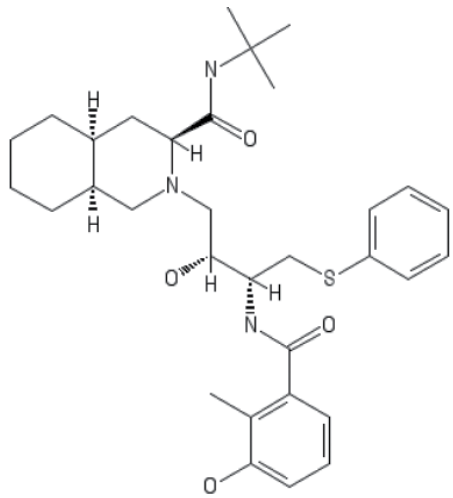
Amprenavir	HIV-1 protease	I84 L90 I54 V82	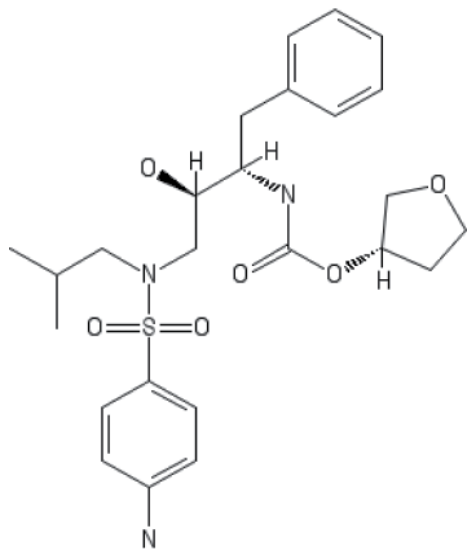

Table 1. The various HIV-1 protease and HIV-1 integrase inhibitors and their structures. The affected residues in HIV-1 protease and HIV-1 integrase binding pocket are shown as well.

of three amino acids—Y143, Q148, or N155—mutate in conjunction with at least one other mutation [27]. The strongest antiviral resistant mutation seems to be the Q148H integrase mutant (IC_{50} > 700 nM), and G140S has been shown to restore the poor replication ability of Q148H to wild-type levels [28]. Even though Raltegravir has seen this resistance profile, pharmaceutical companies still spend lots of money on "me-too" research and the

development on this drug. There should be a distinction made between me-too drugs and second-generation drugs [18]. A second-generation inhibitor needs to exhibit a new mode of action. Secondly, a second-generation drug needs to show significantly improved potency or decreased toxicity. A major problem with second-generation drugs is cross resistance, so these drugs should maintain potency, but avoid this cross-resistance.

2.2.2. Using docking studies to predict the binding mode of S-1360

It is very important to predict a bioactive conformation of a ligand, but the task becomes difficult when the receptor site has a region with unusual conformational flexibility. With the numerous crystal structures available for HIV-1 integrase, there are numerous differences in the active site regions in the core domains of IN. S-1360 was one of the first beta-diketoacid IN inhibitors to enter clinical studies. Dayam and Neamati sought to predict the bioactive (active site bound) conformations of S-1360 [29]. To achieve this, the researchers performed extensive docking studies with three different crystal structures. The study was extended to include 5CITEP and a bis-diketoacid (BDKA).

To predict the binding mode of S-1360, 104 unique conformations within a 20 kcal/mol energy range were generated using catConf module of the Catalyst. All 104 conformations of S-1360 were docked into the active sites A, B, and C (PDB: 1QS4, 1BIS, and 1BL3, respectively). Based on GOLD fitness scores, 10 conformers with highest scores were selected for further analysis. The researchers noted that S-1360 adopted very different binding orientations inside the active sites for A, B, and C. In the A active site, the bound conformation with the highest GOLD fitness score was found 102 times of 200 conformations. S-1360 occupies a space near D64, D116, N120, and Mg^{2+} ion. In active site B, the highly favorable conformation of S-1360 is found 62 times. The triazole and the diketoacid moiety of S-1360 occupy a deep cavity surrounded by I151, N155, V75, and Q62. The groups show favorable van der Waals and electrostatic interactions with D64, I151, E152, and N155 (**Figure 2**). The highly favorable binding conformations of the C active site are found 172 times. The researchers also compared the best binding orientations of S-1360 in the active sites from the three different crystal structures of HIV-1 integrase. Dayam and Neamati observed that S-1360 in the A active site achieves a planar conformation and interacts with various residues throughout the active site. In this orientation, S-1360 forms H-bonding interactions with K159 and N120. The two oxygen

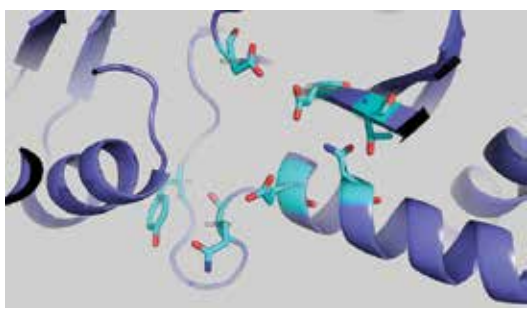

Figure 2. 1BL3 active site with the residues that contribute to antiviral resistance highlighted.

atoms from the furan ring and keto group for coordinate bonds with the Mg^{2+} ions. This conformation appears to be stable because it occurs 102 out of 200 times. The binding site conformation of S-1360 inside the C active site is also very stable because of its 172 appearances out of 200. While these conformations of A and C are stable, this conformation is not in line with experimentally observed results. S-1360 selectively inhibits strand transfer reactions of HIV-1 integrase, but S-1360 in A and C did not interact with amino acids in the strand transfer (ST) cavity. However, S-1360 did form strong interactions with various amino acids and Mg^{2+} ion in the cavity where 3′-processing of IN is believed to be carried out.

Docking in this study was performed using version 1.2 of the Genetic Optimization for Ligand Docking (GOLD) software. This uses a genetic algorithm to explore the ligand conformational flexibility with partial flexibility of the active site [30]. GOLD was tested on a dataset of over 300 complexes. GOLD succeeded in more than 70% of cases in reproducing the experimental bound conformations of the ligand [31]. GOLD requires that users define the specific binding site. For this study, Dayam and Neamati defined a 20 Å radius active site. D64 was selected as the center of the active site. The GOLD program then searches for a cavity within the defined area. The program also considers all the solvent accessible atoms in the defined area as active site atoms. "All docking runs were carried out using standard default settings with a population size of 100, a maximum number of 100,000 operations, a mutation, and crossover rate of 95" [29]. At the end of each run, GOLD reported all the predicted bound conformations based on their fitness score. The fitness score consists of H-bonding, complex energy, and ligand internal energy.

2.2.3. Validating the resistance profiles of "me-too" Raltegravir analogs using docking studies

Serrao et al. sought to validate the resistance profiles of me-too Raltegravir analogs [18]. There are minor variations in the *in vitro* activity of the numerous me-too integrase inhibitors. The researchers believed that the development of me-too compounds could possibly yield a relatively low amount of clinical success due to their similarities [18]. It is still possible for a Raltegravir me-too analog to become a second-generation integrase inhibitor. To elucidate this viewpoint, the researchers utilized the molecular docking program GOLD version 3.2 to conduct a docking study. Serrao et al. used the structure of 1BL3 complexed with an Mg^{2+} ion, and various me-too compounds.

Serrao et al. proposed that residues essential to the compounds' interaction with HIV-1 integrase would be prime candidates for resistance mutation. "Raltegravir makes direct interactions with three residues encompassing the [IN] catalytic motif (D64, D116, E152)" [18]. The researchers wanted to predict the interaction residues of Raltegravir's analogs in a similar way. They wanted to show that the compounds would have little success in viral eradication. Because S-1360 was the one of the first clinical IN inhibitor candidates, the researchers thought it would be interesting to look at the interactions between S-1360 and 1BL3 and compare with that of Raltegravir. The researchers found that there are identical interactions between the two drugs (D64, T66, D116, Y143, Q148, E152, and N155). Raltegravir showed an additional interaction with E92. While this observation has been confirmed by clinical experiments, the E92Q mutation has conferred upwards of a sevenfold viral resistance to Raltegravir [32–34].

The researchers' data could significantly validate the reliability of their docking technique. The researchers then moved on to describing the interactions between HIV-1 integrase and each most potent analog of Raltegravir. On the several compounds that were used in this follow up study, most all of them interacted in the same binding pocket that Raltegravir is active in. If the researchers' predictions are correct, these candidate drugs will fail to replace Raltegravir. The researcher's note, while there is always the possibility for me-too drugs to evolve into blockbuster drugs, the studied HIV-1 integrase "drugs appear to have a small chance of improving the clinical outlook of HIV patients with Raltegravir viral strains" [18].

2.3. HIV-1 protease

An essential element in the HIV life cycle is HIV-1 protease. It is a retroviral aspartyl protease. HIV-1 protease is a homodimer, with each subunit made up of 99 amino acids [35]. Gag and Pol polyproteins are cleaved by this protease [36]. When these are cleaved at the appropriate places, a mature and infectious HIV virion is produced. When an effective HIV protease is blocked, the HIV virus is not infectious [37]. HIV's ability to replicate and infect additional cells can be disrupted by mutation of the HIV protease active site or inhibition [38]. For this reason, HIV protease has seen a massive amount of research money in developing HIV-1 protease inhibitors.

HIV-1 protease is a homodimeric enzyme. Two aspartic acid residues that are essential for catalysis [39], D25 and D25, are located on each monomer. Asp-Thr-Gly sequence is present in HIV-1 protease, but this is conserved among other mammalian aspartic protease enzymes. There are extended beta-sheet regions on each monomer, and these are known as "the flap". This makes up the hydrophobic substrate binding cavity with the two aspartyl residues on the bottom. HIV-1 proteases are highly selective, and very catalytically active in hydrolyzing peptide bonds. While the mechanism is similar to many known features of aspartic proteases, the full detailed mechanism of this enzyme has not been fully understood [40].

2.3.1. Saquinavir and Nelfinavir—HIV-1 protease inhibitors and their ensuing resistance

The ideal HIV-1 protease inhibitor should be potent and specific for HIV-1 protease compared to other mammalian aspartic acid proteases [41]. The drugs should also have good bioavailability and duration in human bodies. There were no known inhibitors of HIV-1 protease when it was first determined to be a good target for antiviral therapy. A good starting place to look was the type of enzyme that HIV-1 protease was, an aspartic acid protease.

When researchers were designing HIV-1 protease inhibitors, it was noted that there was a stereocenter in the drug that correlated with the drug's activity. The transition state hydroxyl group needed to be in the R-stereochemistry or else the drug completely lost its activity. This discovery led researchers to identify Ro-31-8959, or Saquinavir, as a prime candidate for further studies because of this characteristic. Saquinavir has an $IC_{50} < 0.37$ nM for HIV-1 protease and does not inhibit other aspartic acid proteases, making it highly potent. While the drug is potent, it shows poor oral bioavailability—only 4% [41]. Researchers attribute this to the high molecular weight of the drug and the large number of amide bonds. Agouron

Pharmaceuticals and Lilly Research Laboratories collaborated to produce Nelfinavir [42]. The structure of Nelfinavir is very similar to the structure of Saquinavir, but Nelfinavir contains a couple of changes. Labile components in Saquinavir were replaced with a hydroxytoluene amide group, however, this modification resulted in reduced potency. Drug developers replaced the phenyl group with a phenylthio group. This phenylthio group was better able to fill the hydrophobic pocket of the HIV-1 protease active site [43]. With an IC_{50} = 2 nM, Nelfinavir is also a very potent HIV-1 protease inhibitor.

As shown with HIV-1 integrase inhibitors, resistance persists to be a pressing problem in the treatment plans for HIV-1. Because Saquinavir and Nelfinavir have similar structures, there are different, yet highly overlapping sets of amino acids substitution mutations that confer to drug resistance. The mutations that affect the binding site for Saquinavir are G84, I84, or L90. For Nelfinavir, the only difference from the Saquinavir mutation is D30 instead of G48 [41]. While these amino acids affect the binding pocket, there are other overlapping sets of amino acids that when mutated elsewhere in the HIV-1 protease enzyme confers antiviral resistance. These sites include L10, M46, L63, A71, and N88. Because many of the HIV-1 protease inhibitors on the market right now are very similar in structure, it is not surprising that there is a high degree of cross-resistance between the drugs.

2.3.2. Predicting HIV-1 protease resistance with docking studies

There are several different methods to interpret the resistant behavior of HIV-1 from genotypic data. A physics-based approach of docking has seen an influx of use by researchers in evaluating the energy interactions of the protein-inhibitor complexes. This technique has been widely used to look at the interactions between HIV-1 protease and its inhibitors. In 2005, Jenwitheesuk and Samudrala completed a study that used a protein-inhibitor docking approach to determine the correlation between experimentally and computer calculated protease inhibitor binding affinities [44]. The researchers also supplemented their findings with a molecular dynamics protocol [45]. This was used in part because most docking programs utilize a rigid protein protocol. HIV-1 protease has special flaps that are in motion upon binding. Since the structure of target protein is rigid, the opening and closing of the flaps is not performed [46]. This protocol was used to simulate the flexible nature between the ligand and the enzyme. The researchers used the X-ray crystal structures of various wild-type HIV-1 protease-inhibitor complexes. For Saquinavir and Nelfinavir, the researchers selected 1HXB and 1OHR, respectively (**Figures 3** and **4**). The researchers then substituted the wild-type side chains with a mutant side chain.

When preparing the inhibitor structure, the researchers treated them as an all atom entry. By doing so this filled the empty valences with hydrogen. All the rotatable bonds in the inhibitors were also allowed to rotate freely. The researchers used AutoDock version 3.0.5 with a Lamarckian genetic algorithm to carry out docking calculations. Genetic algorithms use the idea of natural genetics and biological evolution. There are specific values describing the ligand with respect to the protein (translation, orientation, and conformation). These are described at state variables and in the genetic algorithm (GA), each state variable corresponds to a gene. In genetic algorithms, the genotype is from the ligand's state, and the phenotype

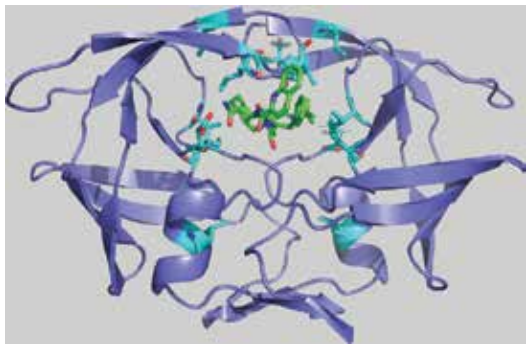

Figure 3. 1HXR mutated with interactions between the binding pocket and Saquinavir.

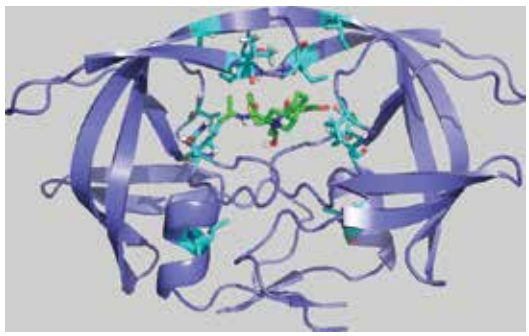

Figure 4. 1OHR mutated with amino acid interactions and Nelfinavir in the binding pocket.

comes from the atomic coordinates [46]. When molecular docking is performed, the fitness of the gene is referred to as the total interaction energy between the ligand and the protein. The GA comes into play by mating random pairs of individuals to induce crossover. In this scenario, some offspring undergo random mutation. The genes are selected from the current generation based off their fitness scores. This process is repeated for multiple generations to produce a ligand and protein interaction that has the most fitness. In the research conducted by Jenwitheesuk and Samudrala [45], there were a total of 27,000 generations. AutoDock generates the energy terms for inter-molecular energy, internal energy of the ligand, and torsional free energy. When the researchers determined the final docked energy of the protein ligand complex, the inter-molecular energy, and the internal energy of the ligand was added.

In the results of this study [45], Jenwitheesuk and Samudrala saw a significant improvement in the correlation coefficient when supplementing their docking procedure with MD simulation to provide a flexible nature of the protein (correlation coefficient changed from 0.38 to 0.87). The researchers were also able to see that their docking with dynamic protocol was 64% accurate for phenotypically resistant profiles and 83% accurate for phenotypically susceptible groups. There was a previous study done by Shenderovich et al. [47]. While this study followed a similar protocol to the one followed by Jenwitheesuk and Samudrala, Shenderovich et al. only used 50 HIV-1 protease sequences. Jenwitheesuk and Samudrala used 1792 HIV-1

protease sequences. This larger sample size could include all of the reported resistant mutations. Jenwitheesuk and Samudrala also added a protein-inhibitor relaxation feature to their protocol. Their protocol was also able to consider the rearrangement of the side chain on the active site surface. The relatively short MD simulation of 0.1 ps had a significant effect on the flap region (which moved away from the binding pocket—RMSD = 0.54 Å), yet was not long enough to affect the main chain of the protein. Using this protocol, the resistance and susceptibility predictions from Nelfinavir and Saquinavir were 86 and 94%, respectively [45].

This study looked at the two key mutations discussed earlier—Asp30Asn and Gly48Val. In this study, docking with the molecular dynamics implementations always failed to identify as a cause of drug resistance. This suggests that researchers should not rely solely on one method or system in making decisions about therapeutic regimens without consulting other methods, resources, and techniques. This study was still able to determine other mutations around the binding pocket. The docking with MD simulation implementation could identify mutations that correspond with high levels of resistance of Amprenavir (another kind of HIV-1 protease inhibitor)—I50V and a combination of I84V + L90 M and I54V + V82A + I84V + L90 M. These mutations are cross resistant with Nelfinavir and Saquinavir.

2.4. Repurposing HIV-1 protease inhibitors

American trypanosomiasis, or Chagas disease, is caused by the protist *Trypanosoma cruzi.* Many times there are no early signs of infection but over the course of the infection symptoms can range from a mild fever, swollen lymph nodes, or headaches. If the infection progresses further, the symptoms can include enlarged ventricles of the heart, which will ultimately lead to heart failure. This infection is most common in Mexico, Central America, and South America, and an estimated 6.6 million people are living with this parasite [48] The most common ways that the disease is spread are eating contaminated food, from mother to her fetus, and blood or organ transfusions [49]. While the knowledge of this parasite has grown remarkably, there have been no medications to treat Chagas disease in the last 40 years [50].

Over the years, there has been a recent interest in drug repurposing (also known as drug repositioning). The process involves using known and approved medications—and sometimes discontinued drugs from other drug trials—and using them for a new clinical applications other than their intended treatment. Drug repurposing is gaining popularity due to the fact that within the past few decades there has been a significant decline in the number of safe and effective drugs being developed for the pharmaceutical market. Pharmaceutical companies are not inclined to fund research or product design because development of a new drug is a long and costly process [51]. One of the major benefits of trying to repurpose drugs is the reduced cost of researching and developing a novel drug from scratch.

Bellera et al. present computer-aided identification of approved drugs Clofazimine, Benidipine, and Saquinavir as potential trypanocidal compounds [50]. The major drug target is cruzipain (Cz). Cz is the major cysteine protease of the parasite. This protease is essential for replication of the intracellular form of the parasite. Bellera et al. compiled a 147 compound dataset. This data set was balanced with 77 Cz inhibitors and 70 non-inhibitors. The researchers then used docking studies on Saquinavir, Benidipine, Clofazimine, and the inactive verapamil. The protein to be

used in the docking studies was 1ME4. This protein was a crystal structure of one reversible inhibitor that was complexed with Cz. The compounds were docked according to the Lamarckian genetic algorithm. The active site was defined as a 19 × 15 × 15 $Å^3$ grid. The researchers performed 100 docking runs for each compound. The docking active site was treated as a rigid molecule and the ligands were treated as flexible. The researchers used Autodock 4.2 to analyze the results of their docking study. The binding results from the docking studies correlated with experimental evidence. The scores for Saquinavir, Benidipine, and Coldazimine were −12.76, −8.42, and −7.36 kcal/mol, respectively. However, the inactive verapamil compound was only −6.37 kcal/mol [50].

3. Identification of medicine for cancer

Cancer is one of the most devastating and destructive diseases that is known to be a persistent public health threat. As of the year 2016, cancer is the second leading cause of death in the United States. There were an estimated 1,685,210 new cases and 595,690 deaths resulting from cancer [52]. Along with the high rate of incidence exacerbating the pressure already felt by researchers to discover a cure, the mechanisms of the disease add another level of complexity that must be outmaneuvered. Many cancer cells lack molecular targets making it extremely difficult for anticancer chemotherapeutics to be fully effective. Toxicity against normal tissues can develop from anticancer therapy, which leads to unwanted side effects. Due to the adverse effects, many anticancer chemotherapeutics are given at suboptimal doses which typically results in failure of therapy, drug resistance, and metastatic disease [53]. The complications associated with cancer demonstrate the critical need for the development of new anticancer therapies that are successful with minimal undesired reactions. In order to aid in the task, many researchers are turning to *in silico* methods to expedite the process. Molecular docking is one of the most popular and reliable softwares available for drug discovery, design, and repurposing. Many researchers utilize molecular docking in cancer research because it provides great insight into protein-ligand interactions, ligand binding mechanisms, and knowledge of the optimal orientation of the ligand bound to its target to form the most stable complex. Molecular docking is an essential computational method that has demonstrated a promising future for the evolution of more effective and potent anticancer therapies.

3.1. Docking for identifying novel proteasome inhibitors and understanding the binding mechanisms

A variety of cancer therapeutics already exists and is available to patients; many of these therapies attempt to have a specific molecular target in order to eradicate the cancerous cells. One protein that receives extensive attention due to its pivotal biological role in eukaryotic cells is the proteasome. There are two major types of proteasomes such as the 20S proteasome, which is responsible for intracellular protein degradation and the 26S proteasome complex, which functions in the ubiquitin pathway as an ATP-dependent proteasome [54]. The 26S proteasome has three proteolytic activities including peptidyl glutamyl peptide hydrolase

(PGPH) in the β1subunit, trypsin-like (T-L) in the β2 subunit and CT-L activities in the β5 subunit [55].

Degradation of proteins in the cytoplasm and nucleus of eukaryotic cells can affect: regulation of cellular pathways particularly cell growth and proliferation, apoptosis, DNA repair, transcription, immune responses, and signaling processes [56]. Inhibition of proteasomes has therefore become an attractive target for anticancer therapies. The drug Bortezomib was developed by Millennium Pharmaceuticals Inc. and received regular approval by the Food and Drug Administration in 2005 as the first proteasome inhibitor to be used for the treatment of multiple myeloma [57]. Bortezomib is a peptide boronate inhibitor of the proteasome and it selectively binds to the protein to inhibit its chymotryptic-like activity [58]. The anticancer effects demonstrated by Bortezomib are mainly observed by the inhibition of the transcription factor NF*k*B and the promotion of apoptosis in rapidly dividing cells. While Bortezomib is considered a successful cancer treatment, many reports of adverse side effects have driven researchers to develop a more potent and selective proteasome inhibitor [59].

In the race to discover a more efficacious proteasome inhibitor, molecular docking has been an extremely beneficial tool utilized by researchers to expedite the exacting process. *In silico* high throughput screening of multiple chemical libraries identified the compound PI-083 as a potential inhibitor due to its potency (IC_{50} = 1 μM). Molecular docking of PI-083 to the 20S proteasome was performed by the GLIDE computer program, version 3.0 (Schrödinger, LLC, New York, NY). The GLIDE program used for the docking and grid generation was set using default options and parameters. The X-ray structure of yeast 20S proteasome complexed with Bortezomib revealed that the pyrazine ring in the Bortezomib forms a hydrogen bond with Asp114 from the β6 subunit of the proteasome. As visualized in **Figure 5**, Bortezomib also forms hydrogen bonds with T21, T1, G47, and A49 residues located in the active site. PI-083 possesses a pyridine ring and it was docked to a model derived from the Bortezomib-proteasome complex (PBD ID: 2F16). The docking studies revealed that PI-083 and Bortezomib have similar binding mechanisms to the active site of the CT-L enzyme within the proteasome [55]. The molecular docking combined with *in vivo* studies of PI-083 are indicative that the compound is successful in tumor suppression which insinuates a need for further clinical research in regards to PI-083 as an anticancer therapy.

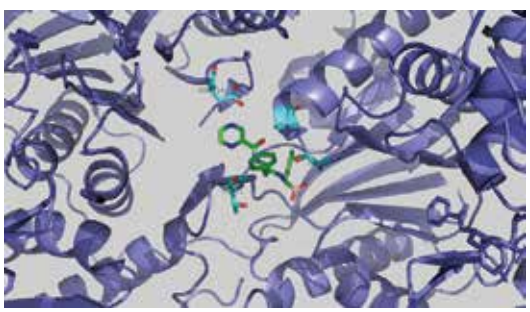

Figure 5. The Bortezomib ligand positioned in the active site of the yeast 20S proteasome crystal structure. The key residues T1, T21, G47, A49, and D114 in the active site are shown.

Molecular docking has not only been successful in identifying potential proteasome inhibitors but it has also been beneficial in understanding the binding mechanism of proteasome inhibitors to the proteasome. One study conducted by Zhang et al. was focused on MG132 (Z-Leu-Leu-Leu-al), which is a structural component of peptide aldehydes selective and potent against the proteasome. Using the Insight II software, the proteins and ligands were prepared for docking. MG132 was then covalently docked to the β5 subunit of the 20S proteasome using GOLD version 4.0. The results showed that the docking of MG132 proposed two binding modes with low docking energies. More thorough analysis and the use of molecular dynamics simulations revealed that binding mode I was more stable than mode II. The computational methods utilized in this study resulted in the generation of a model that was able to re-examine the correlation of the structure and activity of proteasome inhibitors, specifically the interactions that take place at the P2 and P4 sites [60]. Observing the binding mode is advantageous for the improvement of existing proteasome inhibitors but also for the development of more potent inhibitors.

Ma et al. used the binding mechanism of MG132 as a comparison for docking their own series of peptide aldehyde derivatives in which they synthesized. A total of 17 different peptide aldehydes were developed and are listed in **Table 2**. Eight of the peptides are in the Cbz class at the R4 position and the other nine peptides are in the Boc class at the R4 position.

Compounds	R4 position	P3 position	P2 position
1	Cbz	Asp(O^{t}Bu)	Phe
2	Cbz	Asp(O^{t}Bu)	Leu
3	Cbz	Glu(O^{t}Bu)	Phe
4	Cbz	Glu(O^{t}Bu)	Leu
5	Cbz	Phe	Leu
6	Cbz	Arg(NO_2)	Leu
7	Cbz	Arg(Tos)	Leu
8	Cbz	Nap[a]	Leu
9	Boc	Asp(OBzl)	Phe
10	Boc	Asp(OBzl)	Leu
11	Boc	Glu(OBzl)	Phe
12	Boc	Glu(OBzl)	Leu
13	Boc	Pro	Phe
14	Boc	Pro	Leu
15	Boc	Ser(OBzl)	Leu
16	Boc	Thr(OBzl)	Leu
17	Boc	Tyr(OBzl)	Leu

Table 2. Peptide aldehyde derivatives for the inhibition of 20S proteasome activity.

The 17 peptide aldehydes were then docked using GOLD software 4.0 with the β5 of the 20S proteasome based on the crystal structure of the first known inhibitor MG101 complexed with the 20S proteasome. The results of the docking experiment indicated that the size and length of the P3 side chain is critical to the activity of the peptide aldehyde. Compounds 3 and 4 which are part of the Cbz series synthesized by Ma et al. possess Glu(O^tBu) residues at the P3 site providing the most active inhibition. The results from docking indicated that when a phenyl ester was used to replace a tert-butyl ester at P3 in the Boc-series, the Asp(OBzl) residue in compound 10 exhibited more active inhibition than Glu(OBzl) residue in compound 12. Also in the Boc-series, Ser(OBzl) in compound 15 has the most suitable length side chain because it demonstrated the most active inhibition to CT-L active site [61]. The docking results generated from this study highlighted the importance of the P3-position substitutes are vital for inhibitor potency, which is essential for designing more effective proteasome inhibitors.

Peptide aldehydes are not the only compounds being considered as proteasome inhibitors for cancer therapeutics. Santoro et al. investigated whether or not cationic and anionic porphyrins can be used as inhibitors of the proteasome. Porphyrins are hydrophilic compounds that possess tumor localizing properties and are used in conjunction with red light for photodynamic therapy for the treatment of tumorous cells [62]. Cationic and anionic porphyrins were docked using AutoDock Vina to the 20S proteasome complexed with Bortezomib (PDB: 2F16). The cationic porphyrin H_2T4 demonstrated similar inhibitory activity in all three catalytic sites of the proteasome when observed during *in vivo* studies. Docking of planar H_2T4 with the 20S proteasome revealed the binding mechanism of the porphyrin to the proteasome. The results from the docking studies reconcile with the results of the inhibition studies, indicative that H_2T4 has the potential to be a proteasome inhibitor. Along with the active ability of the porphyrin to inhibit the proteasome, the molecules also possess low toxicity, making them an attractive class of compounds to continue to evaluate as a form of anticancer therapy [63].

3.2. Docking for identifying inhibitors of CAs

Besides proteasomes, several isoforms of carbonic anhydrases (CAs) have become an attractive anticancer drug target. Carbonic anhydrases are ubiquitous metalloenzymes broken up into four unrelated gene families; the α-CAs, β-CAs, γ-CAs, and δ-CAs. Mammals have 16 α-CAs isozymes that are different in their tissue distribution, catalytic activity, and subcellular localization [64]. The α-CAs are of particular interest because they have well established catalytic and inhibition mechanisms [65]. One α-CA in particular, CA IX, has potential to act as an anticancer drug target as it has the ability to act as a biological marker for certain tumors [66]. CA IX is an extracellular transmembrane-bound protein located in the gastrointestinal tract. When the enzyme is present in hypoxic conditions, CA IX is overexpressed and is observed to be associated with different types of cancer cells via the hypoxia inducible factor-1 (HIF-1). Overexpression also causes the environmental pH of a tumor to be lowered to acidic conditions [66]. The appeal of the CA IX as a potential anticancer drug is demonstrated by the fact that the enzyme has restricted expression in normal tissues (**Table 2**).

Amresh et al. used molecular docking and several others *in silico* methods to discover five potential CA IX inhibitors. AutoDock 4.2 was used to dock all the inhibitors to the crystal

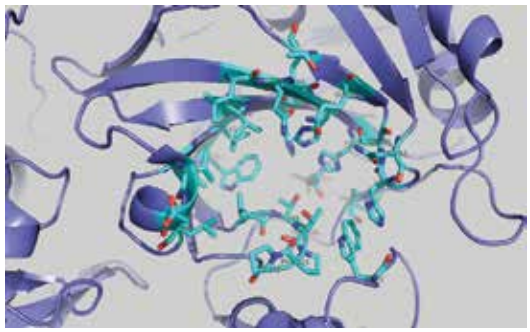

Figure 6. The critical residues in the active site located on the CA IX (PDB: 3IAI): L91, L93, L198, V121, L135, L141, V143, P201, P202, W5, W209, F245, H96, H119, E106, T199, T200, H94, D132, Q92, N62, H64, S65, Q67, T69, and Q92 are displayed.

structure of CA IX (PDB: 3IAI) visualized in **Figure 6**. Coulombic electrostatic potential, van der Waals interaction represented as a Lennard-Jones12-6 dispersion/repulsion term and hydrogen bonding were addressed when evaluating the binding energy during docking. Docking orientations within 2.0 Å in root-mean square deviation tolerance were the parameters set in order to obtain the most favorable free energy of binding. The inhibitors with the best docking poses and scores were then subjected to post-docking energy minimization on Discovery Studio 3.5. The final structures were analyzed using PyMOL visualization programs and the receptor-inhibitor complexes were used to develop the pharmacophore model for further evaluation [67]. Docking simulations were also performed in order to identify the residues present in the active site of CA IX that interact with the inhibitors. The docking study revealed that residues: L91, L93, L198, V121, L135, L141, V143, P201, P202, W5, W209, F245, H96, H119, E106, T199, T200, H94, D132, Q92, and V131 formed either hydrophobic or aromatic interactions with the inhibitor. N62, H64, S65, Q67, T69, and Q92 were identified as the hydrophilic residues in the active site as well [67]. The results of the docking studies established 10 novel compounds as CA IX inhibitors. Further analysis of the docking scores narrowed the list even further to the top five scoring compounds which were: ZINC03363328, ZINC08828920, ZINC12941947, ZINC03622539, and ZINC16650541 [67]. The information obtained from this study has demonstrated the value of molecular docking in identifying new CA IX inhibitors that provide a promising future as an anticancer therapy.

3.3. Docking for identifying inhibitors of EGFR

The epidermal growth factor receptor (EGFR) is another enticing biological target in the development of anticancer therapeutics. The EGFR is a family of tyrosine kinases that regulate many developmental, metabolic, and physiological processes. Binding of the epidermal growth factor to the family of kinases leads to homodimerization or heterodimerization of the EGFR. Mutations of EGFR gene, over expressed copies of the gene and EGFR protein overexpression lead to dysregulated TK activity which is observed in many tumors [68]. Overexpression of EGFR is frequently observed in breast, lung, ovarian, and prostate cancer

and is associated with aggressive tumor behavior [69]. The EGFR is the main activator in the downstream pathways for survival and growth signals such as p42/44 MAPK and PI3K/AKT pathways [70]. Inhibition of these pathways leads to apoptosis of cancer cells, making the EGFR a particularly promising area of cancer research.

The mutations G719S, L858R, T790M, G719S/T790M, and T790M/L858R are commonly seen in patients with cancer because they modify the EGFR kinase activity [71]. García-Godoy et al. used molecular docking in order to study the interactions of EGFR inhibitors on the wild-type EGFR and mutant EGFR. For the wild-type human EGFR, the EGFR (PDB: 4ZAU) was complexed with the ligand AZD9291. Docking was also conducted on the EGFR containing the G719S mutation and the L858R mutation. The EGFR (PBD ID: 2ITN) was used with the G719S mutation and the EGFR (PDB: 2 EB3) was used with the L858R mutation. Both EGFRs were in complex with AMP-PNP. Results of this docking study indicated that in both complexes, M793 was an important residue in facilitating interactions between the ligand and the active site [71]. In the final docking study, docking was performed on the EGFR double mutants T790M/L858R and T790M/G719S. In the instance where the EGFR mutant T790M/L858R was docked, the EGFR (PDB: 4JR5) was used and it was complexed with the ligand 3QY. The double mutant EGFR T790M/G719S (PDB: 3UG2) was also used and it was complexed with getfitinib (PDB: IRE). In both of the docking studies, the results revealed that there is a critical interaction between the ligand and the Met793 residue in the active site of the mutant EGFR [71]. Analysis of the results concluded that the interactions displayed in each case can be crucial evidence to why different cancer patients are more or less sensitive to certain treatments. This provides insight into how certain therapies should be considered circumstantial based on the mutation a patient may possess. The *in silico* methodology utilized in this study set a precedent for other researchers to use molecular docking to discover more drugs for EGFR inhibition.

Mahajan et al. discerned the value of the EGFR as a target for anticancer therapy; using molecular docking they were able to discover potential EGFR inhibitors. Screening of 50,000 compounds was performed by LigPrep (version3.3; Schrodinger, LLC, 2015) in order to prepare a library of drugs to be tested by several *in silico* methods. After the library was prepared with LigPrep, the compounds were then screened against EGFR drug target using e-Pharmacophore, docking, pharmacophore, substructure, and similarity search [72]. The protein used in the docking studies is complexed with the inhibitor tak-285 and it was chosen for the study because it has the best X-ray resolution (1.50 Å) of the EGFR structure (PDB: 3POZ). The downloaded protein was prepared for docking using the Protein Preparation Wizard. Docking the compounds was performed by the Glide module (version3.6; Schrodinger, LLC, 2015) software and the first round of docking studies used the high throughput virtual screening setting. After all compounds had been screened, the top 30% of the best scoring compounds were then re-docked using standard precision (SP) docking. Once those compounds had been docked, the top 30% of the best scoring compounds in SP docking were then re-docked using extra precision (XP) docking. A total of 1534 had been selected as compounds that bound to the EGFR with a respectable docking score [72]. Docking, along with e-Pharmacophore and pharmacophore *in silico* methods were able to narrow 50,000 compounds down to 200 compounds that showed potential for EGFR inhibition. Further computational methodology of the compounds revealed

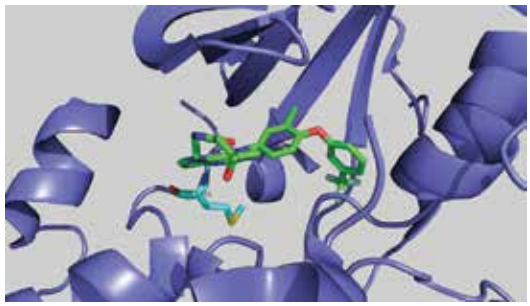

Figure 7. The tak-285 inhibitor complexed with the EGFR tyrosine kinase domain. The critical residue Met793 is shown in the active site of the EGFR tyrosine kinase.

that 87 out of the 200 compounds form an H-bond with M793, a critical residue in the inhibition of EGFR which can be visualized in **Figure 7**. Docking also revealed the structural similarity between the compounds and how the compounds orient themselves in the active site [72]. The 87 compounds were then categorized into 12 structural moieties which provided critical structural modification suggestions that would be beneficial in the development of more potent EGFR inhibitors [72].

3.4. Repurposing approved drugs to anticancer applications

Molecular docking for drug repurposing is another effective and beneficial method that many researchers utilize in order to discover new indications for already existing drugs. The technique is especially favorable when assessing different pharmaceuticals as potential anticancer therapies. Avastin, which was originally developed for metastatic colon cancer and non-small cell lung cancer, has now been approved for metastatic breast cancer. Rituxan, which was intended for non-Hodgkin's Lymphoma has been repurposed for chronic lymphocytic leukemia and rheumatoid arthritis [51]. Molecular docking to make predictions of the physical interactions between the ligand and the target has been a successful practice in drug repurposing.

Avastin and Rituxan are not the only two drugs that have been repurposed for anticancer therapeutics. Oliva et al. used molecular docking to aid in the study of repurposing the FDA approved psychotropic drug Chlorpromazine. Evidence had shown that Chlorpromazine had antiproliferative activity against colon and brain tumors [73]. The drug accomplished this by inhibiting cytochrome c oxidase (CcO), which is the terminal electron acceptor enzyme of the mitochondrial respiratory chain and is composed of 13 subunits [74, 75] . Cytochrome c oxidase subunit 4 isoform 1 (COX4-1) was the focus of the study because in patients with glioblastoma, increased expression of COX4-1 has been associated with Temozolomide chemoresistance [73]. *In vitro* studies indicated that Chlorpromazine inhibited CcO when COX4-1 is expressed, however the binding mechanism was not well understood. Using Schrödinger Suite 2015 (Schrödinger, LLC, New York, NY, 2015), two human CcO homology models were constructed based on the mouse CcO crystal structure (PDB: 2Y69) using the Prime program. The Chlorpromazine ligand was prepared using the LigPrep program and the docking studies were

conducted using the Glide program. The docking results showed that Chlorpromazine binds to a hydrophobic pocket formed by residues from COX4 and transmembrane helices of COX1. L129, K122, M119, and Y126 were identified as being important residues that displayed interactions with the Chlorpromazine [73]. The results also indicated that the Chlorpromazine overlaps with residues of COX11, preventing the subunit from interacting with the rest of the CcO complex [73]. The study provides critical evidence on the repurposing for Chlorpromazine as a treatment for chemoresistant gliomas and persuades future research on Chlorpromazine as an anticancer therapy.

In silico methods have been played an essential role in the battle against many of world's most devastating diseases. Cancer is debilitating, painful, and in some cases lethal; there is a massive urgency for researchers to find a cure so patients no longer have to suffer. Molecular docking has been on the forefront for the development, design, and discovery for new anticancer therapeutics. Among other things, one of the most important features of molecular docking is that it provides researchers with the opportunity to examine specific interactions between the ligand and the molecular target that are not well understood by *in vivo* and *in vitro* methods. Detailed knowledge of the binding interactions and mechanisms of the ligand to the target is critical for the production of new drugs or the improvement of the already existing drugs. Molecular docking is a dependable, economic, and an expeditious process that is of paramount importance in the advancement of anticancer therapeutics.

4. Identification of medicine for other prevalent diseases

4.1. Influenza

Influenza, commonly referred to as the flu, is a viral infection that can be mild or severe, depending on the strain, and the host it infects. Due to the rapidly mutating nature of the influenza virus, new vaccines must be made and administered annually. Each year, researchers must determine which strains of the influenza virus are most likely to become prevalent in the coming flu season; annual flu vaccines are manufactured based on those recommendations [76]. Unfortunately, there is always the threat that the virus may mutate after that decision has been made, rendering vaccines ineffective. In that case, flu outbreaks and even pandemics may occur. In a pandemic, vaccination will no longer be a feasible option, and antiviral agents will become a critical resource [77].

There are two types of antiviral drugs that have been used to treat influenza. The first marketed influenza antivirals were Adamantanes, specifically Amantadine and Rimantadine (**Figure 8A**, **B**). Adamantanes function by blocking the M2 proton channel [78]. This class of drugs was effective against influenza type A, but drug resistance developed rapidly [79, 80]. Hayden et al. conducted a study in which 17 Rimantadine-resistant influenza strains were recovered from 13 patients [81]. The M2 coding sequences of 17 resistant strains were then compared to 8 drug sensitive strains, and it was determined that all resistant strains had a nonsynonymous substitution in RNA segment 7. The most common mutation was S31N,

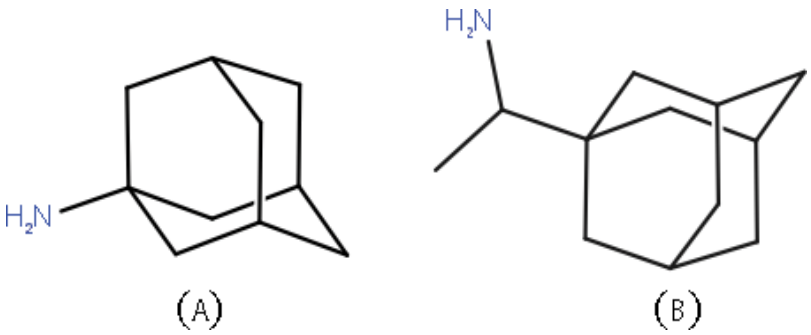

Figure 8. Two dimensional structures of the Adamantanes, (A) amantadine [SMILES: NC13CC2CC(CC(C1)C2)C3] and (B) Rimantadine [SMILES: NC(C)C13CC2CC(CC(C1)C2)C3].

which was found in 14 separate isolates. The other mutations found were A30V, A30T, and V27A. By 2009, all strains of influenza A had become resistant to Adamantanes [82].

The second class of influenza drugs is neuraminidase inhibitors. Neuraminidase, also referred to as sialidase, is an enzyme involved in the release of viral progeny. At the end of the viral replication cycle, neuraminidase cleaves O-sialic acid, also called NeuAc5 (N-acetyl-alpha-neuraminate), during the budding process that releases viral progeny that then infect other cells. Because inhibition of this enzyme greatly reduces the spread of the virus throughout the body, it is an attractive drug target [83]. There are currently two neuraminidase inhibitors on the market: Zanamivir (Relenza) and Oseltamivir (Tamiflu). Zanamivir (4-guanidino-Neu5-Ac2en) was created using computer-assisted rational design based on the X-ray diffraction structure of influenza neuraminidase, which was first solved by Varghese et al. (now PDB: 7NN9) [84]. In further studies, Colman et al. characterized the active site of this protein, identifying a large pocket containing "an unusually large number of charged residues," including R119 and E120[1] [86]. Von Itzstein et al. used GRID software to analyze the active site of influenza neuraminidase and its interactions with various novel inhibitors [87]. The inhibitor with the most energetically favorable interactions was 4-guanidino-Neu5Ac2en, now known as Zanamivir. It was noted that one of the terminal amino groups of Zanamivir's guanidyl group interacted with the glutamic acid 119 carboxyl group (**Figure 9A**, **B**). Von Itzstein et al. went on to conduct Zanamivir trials on influenza infected ferrets and mice, which validated the results of their computational studies [87]. Hayden et al. conducted randomized double blind trials that concluded Zanamivir was both effective and safe for use to treat influenza A and B [88]. The drug became FDA approved in 1999 and has since been used in conjunction with annual vaccines to prevent and minimize influenza outbreaks [89].

4.2. Malaria

Malaria is an infectious disease caused by a parasitic protist and spread by mosquitoes. There are several different species of this parasite; the most deadly, and most prevalent is *Plasmodium*

[1]Colman et al. (1983) refers to Arg 119 and Glu 120 as Arg 118 and Glu 119. This text uses the more up to date numbering used in [85].

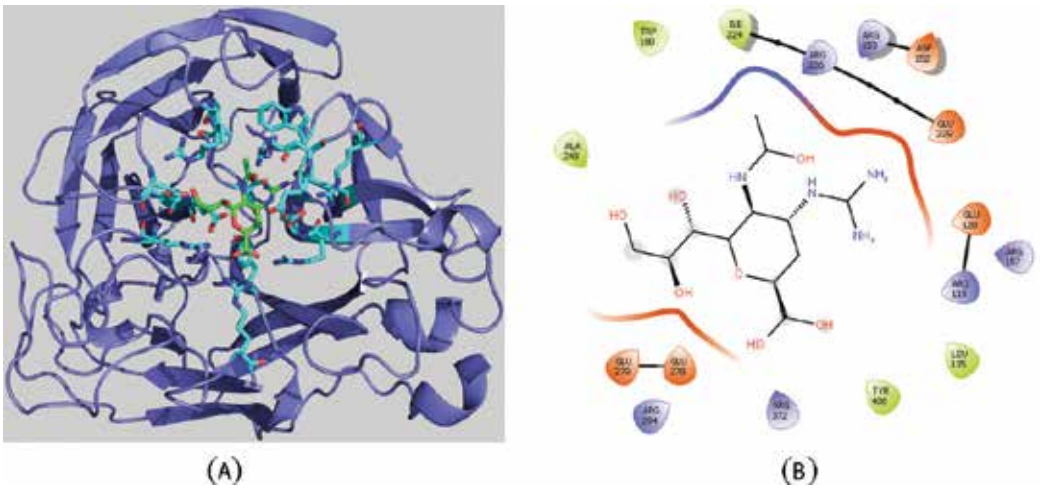

Figure 9. (A) (PDB ID: 5 L17) this structure shows Zanamivir bound to influenza a neuraminidase. Zanamivir, shown with green carbons, interacts with R119, E120, L135, D152, R153, W180, I224, R226, E229, E278, E279, R294, R372, and Y406 (cyan carbons). (B) Ligand interaction diagram showing a closer look at how these residues interact with the ligand. Note the interaction between amino groups and acidic residues (primarily glutamic acid) and the interactions between hydroxyl groups and basic residues (primarily arginine).

falciparum. This disease can cause flu-like symptoms, and can be fatal if left untreated [90]. Malaria is typically treated with quinine drugs such as Chloroquine, Hydroxychloroquine, or Amodiaquine (**Figure 10A**, **B**), which function by interfering with heme polymerization [91]. Interference with this function leads to increased levels of hemoglobin and ferriprotoporphyrin IX (FPIX), which can be toxic to the parasite. *P. falciparum* has developed resistance to chloroquine (and similar drugs); in resistant cells, quinine drugs are actively transported out of the parasitic vacuole [92]. This form of resistance has become widespread, resulting in a need for new antimalarial drugs.

In *P.* falciparum, M18 aspartyl aminopeptidase (*Pf*M18AAP) and its interactions with membrane proteins are essential for parasite survival, making it an attractive antimalarial drug target. Using molecular docking and other computational methods, Kumari et al. determined structural requirements for *Pf*M18AAP inhibitors using GOLD v5.2 and the Schrödinger Maestro 9.1 GLIDE program [12]. This study selected and screened just under 30,000 compounds

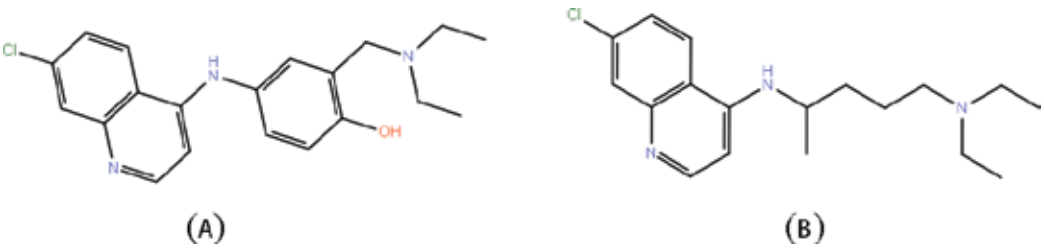

Figure 10. Two-dimensional structures of the common quinine drugs, (A) Amodiaquine [SMILES: Clc1cc2nccc(c2cc1)Nc3cc(c(O)cc3)CN(CC)CC] and (B) Chloroquine [SMILES: Clc1cc2nccc(c2cc1)NC(C)CCCN(CC)CC].

for binding activity. Based on the results, it was concluded that the best inhibitors had one hydrogen donor, one hydrophobic group, and two aromatic rings. Molecular docking and pharmacophore modeling have been used to search for novel inhibitors using those criteria.

The lactate dehydrogenase enzyme of *P. falciparum* (*Pf*LDH) is a target of quinine drugs, and is another potential target for novel antimalarial drugs. This enzyme is important for glycolysis, and its inhibition can potentially result in death of the parasite [93]. Compounds similar to nicotinamide adenine dinucleotide (NADH) are believed to be excellent candidates for *Pf*LDH inhibition [94]. Penna-Coutinho et al. used molecular docking (with software MolDock) to select potential drug candidates [95]. NADH and 50 potential drug candidates were docked to *Pf*LDH in complex with Oxamate (PDB: 1LDG), the substrate that NADH binds to (**Figure 11**); the compounds that had the most similar docking score to NADH were selected for *in vitro* tests. The *in vitro* tests confirmed the activity of the highest scoring compounds, Itraconazole, Atorvastatin, and Posaconazole. In further tests, these same compounds inhibited parasite growth in mice infected with *Plasmodium berghei*, another species of the malaria parasite. These compounds require further testing, but could potentially progress to clinical trials and eventually be marketed as antimalarial drugs.

4.3. Zika

The Zika virus (ZIKV), named for the Ugandan forest in which it was originally found, was first isolated in monkeys [96]. ZIKV belongs to a genus of viruses known as flaviviruses; other viruses belonging to this genus are dengue fever, yellow fever, hepatitis, and West Nile. ZIKV can be transmitted by mosquitoes or sexual contact. Symptoms of the virus include fever, joint pain, and rash for up to 7 days. ZIKV has also been associated with Guillain-Barre syndrome [97], an autoimmune disease. The virus can also be transmitted from mother to fetus, which can result in severe birth defects. From 2007 to 2014, several small outbreaks of the virus were

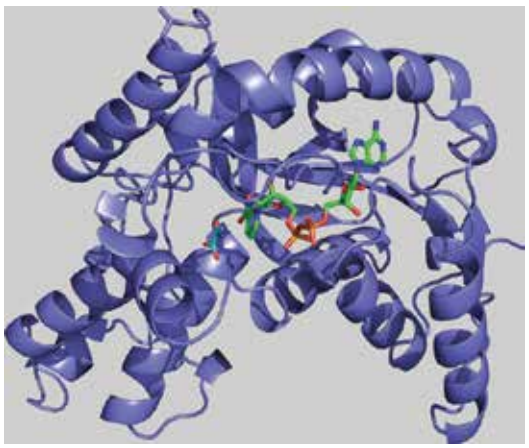

Figure 11. Structure of plasmodium falciparum lactate dehydrogenase in complex with Oxamate and NADH. NADH [SMILES: O=C(N)c1ccc[n+](c1)[C@@H]2O[C@@H]([C@@H](O)[C@H]2O)COP([O-])(=O)OP(=O)(O)OC[C@H]5O[C@@H](n4cnc3c(ncnc34)N)[C@H](O)[C@@H]5O]; Oxamate [SMILES: C(=O)(C(=O)O)N].

reported [97–99]. In 2015, the first ZIKV epidemic began in Brazil. As outbreaks become more and more severe, it is becoming increasingly urgent to find a drug to treat ZIKV.

Non-structural protein 5 methyl transferase (NS5 MTase) is crucial for the maintained stability of a flaviviral genome, and the ability to evade immune response [100] which makes it an attractive target for antiviral activity. Zhang et al. used docking simulations (AutoDock 4.2) to determine potential designs for novel NS5 MTase inhibitors and binding sites [101]; the authors of this study found that dengue virus inhibitor compound 10 found by Lim et al. [102] (PDB: 3P8Z) may bind to ZIKV NS5MTase. Ramharack and Soliman utilized several different computational tools in their study. Preliminary methods included homology modeling, binding site prediction, and pharmacophore modeling [103]. To narrow down the results from these studies, they used molecular docking [AutoDock Vina]. Out of 31 compounds subjected to docking studies, 3 were chosen for the next step, molecular dynamic simulation. It was concluded that two of their compounds showed "substantial stability in complex with the target enzyme (ZIKV NS5)," [103].

Hepatitis C is another virus that is closely related to Zika. Hepatitis C is commonly treated with polymerase inhibitors (Ribavirin and Sofosbuvir). Sacramento et al. used docking simulations (MODELER 9.16) to model binding between Hepatitis C polymerase inhibitors and Zika RNA polymerase (PDB: 4WTG) [104]. These simulations, as well as their *in vitro* trials suggested that these drugs intended for treatment of Hepatitis C may be effective against Zika as well. A study by Elfiky supported these results through further docking simulations (SCIGRESS software with PDB: 2J7U) [105].

4.4. Tuberculosis

Tuberculosis (TB) and infectious disease caused by *Mycobacterium tuberculosis*. Human infection with TB dates back all the way to ancient Egypt, India, and China [106]. TB is spread through the air, usually by a cough or sneeze from an infected person. TB kills nearly 2 million people each year, mostly in Africa [107]. The most effective treatments for non-resistant TB are Isoniazid and Rifampin. Unfortunately, TB drug resistance has become extensive [107]. There are three categories of resistant TB strains: multidrug resistant (MDR), extensively drug-resistant (XDR), and totally drug-resistant (TDR). In order to be classified as MDR TB, the strain must be resistant to both Isoniazid and Rifampin [108]. A TB strain is classified as XDR if it is resistant to Isoniazid, Rifampin, and "is also resistant to three or more of the six classes of second line TB drugs," [108]. TDR strains are resistant to all known TB drugs [109]. Dramatic increases of drug resistance have prompted researchers to seek new drug targets; in order to reduce research costs and get results as quickly as possible, many are turning to docking simulations for preliminary trials.

Shikimate kinase is a protein involved in an amino acid biosynthesis pathway in *M. tuberculosis* [110]. Interruption of this pathway prevents synthesis of essential amino acids, leading to incomplete proteins, which leads to cell death. Vianna and de Azevedo used docking simulations (MOLDOCK) to identify novel SK inhibitors; these compounds were compared to staurosporine, which has demonstrated SK inhibition *in vitro* [111]. The novel inhibitors were

docked to a number of structures for *Mt*SK (PDB: 2DFN, 1U8A, 1WE2, 1ZYU, 2G1K, 2IYQ, 2IYR, 2IYS, 2IYX, 2IYY, 2IYZ, and 3BAF).

Another response to drug resistance is drug repurposing. The advantage of drug repurposing is that potential drugs have already been shown not to have severe side effects, which speeds up the process and saves money. Studies of this nature often utilize molecular docking and other computational methods to save even more time and money by screening more potential drugs in a shorter time frame. Kahlous et al. selected 1991 FDA-approved (nonantibiotic) drugs and tested them for antibiotic activity against *Staphylococcus aureus* [PDB: 2XCS and 2XCT] by docking (OpenEye HYBRID) drug structures to known antibiotic targets [112]. These results were then compared to a variety of market antibiotics. The drug candidates were narrowed down to 34 potential candidates for further testing. Among the top candidates were Diclofenac (antiinflammatory), Drotaverine (antispasmodic), Flurbiprofen (antiinflammatory), Ibuprofen (antiinflammatory), and Niacin (vitamin B_3). Brindha et al. conducted a similar study, specifically targeting tuberculosis [113]. This study screened 1554 FDA-approved drugs (Schrödinger GLIDE) for their ability to bind to protein kinase B of *M. tuberculosis* (PDB: 2FUM), a known antibiotic target. Fourteen of these drugs were determined suitable for further exploration as TB drugs. The top three candidates from this study were Flavin adenine dinucleotide (treats vitamin B_2 deficiency), Valrubicin (treats bladder cancer), and Arcarbose (treat/manage type II diabetes).

5. Summary and discussion

While *in silico* methods must be reaffirmed by *in vitro* and *in vivo* testing, computational methods have been gaining popularity in the drug design industry by proving they are critical in the discovery of medications. Several drugs that are currently available to the public for the treatment of different diseases have been developed based on *in silico* approaches. For example, Zanamivir, used to treat influenza, was developed using computer-assisted design [84]. Through these studies, Zanamivir was identified as the inhibitor having the most energetically favorable interactions with influenza neuraminidase. The results from the docking study of Zanamivir were convincing enough to move forward with *in vivo* testing; the results of *in vivo* studies reaffirmed the results of the *in silico* tests [87]. Nelfinavir and Saquinavar are used in the treatment of HIV and were also developed by computational methods. Docking studies also revealed how the HIV protease developed resistance toward Nelfinavir and Saquinavar which was beneficial in improving the potency of the drugs [45]. Based on these successful examples, it is clear that computational methods are capable of developing new pharmaceuticals and provide evidence to other researchers that this is a reliable and effective technique in drug discovery.

The cost of bringing a drug to market and the amount of drug resistance profiles emerging are major factors that researchers need to address when designing a drug. It may cause more than 1 billion dollars and 10 years to bring a drug to the market [114]. As we have collected millions of pharmaceutical compounds in a database like Pubchem [115] and ChEMBL [116], we will

need several months or even years to screen them all manually or automatically in the lab, if it is possible we can obtain them all. More and more researchers are turning to computational methods to design drugs in an efficient manner that has the possibility to save money for pharmaceutical companies. While these *in silico* methods are not yet ready to replace *in vivo* and *in vitro* methods and have only brought a few medications to the market, such Raltegravir and Dorzolamide [117], they still provide a valuable insight into the molecular interactions between the ligand and protein. As seen above, there are situations in which computational methods are not always able to accurately determine the results. For this reason, many researchers use *in silico* methods in tandem with other research methods to verify or elucidate standing results. Each time these computational methods verify already established experimental results, their validity in the drug design market has the opportunity to go up. It seems that many researchers are starting to rely on computational results from molecular docking and other computational methods in their research. Often these methods cannot solely generate results that will create a novel drug. However, computational methods are slowly solidifying their place in the pharmaceutical industry as a necessary step toward designing new drugs.

To summarize the cases we reported above (Please see **Table 3**):

1. Most of these projects were designed to recognize a new inhibitor(s) to an enzyme which plays an essential role in a key metabolic/proliferation pathway or the infectious procedure of a pathogen.

2. One or more determined PDB structures of the target protein with good resolution were used, and, often, the key residues of the catalytic reaction, binding/inhibition mechanisms, and drug resistances were revealed based on the docking results.

3. Other computational methods or tools were also used in sequence or in parallel, such as structure prediction, binding site prediction, pharmacophore model, QSAR model, and MD simulation.

4. Drug repurposing has received more and more attention.

Enzymes and membrane proteins (receptors) are two major drug targets. According to previous studies, there is severe bias on the number of determined structures deposit on PDB [118, 119]. A large proportion of solved structures belong to soluble proteins, especially enzymes. It not only made structures of enzymes easier to obtain for molecular docking, but it also made scoring functions/force fields of molecular docking and other related computational approaches to be more accurate for enzymes than membrane proteins. However, we have noticed the importance of membrane receptors, glycol-proteins and non-structure proteins. How to create a reliable strategy to determine or predict the structures of these important drug targets remains a big challenge in molecular docking.

Drug resistance is also a major issue in the failures of treatment of both cancers and infectious diseases. Due to the advancement of docking calculation, we will be able to predict the possible drug resistances and side effects before the treatment or even the drug approval in the future. Therefore, the back-up drugs should be developed and utilized even before drug

Disease	Target protein	PDB ID	Docking Software	Drug(s)	Purpose	Other computational method(s) used
HIV	Integrase	1QS4, 1BIS, 1BLE	GOLD	S-1360	To predict the binding mode	
HIV	Protease	1HXB, 1OHR	AutoDock	Saquinavir, Nelfinavir	To predict the drug resistance	MD simulation
Cancer	Proteasome	2F16	Glide, GOLD	PI-083, MG132, peptide aldehydes	To identify new drug, to understand the binding mechanism	MD simulation
Cancer	Carbonic anhydrases IX	3IAI	AutoDock	ZINC03363328, ZINC08828920, ZINC12941947, ZINC03622539, ZINC1665054	To discover inhibitors	Post-docking energy minimization
Cancer	EGFR	2ITN et al.	AutoDock, jMetalCpp	AMPPNP, Dacomitinib, et al.	To study the effects of mutations	Optimization algorithms
Cancer	CcO	2Y69	Glide	Chlorpromazine	Drug repurposing	
Influenza	Neuraminidase	7NN9	GRID	Zanamivir	To analyze the active site	
Malaria	M18 aspartyl aminopeptidase	4EME	GOLD, Glide	CHEMBL588000 et al.	To identify new drugs	Pharmacophore and QSAR models
Malaria	Lactate dehydrogenase	1LDG	MolDock	Itraconazole, Atorvastatin, Posaconazole	To select potential drugs	
Zika	NS5MTase	3P8Z	AutoDock	New candidates	To identify new drugs	MD simulation
Zika	RNA Polymerase	4WTG	Modeler	Ribavirin, Sofosbuvir	To model and compare ligand binding	
TB	Shikimate kinase	2DFN et al.	MOLDOCK	New candidates	To identify new inhibitors	
TB	Shikimate kinase	2XCS, 2XCT, 2FUM	OpenEye HYBRID, Glide	Diclofenac et al.	Drug repurposing	

Table 3. Summary of the cases presented.

resistance occurs. The improved reliability of molecular docking also facilitates the precision medicine.

As we see in **Figure 1**, the computational approaches play key roles in different steps of the drug discovery process: obtaining the protein structures, binding site prediction, virtual drug screening, binding verification, binding affinity estimation, prediction of drug resistances, binding kinetic modeling, and so on. Molecular docking assists in achieving many objectives in the steps mentioned above effectively and efficiently. Often, it is cheaper, faster than performing

experiments in the biological labs, and we can do even more than conventional approaches. For example, we can predict the potential side effects or drug resistances. Other computational tools such as (3D structure or binding site) prediction models, molecular dynamic simulation, and kinetic modeling have been also well established and applied in different steps of drug discovery to provide more information of target protein or drug efficacy, narrow down the searching spaces/reduce computational load, and/or validate the results of docking. Moreover, drug repurposing is another important application of molecular docking that helps us to enhance the cost- and time-effectiveness of drug development.

In the Era of "Big Data", the accumulated number of protein structures and upgraded computation software and hardware generally improved all related computational methods, not just molecular docking. Based on the progress of the knowledge on protein folding, structural flexibility and molecular recognition, molecular docking has matured. As the core technology of virtual drug discovery, molecular docking will be widely applied to many stages of the drug discovery process.

Author details

Mark Andrew Phillips, Marisa A. Stewart, Darby L. Woodling and Zhong-Ru Xie*

*Address all correspondence to: paulxie@uga.edu

Computational Drug Discovery Laboratory, School of Electrical and Computer Engineering, College of Engineering, University of Georgia, Athens, GA, USA

References

[1] Pagadala NS, Syed K, Tuszynski J. Software for molecular docking: A review. Biophysical Reviews. 2017;**9**(2):91-102

[2] Wong CF. Flexible receptor docking for drug discovery. Expert Opinion on Drug Discovery. 2015;**10**(11):1189-1200

[3] Ferreira LG, Dos Santos RN, Oliva G, Andricopulo AD. Molecular docking and structure-based drug design strategies. Molecules. 2015;**20**(7):13384-13421

[4] Yuriev E, Ramsland PA. Latest developments in molecular docking: 2010–2011 in review. Journal of Molecular Recognition. 2013;**26**(5):215-239

[5] Berman HM, Westbrook J, Feng Z, Gilliland G, Bhat TN, Weissig H, Shindyalov IN, Bourne PE. The protein data bank. Nucleic Acids Research. 2000;**28**(1):235-242

[6] Berman HM, Henrick K, Nakamura H, Markley J, Bourne PE, Westbrook J. Realism about PDB. Nature Biotechnology. 2007;**25**(8):845-846

[7] Roche DB, Brackenridge DA, McGuffin LJ. Proteins and their interacting partners: An introduction to protein-ligand binding site prediction methods. International Journal of Molecular Sciences. 2015;**16**(12):29829-29842

[8] Xie ZR, Hwang MJ. Methods for predicting protein-ligand binding sites. Methods in Molecular Biology. 2015;**1215**:383-398

[9] Zhu X, Xiong Y, Kihara D: Large-scale binding ligand prediction by improved patch-based method patch-Surfer2.0. Bioinformatics. 2015;**31**(5):707-713

[10] Abdolmaleki A, Ghasemi JB, Ghasemi F. Computer aided drug design for multi-target drug design: SAR/QSAR, molecular docking and pharmacophore methods. Current Drug Targets. 2017;**18**(5):556-575

[11] Desaphy J, Azdimousa K, Kellenberger E, Rognan D. Comparison and druggability prediction of protein-ligand binding sites from pharmacophore-annotated cavity shapes. Journal of Chemical Information and Modeling. 2012;**52**(8):2287-2299

[12] Kumari M, Chandra S, Tiwari N, Subbarao N. 3D QSAR, pharmacophore and molecular docking studies of known inhibitors and designing of novel inhibitors for M18 aspartyl aminopeptidase of plasmodium falciparum. BMC Structural Biology. 2016;**16**(12)

[13] Weiss R. How does HIV cause AIDS? Science. 1993;**260**:1273-1279

[14] Cunningham AL, Donaghy H, Harman AN, Kim M, Turville SG. Manipulation of dendritic cell function by viruses. Current Opinion in Microbiology. 2010;**13**:524-529

[15] Gilbert PB, McKeague IW, Eisen G, Mullins C, Guéye-Ndiaye A, Mboup S, Kanki PJ. Comparison of HIV-1 and HIV-2 infectivity from a prospective cohort study in Senegal. Statistics in Medicine. 2003;**22**(4):573-593

[16] Zheng Y-H, Lovsin N, Peterlin BM. Newly identified host factors modulate HIV replication. Immunology Letters. 2005;**97**(2):225-234

[17] Fan X, Zhang F-H, Al-Safi RI, Zeng L-F, Shabaik Y, Debnath B, Sanchez TW, Odde S, Neamati N, Long Y-Q. Design of HIV-1 integrase inhibitors targeting the catalytic domain as well as its interaction with LEDGF/p75: A scaffold hopping approach using salicylate and catechol groups. Bioorganic & Medicinal Chemistry. 2011;**19**:4935-4952

[18] Serrao E, Odde S, Ramkumar K, Neamati N. Raltegravir, elvitegravir, and metoogravir: The birth of "me-too" HIV-1 integrase inhibitors. Retrovirology. 2009;**6**:25-25

[19] Hazuda a DJ, Felock a P, Witmer a M, Wolfe a A, Stillmock a K, Grobler a JA, Espeseth a A, Gabryelski a L, Schleif a W, Blau a C, et al. Inhibitors of strand transfer that prevent integration and inhibit HIV-1 replication in cells. Science. 2000;(5453):646

[20] Zhuang L, Wai JS, Embrey MW, Fisher TE, Egbertson MS, Payne LS, Guare JP, Jr., Vacca JP, Hazuda DJ, Felock PJ et al: Design and synthesis of 8-hydroxy-[1,6]naphthyridines as novel inhibitors of HIV-1 integrase in vitro and in infected cells. Journal of Medicinal Chemistry. 2003;**46**(4):453-456

[21] Summa V, Petrocchi A, Matassa VG, Gardelli C, Muraglia E, Rowley M, Paz OG, Laufer R, Monteagudo E, Pace P. 4,5-dihydroxypyrimidine carboxamides and N-alkyl-5-hydroxypyrimidinone carboxamides are potent, selective HIV integrase inhibitors with good pharmacokinetic profiles in preclinical species. Journal of Medicinal Chemistry. 2006;**49**(23):6646-6649

[22] Low A, Mohri H, Markowitz M. Frequency of naturally occurring polymorphisms associated with resistance to integrase inhibitors in a recently infected cohort. In: 14th Conference on Ret- roviruses and Opportunistic Infections: Feb 25–28, 2007; Los Angeles, CA. 2007

[23] Gilbert J, Henske P, Singh A. Rebuilding big pharma's business model. The Business & Medicine Report. 2003;**21**(10):73-80

[24] Grabowski H, Vernon J, DiMasi JA. Returns on research and development for 1990s new drug introductions. PharmacoEconomics. 2002;**20**(15):11-29

[25] Lee TH. "Me-too" products—Friend or foe? New England Journal of Medicine. 2004; **350**(3):211-212

[26] Al-Mawsawi LQ, Al-Safi RI, Neamati N. Anti-infectives clinical progress of HIV-1 integrase inhibitors. Expert Opinion on Emerging Drugs. 2008;**13**(2):213-225

[27] Cooper DA, Steigbigel RT, Gatell JM, Rockstroh JK, Katlama C, Yeni P, Lazzarin A, Clotet B, Kumar PN, Eron JE. Subgroup and resistance analyses of raltegravir for resistant HIV-1 infection. New England Journal of Medicine. 2008;**359**(4):355-365

[28] Delelis O, Malet I, Na L, Tchertanov L, Calvez V, Marcelin A-G, Subra F, Deprez E, Mouscadet J-F. The G140S mutation in HIV integrases from raltegravir-resistant patients rescues catalytic defect due to the resistance Q148H mutation. Nucleic Acids Research. 2009;**37**(4):1193-1201

[29] Dayam R, Neamati N. Active site binding modes of the beta-diketoacids: A multi-active site approach in HIV-1 integrase inhibitor design. Bioorganic & Medicinal Chemistry. 2004;**12**(24):6371-6381

[30] Jones G, Willett P, Glen RC, Leach AR, Taylor R. Development and validation of a genetic algorithm for flexible docking. Journal of Molecular Biology. 1997;**267**(3):727-748

[31] Nissink JWM, Murray C, Hartshorn M, Verdonk ML, Cole JC, Taylor R. A new test set for validating predictions of protein–ligand interaction. Proteins: Structure, Function, and Bioinformatics. 2002;**49**(4):457-471

[32] Fikkert V, Hombrouck A, Van Remoortel B, De Maeyer M, Pannecouque C, De Clercq E, Debyser Z, Witvrouw M. Multiple mutations in human immunodeficiency virus-1 integrase confer resistance to the clinical trial drug S-1360. AIDS. 2004;**18**(15):2019-2028

[33] Billich A. S-1360 Shionogi-GlaxoSmithKline. Current Opinion in Investigational Drugs (London, England: 2000). 2003;**4**(2):206-209

[34] Yoshinaga T, Sato A, Fujishita T, Fujiwara T. S-1360: In vitro activity of a new HIV-1 integrase inhibitor in clinical development. In: 9th conference on retroviruses and opportunistic infections, Seattle, WA: 2002. 55

[35] Davies DR. The structure and function of the aspartic proteinases. Annual Review of Biophysics and Biophysical Chemistry. 1990;**19**(1):189-215

[36] Huang X, Britto MD, Kear-Scott JL, Boone CD, Rocca JR, Simmerling C, Mckenna R, Bieri M, Gooley PR, Dunn BM. The role of select subtype polymorphisms on HIV-1 protease conformational sampling and dynamics. Journal of Biological Chemistry. 2014; **289**(24):17203-17214

[37] Kräusslich H-G, Ingraham RH, Skoog MT, Wimmer E, Pallai PV, Carter CA. Activity of purified biosynthetic proteinase of human immunodeficiency virus on natural substrates and synthetic peptides. Proceedings of the National Academy of Sciences. 1989; **86**(3):807-811

[38] Seelmeier S, Schmidt H, Turk V, Von Der Helm K. Human immunodeficiency virus has an aspartic-type protease that can be inhibited by pepstatin a. Proceedings of the National Academy of Sciences. 1988;**85**(18):6612-6616

[39] Goodman LS. Goodman and Gilman's the Pharmacological Basis of Therapeutics. vol. 1549. New York: McGraw-Hill; 1996

[40] Brik A, Wong C-H. HIV-1 protease: Mechanism and drug discovery. Organic & Biomolecular Chemistry. 2003;**1**(1):5-14

[41] Vacca JP, Condra JH. Clinically effective HIV-1 protease inhibitors. Drug Discovery Today. 1997;**2**(7):261-272

[42] Kalish V, Kaldor S, Shetty B, Tatlock J, Davies J, Hammond M, Dressman B, Fritz J, Appelt K, Reich S. Iterative protein structure-based drug design and synthesis of HIV protease inhibitors. European Journal of Medicinal Chemistry. 1995;**30**:201s-214s

[43] Vacca JP, Guare J, Desolms S, Sanders W, Giuliani E, Young S, Darke P, Sigal I, Schleif W. L-687,908, a potent hydroxyethylene containing HIV protease inhibitor. Journal of Medicinal Chemistry. 1991;**34**(3):1225-1228

[44] Jenwitheesuk E, Samudrala R. Prediction of HIV-1 protease inhibitor resistance using a protein-inhibitor flexible docking approach. Antiviral Therapy. 2005;**10**(1):157-166

[45] Jenwitheesuk E, Samudrala R. Improved prediction of HIV-1 protease-inhibitor binding energies by molecular dynamics simulations. BMC Structural Biology. 2003;**3**(1):2

[46] Morris GM, Goodsell DS, Halliday RS, Huey R, Hart WE, Belew RK, Olson AJ. Automated docking using a Lamarckian genetic algorithm and an empirical binding free energy function. Journal of Computational Chemistry. 1998;**19**(14):1639-1662

[47] Shenderovich MD, Kagan RM, Heseltine PN, Ramnarayan K. Structure-based phenotyping predicts HIV-1 protease inhibitor resistance. Protein Science. 2003;**12**(8):1706-1718

[48] Vos T, Allen C, Arora M, Barber RM, Bhutta ZA, Brown A, Carter A, Casey DC, Charlson FJ, Chen AZ. Global, regional, and national incidence, prevalence, and years lived with disability for 310 diseases and injuries, 1990-2015: A systematic analysis for the global burden of disease study 2015. The Lancet. 2016;**388**(10053):1545

[49] Organization WH. Chagas disease (American trypanosomiasis). Fact sheet No. 340. 2016. In. 2016

[50] Bellera CL, Balcazar DE, Vanrell MC, Casassa AF, Palestro PH, Gavernet L, Labriola CA, Gálvez J, Bruno-Blanch LE, Romano PS. Computer-guided drug repurposing: Identification of trypanocidal activity of clofazimine, benidipine and saquinavir. European Journal of Medicinal Chemistry. 2015;**93**:338-348

[51] Dudley JT, Deshpande T, Butte AJ. Exploiting drug-disease relationships for computational drug repositioning. Briefings in Bioinformatics. 2011;**12**(4):303-311

[52] Siegel RL, Miller KD, Jemal A. Cancer statistics, 2016. CA: a Cancer Journal for Clinicians. 2016;**66**(1):7-30

[53] Allen T. Ligand-targeted therapuetics in anticancer therapy. Nature Reviews Cancer. 2002;**2**(10):750-763

[54] Peters JM. Proteasomes: Protein degradation machines of the cell. Trends in Biochemical Sciences. 1994;**19**(9):377-382

[55] Kazi A, Lawrence H, Guida WC, McLaughlin ML, Springett GM, Berndt N, Yip RM, Sebti SM. Discovery of a novel proteasome inhibitor selective for cancer cells over non-transformed cells. Cell Cycle. 2009;**8**(12):1940-1951

[56] Guedes RA, Serra P, Salvador JAR, Guedes RC. Computational approaches for the discovery of human proteasome inhibitors: An overview. Molecules. 2016;**21**(7):927-953

[57] Kane RC, Farrell AT, Sridhara R, Pazdur R. United States Food and Drug Administration approval summary: Bortezomib for the treatment of progressive multiple myeloma after one prior therapy. Clinical Cancer Research. 2006;**12**(10):2955-2960

[58] Lashinger LM, Zhu K, Williams SA, Shrader M, Dinney CP, McConkey DJ. Bortezomib abolishes tumor necrosis factor-related apoptosis-inducing ligand resistance via a p21-dependent mechanism in human bladder and prostate cancer cells. Cancer Research. 2005;**65**(11):4902-4908

[59] Liu J, Zhang H, Xiao Z, Wang F, Wang X, Wang Y. Combined 3D-QSAR, molecular docking and molecular dynamics study on derivatives of peptide epoxyketone and tyropeptin-boronic acid as inhibitors against the beta5 subunit of human 20S proteasome. International Journal of Molecular Sciences. 2011;**12**(3):1807-1835

[60] Zhang S, Shi Y, Jin H, Liu Z, Zhang L, Zhang L. Covalent complexes of proteasome model with peptide aldehyde inhibitors MG132 and MG101: Docking and molecular dynamics study. Journal of Molecular Modeling. 2009;**15**(12):1481-1490

[61] Ma Y, Xu B, Fang Y, Yang Z, Cui J, Zhang L, Zhang L. Synthesis and SAR study of novel peptide aldehydes as inhibitors of 20S proteasome. Molecules. 2011;**16**(9):7551-7564

[62] Spikes JD, Jori G. Photodynamic therapy of tumours and other diseases using porphyrins. Lasers in Medical Science. 1987;**2**(1):3-15

[63] Santoro AM, Lo Giudice MC, D'Urso A, Lauceri R, Purrello R, Milardi D. Cationic porphyrins are reversible proteasome inhibitors. Journal of the American Chemical Society. 2012;**134**(25):10451-10457

[64] Supuran CT. Carbonic anhydrases: Novel therapeutic applications for inhibitors and activators. Nature Reviews Drug Discovery. 2008;**7**(2):168-181

[65] Krungkrai J, Supuran CT. The alpha-carbonic anhydrase from the malaria parasite and its inhibition. Current Pharmaceutical Design. 2008;**14**(7):631-640

[66] Pinard MA, Boone CD, Rife BD, Supuran CT, McKenna R. Structural study of interaction between brinzolamide and dorzolamide inhibition of human carbonic anhydrases. Bioorganic & Medicinal Chemistry. 2013;**21**(22):7210-7215

[67] Amresh P, Kumar K, Islam A, Hassan MI, Ahmad F. Receptor Chemoprint derived Pharmacophore model for development of CAIX Inihibitors. Carcinogenesis & Mutagenesis. 2013;**S8**(003)

[68] Gazdar AF. Activating and resistance mutations of EGFR in non-small-cell lung cancer: Role in clinical response to EGFR tyrosine kinase inhibitors. Oncogene. 2009;**28**:S24-S31

[69] Anderson NG, Ahmad T, Chan K, Dobson R, Bundred NJ. ZD1839 (Iressa), a novel epidermal growth factor receptor (EGFR) tyrosine kinase inhibitor, potently inhibits the growth of EGFR-positive cancer cell lines with or without erbB2 overexpression. International Journal of Cancer. 2001;**94**(6):774-782

[70] Engelman JA, Cantley LC. A sweet new role for EGFR in cancer. Cancer Cell. 2008;**13**(5): 375-376

[71] Garcia-Godoy MJ, Lopez-Camacho E, Garcia-Nieto J, Nebro AJ, Aldana-Montes JF. Molecular docking optimization in the context of multi-drug resistant and sensitive EGFR mutants. Molecules. 2016;**21**(11)

[72] Mahajan P, Suri N, Mehra R, Gupta M, Kumar A, Sing SK, Nargotra A. Discovery of novel small molecule EGFR inhibitory leads by structure and ligand-based virtual screening. Medicinal Chemistry Research. 2016;**26**(74):74-92

[73] Oliva CR, Zhang W, Langford C, Suto MJ, Griguer CE. Repositioning chlorpromazine for treating chemoresistant glioma through the inhibition of cytochrome c oxidase bearing the COX4-1 regulatory subunit. Oncotarget. 2017;**8**(23):37568-37583

[74] Brunori M, Antonini G, Malatesta F, Sarti P, Wilson MT. Cytochrome-*c* oxidase. European Journal of Biochemistry. 1987;**169**:1-8

[75] Tsukihara T, Aoyama H, Yamashita E, Tomizaki T, Yamaguchi H, Shinzawa-Itoh K, Nakashima R, Yaono R, Yoshikawa S. The whole structure of the 13-subunit oxidized cytochrome c oxidase at 2.8 A. Science. 1996;**272**(5265):1136-1144

[76] Gerdil C. The annual production cycle for influenza vaccine. Vaccine. 2003;**21**(16):1776-1779

[77] Hayden FG. Pandemic influenza: Is an antiviral response realistic? The Pediatric Infectious Disease Journal. 2004;**23**(11 Suppl):S262-S269

[78] Moorthy NS, Poongavanam V, Pratheepa V. Viral M2 ion channel protein: A promising target for anti-influenza drug discovery. Mini Reviews in Medicinal Chemistry. 2014; **14**(10):819-830

[79] Moscona A. Neuraminidase inhibitors for influenza. The New England Journal of Medicine. 2005;**353**(13):1363-1373

[80] Davies WL, Grunert RR, Haff RF, McGahen JW, Neumayer EM, Paulshock M, Watts JC, Wood TR, Hermann EC, Hoffmann CE. Antiviral activity of 1-Adamantanamine (amantadine). Science. 1964;**144**(3620):862-863

[81] Hayden FG, Belshe RB, Clover RD, Hay AJ, Oakes MG, Soo W. Emergence and apparent transmission of rimantadine-resistant influenza A virus in families. The New England Journal of Medicine. 1989;**321**(25):1696-1702

[82] Alves Galvao MG, Rocha Crispino Santos MA, Alves da Cunha AJ. Amantadine and rimantadine for influenza A in children and the elderly. Cochrane Database Systematic Review. 2014;**11**. CD002745

[83] von Itzstein M: The war against influenza: Discovery and development of sialidase inhibitors. Nature Reviews Drug Discovery. 2007;**6**(12):967-974

[84] Varghese JN, Laver WG, Colman PM. Structure of the influenza virus glycoprotein antigen neuraminidase at 2.9 a resolution. Nature. 1983;**303**(5912):35-40

[85] Gubareva LV, Sleeman K, Guo Z, Yang H, Hodges E, Davis CT, Baranovich T, Stevens J. Drug susceptibility evaluation of an influenza a(H7N9) virus by Analyzing recombinant neuraminidase proteins. The Journal of Infectious Diseases. 2017;**216**(suppl_4):S566-S574

[86] Colman PM, Varghese JN, Laver WG. Structure of the catalytic and antigenic sites in influenza virus neuraminidase. Nature. 1983;**303**(5912):41-44

[87] Vonitzstein M, Wu WY, Kok GB, Pegg MS, Dyason JC, Jin B, Phan TV, Smythe ML, White HF, Oliver SW, et al. Rational design of potent sialidase-based inhibitors of influenza-virus replication. Nature. 1993;**363**(6428):418-423

[88] Hayden FG, Osterhaus AD, Treanor JJ, Fleming DM, Aoki FY, Nicholson KG, Bohnen AM, Hirst HM, Keene O, Wightman K. Efficacy and safety of the neuraminidase inhibitor zanamivir in the treatment of influenzavirus infections. GG167 influenza study group. The New England Journal of Medicine. 1997;**337**(13):874-880

[89] Winquist AG, Fukuda K, Bridges CB, Cox NJ. Neuraminidase inhibitors for treatment of influenza A and B infections. In. Edited by Services DoHaH. In: Morbidity and Mortality Weekly Report: Centers for Disease Control and Prevention. Vol. 48. 1999. pp. 1-9

[90] Newton CR, Krishna S. Severe falciparum malaria in children: Current understanding of pathophysiology and supportive treatment. Pharmacology & Therapeutics. 1998;**79**(1):1-53

[91] Wellems TE. Malaria. How chloroquine works. Nature. 1992;**355**(6356):108-109

[92] Chinappi M, Via A, Marcatili P, Tramontano A. On the mechanism of Chloroquine resistance in plasmodium falciparum. PLoS One. 2010;**5**(11)

[93] Egan TJ, Ncokazi KK. Quinoline antimalarials decrease the rate of beta-hematin formation. Journal of Inorganic Biochemistry. 2005;**99**(7):1532-1539

[94] Dunn CR, Banfield MJ, Barker JJ, Higham CW, Moreton KM, Turgut-Balik D, Brady RL, Holbrook JJ. The structure of lactate dehydrogenase from plasmodium falciparum reveals a new target for anti-malarial design. Nature Structural Biology. 1996;**3**(11):912-915

[95] Penna-Coutinho J, Cortopassi WA, Oliveira AA, Franca TC, Krettli AU. Antimalarial activity of potential inhibitors of plasmodium falciparum lactate dehydrogenase enzyme selected by docking studies. PLoS One. 2011;**6**(7):e21237

[96] Sikka V, Chattu VK, Popli RK, Galwankar SC, Kelkar D, Sawicki SG, Stawicki SP, Papadimos TJ. The emergence of Zika virus as a Global Health security threat: A review and a consensus statement of the INDUSEM joint working group (JWG). Journal of Global Infectious Disease. 2016;**8**(1):3-15

[97] Cao-Lormeau VM, Blake A, Mons S, Lastere S, Roche C, Vanhomwegen J, Dub T, Baudouin L, Teissier A, Larre P, et al. Guillain-Barre syndrome outbreak associated with Zika virus infection in French Polynesia: A case-control study. Lancet. 2016;**387**(10027): 1531-1539

[98] Duffy MR, Chen TH, Hancock WT, Powers AM, Kool JL, Lanciotti RS, Pretrick M, Marfel M, Holzbauer S, Dubray C, et al. Zika virus outbreak on Yap Island, Federated States of Micronesia. The New England Journal of Medicine. 2009;**360**(24):2536-2543

[99] Musso D. Zika virus transmission from French Polynesia to Brazil. Emerging Infectious Diseases. 2015;**21**(10):1887

[100] Dong HP, Fink K, Zust R, Lim SP, Qin CF, Shi PY. Flavivirus RNA methylation. Journal of General Virology. 2014;**95**:763-778

[101] Zhang C, Feng T, Cheng J, Li Y, Yin X, Zeng W, Jin X, Li Y, Guo F, Jin T. Structure of the NS5 methyltransferase from Zika virus and implications in inhibitor design. Biochemical and Biophysical Research Communications; 2016

[102] Lim SP, Sonntag LS, Noble C, Nilar SH, Ng RH, Zou G, Monaghan P, Chung KY, Dong H, Liu B, et al, Small molecule inhibitors that selectively block dengue virus methyltransferase. The Journal of Biological Chemistry. 2011;**286**(8):6233-6240

[103] Ramharack P, Soliman MES. Zika virus NS5 protein potential inhibitors: An enhanced in silico approach in drug discovery. Journal of Biomolecular Structure & Dynamics. 2017:1-16

[104] Sacramento CQ, de Melo GR, de Freitas CS, Rocha N, Hoelz LV, Miranda M, Fintelman-Rodrigues N, Marttorelli A, Ferreira AC, Barbosa-Lima G et al: The clinically approved antiviral drug sofosbuvir inhibits Zika virus replication. Scientific Reports. 2017;**7**:40920

[105] Elfiky AA. Zika viral polymerase inhibition using anti-HCV drugs both in market and under clinical trials. Journal of Medical Virology. 2016;**88**(12):2044-2051

[106] Hershkovitz I, Donoghue HD, Minnikin DE, Besra GS, Lee OY, Gernaey AM, Galili E, Eshed V, Greenblatt CL, Lemma E, et al. Detection and molecular characterization of 9,000-year-old mycobacterium tuberculosis from a Neolithic settlement in the eastern Mediterranean. PLoS One. 2008;**3**(10):e3426

[107] Keshavjee S, Farmer PE. Tuberculosis, drug resistance, and the history of modern medicine. The New England Journal of Medicine. 2012;**367**(10):931-936

[108] Centers for Disease Control and Prevention. Plan to Combat Extensively Drug-Resistant Tuberculosis: Recommendations of the Federal Tuberculosis Task Force. MMWR Recomm Report. 2009;**58**(RR-3):1-43

[109] Velayati AA, Masjedi MR, Farnia P, Tabarsi P, Ghanavi J, ZiaZarifi AH, Hoffner SE. Emergence of new forms of totally drug-resistant tuberculosis bacilli: Super extensively drug-resistant tuberculosis or totally drug-resistant strains in iran. Chest. 2009;**136**(2): 420-425

[110] Ratledge C, Patel PV, Mundy J. Iron transport in mycobacterium smegmatis: The location of mycobactin by electron microscopy. Journal of General Microbiology. 1982;**128**(7): 1559-1565

[111] Vianna CP, de Azevedo WF, Jr.: Identification of new potential mycobacterium tuberculosis shikimate kinase inhibitors through molecular docking simulations. Journal of Molecular Modeling. 2012;**18**(2):755-764

[112] Kahlous NA, Bawarish MA, Sarhan MA, Kupper M, Hasaba A, Rajab M. Using Chemoinformatics, bioinformatics, and bioassay to predict and explain the antibacterial activity of nonantibiotic Food and Drug Administration drugs. Assay and Drug Development Technologies. 2017;**15**(3):89-105

[113] Brindha S, Vincent S, Velmurugan D, Ananthakrishnan D, Sundaramurthi JC, Gnanadoss JJ. Bioinformatics approach to prioritize known drugs towards repurposing for tuberculosis. Medical Hypotheses. 2017;**103**:39-45

[114] DiMasi JA, Grabowski HG, Hansen RW. Innovation in the pharmaceutical industry: New estimates of R&D costs. Journal of Health Economics. 2016;**47**:20-33

[115] Kim S, Thiessen PA, Bolton EE, Chen J, Fu G, Gindulyte A, Han L, He J, He S, Shoemaker BA, et al. PubChem substance and compound databases. Nucleic Acids Research. 2016;**44**(D1):D1202-D1213

[116] Gaulton A, Bellis LJ, Bento AP, Chambers J, Davies M, Hersey A, Light Y, McGlinchey S, Michalovich D, Al-Lazikani B, et al. ChEMBL: A large-scale bioactivity database for drug discovery. Nucleic Acids Research. 2012;**40**(Database issue):D1100-D1107

[117] Kubinyi H. Chance favors the prepared mind–from serendipity to rational drug design. Journal of Receptor and Signal Transduction Research. 1999;**19**(1–4):15-39

[118] Peng K, Obradovic Z, Vucetic S: Exploring bias in the protein data Bank using contrast classifiers. Pacific symposium on Biocomputing Pacific Symposium on Biocomputing 2004:435-446

[119] Xie ZR, Liu CK, Hsiao FC, Yao A, Hwang MJ. LISE: A server using ligand-interacting and site-enriched protein triangles for prediction of ligand-binding sites. Nucleic Acids Research. 2013;**41**(Web Server issue):W292-W296

Edited by Dimitrios P. Vlachakis

Molecular docking has always been and will be on the forefront of developments in the eminent field of drug design and medicinal chemistry. At the early days, drug discovery was based on blackboard drawings and expert intuition. However, as times move on, the amount of available information and overall knowledge base that needs to be analyzed cannot be processed manually. This, coupled by the rapid growth in computational infrastructure and processing power, has allowed for the efficient use of molecular docking tools and algorithms to be considered in the greater field of drug discovery. In the postgenomic era, molecular docking has become the key player for the screening of hundreds of thousands of compounds against a repertoire of pharmacological targets.

Published in London, UK

IntechOpen

ISBN 978-1-83881-432-8